Design of Nitrone-based antioxidant as neuroprotective agents

Anaïs Deletraz

▶ **To cite this version:**

Anaïs Deletraz. Design of Nitrone-based antioxidant as neuroprotective agents. Medicinal Chemistry. Université d'Avignon, 2019. English. NNT : 2019AVIG0272 . tel-02534818

HAL Id: tel-02534818
https://theses.hal.science/tel-02534818

Submitted on 7 Apr 2020

HAL is a multi-disciplinary open access archive for the deposit and dissemination of scientific research documents, whether they are published or not. The documents may come from teaching and research institutions in France or abroad, or from public or private research centers.

L'archive ouverte pluridisciplinaire **HAL**, est destinée au dépôt et à la diffusion de documents scientifiques de niveau recherche, publiés ou non, émanant des établissements d'enseignement et de recherche français ou étrangers, des laboratoires publics ou privés.

ACADÉMIE D'AIX-MARSEILLE
AVIGNON UNIVERSITÉ

Laboratoire de Chimie Bioorganique et Systèmes Amphiphiles
Institut des Biomolécules Max Mousseron - UMR 5247

ED 536 « Agrosciences & Sciences »

THÈSE

Présentée à Avignon Université

En vue de l'obtention du grade de Docteur en Sciences

Spécialité : Chimie organique

Développement d'antioxydants de type nitrone comme agents neuroprotecteurs

Présentée par

Anaïs DELETRAZ

Soutenue le 20 Décembre 2019 devant le jury composé de :

Dr Fabienne PEYROT : Maître de Conférences-HDR, Université Paris-Descartes	Rapporteure
Dr Olivier OUARI : Maître de Conférences-HDR, Université d'Aix-Marseille	Rapporteur
Pr Sandrine PY : Directrice de Recherche-CNRS, Université Grenoble Alpes	Examinatrice
Dr Béatrice TUCCIO : Maître de Conférences-HDR, Université d'Aix-Marseille	Examinatrice
Pr Olivier DANGLES : Professeur, Avignon Université	Examinateur
Pr Patrick MEFFRE : Professeur, Université de Nîmes	Examinateur
Pr Patrick TROUILLAS : Professeur, Université de Limoges	Examinateur
Dr Noëlle CALLIZOT : Responsable scientifique, Neuro-Sys	Invitée
Dr Grégory DURAND : Maître de Conférences-HDR, Avignon Université	Directeur de thèse

Remerciements

Ces travaux de thèse ont été réalisés au laboratoire de Chimie Bioorganique et Systèmes Amphiphiles (CBSA) de l'Université d'Avignon, actuellement dirigée par la Dr Christine Contino-Pépin. Ils ont reçu le soutien financier de la start-up Neuro-Sys, dirigée par M. Yann Jaudouin, et de la Région Provence Alpes Côtes d'Azur. Je les remercie grandement d'avoir permis la réalisation de ce travail.

Je remercie vivement les Drs Fabienne Peyrot et Olivier Ouari pour avoir accepté de juger mon travail de thèse en tant que rapporteurs. Je tiens également à remercier les Prs Sandrine Py et Patrick Trouillas ainsi que les Drs Béatrice Tuccio et Noëlle Callizot pour avoir accepté de faire partie de mon jury de thèse. Merci à vous tous de l'intérêt que vous avez manifesté à l'égard de ce travail.

Je tiens ensuite à adresser mes remerciements à mon directeur de thèse, Grégory Durand, pour m'avoir donné l'opportunité d'effectuer cette thèse et m'avoir encadré pendant ces trois années. J'ai particulièrement apprécié la confiance et l'autonomie que tu m'as accordées.

Plusieurs collaborations ont permis l'aboutissement de ce travail et je tiens à remercier chacune d'entre elles car, sans elles, ce travail n'aurait pas été si riche et varié. Merci à M. Yann Jaudouin, président de Neuro-Sys et à Mme Noëlle Callizot, responsable scientifique de Neuro-Sys pour leurs discussions enrichissantes sur les résultats obtenus. Merci également à Mme Maud Combes pour la réalisation des tests sur cellules. Un grand merci aux Drs Béatrice Tuccio et Robert Lauricella pour m'avoir formé et aidé à la réalisation des études cinétiques par RPE. De même, je tiens à remercier les Prs Paul-Louis Fabre et Karine Reybier pour m'avoir très bien reçu dans leur laboratoire et initié à la voltampérométrie cyclique. Je remercie également le Pr Patrick Trouillas et le Dr Florent Di Meo pour avoir contribué à donner plus de sens à mes travaux de recherche par l'acquisition de données théoriques. Merci également à Jamila Chetouani pour avoir réalisé un très bon travail de stage. Enfin, je remercie le Pr Michel Vignes pour la réalisation des tests biologiques.

Je tiens à remercier chaleureusement tous les collègues que j'ai côtoyés, et qui ont contribués de loin ou de près à ces trois années de thèse : Carole, Céline, Delphine, Nathalie, Hughes, Valérie, Manu et Cyril. Je remercie plus particulièrement Karine pour sa grande disponibilité et son aide précieuse et Saad pour sa gentillesse et sa bonne humeur.

J’adresse mes remerciements les plus sincères aux autres membres de l’équipe : Pierre pour ses blagues et pour m’avoir permis de créer de très belles figures grâce à sa formation sur Igor ; Victoria, Christine et Françoise pour leur très bon accueil et leur gentillesse ; Simon pour sa bonne humeur contagieuse ; Maxence pour sa disponibilité ; Damien pour ses précieux conseils en chimie et son envie de transmettre aux autres ; Marine pour sa volonté sans faille pour améliorer le quotidien du laboratoire ; Moheddine pour nos discussions profondes sur l’avenir et ses deux acolytes Nasreddine et Vinay. Un grand merci également aux stagiaires Ludivine, Emilie et Cécile à qui je souhaite bonne chance pour la suite.

Je remercie tout spécialement : Alice pour m’avoir bien fait rire avec ses drôles d’aventures, J.-B. pour ses conseils en matière de chimie mais également en vin ; Stéphane pour sa grande disponibilité et ses petites blagounettes quotidiennes (ne détruit pas le tram quand même !) ; Kam pour avoir contribué à l’obtention de données RPE ainsi que pour ses conseils précieux et son soutien ; Christophe pour m’avoir beaucoup aidé, écouté et encouragé ; Valou pour sa joie de vivre et ses discussions rigolotes ; Val pour ses ragots et ses connaissances culinaires et enfin Emilie pour nos longues discussions sur la vie, sa grande aide et pour toujours réussir à me mettre une chanson dans la tête ;).

Un grand merci également à Shiraz pour son soutien et nos discussions très enrichissantes ; Elodie pour son aide administrative et son rire communicatif ; Adrien pour ses conseils et son amour de la grenadine ; Fatina pour être toujours de bonne humeur et ses gâteaux libanais ; Vincent pour sa gentillesse et sa galanterie ; Marie ; Louise ; Mylan ; Florian ; Léa ; Aurélia et tous ceux que j’ai oublié de mentionner.

Merci à vous tous de m’avoir permis d’aller jusqu’au bout de cette aventure.

Pour finir, j’adresse un grand merci à tous mes proches, amis et famille. Merci à ma maman et à Pierre pour leur présence et pour m’avoir toujours soutenu ; à mon père que j’ai peu connu mais à qui je pense souvent et à mon frère pour s’intéresser à ce que je fais même s’il n’y comprend pas grand-chose ; aux schlass DJA, MR et Cecilix pour m’avoir encouragé et conseillé ; à Lisa, Marie, Alizée, Marion et Amande pour m’avoir permis de me vider la tête de temps en temps et enfin un merci tout particulier à Jeremy pour m’avoir supporté durant ces trois années mais surtout pour m’avoir toujours écouté, encouragé et soutenu (<3).

Résumé

Le stress oxydant est associé à de nombreuses pathologies humaines telles que les maladies neurodégénératives. Les nitrones sont des antioxydants capables de protéger les cellules contre les dommages induits par un stress oxydant. Elles sont aussi capables de réagir avec les radicaux libres pour former un adduit de spin nitroxyde persistant et détectable en spectroscopie par résonance paramagnétique électronique (RPE). Elles ont été ainsi très largement utilisées comme sondes analytiques afin d'étudier les processus radicalaires se produisant dans des environnements biochimiques. Dans ce travail de thèse, nous nous sommes intéressés à l'α-phenyl-*N*-tert-butyl nitrone (PBN), une nitrone linéaire possédant de bonnes propriétés de piégeage ainsi qu'une activité protectrice dans des modèles animaux de maladies neurodégénératives. Le but de ce travail était d'étudier l'impact de la nature, de la position et du nombre de substituants de part et d'autre de la fonction nitronyle (cycle phényle et partie *N*-*tert*-butyle) sur les propriétés de la nitrone et d'améliorer son activité. Différentes séries de nitrones de type PBN ont ainsi été synthétisées et leur capacité de piégeage du radical hydroxyméthyle ($^{\bullet}CH_2OH$) ainsi que leurs propriétés électrochimiques et de neuroprotection ont été évaluées. Il ressort de cette étude que l'introduction d'un groupement électroattracteur en position *para* du cycle phényle ou sur la partie *N*-*tert*-butyle améliore les capacités de piégeage du radical nucléophile $^{\bullet}CH_2OH$. Au contraire, la fonctionnalisation de la PBN avec un substituant électrodonneur a tendance à diminuer sa capacité de piégeage. Lorsque des substituants sont introduits à la fois en *para* du cycle et sur la fonction *N*-*tert*-butyle, les effets vont dans le même sens sans pour autant s'additionner complètement. En revanche, l'influence des substituants sur la neuroprotection des nitrones n'a pu être identifiée. Finalement, des nitrones avec des activités de piégeage de radicaux et/ou de neuroprotection prometteuses ont été identifiées.

Mots clés : nitrones, stress oxydant, piégeage de radicaux, spectroscopie par résonance paramagnétique électronique (RPE), électrochimie, antioxydant, neuroprotection

Abstract

Oxidative stress is associated with many human pathologies such as neurodegenerative diseases. Nitrones are antioxidants able to protect the cells against oxidative stress-induced damage in *in vitro* and *in vivo* models. They are also able to react with free radicals to form a persistent nitroxide spin adduct, detectable by electron paramagnetic resonance (EPR) spectroscopy. They have thus been widely used as analytical probes to study the radical processes occurring in biochemical environments. In this thesis work, we focused on the α-phenyl-*N*-tert-butyl nitrone (PBN), a linear nitrone with good spin-trapping properties as well as protective activity in animal models of neurodegenerative diseases. The aim of this work was to study the impact of the nature, the position and the number of substituents on both sides of the nitronyl function (phenyl ring and *N*-*tert*-butyl part) on the properties of the nitrone and to improve its activity. Different series of PBN-type nitrones were thus synthesized and their spin-trapping ability towards hydroxymethyl radical ($^{\bullet}CH_2OH$), as well as their electrochemical and neuroprotective properties were evaluated. It emerges from this study that the introduction of an electron-withdrawing group in the *para* position of the phenyl ring or in the *N*-*tert*-butyl part improves the trapping capacities of the nucleophilic radical $^{\bullet}CH_2OH$. In contrast, the functionalization of PBN with an electron-donating substituent tends to decrease its spin-trapping ability. When substituents are introduced both in the *para* position of the phenyl ring and in the *N*-*tert*-butyl function, the effects go in the same direction without completely adding up. In contrast, the influence of substituents on the neuroprotection of nitrones could not be identified. Finally, nitrones with promising trapping and/or neuroprotective activities were identified.

Keywords: nitrones, oxidative stress, spin-trapping, electron paramagnetic resonance (EPR) spectroscopy, electrochemistry, antioxidant, neuroprotection

Table des matières

Liste des abréviations et acronymes

Ac: acetyl

ACN: acetonitrile

ATP: adenosine triphosphate

DCM: dichloromethane

DFT: density functional theory

DMD: dimethyldioxirane

DMPO: 5,5-dimethyl-1-pyrroline *N*-oxide

DMSO: dimethyl sulfoxide

DNA: deoxyribonucleic acid

DTPA: diethylenetriaminepentaacetic acid

EPPN: *N*-benzylidene-1-ethoxycarbonyl-1-methylethylamine *N*-oxide

EPR: electron paramagnetic resonance

Equiv: equivalent

ESI+: positive electrospray ionization

GC: glassy carbon

Hfsc: hyperfine splitting constant

HOMO: highest occupied molecular orbital

HPLC: high pressure liquid chromatography

HR-MS: high resolution mass spectrometry

IP: ionization potential

MCPBA: *m*-chloroperbenzoic acid

Me: methyl

Mp: melting point

MTO: methyltrioxorhenium

MTT: 3-(4,5-dimethylthiazol-2-yl)-2,5-diphenyltetrazolium bromide

NBO: natural bond orbital

NMR: nuclear magnetic resonance

NPA: natural population analysis

NXY-059: disodium [(*tert*-butylimino)methyl]-benzene-1,3-disulfonate *N*-oxide

PBN: α-phenyl-*N*-tert-butyl nitrone

pH: hydrogen potential

Ph: phenyl

PPN: *N*-benzylidene-1-diethoxyphosphoryl-1-methylethylamine *N*-oxide

R_f: retardation factor

RNS: reactive nitrogen species

ROS: reactive oxygen species

RSS: reactive sulfur species

Rt: room temperature

TBAP: *tetra*-butylammonium perchlorate

***t*Bu**: *tert*-butyl

THF: tetrahydrofuran

TLC: thin-layer chromatography

TN: 1,3,5-tri[(*N*-(1-diethylphosphono)-1-methylethyl) *N*-oxy-aldimine] benzene

TOF: time-of-flight analyzer

UHP: urea-hydrogen peroxide

UV: ultraviolet

Introduction générale

Introduction générale

Table des matières

1. Avant-propos

Nous avons fait le choix de rédiger ce manuscrit en anglais, sous forme de thèse d'articles. Le manuscrit commence par une introduction générale en français comprenant une mise en contexte et une présentation générale du projet de thèse et de ses objectifs, une description des différentes collaborations et techniques qui ont permis de mener à bien ce projet ainsi qu'une présentation des différents chapitres de thèse. Un chapitre d'introduction bibliographique en anglais est ensuite présenté afin de mieux comprendre le positionnement de ce projet de thèse dans le contexte scientifique et fera par la suite l'objet d'une revue. Les travaux obtenus au cours de ces trois années de thèse sont ensuite décrits dans trois chapitres, chacun correspondant à un article publié ou prêt à l'être. Ainsi, le deuxième chapitre a été publié dans *New Journal of Chemistry* et le troisième et le quatrième chapitres sont en cours de finalisation pour être prochainement soumis dans des revues à comité de lecture. Ce manuscrit de thèse se conclut par une analyse et une discussion globale des résultats en français présentant également différentes perspectives envisagées.

2. Les espèces réactives de l'oxygène (ERO) et de l'azote (ERA) et leur régulation par les défenses antioxydantes

Les espèces réactives de l'oxygène (ERO) et de l'azote (ERA) sont de petites molécules très importantes, qui participent à la signalisation cellulaire dans les systèmes biologiques.[1,2] Elles peuvent être radicalaires ou non, sous forme ionique ou neutre. Ce sont des sous-produits naturels du métabolisme du dioxygène, formés en particulier au cours du processus de respiration cellulaire se déroulant dans la membrane mitochondriale interne.[3] Ce processus permet de produire l'énergie nécessaire aux cellules (sous forme d'ATP) par l'intermédiaire de chaînes de transport d'électrons. Lors du métabolisme normal, le dioxygène est réduit en eau par capture de quatre électrons et donne naissance à des intermédiaires beaucoup plus réactifs que lui-même : les ERO, comme résumé dans le Schéma 1.[4] Ainsi, environ 2% du dioxygène consommé dans les mitochondries est transformé en radical superoxyde $O_2^{\bullet-}$ lors de la première réduction électronique du dioxygène. Le radical superoxyde est très réactif et réagit rapidement avec d'autres espèces, conduisant à la production de radicaux hautement toxiques. La superoxyde dismutase catalyse la dismutation du radical superoxyde en dioxygène et peroxyde d'hydrogène H_2O_2, permettant ainsi l'élimination du radical

superoxyde mais la production de H_2O_2, un oxydant puissant. Le H_2O_2 ainsi formé peut réagir avec des cations métalliques comme Fe^{2+} et Cu^{+} présents dans les cellules et donner naissance par une réaction de Fenton à l'espèce radicalaire la plus délétère : le radical hydroxyle $HO^{\bullet}$.[5] D'autres ERO sont également présentes dans les cellules telles que les radicaux peroxyles ($RO_2^{\bullet}$), les hydroperoxydes (RO_2H) ainsi que les radicaux alkoxyles ($RO^{\bullet}$). Les ERO peuvent aussi être produites par des facteurs exogènes tels que les radiations UV, les rayonnements ionisants et les toxiques environnementaux. Les ERA, quant à elles, proviennent de réactions avec le monoxyde d'azote ($NO^{\bullet}$), produit dans le corps humain par les NO synthases (NOS).[6] On peut citer l'anion peroxynitrite (ONO_2^{-}), un oxydant puissant des tissus biologiques, qui peut se décomposer en radical hydroxyle et en radical nitro ($NO_2^{\bullet}$).[7]

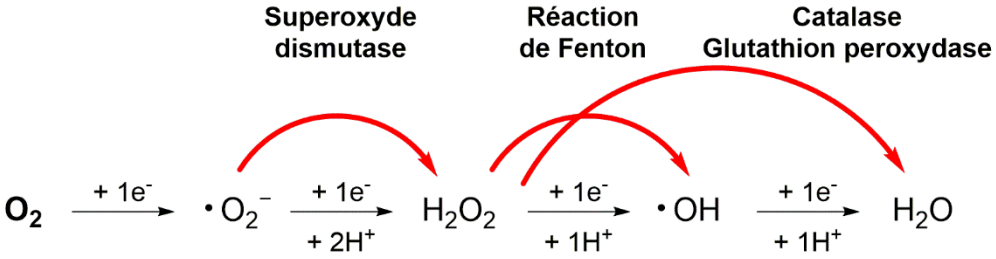

Schéma 1. Les quatre étapes de la réduction du dioxygène en eau, entraînant la formation d'ERO.

Les ERO et ERA interviennent dans la régulation d'une variété de fonctions physiologiques (la transduction de signal, les réponses mitogéniques et la défense contre les agents infectieux) et sont donc bénéfiques pour l'organisme mais, lorsque qu'elles sont présentes en trop forte concentration, elle deviennent toxiques et entraînent d'importants dommages cellulaires ; c'est ce que l'on appelle le paradoxe des ERO/ERA.[8] Pour se défendre contre ces espèces très réactives, l'organisme a développé des systèmes de défense très efficaces, les antioxydants, permettant la régulation du taux d'ERO/ERA dans les cellules par leur élimination. Par exemple, la production du superoxyde est régulée par la superoxyde dismutase, qui catalyse sa dismutation en H_2O_2. La quantité de H_2O_2 est elle-même régulée grâce à l'enzyme héminique catalase qui accélère sa dismutation et à la glutathion peroxydase qui catalyse sa réduction par le glutathion. Dans ces exemples, les antioxydants sont des enzymes produites par les cellules. Des systèmes antioxydants non enzymatiques sont également présents dans l'organisme tels que le glutathion, l'acide urique, la mélanine, la mélatonine et l'acide lipoïque. A ces antioxydants endogènes s'ajoutent des substances

exogènes apportées par l'alimentation regroupant les micronutriments comme les vitamines (E ou C), les polyphénols, les caroténoïdes et certains métaux tels que le zinc et le sélénium.[9]

3. Le stress oxydant et les maladies neurodégénératives

En absence de conditions pathologiques, la balance prooxydants/antioxydants est en équilibre. Lorsque cet équilibre est rompu, soit par une production excessive d'ERO/ERA, soit par une diminution des capacités antioxydantes, on parle de stress oxydant. Les ERO/ERA vont alors attaquer les constituants cellulaires et entraîner des dommages au niveau des lipides, des protéines et de l'ADN des cellules. Il a ainsi été démontré que le stress oxydant intervient dans de nombreuses pathologies telles que les maladies cardiovasculaires, certains cancers et les maladies neurodégénératives.[9]

Les maladies neurodégénératives représentent un enjeu sociétal important. Elles englobent plus de 600 pathologies dont les plus connues sont la maladie d'Alzheimer, la maladie de Parkinson et la maladie de Huntington. Ces maladies sont caractérisées par une neurodégénérescence, c'est-à-dire une situation pathologique affectant une population ciblée et délimitée de cellules nerveuses, jusqu'à la perte progressive de leurs structures et de leurs fonctions, entraînant des complications cognitives, motrices ou perceptives. Ces maladies touchent particulièrement les personnes âgées de plus de 65 ans, leur facteur de risque majeur étant le vieillissement. En 2014, plus d'un million de français ont été touchés par ces pathologies et le nombre de nouveaux cas recensés ne cesse d'augmenter d'année en année.[10] En région PACA, en 2015, près de 67 000 personnes étaient touchées par les maladies neurodégénératives, soit environ 1,3% de la population, dont une majorité de femmes. A l'horizon 2028, entre 1,6 et 2,0% de la population régionale pourrait être affectée par l'une de ces maladies ; cela représenterait une hausse de 25% par rapport à 2015, sous l'effet de l'évolution démographique.[11] Les multiples causes de ces maladies sont peu connues mais des avancées scientifiques montrent l'implication du stress oxydant dans les mécanismes du processus neurodégénératif et de la mort neuronale.[9] De plus, les médicaments qui existent actuellement ne permettent pas de soigner les maladies neurodégénératives, mais seulement de réduire les symptômes, sans empêcher leur apparition ou leur progression.[12] C'est pourquoi, en France et dans le monde, de nombreuses équipes de recherche s'intéressent de près aux causes de ces maladies et au développement de nouvelles stratégies thérapeutiques.

Dans cette perspective, le gouvernement français a créé en 2014 un plan maladies neurodégénératives (PMND) afin de lutter contre ces maladies, tout en prenant en compte les spécificités de chacune.[13]

4. Les nitrones, des composés piégeurs de radicaux libres et antioxydants

Afin de limiter les effets néfastes engendrés par le stress oxydant, les chercheurs travaillent depuis de nombreuses années sur l'élaboration d'antioxydants naturels ou synthétiques.[14] Ils étudient également les processus pathologiques liés au stress oxydant afin de mieux comprendre leurs mécanismes et les radicaux impliqués. De nouvelles molécules capables de piéger les radicaux libres d'origine biologique ont donc vues le jour, c'est le cas des nitrones. Les nitrones sont des molécules caractérisées par la présence d'une fonction $–C=N^{+}(O^{-})–$, comportant une double liaison carbone-azote et une liaison covalente entre l'azote et l'oxygène. Les nitrones possèdent différents sites réactifs (Figure 1) et sont largement utilisées comme intermédiaires réactionnels d'espèces bioactives.[15] Elles possèdent la même réactivité que les composés carbonylés, le carbone de la fonction nitronyle (carbone α) pouvant subir des attaques nucléophiles. Elles sont également capables d'agir comme dipôles 1,3 et donc de subir des cycloadditions 1,3-dipolaires avec des alcènes pour donner des isoxazolidines.[16] La charge négative portée par l'oxygène, peut donner lieu à des réactions de chélation sur des métaux.

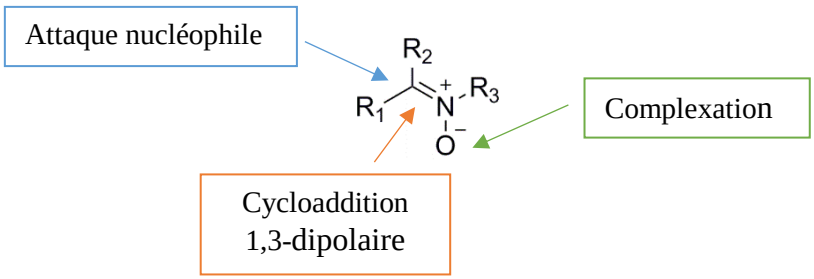

Figure 1. Les différents sites réactifs de la nitrone.

L'une des propriétés chimiques les plus remarquables des nitrones est leur capacité à piéger des radicaux libres. Le radical $R^{\bullet}$ vient s'additionner sur le carbone électrophile de la double liaison de la fonction nitronyle conduisant à la formation d'un adduit de spin de type

nitroxyde stable (voir Schéma 2), pouvant être détecté en spectroscopie par résonance paramagnétique électronique (RPE). Cette technique appelée spin-trapping a permis la détection et l'identification de radicaux libres très réactifs ayant des temps de demi-vie très courts et ne pouvant être directement détectés par RPE.[17] Les nitrones sont alors devenues un outil d'analyse populaire permettant une meilleure compréhension des processus radicalaires intervenant dans des pathologies liées au stress oxydant.[17,18] Les nitrones ont ensuite montré de nombreuses propriétés protectrices dans des modèles animaux tels que les maladies neurodégénératives, l'accident vasculaire cérébral (AVC) ischémique, les maladies cardiovasculaires, les pathologies oculaires ou encore certains cancers.[19]

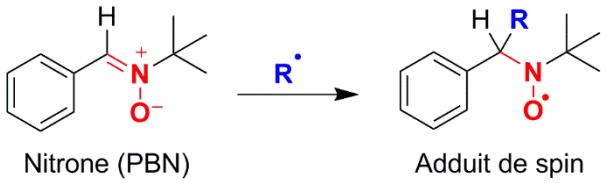

Schéma 2. Mécanisme de piégeage de radicaux par la PBN (spin-trapping).

Deux grandes familles de nitrones ont largement été étudiées : les nitrones cycliques dérivées de la 5,5-dimethyl-1-pyrroline *N*-oxide (DMPO) et les nitrones linéaires dérivées de l'α-phenyl-*N*-*tert*-butyl nitrone (PBN). Depuis de nombreuses années, plusieurs équipes de recherche ont travaillé sur la synthèse et l'étude de dérivés de la DMPO et de la PBN afin d'améliorer leurs propriétés de piégeage de radicaux libres et/ou leurs activités thérapeutiques. En général, les nitrones cycliques ont un meilleur taux de piégeage vis-à-vis des radicaux centrés sur l'oxygène et une meilleure stabilité des adduits de spin formés.[20] Les nitrones linéaires, quant à elles, ont des meilleures propriétés de piégeage envers les radicaux centrés sur le carbone. La PBN possède une lipophilie plus grande que la DMPO et a montré de meilleures propriétés de piégeage en milieu biologique, grâce à sa bonne distribution à travers les tissus et les cellules. Elle s'est également avérée plus efficace en tant qu'agent thérapeutique. Novelli *et al.* ont été les premiers à démontrer en 1986 une baisse de la mortalité de rats préalablement traités avec de la PBN et soumis à un choc septique.[21] Les recherches sur les effets protecteurs de la PBN se sont ensuite intensifiées et la PBN a montré d'excellentes propriétés neuroprotectrices dans des modèles d'ischémie cérébrale. Floyd *et al.* ont montré que la PBN possède des propriétés protectrices envers les dommages induits par un AVC ischémique chez la gerbille et cela même lorsqu'elle est administrée 1 h après la réperfusion.[22] Un dérivé de la PBN possédant deux groupements sulfonates sur le cycle

aromatique, la 2,4-disulfonyl-phenyl-*tert*-butylnitrone (NXY-059) a atteint la phase III des essais cliniques pour le traitement de l'AVC ischémique. Ces essais ont été conduits en deux parties, la première (SAINT-1) sur 1 700 patients et la deuxième (SAINT-2) sur 3 200 patients mais malheureusement ces essais n'ont pas montré une efficacité significative du composé NXY-059.[23,24] Le passage de NXY-059 en phase III des essais cliniques restera tout de même un fait marquant et encourageant dans le développement des nitrones. De nombreux dérivés de la PBN ont par la suite été synthétisés, les nitrones linéaires permettant une fonctionnalisation relativement aisée à la fois sur le cycle aromatique et sur la partie *N*-*tert*-butyle, donnant accès à une plus grande variété de dérivés. Les nitrones linéaires sont également plus facilement synthétisées et purifiées que leurs analogues cycliques ; étant souvent solides à température ambiante, elles peuvent être recristallisées, permettant ainsi d'obtenir des lots sans trace d'impuretés paramagnétiques, qui peuvent compliquer l'interprétation des spectres RPE.

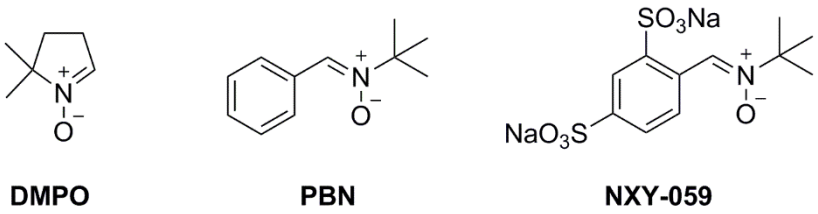

Figure 2. Structure chimique de la PBN, de la DMPO et de NXY-059.

5. Le projet de thèse et les différentes collaborations mises en place

C'est dans cette optique que depuis de nombreuses années, notre laboratoire travaille sur le développement de nitrones linéaires de type PBN comportant des modifications structurales variées. Notre laboratoire s'est en particulier intéressé à l'amélioration de la biodisponibilité de ces motifs nitrones en les greffant sur des transporteurs monomoléculaires amphiphiles, leur conférant ainsi une bonne solubilité dans l'eau ainsi qu'une lipophilie suffisante pour assurer un passage membranaire. Parallèlement, depuis une dizaine d'années, notre laboratoire a démarré une nouvelle approche qui vise à synthétiser un grand nombre de dérivés de la PBN comportant des modifications simples afin de réaliser une étude des relations structure-activité. L'objectif de cette approche est d'améliorer les propriétés intrinsèques de la fonction nitrone. Une fois que les propriétés et l'activité de la nitrone seront améliorées, un greffage sur un transporteur amphiphile pourra être envisagé.

Les travaux menés au cours de cette thèse ont consisté à poursuivre cette thématique de recherche en synthétisant des dérivés de la PBN possédant divers substituants et en étudiant l'impact de la nature, du nombre et de la position de ces substituants sur les propriétés de piégeage de radicaux libres et la capacité antioxydante de la nitrone. Pour cela nous nous sommes intéressés à l'introduction de substituants de part et d'autre de la fonction nitronyle (voir Figure 3) : soit sur la partie aromatique (en position *ortho*, *meta* ou *para*), soit sur la fonction *N*-*tert*-butyle (en position α ou β) et nous avons également combiné les modifications à la fois sur le cycle aromatique et sur la fonction *N*-*tert*-butyle afin d'étudier l'impact de l'addition des effets. L'objectif principal de la thèse est d'obtenir des dérivés ayant une activité de piégeage de radicaux libres ou de neuroprotection supérieure à la nitrone linéaire de référence, la PBN, et d'avoir une meilleure compréhension de l'influence de ces substituants sur la réactivité de la nitrone.

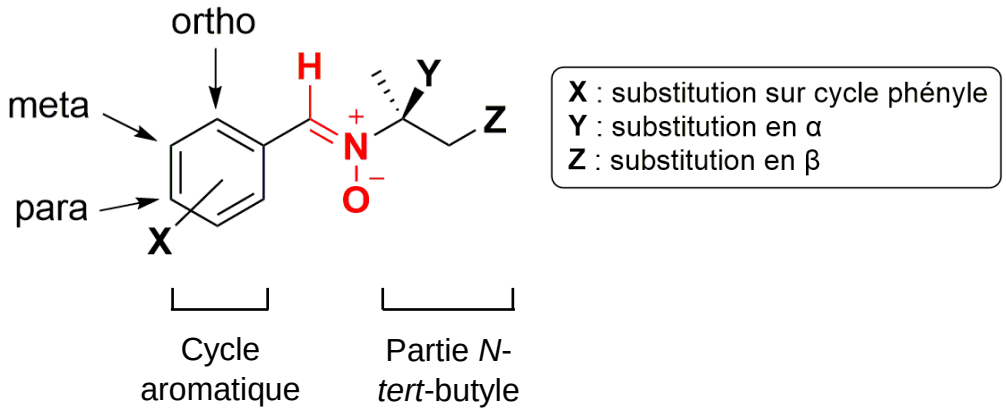

Figure 3. Modifications structurales envisagées sur la PBN.

Afin d'étudier l'impact des substituants sur les propriétés et la réactivité des différentes nitrones synthétisées au cours de cette thèse, nous avons utilisé plusieurs outils d'étude. Nous avons étudié à la fois leurs propriétés de piégeage de radicaux libres et leur capacité antioxydante, afin de déterminer quelles étaient les nitrones les plus efficaces et de mettre en évidence (ou non) un lien entre les deux activités.

La capacité des dérivés à piéger le radical hydroxymethyl ($^{\bullet}CH_2OH$) a été évaluée par RPE en déterminant la vitesse de piégeage de chaque dérivé par rapport à la PBN. Le radical $^{\bullet}CH_2OH$ est un radical centré sur le carbone, qui constitue un bon modèle d'étude puisqu'il peut être généré en milieu biologique en situation de stress oxydant. De plus, il est produit facilement par une réaction de Fenton dans le méthanol, un solvant pouvant solubiliser toutes les

nitrones. Ce travail a été réalisé en collaboration avec le docteur Béatrice Tuccio (ICR, UMR 7273, Aix-Marseille Université) et certaines manipulations ont pu être réalisées directement dans notre laboratoire grâce au spectromètre Bruker EMX Plus acquis récemment.

Afin d'étudier les propriétés antioxydantes des nitrones, nous avons tout d'abord analysé leur comportement électrochimique par voltampérométrie cyclique. Ce travail a été effectué grâce à une collaboration avec les professeurs Karine Reybier et Paul-Louis Fabre (Pharma-Dev, UMR 152, Université Paul Sabatier – Toulouse III). Les nitrones sont à la fois capables d'être réduites en radical anion et oxydées en radical cation. La connaissance de leurs potentiels de réduction et d'oxydation, des données caractéristiques des dérivés, permet donc d'avoir une meilleure compréhension de leur activité antioxydante. Le caractère neuroprotecteur des nitrones après induction d'un stress oxydant a également été évalué *in vitro* sur deux modèles d'étude. La première étude a été réalisée par le professeur Michel Vignes (IBMM, UMR 5247, Université de Montpellier) et porte sur des cellules gliales intoxiquées à l'hydroperoxyde de *tert*-butyle. La deuxième étude a été réalisée par la société Neuro-Sys (Gardanne), partenaire de cette thèse et spécialisée dans les modèles *in vitro* de maladies neurodégénératives. Neuro-Sys a étudié l'effet neuroprotecteur des dérivés synthétisés sur des neurones corticaux primaires après une intoxication au glutamate. Les deux modèles d'étude utilisés donnent une idée de la protection des nitrones vis-à-vis des maladies neurodégénératives et sont complémentaires, puisque les cultures de neurones contiennent des cellules gliales (20-30%). Nous avons également étudié le lien entre les propriétés électrochimiques des nitrones et leur activité neuroprotectrice.

Une collaboration avec le professeur Patrick Trouillas (INSERM, U1248 IPPRITT, Université de Limoges) nous a également permis d'obtenir des données théoriques par modélisation moléculaire (charges atomiques partielles, potentiels d'ionisation) sur les nitrones synthétisées. L'acquisition de ces données nous a permis de mieux comprendre l'influence de la nature, de la position et du nombre de substituants sur les répartitions de charge au niveau de la fonction nitronyle, et également de mettre en évidence des corrélations entre ces paramètres théoriques et les paramètres expérimentaux déterminés.

6. La spectroscopie par Résonance Paramagnétique Electronique (RPE) et l'étude de la capacité à piéger les radicaux libres

Principe de la RPE. La RPE est la seule technique spectroscopique permettant la détection d'espèces chimiques paramagnétiques, possédant un ou plusieurs électrons célibataires, tels que les radicaux libres ou certains sels et complexes de métaux de transition. Le premier développement de la RPE a été effectué en 1944 par un physicien russe Y. Zavoisky à Kazan (URSS) lors de l'étude de cristaux paramagnétiques de $CuCl_2.2H_2O$. La RPE partage les mêmes concepts que la spectroscopie RMN, la grande différence provenant d'un moment magnétique plus grand des spins électroniques (rapport de 600 / à celui du proton), rendant la RPE plus sensible que la RMN. La RPE, de par son nom, désigne la capacité de certains électrons à absorber, puis réémettre l'énergie d'un rayonnement électromagnétique lorsqu'ils sont placés dans un champ magnétique. Seuls les électrons non appariés présentent cette propriété. La RPE permet donc de mettre en évidence spécifiquement la présence d'espèces paramagnétiques dans des solides, des liquides et des gaz et de déterminer leur environnement.

Le principe de la RPE repose sur l'effet Zeeman : sous l'action d'un champ magnétique extérieur, l'électron caractérisé par le nombre quantique S = 1/2 se sépare en 2 états de spin d'énergies différentes (2S+1), chacun caractérisé par un nombre quantique de spin m_s = -1/2 et m_s = +1/2 et correspondant à une orientation dans l'espace différente (parallèle ou antiparallèle au champ magnétique). On dit que le champ appliqué lève la dégénérescence entre les deux états de spin (Figure 4). Cette séparation des niveaux est d'autant plus grande que la valeur du champ magnétique (B_0) est intense.

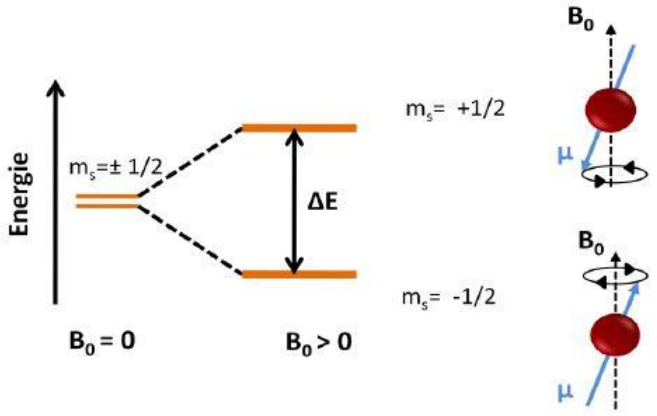

Figure 4. Représentation schématique de la levée de la dégénérescence.

La répartition des électrons suit la distribution de Boltzmann selon laquelle le niveau énergétique inférieur (*i.e.* parallèle au champ) est légèrement plus peuplé que le niveau supérieur. Lorsqu'une radiofréquence appartenant à la gamme des micro-ondes est appliquée et correspond à la différence d'énergie entre les deux niveaux, une transition des électrons entre ces deux niveaux est induite ; c'est le phénomène de résonance. Le système est alors hors équilibre et les processus de relaxation le font revenir à l'état fondamental. Pour que la transition se produise, le champ magnétique appliqué doit posséder une intensité bien spécifique, de sorte que l'écart d'énergie entre les deux niveaux corresponde à la fréquence micro-onde appliquée. Pour atteindre cette condition, on fait varier progressivement le champ magnétique de l'aimant externe tout en exposant l'échantillon à une fréquence fixe. Lorsque le champ magnétique et la fréquence appliquée permettent de faire transiter les électrons entre les deux niveaux d'énergie, on parle alors de condition de résonance. Les spectres enregistrés présentent donc l'absorbance ou sa dérivée en ordonnée et le champ magnétique en abscisse, exprimé en Gauss. A la différence de la RMN, on enregistre la dérivée première de la courbe d'absorption afin d'obtenir une plus grande sensibilité et une meilleure résolution.

Chaque spectre RPE enregistré permet d'identifier des paramètres caractéristiques du radical étudié. Le facteur g (facteur de Landé) traduit l'intensité du couplage entre le moment cinétique orbitalaire et le moment cinétique de spin du radical libre. Cette interaction dépend de l'environnement électronique du radical. Le facteur g varie peu d'un radical à l'autre, excepté pour les sels métalliques, mais sa valeur est typique du radical étudié et peut être associée au déplacement chimique (δ) en RMN. Pour les radicaux centrés sur le carbone, la valeur du facteur g est très proche de celle de l'électron libre (g = 2,0036). Lorsqu'un électron se trouve au voisinage d'un atome de spin nucléaire non nul, il y a interaction entre les moments magnétiques de l'électron et des noyaux environnants ; c'est l'interaction hyperfine. Elle se manifeste par l'éclatement des raies RPE en 2nI+1 raies avec n : le nombre de noyau équivalent et I : la valeur du spin nucléaire du noyau. On peut alors mesurer les constantes hyperfines de couplage des atomes (symbole a, exprimées en G, mT ou MHz) entre les différentes raies des spectres, qui correspondent aux constantes de couplage en RMN.

Principe de la technique du spin-trapping. Les radicaux libres ont des durées de vie souvent trop courtes pour être détectés par RPE conventionnelle. On peut alors utiliser la méthode indirecte appelée spin-trapping ou piégeage de spin. Il s'agit d'utiliser une molécule

diamagnétique, le piège (P), qui réagit avec le radical libre $R^{\bullet}$ pour conduire à un adduit de spin paramagnétique $(PR)^{\bullet}$ plus stable et ayant une durée de vie suffisante pour être détecté par RPE. A partir du spectre obtenu, on peut en déduire des renseignements sur le radical piégé (voir Schéma 3). Pour être un bon piégeur de radicaux, la molécule utilisée doit être stable chimiquement dans les conditions expérimentales, réagir spécifiquement avec le radical étudié et avoir un taux de piégeage assez élevé. Il faut également que l'adduit de spin formé soit suffisamment stable pour être observé. De plus, si on veut utiliser le piège en milieu biologique, celui-ci ne doit pas être cytotoxique, doit être soluble dans l'eau, stable et non dégradable en milieu biologique : il ne doit pas former par décomposition des espèces paramagnétiques pouvant compliquer l'interprétation des spectres RPE de l'adduit $(PR)^{\bullet}$. Il existe deux grandes classes de molécules pièges : les nitroso (R-N=O) et les nitrones (R^1-$N^+(O^-)$=C-R^2), les deux conduisant après piégeage du radical à un adduit de spin nitroxyde. Les nitroso ont d'énormes inconvénients (cytotoxicité, photosensibilité) empêchant leur utilisation en milieu biologique et leurs adduits de spin de radicaux centrés sur l'oxygène ne sont pas persistants. Les nitrones, quant à elles, ne présentent pas ces inconvénients.

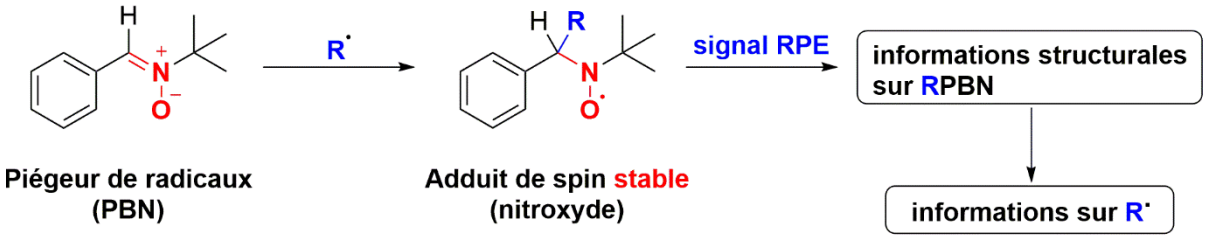

Schéma 3. Schéma du principe du spin-trapping.

Interprétation du spectre RPE. Les spectres RPE de tous les nitroxydes présentent au moins 3 raies dues à l'interaction hyperfine entre l'électron célibataire et le noyau de l'azote de spin 1 (2nI+1 = 2×1×1+1 = 3). Ce signal typique des adduits nitroxydes peut être démultiplié par les interactions hyperfines avec d'autres noyaux paramagnétiques en position β, et plus rarement γ, du centre radicalaire. Dans le cas de la nitrone linéaire PBN, un couplage hyperfin avec le proton situé en position β du centre radicalaire est également observé, ce qui entraîne le dédoublement des raies. On observe alors deux couplages hyperfins donnant lieu à deux valeurs de constantes : a_N et a_H. Les spectres expérimentaux sont simulés en utilisant des logiciels spécifiques comme par exemple WINSIM qui est disponible gratuitement

(http://www.niehs.nih.gov/research/resources/software/tox-pharm/tools/). A partir du spectre simulé, les constantes hyperfines de couplage sont déterminées.

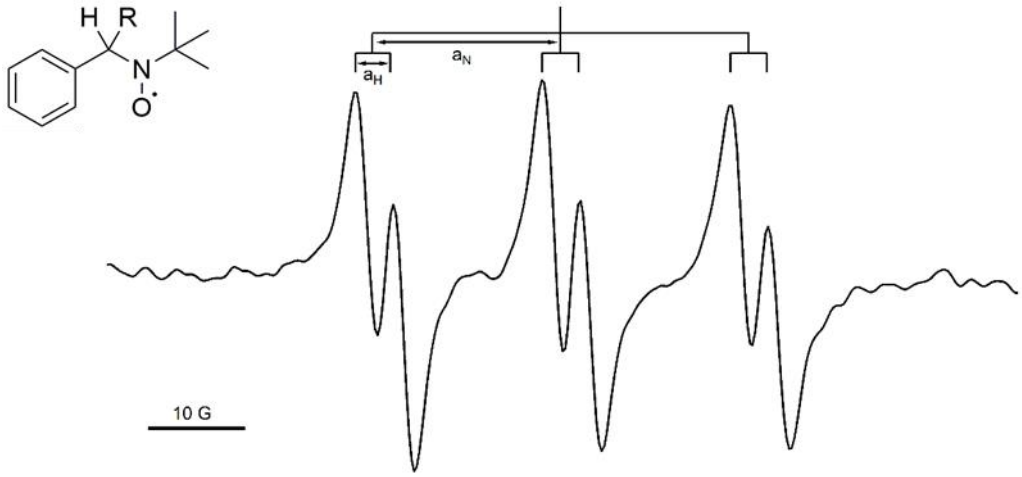

Figure 5. Spectre RPE de l'adduit de spin PBN-R obtenu après le piégeage du radical R$^{\bullet}$ par la PBN.

Cinétiques de piégeage. Dans le but d'étudier les propriétés de piégeage du radical R$^{\bullet}$ des différentes nitrones N synthétisées, la méthode de compétition cinétique développée par Janzen *et al.* a été employée, en utilisant la poly-nitrone 1,3,5-tri[(*N*-(1-diethylphosphono)-1-methylethyl) *N*-oxy-aldimine] benzene notée TN comme piégeur compétitif (Figure 6).[25] Il a été démontré que la TN ne piège qu'un seul radical malgré ses trois fonctions nitronyles.

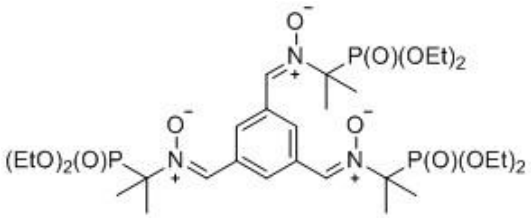

Figure 6. Structure chimique de la TN, utilisée comme piégeur compétitif.

Pour évaluer le taux de piégeage d'une nitrone N, on solubilise N en présence de TN et on génère le radical R$^{\bullet}$ souhaité *in situ*. L'expérience est suivie par RPE et on observe deux signaux différents : celui correspondant à l'adduit N-R et celui de l'adduit TN-R (Figure 7). TN possédant un atome de phosphore de spin nucléaire non nul, un couplage supplémentaire est observé et les raies sont dédoublées. On regarde ainsi les signaux RPE obtenus à un temps t = 2 min, correspondant à une vitesse de piégeage de la nitrone initiale ; nous permettant ainsi

de nous affranchir de la cinétique de dégradation de l'adduit de spin formé. En supposant que la concentration en radical $R^{\bullet}$ est constante en début de réaction, le modèle cinétique peut être décrit par les équations (1) à (4) (Schéma 4), dans lesquelles k_N et k_{TN} représentent les constantes de vitesse de piégeage du radical $R^{\bullet}$ par la nitrone N étudiée et la TN, respectivement. *R* et *r* représentent le taux de piégeage à la fois par N et TN, et par TN seulement. Alors l'équation (5) est obtenue en divisant l'équation (3) par l'équation (4). Le taux de piégeage de la nitrone N étudiée est déterminé en mesurant l'intensité des signaux N-R+TN-R (*R*) et TN-R (*r*) pour différents rapports de concentrations [N]/[TN]. En traçant le rapport *R*/*r* en fonction de [N]/[TN] une droite est obtenu et le coefficient directeur est égal au rapport k_N/k_{TN}. En réalisant la même expérience en remplaçant la nitrone N par la PBN, le rapport k_{PBN}/k_{TN} est déterminé, nous permettant d'en déduire la constante de vitesse de piégeage relative k_N/k_{PBN} de la nitrone N étudiée par rapport à la PBN.

$$R^{\bullet} + N \xrightarrow{k_N} N\text{-}R \qquad (1)$$

$$R^{\bullet} + TN \xrightarrow{k_{TN}} TN\text{-}R \qquad (2)$$

$$R = k_{TN}\,[TN][R^{\bullet}] + k_N\,[N][R^{\bullet}] \qquad (3)$$

$$r = k_{TN}\,[TN][R^{\bullet}] \qquad (4)$$

$$\frac{R}{r} = 1 + \frac{k_N}{k_{TN}}\,\frac{[N]}{[TN]} \qquad (5)$$

Schéma 4. Modèle cinétique de la compétition entre la nitrone N étudiée et la TN pour le piégeage du radical $R^{\bullet}$.

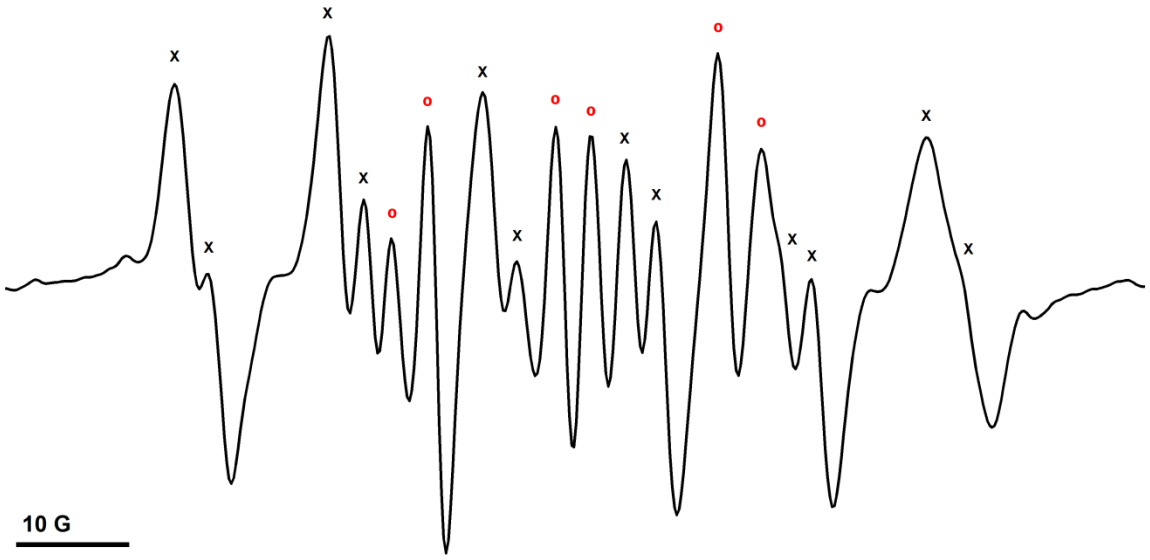

Figure 7. Signaux RPE des adduits TN-CH_2OH et N-CH_2OH obtenus après piégeage du radical $^{\bullet}CH_2OH$ par la TN et la nitrone N, respectivement, avec un ratio [N]/[TN] = 2. Les pics marqués d'une croix (×) correspondent à l'adduit TN-CH_2OH tandis que ceux marqués d'un rond rouge (○) correspondent à l'adduit N-CH_2OH.

7. La voltampérométrie cyclique et la mesure des potentiels redox

Principe de la voltampérométrie cyclique. La voltampérométrie cyclique est l'une des techniques les plus utilisées pour obtenir des informations qualitatives sur les réactions électrochimiques, permettant une caractérisation simple et rapide d'un système électrochimique. Ce n'est par contre pas une technique appropriée pour des analyses quantitatives. Le principe consiste à appliquer un potentiel contrôlé au système redox et à mesurer la réponse du courant. Ce courant est la somme d'un courant capacitif, dû à la charge de l'électrode et d'un courant faradique, qui résulte d'un transfert depuis/vers l'électrode d'électrons impliqués dans des réactions d'oxydo-réduction. Au cours d'une expérience de voltampérométrie cyclique, on explore une fenêtre de potentiels, en balayant le potentiel d'électrode linéairement avec le temps entre deux limites, appelées « potentiels d'inversion ». Le premier balayage appelé « aller » s'effectue à partir du potentiel de départ puis, lorsque la première limite est atteinte, le sens du balayage change pour revenir au potentiel de départ, c'est le balayage « retour ». Ce cycle peut être répété et la vitesse de balayage peut varier.

Tracé et interprétation d'un voltammogramme cyclique. Afin de mesurer les potentiels d'oxydo-réduction, les nitrones (analytes), qui sont des espèces électroactives, sont dissoutes en solution. Un électrolyte, comme le *tétra*-butylammonium perchlorate (TBAP), est ajouté afin de fournir des ions et d'assurer une conductivité suffisante. Un dispositif à trois électrodes est utilisé :

- Une électrode de travail (disque de carbone vitreux), auprès de laquelle la réaction d'intérêt a lieu, le potentiel de l'électrode de travail variant linéairement avec le temps ;
- Une électrode de référence (fil d'argent), qui maintient un potentiel constant et précis ;
- Une électrode auxiliaire ou contre-électrode (fil de platine), qui conduit l'électricité de la source du signal vers l'électrode de travail.

Le potentiel est mesuré entre l'électrode de référence et l'électrode de travail et le courant entre l'électrode de travail et l'électrode auxiliaire. Un système de voltampérométrie cyclique se compose d'une cellule d'électrolyse, d'un potentiostat, d'un convertisseur courant-potentiel, et d'un système d'acquisition de données. Ce dernier permet le tracé du voltammogramme cyclique : évolution du courant (I) qui traverse le système électrochimique en fonction du potentiel appliqué (E). La Figure 8 représente l'allure générale d'un voltammogramme cyclique. En l'absence de réaction chimique, seulement un courant capacitif est observé. Dès qu'une réaction chimique se déroule à la surface de l'électrode, le courant augmente.

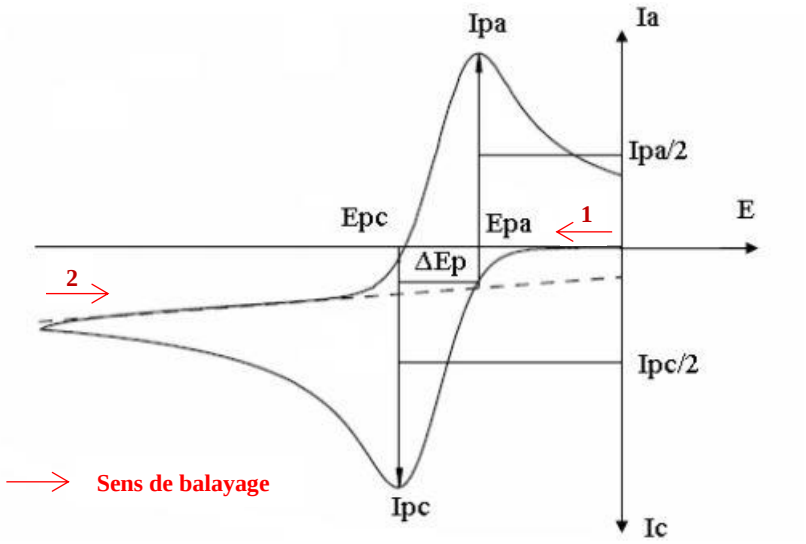

Figure 8. Allure générale d'un voltammogramme cyclique.

En balayant les potentiels, on observe une augmentation du courant vers les intensités négatives lorsque le potentiel de réduction (potentiel cathodique) est atteint. Le courant passe par un maximum avant d'atteindre un palier. Cette forme particulière s'explique par l'évolution de la concentration en analyte près de la surface de l'électrode. Dans le cas d'une réaction réversible, après inversion du sens du balayage, le potentiel atteint une valeur où le produit de réduction formé se réoxyde, et un courant de signe opposé est observé. Si les deux signaux observés sont symétriques, le produit de la réduction est stable pendant le temps de la mesure ; on parle alors d'un système réversible. Par contre, si le produit de la réduction se décompose avant le retour du balayage de potentiel, il n'y a pas de pic retour ; on parle alors d'un système irréversible. Le même phénomène lié à l'oxydation de l'analyte est également observé. Si l'analyte peut atteindre plusieurs degrés de réduction ou d'oxydation, le voltammogramme cyclique présente plusieurs pics successifs. A partir d'un voltammogramme cyclique, plusieurs informations peuvent être déterminées : le courant du pic cathodique $I_p(c)$ et anodique $I_p(a)$, le potentiel du pic cathodique $E_p(c)$ et anodique $E_p(a)$ et la différence entre le potentiel cathodique et anodique ΔEp.
Si le transfert électronique à la surface est rapide et que le courant est limité par la diffusion des espèces vers la surface de l'électrode, l'intensité du pic de courant est directement proportionnelle à la racine carrée de la vitesse de balayage. On obtient alors un signal symétrique et le potentiel redox de l'analyte est égal à la moyenne des potentiels de réduction et d'oxydation. En revanche, si l'analyte étudié est adsorbé sur la surface de l'électrode, l'intensité du pic de courant est proportionnelle à la vitesse de balayage.

Application aux nitrones. Les nitrones sont à la fois capables d'être réduites et oxydées, elles possèdent donc deux potentiels : un potentiel de réduction $E_p(c)$ et un potentiel d'oxydation $E_p(a)$. Afin d'étudier leur comportement électrochimique, nous avons fait varier le potentiel en partant de 0 V jusqu'à -3 V puis de -3 V à 2,5 V pour enfin revenir à 0 V. Un seul cycle est réalisé à une vitesse de balayage de 0,1 V/s. Le potentiel de réduction de la fonction nitronyle est observé entre -1,7 et -2,6 V et le potentiel d'oxydation entre 1,1 et 1,9 V ; les pics n'étant en général pas réversibles. Afin de connaître le nombre d'électrons impliqués dans les réactions d'oxydo-réduction, qui est directement proportionnel à l'intensité du courant, une calibration au ferrocène $(FeC_5H_5)_2$ est effectuée. On étudie pour cela l'oxydation d'une solution de ferrocène à 115 mM dans l'ACN et contenant du TBAP par voltampérométrie cyclique (Figure 9). On mesure alors l'intensité du courant anodique dû à

l'oxydation du ferrocène : I = 16 µA dans les conditions expérimentales utilisées et pour une vitesse de balayage de 0.1 V/s. Sachant que cette réaction implique un électron, on obtient la valeur d'intensité correspondant à un électron. Par conséquent, en mesurant les intensités des courants cathodique et anodique des nitrones étudiées et en les comparant avec la valeur du ferrocène, on peut en déduire le nombre d'électrons impliqués dans la réduction et l'oxydation de la fonction nitronyle.

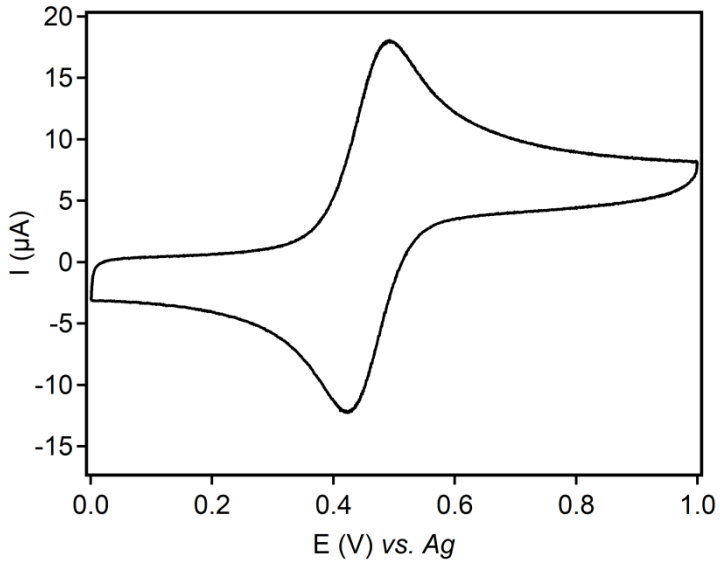

Figure 9. Voltammogramme cyclique de l'oxydation du ferrocène dans l'ACN contenant 0,1 M de TBAP à une vitesse de balayage de 0,1 V/s vs. Ag.

A titre d'exemple, la réduction de la PBN dans l'acétonitrile se fait de manière irréversible en une seule étape à un potentiel $E_p(c)$ = -2,12 V et fait intervenir deux électrons ($I_p(c)$ = 34 µA). Ce transfert d'électrons peut être représenté par un schéma ECEC avec E désignant une réaction électrochimique lente et C une réaction chimique rapide, empêchant l'observation d'un pic retour.

$$\text{E: } \text{Ar-CH=N}^{+}(\text{O}^{-})\text{-R} + \text{e}^{-} \rightarrow \text{Ar-C}^{-}\text{(H)-N(O}^{\bullet}\text{)-R} \qquad (6)$$

$$\text{C: } \text{Ar-C}^{-}\text{(H)-N(O}^{\bullet}\text{)-R} + \text{H}^{+} \rightarrow \text{Ar-CH}_2\text{-N(O}^{\bullet}\text{)-R} \qquad (7)$$

$$\text{E: } \text{Ar-CH}_2\text{-N(O}^{\bullet}\text{)-R} + \text{e}^{-} \rightarrow \text{Ar-CH}_2\text{-N(O}^{-}\text{)-R} \qquad (8)$$

$$\text{C: } \text{Ar-CH}_2\text{-N(O}^{-}\text{)-R} + \text{H}^{+} \rightarrow \text{Ar-CH}_2\text{-N(OH)-R} \qquad (9)$$

Schéma 5. Schéma ECEC du transfert d'électrons décrivant la réduction d'une nitrone de type PBN dans l'ACN.

L'oxydation de la PBN n'implique quant à elle qu'un seul électron (I_p(a) = 15 µA). Elle est également irréversible et a lieu à un potentiel E_p(a) = 1,60 V (Figure 10). On peut également noter la présence d'un très faible pic d'oxydation à -1,79 V ainsi que l'apparition de pics de réduction à ≈ 0,5 V et ≈ 0,1 V lors du balayage retour. Ces pics de réduction sont attribués aux intermédiaires du processus d'oxydation.[26]

$$\text{E: } \text{Ar-CH=N}^{+}(\text{O}^{-})\text{-R} \rightarrow \text{Ar-C}^{+}\text{(H)-N(O}^{\bullet}\text{)-R} + \text{e}^{-} \quad (10)$$

$$\text{C: } \text{Ar-C}^{+}\text{(H)-N(O}^{\bullet}\text{)-R} + \text{H}_2\text{O} \rightarrow \text{Ar-CHOH-N(O}^{\bullet}\text{)-R} + \text{H}^{+} \quad (11)$$

$$\text{C: } \text{Ar-CHOH-N(O}^{\bullet}\text{)-R} \rightarrow \text{Ar}^{\bullet}\text{-CH}_2\text{-NO-R} \quad (12)$$

$$\text{E: } \text{Ar}^{\bullet}\text{-CH}_2\text{-NO-R} \rightarrow \text{Ar}^{\bullet+}\text{-CH}_2\text{-NO-R} + \text{e}^{-} \rightarrow \text{condensation} \quad (13)$$

Schéma 6. Schéma ECCE du transfert d'électrons décrivant l'oxydation d'une nitrone de type PBN dans l'ACN.

Dans l'eau (tampon phosphate salin pH 7,4), l'étude est limitée à la réduction de la PBN car le processus d'oxydation est confondu avec celui du solvant. La réduction de la PBN se fait en deux étapes et conduit à la formation d'une amine à travers le transfert de quatre électrons et quatre protons.

$$\text{Ar-CH=N}^{+}(\text{O}^{-})\text{-R} + 2\,\text{e}^{-} + 2\,\text{H}^{+} \rightarrow \text{Ar-CH}_2\text{-N(OH)-R (ou Ar-CH=N-R)} \quad (14)$$

$$\text{Ar-CH}_2\text{-N(OH)-R} + 2\,\text{e}^{-} + 2\,\text{H}^{+} \rightarrow \text{Ar-CH}_2\text{-NH-R} + \text{H}_2\text{O} \quad (15)$$

Schéma 7. Schéma du transfert d'électrons décrivant la réduction d'une nitrone de type PBN dans l'eau.

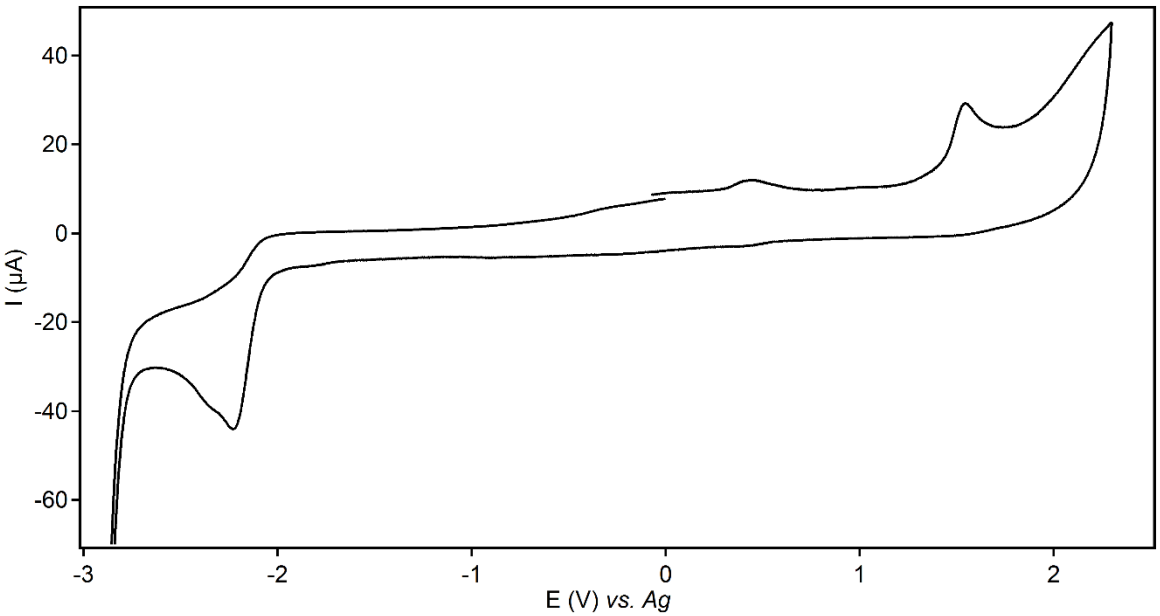

Figure 10. Voltammogramme cyclique de la PBN dans l'ACN contenant 0,1 M de TBAP, à une vitesse de balayage de 0,1 V/s vs. Ag.

Les mêmes comportements sont généralement observés pour les dérivés de la PBN, les potentiels variant en fonction des substituants introduits. Si les dérivés possèdent également des fonctions susceptibles d'être réduites ou oxydées, d'autres pics, en plus de ceux correspondant à la réduction et à l'oxydation de la fonction nitronyle, sont observés. Plus le potentiel de réduction $E_p(c)$ (en valeur absolue) ou d'oxydation $E_p(a)$ de la nitrone est faible, plus la nitrone peut facilement se réduire ou s'oxyder. Ainsi, un bon antioxydant devrait avoir un potentiel d'oxydation faible.

Dans le cas des nitrones, on s'intéresse également au domaine de stabilité des dérivés, qui correspond à la différence entre le plus grand potentiel d'oxydation et le plus faible potentiel de réduction obtenus. Il correspond à la fenêtre de potentiel pouvant être appliquée au dérivé sans risquer de l'oxyder ou de le réduire. Il est important de connaître le domaine de stabilité des dérivés lorsque l'on veut effectuer une expérience de spin-trapping par RPE où le radical est généré de manière électrochimique. En effet, la fonction nitronyle est oxydée ou réduite en cation ou en anion radicalaire, pouvant ensuite réagir avec un nucléophile (Nu^-) ou un électrophile (E^+) pour conduire à la formation d'un radical aminoxyle, comme le montre le Schéma 8 (processus de spin-trapping inversé).[27,28] Ce radical ne vient pas de l'addition d'un radical sur la fonction nitronyle et sa présence peut perturber l'interprétation du signal.

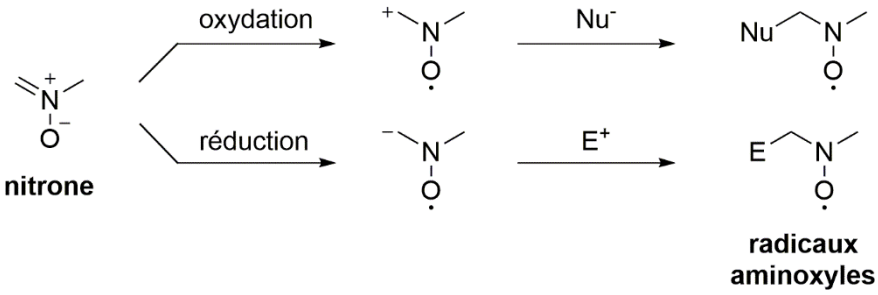

Schéma 8. Conversion de la nitrone en radicaux aminoxyles par le processus de spin-trapping inversé.

8. Modèles d'étude *in vitro* de l'activité neuroprotectrice

La capacité neuroprotectrice des dérivés synthétisés a été évaluée sur deux modèles d'étude *in vitro*. Le premier réalisé par Michel Vignes étudie la survie de cellules gliales de rats (cellules C6) intoxiquées par de l'hydroperoxyde de *tert*-butyle (*t*BuOOH), un inducteur de stress oxydant. Le *t*BuOOH est une substance modèle pour l'évaluation des mécanismes d'altération cellulaire résultant du stress oxydant dans les cellules et les tissus. Les cellules sont mises en contact avec les nitrones étudiées 24 h avant induction du stress oxydant, afin de mettre en évidence un effet protecteur à long terme. Le stress oxydant est alors produit en traitant les cellules avec du *t*BuOOH (300 µM) pendant 24 h puis la survie cellulaire est mesurée par un test MTT. Le test MTT est une méthode colorimétrique rapide de numération des cellules vivantes. On utilise pour cela du sel de tétrazolium MTT (bromure de 3-(4,5-dimethylthiazol-2-yl)-2,5-diphenyl tetrazolium) qui va être réduit en formazan par la succinate deshydrogénase mitochondriale des cellules vivantes actives. Cette réaction entraîne la formation d'un précipité violet dans la mitochondrie ; la quantité de précipité violet étant directement proportionnelle à la quantité de cellules vivantes, et est réalisée grâce à une incubation des cellules à 37 °C. Après incubation, l'ajout de DMSO permet de dissoudre les cellules, leurs mitochondries et donc les précipités violets. Un dosage de la densité optique à 550 nm en spectroscopie UV permet alors de connaître la quantité relative de cellules vivantes et actives métaboliquement. Les résultats sont alors exprimés en % de survie cellulaire par rapport au contrôle (pas d'intoxication = 100%). On peut alors comparer les résultats obtenus en présence et en absence de nitrone afin d'en déduire l'effet protecteur (différence positive) ou toxique (différence négative) de la nitrone.

Le deuxième test a été réalisé par la société Neuro-Sys et consiste à étudier des neurones corticaux primaires de rats intoxiqués par du glutamate. Le glutamate est un

neurotransmetteur d'importance majeure. En concentrations trop élevées dans le cerveau, il déclenche un processus dit d'excitotoxicité qui entraîne la destruction des neurones et est reconnu comme étant l'un des mécanismes physiopathologiques à l'origine de nombreuses maladies neurodégénératives telles qu'Alzheimer, Parkinson et la sclérose latérale amyotrophique. L'excitotoxicité du glutamate entraine la génération d'ERO/ERA, ce qui produit un stress oxydant. Les cellules sont pré-incubées avec les nitrones étudiées 1 h avant une exposition au glutamate pendant 20 min. Le glutamate est ensuite lavé et 48 h après l'intoxication, le test MTT est réalisé. Les résultats sont alors exprimés en % de survie cellulaire par rapport au contrôle (pas d'intoxication = 100%). Des études statistiques (ANOVA suivi d'un test Fischer PLSD) ont été réalisées.

Les deux modèles d'étude utilisés donnent une idée de la protection des nitrones vis-à-vis des maladies neurodégénératives et sont complémentaires, puisque les cultures de neurones contiennent des cellules gliales (20-30%).

9. Présentation des chapitres du manuscrit

Le premier chapitre de ce manuscrit de thèse est présenté sous forme d'introduction bibliographique, dressant l'état de l'art des différentes stratégies de synthèse mises en place pour obtenir des nitrones et de leurs avantages et inconvénients. Il décrit également les nombreux dérivés de la PBN et de la DMPO synthétisés depuis plusieurs années et comment l'introduction de substituants de nature variée influence les propriétés et l'activité de la fonction nitronyle. Dans ce chapitre d'introduction bibliographique, l'accent a été mis sur la capacité des nitrones à piéger les radicaux libres, notamment les radicaux superoxydes $O_2^{\bullet-}$, précurseurs majeurs d'espèces réactives, et les radicaux hydroxyles $HO^{\bullet}$, espèces réactives les plus délétères, mais également sur leurs propriétés physicochimiques. Des nitrones ayant montré des effets neuroprotecteurs dans des modèles d'étude *in vitro* et *in vivo* sont aussi présentées.

Dans le second chapitre, nous nous sommes intéressés à l'étude de dérivés de la PBN, de la *N*-benzylidene-1-diethoxyphosphoryl-1-methylethylamine *N*-oxide (PPN) et de la *N*-benzylidene-1-ethoxycarbonyl-1-methylethylamine *N*-oxide (EPPN) comportant des groupements methoxy (MeO) sur le cycle aromatique (Figure 11). Des études antérieures dans notre laboratoire sur des dérivés de la PBN substitués en position *para* ont montré que le

dérivé 4-MeO-PBN est un composé prometteur.[26] En effet, il possède un faible potentiel d'oxydation et pourrait présenter de bonnes propriétés antioxydantes, ainsi que de bonnes capacités à piéger le radical $Ph^{\bullet}$, dus au groupement MeO électrodonneur introduit sur le cycle aromatique. C'est pourquoi nous avons décidé d'étudier l'influence de ce groupement en position *para* sur la réactivité de la nitrone à travers trois nitrones classiques : la PBN, la PPN et la EPPN et d'analyser par la même occasion l'impact de l'introduction d'un groupement électroattracteur (diethoxyphosphoryl et ethoxycarbonyl) en position α de la partie *N-tert*-butyle. Nous avons également étudié l'influence sur les propriétés de la nitrone de type PBN de la position et du nombre de substituants MeO sur le cycle aromatique. Afin de répondre aux problématiques posées, nous avons mesuré les potentiels d'oxydo-réduction des dérivés synthétisés par voltampérométrie cyclique, étudié leur cinétique de piégeage par RPE et déterminé des paramètres théoriques par modélisation moléculaire.

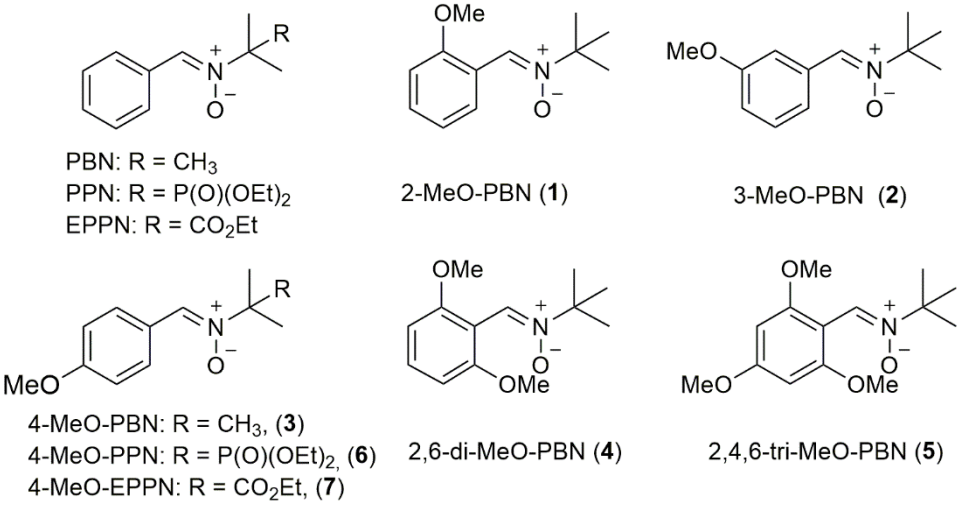

Figure 11. Structure chimique des dérivés étudiés dans le chapitre 2.

Dans le troisième chapitre, nous nous sommes intéressés à l'influence de la nature électronique des substituants en position *para* du cycle aromatique de la nitrone de type PBN et à l'amélioration de ses propriétés intrinsèques. Pour cela, nous avons étudié de nouveaux dérivés possédant des groupements électrodonneurs ou électroattracteurs en position *para* (Figure 12) et nous avons également inclus dans l'étude des dérivés précédemment synthétisés dans notre laboratoire.[26] La constante de Hammett (σ_p) est un paramètre issu de la littérature permettant de classer l'électronégativité du substituant.[29] Nous avons donc essayé d'établir des corrélations entre ce facteur et différents paramètres expérimentaux déterminés. En effet, nous avons évalué les capacités de piégeage de radicaux libres des dérivés par RPE,

mesuré leur potentiel d'oxydo-réduction par voltampérométrie cyclique et évalué leur neuroprotection sur deux modèles d'études *in vitro*. Nous avons également obtenu des données théoriques (charges partielles et potentiels d'ionisation) afin d'avoir une idée plus claire de la réactivité de la fonction nitronyle.

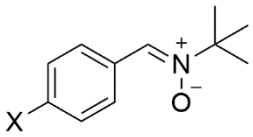

PBN	X = H	**7**	X = MeCONH
1	X = Me_2N	**8**	X = F
2	X = MeO	**9**	X = CF_3O
3	X = iPr	**10**	X = MeNHCO
4	X = $AcNHCH_2$	**11**	X = HOOC
5	X = Ph	**12**	X = CF_3
6	X = MeS	**13**	X = NC

Figure 12. Structure chimique des dérivés étudiés dans le chapitre 3.

Dans le quatrième chapitre, nous avons exploré l'impact de la bi-fonctionnalisation sur le cycle aromatique et sur la partie *N-tert*-butyle de la PBN. Nous avons étudié plusieurs séries de molécules (voir Figure 13). La première série comprend des dérivés possédant une fonction acide en *para* du cycle aromatique et des groupements variés en position β de la fonction nitronyle (H, OH, OAc, NHAc), il s'agit de la série 4-HOOC-PBN-CH_2Y. Dans la deuxième série, au contraire, nous avons fixé le groupement en position β et avons fait varier le substituant en position *para* du cycle aromatique (HOOC-, $AcNHCH_2$- et MeO-), c'est la série 4-X-PBN-CH_2NHAc. Pour la troisième série, nous avons décidé d'introduire un motif naphtalène à la place du motif phényle afin d'étudier l'impact des effets mésomères sur la réactivité de la fonction nitronyle. Nous avons également fait varier les groupements en position β de la fonction nitronyle (H, OH, OAc, NHAc), il s'agit de la série NBN-CH_2Y. Dans ce chapitre, nous avons étudié l'activité de piégeage de radicaux libres des dérivés par RPE, mesuré leurs potentiels d'oxydo-réduction par voltampérométrie cyclique et évalué leur activité neuroprotectrice sur deux modèles d'étude. Nous avons également comparé ces données à celles des composés mono-substitués PBN-CH_2OH, PBN-CH_2OAc et PBN-CH_2NHAc, précédemment synthétisés dans notre laboratoire,[30] afin d'identifier l'impact de la bi-fonctionnalisation sur la réactivité de la fonction nitronyle et d'identifier une possible additivité des effets de part et d'autre de la fonction nitronyle. Des données théoriques sont

actuellement en cours d'acquisition grâce à une collaboration avec le professeur Frederick Villamena (College of Medicine, The Ohio State University) et nous permettront d'obtenir une meilleure compréhension de la réactivité de la fonction nitronyle.

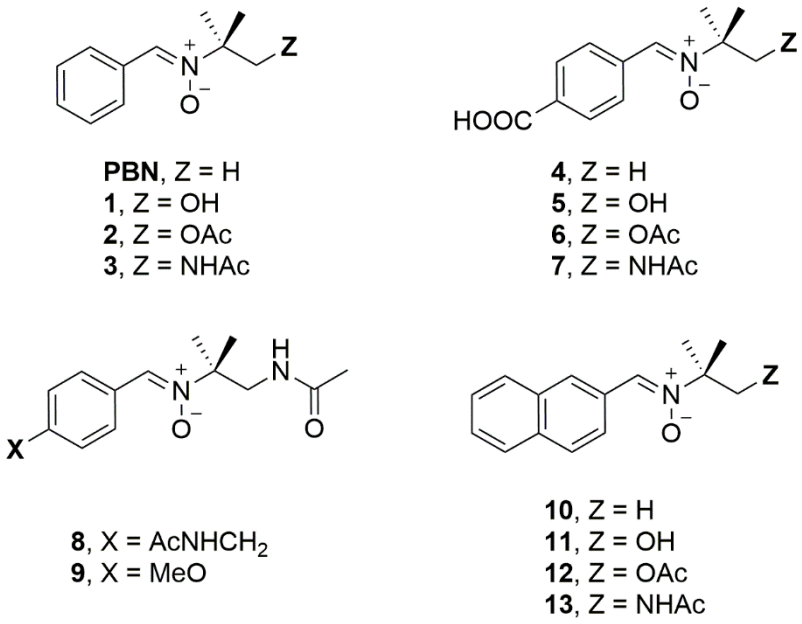

PBN, Z = H
1, Z = OH
2, Z = OAc
3, Z = NHAc

4, Z = H
5, Z = OH
6, Z = OAc
7, Z = NHAc

8, X = $AcNHCH_2$
9, X = MeO

10, Z = H
11, Z = OH
12, Z = OAc
13, Z = NHAc

Figure 13. Structure chimique des dérivés étudiés dans le chapitre 4.

REFERENCES

1 B. Halliwell and J. M. C. Gutteridge, *Free Radicals in Biology and Medicine*, Oxford University Press, 2015.
2 C. C. Winterbourn, *Nat. Chem. Biol.*, 2008, **4**, 278–286.
3 E. Cadenas and K. J. A. Davies, *Free Radic. Biol. Med.*, 2000, **29**, 222–230.
4 W. H. Koppenol, D. M. Stanbury and P. L. Bounds, *Free Radic. Biol. Med.*, 2010, **49**, 317–322.
5 B. Halliwell and J. M. C. Gutteridge, *FEBS Lett.*, 1992, **307**, 108–112.
6 M. C. Martínez and R. Andriantsitohaina, *Antioxid. Redox Signal.*, 2009, **11**, 669–702.
7 J. S. Beckman, T. W. Beckman, J. Chen, P. A. Marshall and B. A. Freeman, *Proc. Natl. Acad. Sci.*, 1990, **87**, 1620–1624.
8 B. H. J. Bielski, D. E. Cabelli, R. L. Arudi and A. B. Ross, *J. Phys. Chem. Ref. Data*, 1985, **14**, 1041–1100.
9 J. Delattre, J.-L. Beaudeux and D. Bonnefont-Rousselot, *Radicaux libres et stress oxydant: Aspects biologiques et pathologiques*, Lavoisier, 2007.
10 Maladies neurodégénératives, santepubliquefrance.fr/maladies-et-traumatismes/maladies-neurodegeneratives, (accessed October 23, 2019).
11 Observatoire Régional de la Santé, *Projections des maladies chroniques en région Provence-Alpes-Côte-D'Azur à l'horizon 2028*, 2017.
12 A. Nieoullon, *J. Appl. Biomed.*, 2011, **9**, 173–183.
13 Le plan maladies neuro-dégénératives 2014-2019, https://www.gouvernement.fr/action/le-plan-maladies-neuro-degeneratives-2014-2019, (accessed October 23, 2019).
14 L. Packer and E. Cadenas, *Handbook of Synthetic Antioxidants*, Marcel Dekker, Inc., 1997.
15 H. Feuer, *Nitrile oxides, Nitrones, and Nitronates in Organic Synthesis: Novel Strategies in Synthesis*, NJ, USA, John Wiley & Sons, Inc., 2008.
16 K. V. Gothelf and K. A. Jørgensen, *Chem. Rev.*, 1998, **98**, 863–910.
17 M. J. Davies, *Methods*, 2016, 21–30.
18 G. M. Rosen, B. E. Britigan, H. J. Halpern and S. Pou, *Free Radicals: Biology and Detection by Spin Trapping*, Oxford University Press, 1999.
19 F. A. Villamena, A. Das and K. M. Nash, *Future Med. Chem.*, 2012, **4**, 1171–1207.
20 F. A. Villamena, *Reactive Species Detection in Biology: From Fluorescence to Electron Paramagnetic Resonance Spectroscopy*, Elsevier., 2017.
21 G. P. Novelli, P. Angiolini, R. Tani, G. Consales and L. Bordi, *Free Radic. Res. Commun.*, 1986, **1**, 321–327.
22 R. A. Floyd, H. C. Castro Faria Neto, G. A. Zimmerman, K. Hensley and R. A. Towner, *Free Radic. Biol. Med.*, 2013, **62**, 145–156.
23 K. R. Lees, J. A. Zivin, T. Ashwood, A. Davalos, S. M. Davis, H.-C. Diener, J. Grotta, P. Lyden, A. Shuaib and H.-G. H\a ardemark, *N. Engl. J. Med.*, 2006, **354**, 588–600.
24 A. Shuaib, K. R. Lees, P. Lyden, J. Grotta, A. Davalos, S. M. Davis, H.-C. Diener, T. Ashwood, W. W. Wasiewski and U. Emeribe, *N. Engl. J. Med.*, 2007, **357**, 562–571.
25 V. Roubaud, H. Dozol, C. Rizzi, R. Lauricella, J.-C. Bouteiller and B. Tuccio, *J. Chem. Soc. Perkin Trans. 2*, 2002, 958–964.

26 M. Rosselin, B. Tuccio, P. Pério, Frederick. A. Villamena, P.-L. Fabre and G. Durand, *Electrochimica Acta*, 2016, **193**, 231–239.
27 L. Eberson, *J. Chem. Soc. Perkin Trans. 2*, 1992, 1807–1813.
28 L. Eberson, *J. Chem. Soc. Perkin Trans. 2*, 1994, 171–176.
29 C. Hansch, A. Leo and R. W. Taft, *Chem. Rev.*, 1991, **91**, 165–195.
30 M. Rosselin, F. Choteau, K. Zéamari, K. M. Nash, A. Das, R. Lauricella, E. Lojou, B. Tuccio, F. A. Villamena and G. Durand, *J. Org. Chem.*, 2014, **79**, 6615–6626.

Chapitre 1

Nitrones derivatives as spin traps and neuroprotective agents

Ce chapitre fera l'objet d'une revue

Chapitre 1 - Nitrones derivatives as spin traps and neuroprotective agents

Table of Contents

ABSTRACT

Nitrones were first developed in the late 1960s as probes for the indirect detection of short-lived free radical species using electron paramagnetic resonance (EPR) spectroscopy. This technique, called spin-trapping, has provided valuable information on the nature and structure of radicals, especially in biological systems. Since the 90s nitrones have also been used as antioxidants to prevent damages from oxidative stress. Many studies have shown the protective effects of α-phenyl-*N*-*tert*-butyl nitrone (PBN) and its derivatives on various experimental models such as cerebral ischemia or Huntington disease. Nitrones can be easily obtained by several organic synthetic methods. Their reactivity depends mainly on the nature and the position of the substituents on the nitronyl function. Therefore, many laboratories have worked on the chemical modification of PBN and 5,5-dimethyl-1-pyrroline-*N*-oxide (DMPO) in order to improve biological and spin-trapping properties of nitrones. In this chapter, we give a non-exhaustive overview of nitrone analogues that have been synthesized and studied in the past decades and how the chemical modifications have improved the reactivity of the nitronyl moiety.

KEYWORDS

Nitrones, Electron Paramagnetic Resonance (EPR) spectroscopy, Spin-Trapping, Antioxidants, Neuroprotection.

1. INTRODUCTION

Nitrones were initially designed in the late 1960s as probes for the indirect detection of free radical species whose half-lives are very short. This technique called spin-trapping involves the addition of a free radical to the nitrogen-carbon double bond of the diamagnetic nitrone, yielding a persistent paramagnetic aminoxyl spin adduct (Scheme 1). The formed adduct, whose half-life is significantly longer, is then detected and characterized by electron paramagnetic resonance (EPR) spectroscopy. The EPR spectral profiles obtained can be characteristic of the radical trapped and therefore provide information in terms of mechanisms, kinetics and dose dependence of radical production in biological systems.[1] When used as spin traps, it is important to design nitrones with high rate constant of free radical trapping as well as a high persistence of the corresponding aminoxyl spin adduct to ensure efficient detection.[2]

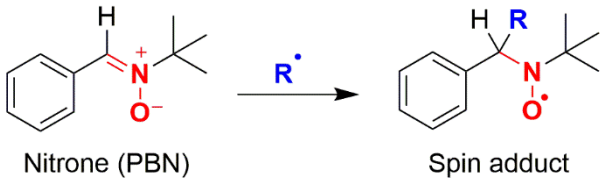

Scheme 1. The spin-trapping mechanism of PBN.

Nitrones have been divided into two major classes: the cyclic ones derived from the 5,5-dimethyl-1-pyrroline-*N*-oxide (DMPO) and the linear ones derived from the α-phenyl-*N*-*tert*-butyl nitrone (PBN). The cyclic nitrones have shown better ability to trap oxygen-centered radicals (*e.g.* superoxide ($O_2^{\bullet-}$) or hydroxyl radicals ($HO^{\bullet}$)), with high rate constants of radicals trapping, persistence and more distinctive EPR spectra of the corresponding spin adducts formed. For instance, DMPO yields distinct and sufficiently persistent spin adducts with the $O_2^{\bullet-}$ and $HO^{\bullet}$ radicals (named DMPO-O_2H and DMPO-OH, respectively) and therefore has been the most frequently used spin trap in isolated heart studies.[3] $O_2^{\bullet-}$ radical is a major precursor of the most highly reactive species known to exist in biological systems, such as $HO^{\bullet}$ radical. Formation of $O_2^{\bullet-}$ shows the first sign of oxidative stress and, therefore, its detection in biological systems is important. The distribution of PBN within tissues and cells is much higher than that of DMPO, allowing PBN to be widely used in *ex vivo* and *in vivo* studies of radical production in whole animals.[4–6] Linear nitrones are also easier to synthesize

and purify as they are often solid at room temperature and can be recrystallized to afford paramagnetic impurity free samples.

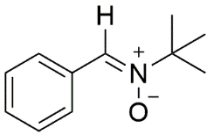

PBN

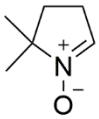

DMPO

Figure 1. Chemical structure of PBN and DMPO.

Aside their ability in trapping free radicals inside the cells and tissues, nitrones have been used since the 90s as pharmacological agents to prevent damage from oxidative stress.[7] The pharmaceutical application of nitrones was first proposed by Novelli *et al.* who demonstrated that administration of PBN confers protection on rats from lethal whole-body trauma or circulatory shock.[8,9] Nitrones have been then used against several disorders implicating free radicals such as neurodegenerative diseases,[10] stroke,[11,12] cardiovascular diseases,[13] retinal degeneration,[14] cancer,[15] and other age-related diseases.[16] The disodium [(*tert*-butylimino)methyl]-benzene-1,3-disulfonate *N*-oxide (NXY-059) was the first neuroprotective agent to reach phase III clinical trials in the USA for the treatment of acute stroke.[17,18] Moreover, the toxicity of nitrones is low, rendering their use in biological system safe without inducing any severe side effects.[19]

The biological activity of nitrones had been first explained by their ability to trap free radicals but experimental evidence has demonstrated the contrary, suggesting other mechanisms. The concentration of nitrones in target tissues is far too low (≈ 50 μM) to trap all the radical species. Moreover, PBN has been shown to act as an anti-inflammatory and anti-apoptotic agent in the brain[20,21] and the eyes.[22] Nitrones also exhibit NO-releasing properties which may be partly responsible for their biological activities, especially during ischemia-reperfusion syndromes.[13,23,24]

However, the use of DMPO and PBN in biological environment has encountered some limitations for *in vivo* applications of spin traps or therapeutic agents. For example, the DMPO-O_2H spin adduct decomposes quickly to DMPO-OH in polar milieu and its biological use to extracellular spin-trapping is limited by its hydrophilicity.[25] Likewise, the spin-trapping properties of PBN are rather limited with the low stability of its spin adducts in aqueous solution, requiring an extraction with an organic solvent before EPR analysis.[26] This

extraction could cause the loss of spin adducts and introduce a solvent effect. To overcome these problems, much effort has been devoted to the design of analogues of DMPO and PBN that could give better spin-trapping and biological activities. In fact, the chemical and pharmacological properties of nitrones depend mainly on the nature and the position of the substituents on the nitronyl function. In this regard, the antioxidant properties of various nitrones have been recently reviewed by our group.[27] We describe herein different synthetic methods developed to obtain nitrones as well as the different derivatives of DMPO and PBN synthesized over the past few years without being exhaustive. This chapter focuses on the evolution of the spin-trapping properties of the derivatives, in particular towards superoxide and hydroxyl radicals, according to their structural modifications. We present also in this chapter different nitrones that have shown neuroprotective activities in *in vitro* and *in vivo* models.

2. NITRONES SYNTHETIC METHODS

Several methods for the synthesis of nitrones are available from the literature: either oxidative methods, generally from amine compounds, or methods that do not involve oxidation.

2.1. Oxidative methods

Many methods used for the synthesis of nitrones are based on the oxidation of compounds. The precursors employed are imines, secondary amines and hydroxylamines.

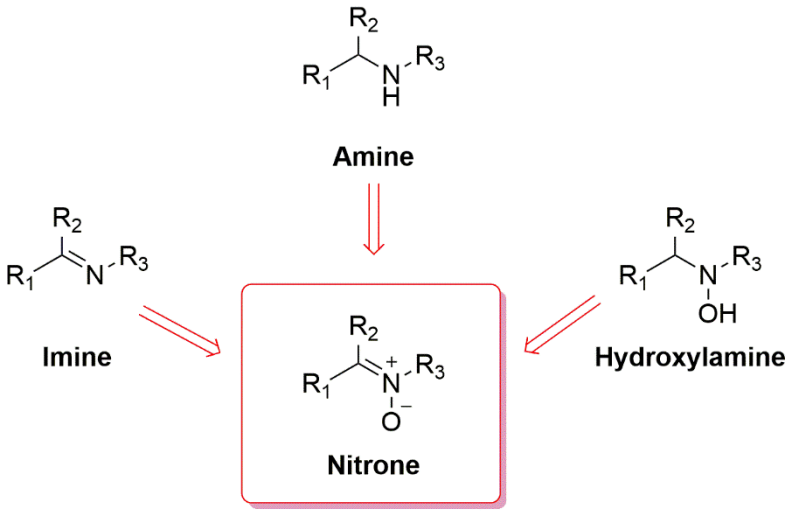

Figure 2. Precursors of nitrones by oxidative pathway.

2.1.1. Imine oxidation

Peracids such as *m*-chloroperbenzoïque acid (MCPBA) can be used to oxidize imines. This reaction often leads to oxaziridines as the main products, which have been identified as the "normal" products from peroxyacid oxidation of imines, but sometimes nitrones were found to be the major products. The nitrone is generally formed after a rearrangement of the oxaziridine intermediate (Scheme 2). Some papers attempted to rationalize the different factors which influence the oxaziridine:nitrone ratio obtained and demonstrated that electronic factors as well as steric effects favour the isomerization of oxaziridines to nitrones.[28,29]

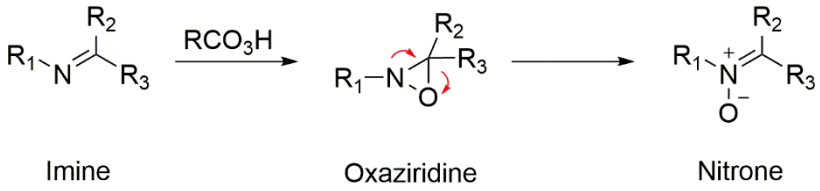

Scheme 2. General mechanism of the formation of a nitrone by oxidation of an imine.

Other reagents can be used to directly oxidize imines to nitrones. Dimethyldioxirane (DMD) is an electrophilic oxidant capable of producing nitrones without evidence of oxaziridine formation.[30] Permanganate ion (MnO_4^-) can oxidize imines to nitrones in reasonable yields under phase-transfer catalyst conditions. The presence of water is necessary and the best phase-transfer catalysts are long-chained tetraalkylammonium salts.[31] Nitrones can also be obtained by photochemistry oxidation of aldimines with TiO_2 in the presence of oxygen.[32] More recently, a chemo- and regioselective oxidative method of imines with urea hydrogen peroxide (UHP) has been described, using methyltrioxorhenium (MTO, CH_3ReO_3) as a catalyst.[33]

2.1.2. Amine oxidation

The oxidant reagent usually used to oxidize secondary amines is a 30% H_2O_2 solution in the presence of a metal catalyst as Na_2WO_4, leading to nitrones with yields up to 95%.[34] Other catalysts such as $VO(acac)_2$, $Ti(OBu)_4$, and $MoO_2(acac)_2$ (acac = acetylacetonate) can be used, giving high yields of nitrones, but their conversions were lower. Urea-Hydrogen peroxide complex (UHP) in the presence of metal catalysts can be used instead of

concentrated solutions of H_2O_2 and constitutes a safer alternative. The best yields (90%) have been obtained with Na_2WO_4 as a catalyst.[35] Methyltrioxorhenium-hydrogen peroxide (MTO/H_2O_2) can also be used to synthesize nitrones in good yields. This reaction occurs in two oxidation steps: the secondary amine is first converted to hydroxylamine and then the nitrone is obtained.[36] This system works even when the UHP complex is used as H_2O_2 source.[37]

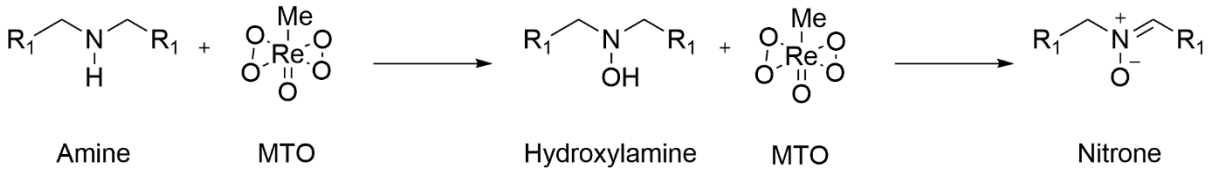

Scheme 3. Oxidation mechanism of secondary amines by MTO.

The application of MTO to oxidize amine compounds has allowed the development of an oxidative method involving the use of molecular oxygen instead of H_2O_2. This new system MTO/O_2 can convert quickly secondary amines to nitrones with yields near 100%.[38] Other reagents allow the oxidation of secondary amines without using metals. Dimethyldioxirane (DMD) can only convert secondary amines containing α-hydrogen to nitrones. If the amine does not have α-hydrogen, a nitroxide is obtained.[39] With one equivalent of dimethyldioxirane, the hydroxylamine derivative is formed. With two equivalents, the reaction continues until the formation of the nitrone.

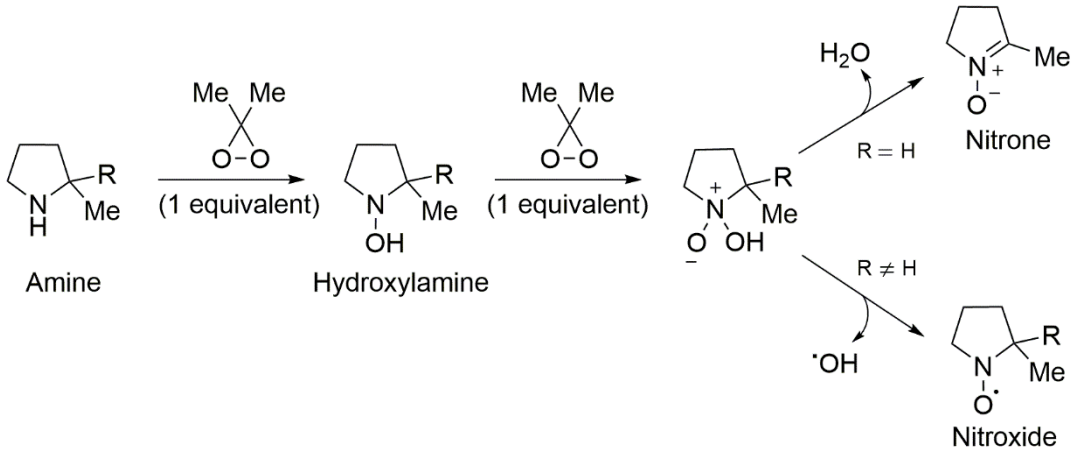

Scheme 4. Oxidation mechanism of secondary amines by DMD.

Another heterocyclic oxidant, the 2-phenylsulfonyl-3-phenyloxaziridine, also called Davis' reagent, is often used to synthesize nitrones. Its mechanism is similar to that of DMD.[40] A

protocol using oxone in a biphasic basic medium has been developed. This method is general, ecological and the oxone does not interfere with other functional groups or existing stereogenic centers.[41]

2.1.3. N,N-disubstituted hydroxylamine oxidation

The oxidation of hydroxylamine to nitrone is an easy method which uses mild conditions. The reaction proceeds via the primary formation of a nitroxide radical, and then, after a reaction of dismutation, the nitrone is obtained accompanied by the starting hydroxylamine, which can be oxidized again. The reaction of dismutation requires the presence of at least one α-hydrogen on the nitroxide function. First, the mercuric oxide (HgO) was used as oxidant agent but because of its acute toxicity and the high quantities needed, it was replaced by MnO_2.[42]

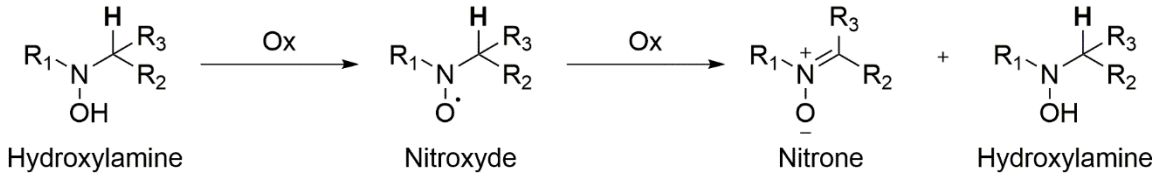

Scheme 5. Oxidation mechanism of hydroxylamines.

This reaction can be catalysed by Mn(III) complexes in the presence of hydrogen peroxide (H_2O_2), sodium hypochlorite (NaOCl) or iodosylbenzene (PhIO) as stoichiometric oxidant and under these conditions it is enantioselective.[43] NaOCl represents an ecologic and cheap system.[44] More recently, nitrones have been synthesized by the aerobic oxidation of hydroxylamines with molecular oxygen catalysed by nanoporous gold (AuNPore). The gold catalyst was recoverable and reusable many times with no leaching of gold.[45]

2.2. Non-oxidative methods

2.2.1. Condensation of a N-substituted hydroxylamine and a carbonyl derivative

The most direct approach for the synthesis of nitrones is the condensation of *N*-substituted hydroxylamines with aromatic aldehydes or ketones.[46] This method is highly used due to the large accessibility of aromatic or aliphatic carbonyl compounds and can be achieved at room

temperature in ether or ethanol. This reaction is easier and gives better yields with aldehydes than with ketones. A Lewis acid ($ZnCl_2$, $AlCl_3$, $MgBr_2$) can be used as activating agent to synthesize ketonitrones.[47] The yield and kinetic can be increased by adding drying agents (Na_2SO_4, $MgSO_4$)[48] or molecular sieves 4Å.

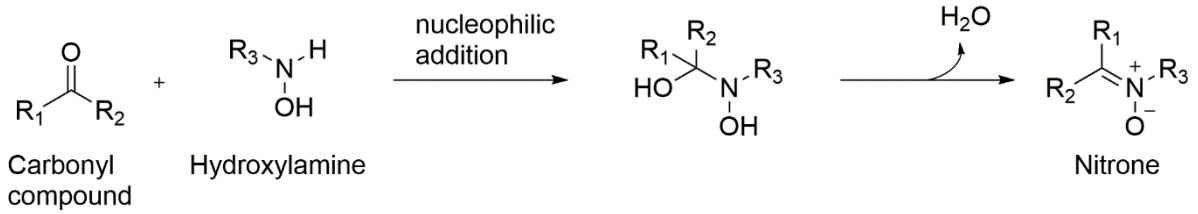

Scheme 6. Condensation reaction between a carbonyl compound and a hydroxylamine.

This synthetic method is widely used to obtain linear nitrones derived from PBN but its limitation results in the poor accessibility and stability of the hydroxylamines. This problem can be overcome by generating the requisite hydroxylamine *in situ* from more accessible precursors (nitro and oxime compounds).[49] Oxime can be reduced by BH_3-THF or $NaCNBH_3$ [50] and nitro by Zn in the presence of a weak acid like NH_4Cl or AcOH.[51] The reduction by Zn is not expensive, the reaction time is relatively short and a large number of substrates are stable under these conditions.[52] The only limitation results in the use of not sensitive substituents to the reduction conditions. In this case, the hydroxylamine is first obtained by reduction of its nitro derivative, purified, and then condensed with the aldehyde derivative. This allows milder conditions of coupling.

More recently, Morales and co-workers have developed a protocol using pyrrolidine as a catalyst to form nitrones from the condensation between aldehydes and *N*-substituted hydroxylamine hydrochlorides. Pyrrolidine allows the complete liberation of the hydroxylamine hydrochloride and accelerates the reaction by forming an iminium ion, much more reactive than the corresponding aldehyde. This method provides nitrones in a matter of minutes under very mild conditions and only a filtration through a short pad of silica gel is necessary to purify the crude nitrone.[53]

With the development of green chemistry, Colacino and co-workers have developed a solvent-free synthesis of nitrones in a ball-mill apparatus. This synthesis occurs via condensation of an equimolar amount of *N*-substituted hydroxylamines and aldehydes and affords nitrones in high yields and in pure form.[54] This method allowed the synthesis of alkyl and aryl-*N*-methylnitrones in the presence of Na_2CO_3-Na_2SO_4 with complete overall

conversion and in a relatively short-time (3-10 min).[55] It can also be applied on the surface of MgO and allowed the synthesis of various nitrones.[56] Nitrones can also be synthesized under microwave irradiation. These reactions are very fast, with no need to reflux the reaction during several days and/or to use excess of hydroxylamines to obtain good yields. *N*-aryl, *N*-alkyl[57] and hydroxyphenyl[58] nitrones were synthesized by this method.

2.2.2. N-alkylation of oximes

Nitrones can also be synthesized from oximes by an alkylation of the oxime nitrogen atom with electrophilic alkenes activated by a withdrawing group.

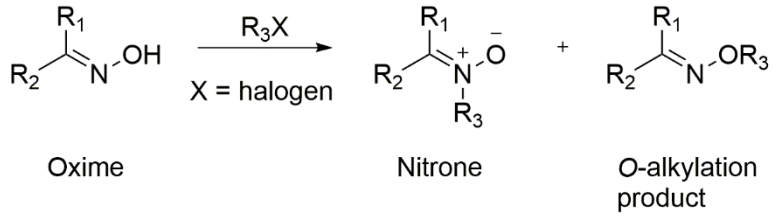

Scheme 7. Synthesis of nitrones from oxime.

This method is seldom used because of the formation of a *O*-alkylated co-product which is difficult to separate from the nitrone.[59] To avoid this problem, it is possible to convert the oxime to a *O*-trimethylsilyloxime and then the nitrone is easily obtained by using a trialkyloxonium tetrafluoroborate or an alkyl triflate.[60]

2.2.3. Condensation/oxidation of aldehydes and primary amines

Recently, Cordona and co-workers reported a one-pot condensation/oxidation of aldehydes and primary amines using MTO as a catalyst in combination with UHP as stoichiometric oxidant. This method allows a regioselective synthesis of nitrones, in contrast to other oxidation methods that use secondary amines or hydroxylamines as starting materials.[61]

This reaction can also occur using Nafion-immobilized $MoOCl_4$[62] and silica-immobilized oxo-rhenium[63] as recyclable catalysts with solid UHP as the oxidant. The activity of the immobilized catalysts is higher than that of their analogous homogeneous catalysts and they can be easily recycled without losing activity. More recently, a new and simple method using

graphite oxide (GO) and oxone as the oxidant has been developed and provides nitrones under very mild reaction conditions and in short reaction times.[64]

2.2.4. Addition of a carbonyl carbon to nitroso arenes

The conventional synthesis pathways involve the addition of a nucleophilic reagent to an electrophilic site, making selectivity difficult when several electrophilic sites are present on the molecule. Chavannavar and co-workers have developed a method that provides ketonitrones with an α-electron withdrawing group. This method uses a phosphine-mediated addition of 1,2-dicarbonyls to nitroso compounds and provides a high degree of chemoselectivity even in the presence of other electrophilic sites.[65]

a. Conventional formation of nitrones: condensation of carbonyl compounds with hydroxylamines

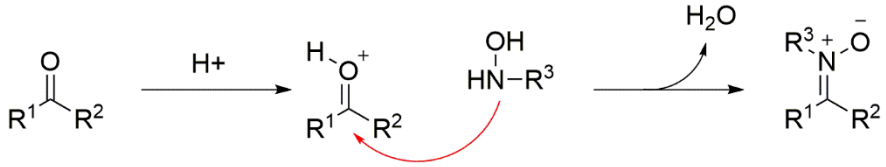

b. Polarity inversion: addition of a carbonyl carbon to nitroso arenes

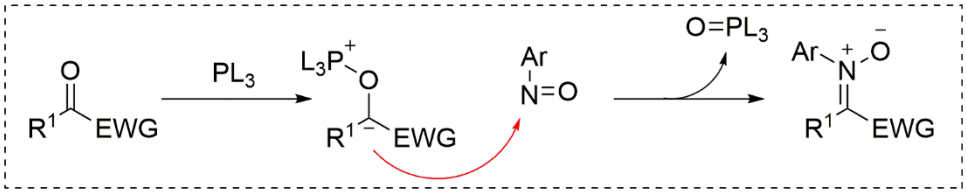

Scheme 8. Comparison of two synthesis pathways. (a) Classic condensation approach. (b) Umpolung approach.

3. NITRONES AS SPIN TRAPS

3.1. DMPO-type derivatives

DMPO was initially synthesized according to the procedure developed by Bonnett *et al.*[66] where the nitronyl function was formed by an intramolecular condensation of aldehyde and hydroxylamine moieties (Scheme 9). The synthetic route begins with a simple Michael addition in which acrolein is carefully added to the anion of 2-nitropropane (**2**), giving 4-

methyl-4-nitro-1-pentanal (**3**). The anion can be generated by slowly adding 2-nitropropane (**1**) to sodium methoxide at low temperature[67] or in the presence of a base such as benzyltrimethylammonium hydroxide.[68] The aldehyde was protected as 2-(3-methyl-3-nitrobutyl)-1,3-dioxolane (**4**) prior to reduction, thereby avoiding the formation of pyrrolidines. The acetal was formed according to standard procedures in which ethylene glycol is added to a refluxing toluene solution containing aldehyde (**3**) and the catalyst *p*-toluenesulfonic acid. The 1,3-dioxolane (**4**) was then reduced by Zn in the presence of NH_4Cl to give the corresponding hydroxylamine, which, upon acid hydrolysis to remove the protective group, leads to the desired nitrone (**5**). There have been several attempts to shorten the synthesis of DMPO. One approach consists to directly reduce the nitro function of aldehyde (**3**) by Zn in the presence of AcOH, avoiding the aldehyde protection/deprotection steps.[69] However, variability in the percentage of the isolatable nitrone was observed and was due to a great difficulty in removing the by-products arising during zinc reduction.

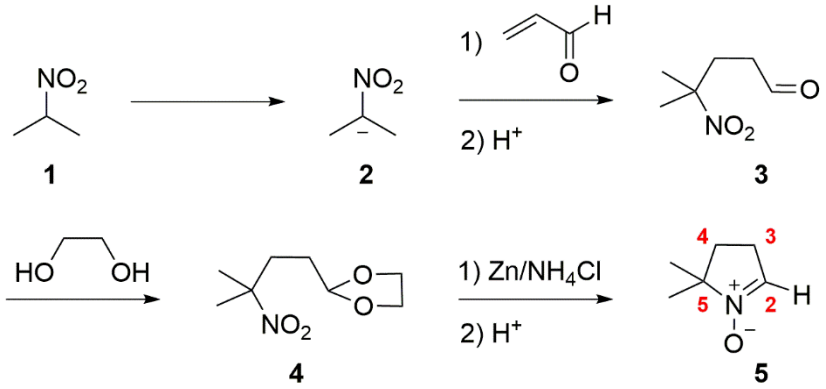

Scheme 9. Synthesis of DMPO by the procedure developed by Bonnett et al.[66]

Various DMPO derivatives have been next synthesized and studied, by introducing different substituents on the carbon-5, carbon-4 or carbon-3 positions, in order to improve the properties and activities towards radicals, more particularly the superoxide radical $O_2^{\bullet-}$.

3.1.1. C5-phosphorylated cyclic nitrones

In 1994, the first member of a new class of DMPO analogues bearing a phosphorylated substituent at the carbon-5 position, the 5-diethoxyphosphoryl-5-methyl-1-pyrroline *N*-oxide (DEPMPO) was synthesized by Tordo and coworkers. DEPMPO (**8**) was obtained from a

two-step procedure (Scheme 10) by first bubbling ammonia into an ethanolic solution of 5-chloropentan-2-one (**6**) and diethyl phosphite. The resulting diethyl (2-methyl-2-pyrrolidinyl)phosphonate (**7**) produced was then oxidized by *m*-chloroperbenzoic acid to DEPMPO (**8**).[25]

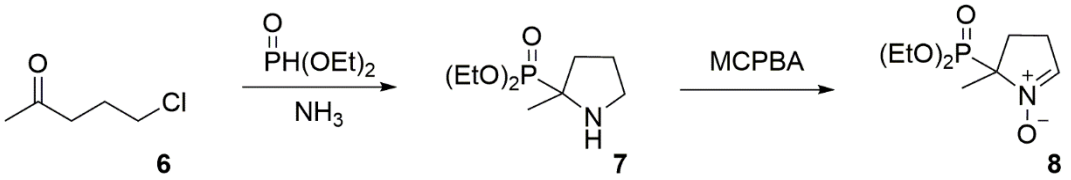

Scheme 10. Synthesis of DEPMPO.

DEPMPO exhibits an octanol-phosphate buffer partition coefficient K_p of only 0.06, very similar to that of DMPO. Its spin-trapping rates for hydroxyl and superoxide radicals were similar to those reported for DMPO. However, the DEPMPO superoxide spin adduct (DEPMPO-O_2H) was significantly more persistent ($t_{1/2}$ = 14.8 min) than that of DMPO ($t_{1/2}$ = 1 min) in phosphate buffer at pH 7, allowing the detection of superoxide during reperfusion experiments performed on ischemic isolated rat hearts.[25,70] The decay of hydroperoxyl spin adduct of DEPMPO and DMPO in buffered solutions was strongly pH-dependent and was slower at acid pH, especially for DEPMPO-O_2H. DEPMPO-O_2H was also more persistent than DMPO-O_2H in organic media with half-lives ranging from 35 to 45 min, which is five times more than those of DMPO. In addition, no paramagnetic species was observed during the decay of DEPMPO-O_2H.[71] In 1997, a study on ischemic isolated rat hearts showed that DEPMPO was able to improve the recovery of post-ischemic heart function.[72] A series of cyclic and acyclic derivatives have been then developed to further improve its properties.

Tordo *et al.* showed that the introduction of a methylene spacer between the nitronyl function and the phosphorylated group greatly decreased the stability of the superoxide adduct formed compared to DEPMPO, suggesting that the electron-withdrawing effect of the phosphorylated group takes part in the stabilization of DEPMPO-O_2H.[73] A derivative bearing two diethoxyphosphorylated groups on the carbon-5 (DEDPPO, **10**) was synthesized by the oxidation of the corresponding aminobis-phosphonate (**9**), previously prepared, with dimethyldioxirane (DMD), as shown in Scheme 11. Unfortunately, DEDPPO (**10**) presented the same limitations in detecting superoxide as those observed with DMPO: a low persistence of the superoxide adduct and a fast decomposition into the hydroxyl adduct. This indicates

that the steric hindrance of the diethoxyphosphorylated group also plays a role in the stabilization of the DEPMPO-O_2H adduct. It was further demonstrated that when only one group is present at C-5, the nitrone adopts low-energy conformations with the phosphorylated group in pseudo-axial position whereas when a second group is introduced in a *gem*-position, one group is forced to occupy a high-energy pseudo-equatorial position.[74]

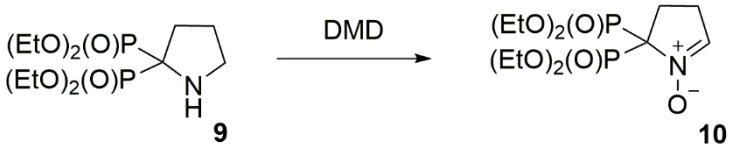

Scheme 11. Formation of the nitronyl function to obtain DEDPPO.

The use of DEPMPO for the detection of radicals in the lipid phase is limited because of its high hydrophilicity. Three derivatives of DEPMPO with increasing degree of lipid solubility have thus been synthesized using the procedure developed by Frejaville *et al.*[25] consisting in oxidation of the corresponding amine with MCPBA: 5-(di-*n*-propoxyphosphoryl)-5-methyl-1-pyrroline *N*-oxide (DPPMPO), 5-(di-*n*-butoxyphosphoryl)-5-methyl-1-pyrroline *N*-oxide (DBPMPO), and 5-(bis-(2-ethylhexyloxy)phosphoryl)-5-methyl-1-pyrroline *N*-oxide (DEHPMPO). DPPMPO and DBPMPO are sufficiently water-soluble to allow an efficient detection of the superoxide radical in phosphate buffer. The stability of their superoxide spin adducts formed was about 30% lower compared to DEPMPO (Table 1) and it was considerably increased in organic solvents. DPPMPO and DBPMPO, as well as DEPMPO itself were also successfully used for the detection of carbon-centered radicals that are generated as secondary products in lipid peroxidation. Due to the presence of hexyl group and very low water-solubility, the use of DEHPMPO was limited to lipid environment only.[75]

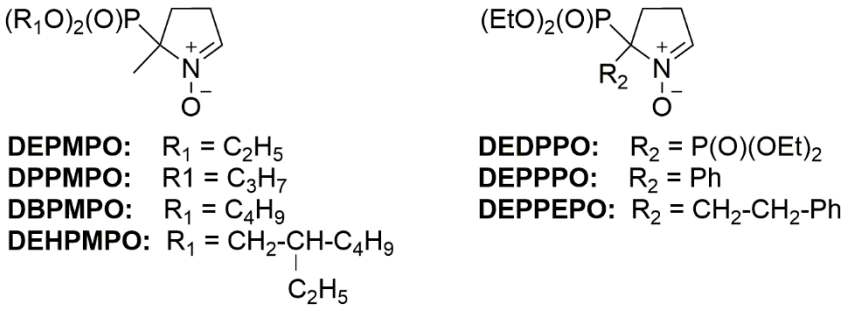

Figure 3. Chemical structure of DEPMPO-type nitrones.

Two other derivatives: 2-(diethoxyphosphoryl)-2-phenyl-3,4-dihydro-2*H*-pyrrole 1-oxide (DEPPPO)[76] and 2-(diethoxyphosphoryl)-2-phenethyl-3,4-dihydro-2*H*-pyrrole-1-oxide (DEPPEPO),[77] bearing bulky groups on the same carbon as the diethoxyphosphoryl group were synthesized in order to evaluate if stereoelectronic effects could influence the stability of the superoxide adduct. For DEPMPO and DEPPEPO, the diethoxyphosphoryl group is preferably in a pseudo-axial geometry, favoring the radical addition on the opposite face due to its bulkiness in this position and making the reaction stereoselective. On the contrary, for DEPPPO, the pseudo-equatorial geometry is favored and the two faces are hindered, making the radical additions not stereoselective and the EPR spectra analysis more complicated. However, the half-lives of DEPMPO, DEPPPO and DEPPEPO superoxide adducts were similar (Table 1), indicating that the conformational geometry of the diethoxyphosphoryl group and the introduction of a phenalkyl group in the carbon-5 position do not influence the stability of the adducts.

Table 1. Octanol-water partition coefficients (K_p) of DMPO-type spin traps and half-lives ($t_{1/2}$) of the superoxide adducts formed in phosphate buffer at pH 7.4.

Nitrone N	Lipophilicity	N-O_2H adduct[a]		Ref
	K_p	[N] (mmol.L^{-1})	$t_{1/2}$ (min)	
DMPO	≤ 0.1	10	0.75	75
DEPMPO	0.1	100	14.8	25,70
DPPMPO	1.4	10	7	75
DBPMPO	13	10	8	75
DEHPMPO	2200	10	nd[b]	75
DEPPPO	2.4	100	13.1	76
DEPPEPO	7.6	50	13.4	77

[a] Superoxide was generated by the xanthine/xanthine oxidase system (Xa/XOD).
[b] Not determined because of a lower spectral resolution.

3.1.2. C5-alkoxycarbonyl cyclic nitrones

2-ethoxycarbonyl-2-methyl-3,4-dihydro-2*H*-pyrrole-l-oxide (EMPO), a DMPO derivative with an electron-withdrawing ethoxycarbonyl group at C-5 was next studied as free radical trap. It was synthesized according to the procedure of Bonnett *et al.* with some modifications (Scheme 12).[78] First, acrolein (**12**) reacted with the anion of ethyl 2-nitropropanoate (**11**), generated *in situ* in the presence of triethylamine, to form ethyl(4-formyl-2-methyl-2-nitro)butanoate (**13**). Then, an aqueous solution of NH_4Cl was added to **13** as well as Zn in

order to reduce the nitro function into hydroxylamine and to obtain EMPO (**14**) after an intramolecular cyclization.

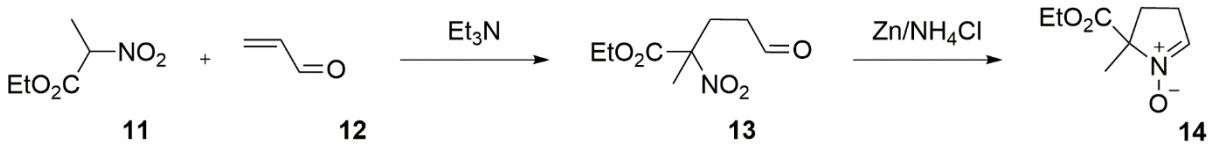

Scheme 12. Synthesis of EMPO.

EMPO exhibited a significantly more persistent superoxide adduct (EMPO-O_2H) than that of DMPO, with a half-life of 4.8 min in phosphate buffer at pH 7, without decomposition into EMPO-OH. In contrast to DEPMPO, EPR spectra of the spin adducts of EMPO are similar to those of DMPO and are very easy to interpret.[78] The apparent rate constants and the stability of hydroxyl adducts of EMPO and DEPMPO were significantly higher compared to DMPO but similar between them (Table 2). Theoretical calculations showed that the presence of electron-withdrawing alkoxycarbonyl and dialkoxyphosphoryl groups improves reactivity towards $HO^{\bullet}$. This could be explained by the more positive charge density on the nitronyl-carbon of the substituted-nitrones compared to DMPO, favoring a nucleophilic addition.[79] The stability of the formed spin adducts may be predicted by looking at the presence of intramolecular H-bonds as well as the relative magnitude of atomic charges on nitronyl-N, -O, C-2 and C-5.[80]

Table 2. Apparent rate constants (k_{app}) and half-lives ($t_{1/2}$) of the adducts N-OH for the spin-trapping of hydroxyl radicals by DMPO, EMPO and DEPMPO.

Nitrone N	N-OH adduct[a]		Ref
	k_{app} (10^{-9} $M^{-1}.s^{-1}$)	$t_{1/2}$ (min)	
DMPO	1.93	0.9	80
EMPO	4.99	2.1	80
DEPMPO	4.83	2.2	80

[a] Hydroxyl radical was generated by the UV photolysis of H_2O_2 and the spin trap concentration was 50 mM.

Considering the benefit obtained by replacing a methyl group by an ester, the nitrone 2,2-diethoxycarbonyl-3,4-dihydro-2*H*-pyrrole-1-oxide (DEPO), bearing two ethoxycarbonyl groups at C-5 position (Figure 4) was later synthesized using the same synthetic route as EMPO from diethyl nitromalonate. It was expected that one ethoxycarbonyl group of DEPO

was in equatorial position and could facilitate the approach of the attacking radical.[81] This was experimentally confirmed with DEPO trapping superoxide in aqueous media at pH 7.2 three times faster than EMPO, its monoester analogue. However, the stability of DEPO-O_2H was found lower than that of EMPO-O_2H, particularly at high nitrone concentration. For example, at a nitrone concentration of 0.01 M, DEPO-O_2H decayed twice faster than EMPO-O_2H. Therefore, EMPO should be preferred to detect superoxide but DEPO is to date the only nitrone described to be capable to detect the superoxide at a concentration lower than 0.005 M.[82] The nitrone 2-(2-ethoxy-2-oxoethyl)-2-(ethoxycarbonyl)-3,4-dihydro-*2H*-pyrrole 1-oxide (EMEPO), another diester analogue of DMPO (Figure 4), was able to significantly reduced $O_2^{\bullet-}$ and elevated NO levels in altered ventricular myocytes, restoring both $O_2^{\bullet-}$ and NO levels and could be used in the treatment of various cardiomyopathies, in which $O_2^{\bullet-}$ and NO levels are altered.[83]

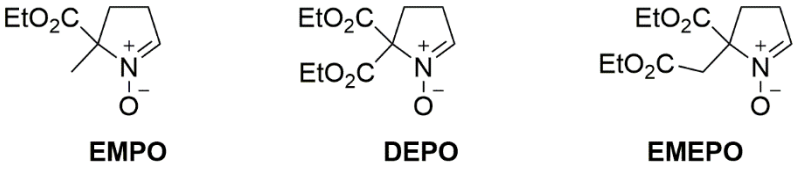

Figure 4. Chemical structure of EMPO, DEPO and EMEPO.

Other EMPO derivatives, where the ethoxycarbonyl group and/or the methyl group were replaced by bulky alkyl substituents were synthesized in analogy to the synthesis of EMPO.[84–88] The rate constants of $O_2^{\bullet-}$ addition were found similar to that of DEPMPO but the stability of the adducts was found higher than that of DEPMPO superoxide adduct for the most sterically hindered substituents (Table 3). For example, tBuMPO-O_2H and iBuMPO-O_2H adducts were more stable than BuMPO-O_2H adduct. The most persistent superoxide adducts were formed with *s*BuMPO and *i*PrEPO.[87,88]

The cytotoxicity of the EMPO derivatives in different human tumour cell lines and in cultured human fibroblasts was studied and the following toxicity rank was obtained: *t*BuMPO > BuMPO > *s*BuMPO > PrMPO > *i*PrMPO ≈ DEPMPO ≈ EMPO.[89] Thanks to their low toxicity and high superoxide-adduct stability, DEPMPO and *i*PrMPO appeared as good candidates for superoxide detection in living cells.

Table 3. Octanol-water partition coefficients (K_p) of EMPO-type spin traps and half-lives ($t_{1/2}$) of the superoxide adducts formed in phosphate buffer at pH 7.4.

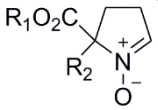

Nitrone N	Structure		Lipophilicity	N-O_2H adduct[a]	Ref
	R_1	R_2	K_p	$t_{1/2}$ (min)	
EMPO	Et	Me	0.15	8.6	85
PrMPO	Pr	Me	0.50	4.6	85
***i*PrMPO**	*i*Pr	Me	0.20	18.8 (or 16.0)	87,88
BuMPO	Bu	Me	1.32	1.1 (or 8.9)	85,87
***s*BuMPO**	*s*Bu	Me	1.06	26.3	88
***t*BuMPO**	*t*Bu	Me	0.80	15.7 (or 22.8)	87,88
EEPO	Et	Et	0.25	18.0	88
PrEPO	Pr	Et	0.78	20.0	88
***i*PrEPO**	*i*Pr	Et	0.66	23.3	88
BuEPO	Bu	Et	2.88	18.0	88
***s*BuEPO**	*s*Bu	Et	1.89	14.1	88
***t*BuEPO**	*t*Bu	Et	1.53	18.2	88
EPPO	Et	Pr	0.81	13.2	88
PrPPO	Pr	Pr	2.64	1.1	88
***i*PrPPO**	*i*Pr	Pr	1.93	0.8	88
BuPPO	Bu	Pr	7.79	0.5	88
***s*BuPPO**	*s*Bu	Pr	5.73	15.5	88
***t*BuPPO**	*t*Bu	Pr	2.69	13.5	88

[a] Superoxide was generated by the xanthine/xanthine oxidase system (Xa/XOD) and the spin trap concentration was 40 mM.

Stolze *et al.* synthesized in 2005 another series of lipophilic EMPO derivatives bearing a butyl side chain at C-5 position as well as a series of 3,5- and 4,5-dimethylated pyrroline derivatives (Table 4). The superoxide adducts obtained with the derivatives bearing an extra methyl group at C-3 or C-4 position were very stable in aqueous media ($t_{1/2}$ = 12-55 min).[90,91] The persistence of the superoxide adducts of *trans*-3,5-EDPO, *trans*-DPPO and *trans*-DIPPO even exceeded those of *i*PrMPO and DEPMPO, probably thanks to steric shielding rather than electronic effects as already mentioned previously.[88] The diastereomers exhibited significantly different spin adduct stabilities, with the half-lives of *cis*-3,5-EDPO and *trans*-

3,5-EDPO being 11.5 and 44.2 min, respectively. These derivatives were also able to detect various oxygen- and carbon-centered radicals.[91]

Table 4. Octanol-water partition coefficients (K_p) of another series of EMPO-type spin traps and half-lives ($t_{1/2}$) of the superoxide adducts formed in phosphate buffer at pH 7.4.

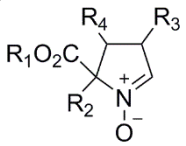

Nitrone N	Structure				Lipophilicity	N-O_2H adduct[a]	Ref
	R_1	R_2	R_3	R_4	K_p	$t_{1/2}$ (min)	
EBPO	Et	Bu	H	H	4.92	4.2	90
PBPO	Pr	Bu	H	H	14.48	0.36	90
***i*PBPO**	*i*Pr	Bu	H	H	11.79	15.8	90
BBPO	*n*Bu	Bu	H	H	55.62	6.4	90
***s*BBPO**	*s*Bu	Bu	H	H	39.03	6.8	90
***t*BBPO**	*t*Bu	Bu	H	H	22.75	17.6	90
3-BEMPO	Et	Bu	Me	H	10.84	47.2	90
4-BEMPO	Et	Bu	H	Me	10.33	36.2	90
3,5-EDPO	Et	Me	Me	H	0.45 (*cis*-) 0.46 (*trans*-)	11.5 (*cis*-) 44.2 (*trans*-)	91
4,5-EDPO[b]	Et	Me	H	Me	0.44	44.6	91
3,5-DPPO	Pr	Me	Me	H	1.66 (*trans*-)	47.3 (*trans*-)	91
4,5-DPPO[c]	Pr	Me	H	Me	1.36	47.0	91
3,5-DIPPO[d]	*i*Pr	Me	Me	H	0.90 (*cis*-) 1.12 (*trans*-)	nd[f] (*cis*-) 55.0 (*trans*-)	91
4,5-DIPPO[e]	*i*Pr	Me	H	Me	1.03	42.8	91

[a] Superoxide was generated by the xanthine/xanthine oxidase system (Xa/XOD) and the spin trap concentration was 40 mM.
[b] *cis*/*trans* = 21/79.
[c] *cis*/*trans* = 29.6/70.4.
[d] ca. 95% *cis* form.
[e] *cis*/*trans* = 24/76.
[f] not determined.

The cytotoxicity effects of the 3- and 4-methylated pyrroline derivatives were investigated in three different cell types (primary rat hepatocytes and cultured human colon carcinoma SW480 cells and hepatocarcinoma HepG2 cells). The derivatives 3-BEMPO, 4-BEMPO and 4,5-DPPO exhibited high toxicity even at a concentration of 10 mM and therefore are not suitable for radical detection in living cells. On the contrary, the low toxicity of *cis*-3,5-EDPO, 4,5-EDPO and 3,5-DIPPO make them good candidates for superoxide detection in

living cells.[92] A series of 5-phenyl- and 5-*n*-pentyl pyrroline derivatives was also synthesized,[93] as well as several ethyl- and hydroxymethyl-substituted EMPO derivatives[94,95] but without improving the spin-trapping properties compared to previous spin traps.

To conclude, compared to their α-phosphorylated analogues, ester-nitrones present certain advantages: they are often easily synthesized at high purity, yields adducts with simpler EPR spectra and as persistent as DEPMPO-O_2H for some derivatives.

3.1.3. C5-carbamoyl cyclic nitrones

In 2004, Villamena *et al.* predicted with a computational approach that 5-carbamoyl-5-methyl-1-pyrroline *N*-oxide (AMPO), bearing a carbamoyl substituent at C-5 position, could be a good spin trap towards nucleophilic radicals such as superoxide and could form stable spin adducts due to the high positive charge on the nitronyl-carbon.[79] AMPO (**15**) was later synthesized from EMPO (**14**) by adding ammonium hydroxide (Scheme 13). It is a solid which is easily purified, affording paramagnetic impurity free samples.[96] Its partition coefficient value K_p is similar to that of DMPO and DEPMPO.[97] AMPO exhibited characteristic EPR spectra with various radicals, allowing for example an easy differentiation between AMPO-O_2H and AMPO-OH spectra. The half-life of AMPO-O_2H adduct in phosphate buffer at pH 7.2 ($t_{1/2}$ = 8.3 min) was much longer than that of DMPO-O_2H ($t_{1/2} \approx 1$ min), similar to that of EMPO-O_2H ($t_{1/2}$ = 9.9 min) but shorter than that of DEPMPO-O_2H ($t_{1/2}$ = 15.5 min).[96]

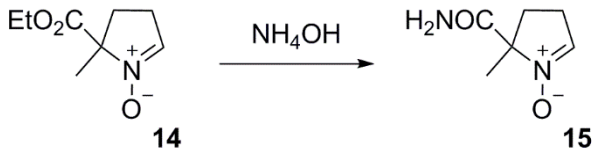

14 **15**

Scheme 13. Synthesis of AMPO.

Using density functional theory (DFT) calculations and stopped-flow kinetics, Villamena *et al.* demonstrated that the use of *N*-monoalkylsubstituted amide or an ester as substituents at C-5 may improve the spin-trapping properties and allow target specificity using specific ligand. This could be used to detect radicals *in vivo* at the site of superoxide formation. The positive charge on the nitronyl-carbon and the presence of strong intramolecular H-bonds between the

hydroperoxyl-H and the carbonyl-O in the transition state for these derivatives facilitate the superoxide adduct formation.[98,99]

A series of AMPO derivatives bearing different 5-alkyl substituents were then synthesized by Stolze *et al.* using the same synthetic route as AMPO, which consists in first obtaining the corresponding EMPO-type derivative and then reacting it with aqueous ammonia. The half-lives of their superoxide adducts were slightly higher than that of EMPO, with the most stable adduct CAEPO-O_2H being as persistent as DEPMPO-O_2H (Table 5). The hydroxyl adducts of AMPO, CAEPO and CAPPO were stable for 30 min or more, whereas the respective adducts of CABPO and CAPtPO were only stable for a couple of minutes, forming unknown secondary products. The derivatives trapped effectively carbon-centered radicals but for methoxyl and ethoxyl radicals, the adducts were unstable and difficult to detect.[100]

Table 5. Octanol-water partition coefficients (K_p) of AMPO-type spin traps and half-lives ($t_{1/2}$) of the superoxide adducts formed in phosphate buffer at pH 7.4.

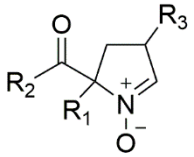

Nitrone N	Structure			Lipophilicity	N-O_2H adduct[a]	Ref
	R_1	R_2	R_3	K_p	$t_{1/2}$ (min)	
AMPO	Me	NH_2	H	0.016	8.58	100
CAEPO	Et	NH_2	H	0.056	16.76	100
CAPPO	Pr	NH_2	H	0.211	10.40	100
CABPO	Bu	NH_2	H	0.668	10.65	100
CAPtPO	Pent	NH_2	H	2.72	11.13	100
CADMPO	Me	NH_2	Me	0.049	nd[b] (14.5)[c]	101
DMMCAPO	Me	$NH(CH_3)$	Me	0.068	11.2 (10.1)[c]	101
CAEMPO	Me	NH_2	Et	0.143	nd[b] (17.4)[c]	101
EMMCAPO	Me	$NH(CH_3)$	Et	0.216	36.6[d] (19.8)[c]	101

[a] Superoxide was generated by the xanthine/xanthine oxidase system (Xa/XOD) and the spin trap concentration was 20 mM.
[b] Not determined as none of the species observed could be attributed to a superoxide adduct.
[c] KO_2 system at a spin trap concentration of 40 mM.
[d] Sum of $^{\bullet}O_2H$ and $^{\bullet}OH$ signals.

Another series of AMPO derivatives with an additional methyl or ethyl substituent at C-3 position and with the carbamoyl group being replaced by a methylcarbamoyl substituent was

also synthesized (Table 5). These derivatives are not appropriate for the detection of superoxide due to the presence of different isomers and secondary products (Hofmman degradation products and hydroxyl radical adducts) that make the interpretation of their EPR spectra difficult. In addition, Hofmann degradation products were also observed for hydroxyl radical detection with CADMPO and CAEMPO. However, these AMPO derivatives trap effectively carbon-centered radicals, and allow the distinction between small radicals (methyl, hydroxymethyl, hydroxyethyl and carbon dioxide anion radicals) as the ratio between their two major diastereomers strongly depends on the size of the trapped radical.[101]

3.1.4. Other DMPO-type nitrones

The bicylic nitrone 1,3,3-trimethyl-6-azabicyclo[3.2.1]oct-6-ene-*N*-oxide (Trazon) is a crystalline solid with an excellent stability and thanks to long-range hyperfine splitting constants and the presence of distinguishable stereoisomers, the EPR spectra of Trazon spin adducts provided additional structural informations compared to DMPO and DEPMPO.[102] The Trazon spin adducts formed with alkoxyl radicals were more stable than those previously reported for DMPO and more selective for detection in lipid phases than PBN. Trazon can then be recommended for the detection of lipid-derived alkoxyl radicals formed during lipid peroxidation. However, Trazon-O_2H was poorly stable ($t_{1/2}$ = 3.6 min), making Trazon not suitable for the superoxide detection.[85]

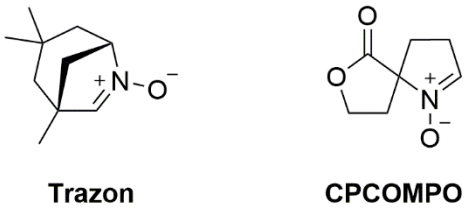

Figure 5. Chemical structure of Trazon and CPCOMPO.

The 6,7-oxa-1-azaspiro[4.4]-non-1-en-6-one 1-oxide (CPCOMPO), a cyclic nitrone with a rigid spirolactonyl hydrogen-bond acceptor at C-5 position, was computationally analyzed and was expected to have a high rate constant for the trapping of superoxide.[79,98,103] This was further confirmed with the highest rate constant for the superoxide addition so far observed at neutral pH for any nitrones (k_t = 60 $M^{-1}.s^{-1}$). However, the half-life of CPCOMPO-O_2H was only ≈ 2.4 min, probably because of the presence of a rigid H-bond acceptor.[103]

3.2. PBN-type derivatives

PBN (**17**) was first synthesized in 1957 by condensation of benzaldehyde (**16**) with *tert*-butylhydroxylamine (Scheme 14).[104] The ease of preparation of α-aryl-*tert*-butyl-nitrones by this method and the availability of a wide variety of aromatic aldehydes makes this class of nitrones ideal for exploring the influence of chemical modifications on the reactivity of the nitrone. Alternative synthetic methods have also been employed to synthesize PBN and its aryl-derivatives. One of them involves the condensation of *tert*-butylamine with the desired aldehyde, followed by an oxidation of the imine thus obtained (**18**) with peracetic acid to form an oxazirane (**19**). Finally, after a rearrangement, the desired nitrone (**17**) is obtained (Scheme 14).[104] However, the overall yields of this synthetic route are generally low and the oxidation step requires the use of a solution of 90% H_2O_2 which is potentially explosive. Another synthetic method used is the one-step reduction/condensation of nitro precursors in the presence of metallic zinc and AcOH (Scheme 14).[49]

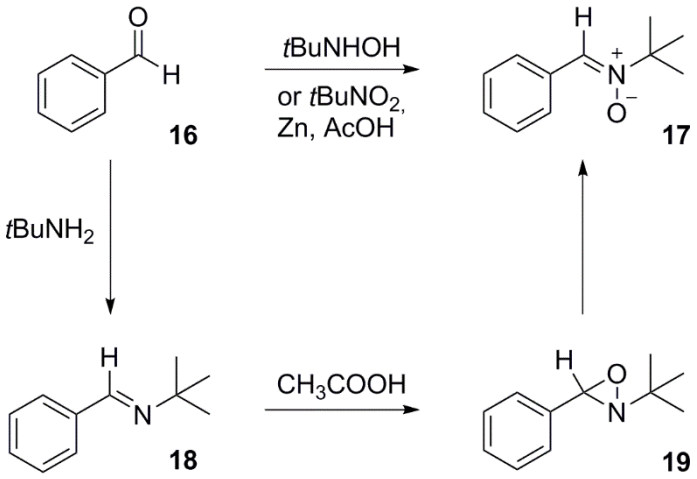

Scheme 14. Synthetic routes of PBN.

3.2.1. Introduction of various substituents on the phenyl ring

Over the past years, PBN derivatives bearing various substituents on the phenyl ring of the molecule, mostly in *para*, have been developed in order to identify the most promising group for improved and optimal spin-trapping and biological activities. This would also provide a wide range of derivatives with different properties (water solubility, lipophilicity). In order to be able to selectively choose a spin trap depending on the type of radical we want to trap

(lipid-soluble or water-soluble), the octanol/water partition coefficients log *P* of substituted PBN derivatives were reported by Janzen *et al.*[105]

With regards to the spin-trapping activity, it has been shown that the electronic nature of the substituent has an influence on the EPR spectra of the radical adducts. In particular, the substituent effects on the EPR hyperfine splitting constants (hfsc's) have been investigated in various radicals.[51,106,107] Both the nitrogen and the hydrogen hfsc's decrease when the electron-withdrawing nature of the substituent increases. This could be due to a higher contribution of the resonance form B compared to form A in the presence of electron-withdrawing group (Scheme 15), resulting in the decrease of spin density on nitrogen.[51,108] Linear correlations between the nitrogen hfsc's and the Hammett constants of *para*- and *meta*-substituents (σ_p/σ_m) have been highlighted but it is not necessarily the case for the hydrogen hfsc's due to a through-space dipole-dipole interaction between the benzylic C-H bond and the substituents. This has an influence on the spin density at the hydrogen and affects the coupling between the hydrogen and the radical.[106]

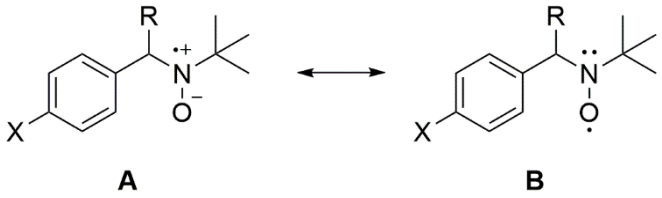

Scheme 15. Resonance structures for 4-X-PBN-R adducts.

It has also been demonstrated that the nature of the substituent influences the trapping rate of the nitrones. Janzen and Evans studied the trapping of *tert*-butoxy and benzoyloxy radicals by EPR and found a smaller effect of the substituents for the former radical[109] compared to the latter,[110] demonstrating that the substituent effect depends on the studied radical. An electron-donating group in the *para*-position enhances the trapping rate of electrophilic radicals whereas the presence of an electron-withdrawing group increases the trapping rate of nucleophilic radicals. This trend was then confirmed by several spin-trapping studies on various radicals that followed Hammett's equation with good correlations between the trapping rates and σ_p. It has been established that positive values of the slope ρ are due to the nucleophilic character of the radicals as observed for *n*-alkyl,[111,112] α-hydroxyalkyl,[113,114] hydroxyl and phenyl radicals[115] whereas negative slopes are due to electrophilic radicals such as *tert*-butoxyl radicals.[116] The work of Hirota and co-workers on the trapping of substituted

phenyl free radicals by PBN derivatives showed that an electron-deficient aryl free radical reacts favourably with an electron-rich spin trap, and *vice versa*. They demonstrated by molecular-orbital calculations that the mechanism involves the participation of an electron-transfer between the frontier orbitals of the reactants, which is favourable when the energy difference between the two orbitals is as small as possible.[116,117] In the case of *ortho*-substituents on the phenyl ring of the PBN-type nitrone not only an electronic effect occurs but also a steric contribution.

A computational approach was used to investigate the polar effect of the substituents on the partial charges of the nitronyl atoms and good correlations between the σ_p and the partial charges have been observed.[108] In the case of superoxide[108] and unsubstituted phenyl radicals[114] no correlation was observed between the rate constants of *para*-PBN derivatives and charge densities or σ_p values, showing the absence of any marked polar effect. It was concluded that these two radicals are intermediate cases. On the contrary, $HO_2^{\bullet}$ addition to nitrones appeared more favoured when the nitronyl-carbon partial charge is lower, suggesting that this reaction is electrophilic in nature. The trapping rate of this reaction was increased in the presence of electron-withdrawing substituents, which is inconsistent with the conclusions reported in the literature that suggested a positive ρ value may be due to the nucleophilic character of the radical. This demonstrated that the sign of ρ value is generally not dependent on the intrinsic characteristic of the radical itself but on the nature of the radical addition.

3.2.2. α-phosphorylated linear nitrones

DEPMPO, a DMPO derivative with a diethoxyphosphoryl group at C-5 position, gives rise to a very persistent superoxide-adduct both in aqueous and organic media.[71] Moreover, the EPR spectra of the spin adducts obtained with DEPMPO provide additional information due to the large phosphorus coupling. DEPMPO is therefore a promising candidate for the detection of oxygen-centered radicals but it is not recommended for the detection of lipophilic radicals because of its weak lipophilicity (K_p = 0.1) compared to PBN (K_p = 10.4). For these reasons, Tordo and co-workers synthesized in 1995 three phosphorylated linear nitrones derived from PBN and *α*-(1-oxidopyridin-1-ium-4-yl)-*N*-*tert*-butylnitrone (4-PyOBN), a pyridine analogue of PBN, namely: *N*-benzylidene-1-diethoxyphosphoryl-1-methylethylamine *N*-oxide (PPN, **23**), 1-diethoxyphosphoryl-1-methyl-*N*-[(1-Oxidopyridin-1-ium-4-yl)methylidene]ethylamine

N-oxide (4-PyOPN, **24**) and *N*-4-chloro-benzylidene-1-diethoxyphosphoryl-1-methylethylamine *N*-oxide (4-Cl-PPN, **25**). These derivatives were prepared from the oxidation of 1-amino-1-methyl phosphonate (**21**) to 1-methyl-1-nitroethyl phosphonate (**22**). Then, a one-pot reduction/condensation of **22** onto the appropriate aldehyde in the presence of Zn and a weak acid gave the desired nitrone (**23**-**25**), as shown in Scheme 16.[118,119] PPN, 4-PyOPN and 4-Cl-PPN showed efficient trapping of oxygen-centered radicals both in aqueous and organic media[118,119] with a better stability of the corresponding superoxide-adducts compared to PBN and 4-PyOBN (Table 6). For example, PBN-O_2H EPR signal decreased 3.3 times more rapidly in DMF than its phosphorylated analogue.[120]

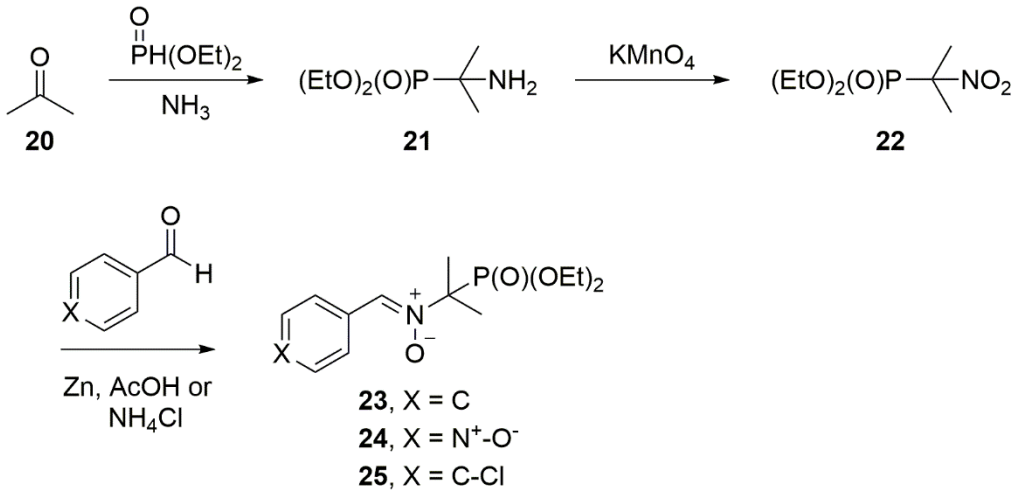

Scheme 16. Synthesis of PPN, 4-PyOPN and 4-Cl-PPN.

Liu *et al.* have shown with an examination of the optimized geometries of the derivative 4-HO-PPN and PBN that the introduction of a phosphorylated group efficiently stabilizes the superoxide spin adduct through strong-intramolecular interactions (H-bonds and non-bonding attractive interactions), as well as a larger steric protection.[121] Otherwise, the presence of an additional hfsc due to the coupling with the phosphorus atom allows an easier distinction between hydroxyl and hydroperoxyl radical adducts. PPN, 4-PyOPN and 4-Cl-PPN were also efficient spin traps for various carbon-centered radicals in buffered solution with spectra characteristic of the added radical.[119]

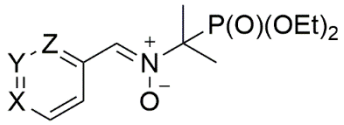

	X	Y	Z
PPN:	CH	CH	CH
4-PyOPN:	N^+-O^-	CH	CH
4-Cl-PPN:	C-Cl	CH	CH
4-HO-PPN:	C-OH	CH	CH
2-PyPN:	CH	CH	N
3-PyPN:	CH	N	CH
4-PyPN:	N	CH	CH
4-NO_2-PPN:	C-NO_2	CH	CH

Figure 6. Chemical structure of PPN-type nitrones.

In 1997, eight new α-phosphorylated spin traps were synthesized using an improved synthetic method (Scheme 17): the direct condensation of the appropriate benzaldehyde with diethyl [1-hydroxyamino)-1-methylethyl]phosphonate (**26**), first prepared following the procedure of Petrov *et al.*[122] The octanol-phosphate buffer partition coefficient of these PPN-type derivatives, *i.e.* K_p, was determined by HPLC and showed that the nature of the aromatic ring alters significantly the lipophilicity (Table 6). Furthermore, it was found that these PPN-type nitrones trap a large variety of carbon-centered radicals with characteristic EPR spectra. It also appeared that small changes in the aromatic moiety of the nitrone could induce important modifications in the EPR spectra of the spin adducts. However, among this series no nitrone proved to efficiently trap superoxide and hydroxyl radicals in aqueous environnement.[123]

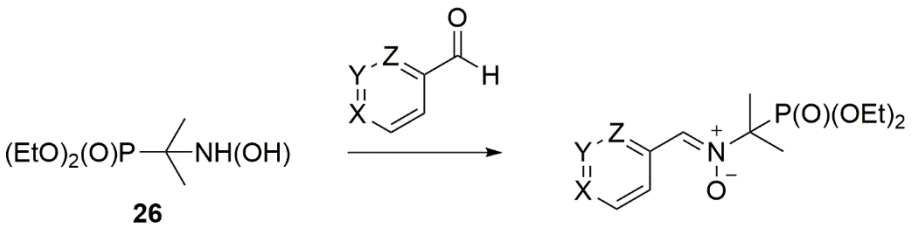

Scheme 17. Improved synthetic route of PPN derivatives.

Table 6. Partition coefficient (K_p) of PPN-type nitrones and half-lives ($t_{1/2}$) of the nitrone-superoxide spin adducts determined in organic media or aqueous environment at pH 5.8.

Nitrone N	**Lipophilicity**	**$t_{1/2}$ of N-O_2H adduct[a] (min)**			**Ref.**
	***K*$_p$**	**DMF**	**Pyridine**	**Phosphate Buffer**	
PPN	10.2	13.8	19.0	5.1	120,123
4-PyOPN	0.21	16.2	21.1	7.1	120,123
4-Cl-PPN	273.3	15.2	20.2	nd[b,c]	120,123
PBN	10.4	4.2	4.4	nd[b,c]	120,124
4-PyOBN	0.09	5.1	5.2	0.3	120,124
DMPO	0.08	7.6	5.2	1.1	120,124
4-HO-PPN	nd[b]	nd[b]	nd[b]	8.8	121
2-PyPN	4.8	nd[b]	nd[b]	nd[b,c]	123
3-PyPN	2.6	nd[b]	nd[b]	nd[b,c]	123
4-PyPN	2.1	nd[b]	nd[b]	nd[b,c]	123
4-NO_2-PPN	26.9	nd[b]	nd[b]	nd[b,c]	123

[a] Superoxide was generated with a light-lumiflavin-DTPA system and the nitrone concentration was 100 mM except for 4-HO-PPN (45 mM).
[b] Not determined.
[c] The EPR signals observed were too weak to be correctly analysed.

In order to increase the spin-trapping ability of PPN-type nitrones, Tuccio *et al*. synthesized and characterized four new poly(α-phosphorylated nitrones): the 1,3,5-tris[*N*-(1-diethylphosphono-1-methylethyl)-*N*-oxidoiminiomethyl]benzene (TN), the 1,3-bis[*N*-(1-diethylphosphono-1-methylethyl)-*N*-oxidoiminiomethyl]benzene (MDN), the 1,4-bis[*N*-(1-diethylphosphono-1-methylethyl)-*N*-oxidoiminiomethyl]benzene (PDN), and the 1,2-bis[*N*-(1-diethylphosphono)-1-methylethyl)-*N*-oxidoiminiomethyl]benzene (ODN). These derivatives were obtained by direct condensation of diethyl [1-(hydroxyamino)-1-methylethyl]phosphonate (**26**)[122] with the corresponding poly-aldehyde.[125] They are more lipophilic than DMPO, PBN and PPN (Table 7). ODN did not trap efficiently carbon-centered radicals compared to TN, MDN and PDN. The superoxide adduct decay for TN, MDN and PDN was studied at pH 5.8 and 7.2 (Table 7). No significant change was observed between the two pH, contrary to DMPO, DEPMPO or EMPO. Their half-lives were significantly longer than those observed for DMPO-O_2H ($t_{1/2}$ = 50 s at pH = 7),[71] EMPO-O_2H ($t_{1/2}$ = 4.8 min at pH = 7)[78] and PPN-O_2H ($t_{1/2}$ = 5.1 min at pH = 5.6).[120] However, DEPMPO-O_2H remained the most persistent superoxide adduct ($t_{1/2}$ = 13 min at pH = 7).[71] These three nitrones failed to trap $HO^{\bullet}$, which decomposes rapidly in aqueous media.[125]

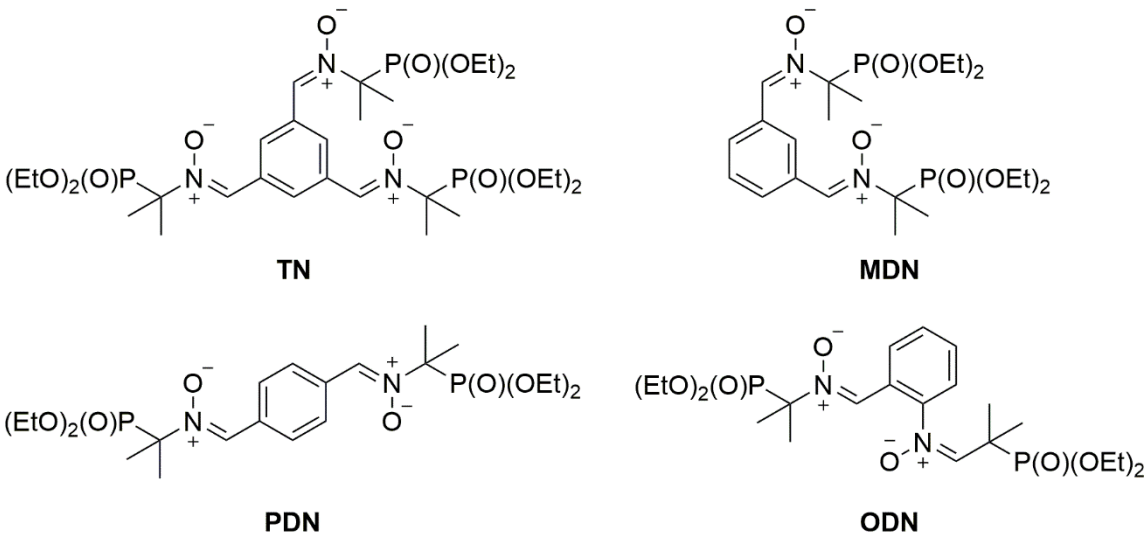

Figure 7. Chemical structure of TN, MDN, PDN and ODN.

Table 7. Partition coefficient (K_p) of poly-α-phosphorylated nitrones and half-lives ($t_{1/2}$) of the nitrone-superoxide spin adducts determined in phosphate buffer at pH 5.8 and 7.2.

Nitrone N	**Lipophilicity**	**$t_{1/2}$ of N-O_2H adduct[a] (min)**		**Ref.**
	***K*$_p$**	**pH 5.8**	**pH 7.2**	
TN	> 300	5.3	5.2	125
MDN	20	8.4	6.6	125
PDN	65	11.6	10.5	125
ODN	11.5	nd[b]	nd[b]	125

[a] Half-life time ($t_{1/2}$) of the nitrone-superoxide adducts. Superoxide was generated with a light-lumiflavin-DTPA system and the nitrone concentration was 5 mM.
[b] Not determined due to complex EPR spectra with this spin trap.

More recently, Pietri and co-workers synthesized novel PPN derivatives bearing various substituted aromatic ring inspired from phenolic acids. Among the whole series, four derivatives deriving from caffeic, gallic, ferulic and sinapic acids emerged as potential drug candidates with vasorelaxant activity and significant protection against ROS-induced vascular protein oxidation.[126]

3.2.3. α-alkoxycarbonyl linear nitrones

In 1993, the nitrone *N*-2-(2-ethoxycarbonyl-propyl) α-phenylnitrone (EPPN, **29**), the linear derivative of EMPO, bearing an ethoxycarbonyl group in the α-position of the nitronyl function was synthesized by Kliegel *et al.* (Scheme 18).[127] First, ethyl 2-bromo-2-

methylpropionate (**27**) was converted to ethyl 2-methyl-2-nitropropionate (**28**) in the presence of sodium nitrite. Then, EPPN (**29**) was obtained by the one-pot reduction/condensation of **28** onto the benzaldehyde in the presence of Zn and NH_4Cl. When compared to their α-phosphorylated analogues, α-alkoxycarbonyl nitrones present some advantages: they are easily synthesized with high purity and yield adducts with simpler EPR spectra.

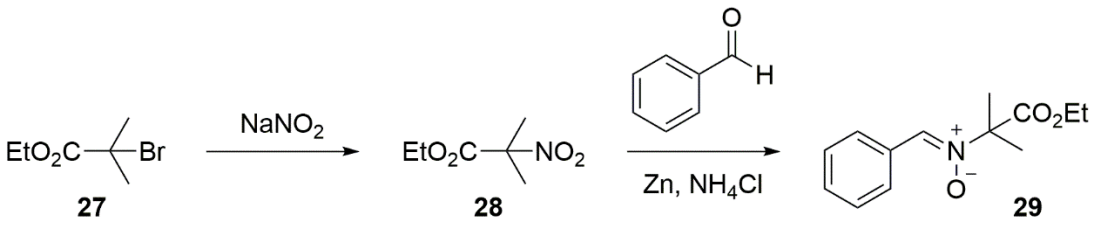

Scheme 18. Synthesis of EPPN.

The octanol-phosphate buffer partition coefficient K_p of EPPN is 29.8, showing that EPPN is more lipophilic than PBN. It is also easily solubilized in water up to 60 mmol/L. It failed to trap hydroxyl radical in aqueous environment but it is a very efficient tool for the detection of carbon-centered radicals. The half-life $t_{1/2}$ of the superoxide adduct EPPN-O_2H in aqueous milieu was 6.8 min at pH 5.8 and 5.3 min at pH 7.[128] EPPN-O_2H was more persistent than the superoxide adducts of DMPO, EMPO, PBN, POBN and PPN but DEPMPO-O_2H remains the more stable superoxide adduct of all these derivatives. As observed with the PPN-type nitrones, it appeared that the presence of an electron-withdrawing group in the α-position of the nitronyl function greatly enhances the superoxide adduct stability.

Tuccio and co-workers then prepared two new nitrones derived from EPPN: *N*-benzylidene-1,1-bis(ethoxycarbonyl)ethylamine *N*-oxide (DEEPN) and *N*-[(1-oxidopyridin-1-ium-4-yl)methylidene]-1-ethoxycarbonyl-1-methylethylamine *N*-oxide (EPPyON). For the nitrone EPPyON, the replacement of the phenyl ring by a more polar oxidopyridinium group enhanced the hydrophilicity, making this spin trap more suitable for aqueous phase (Table 8). Like many other nitrones, DEEPN and EPPyON efficiently trapped carbon-centered radicals in aqueous media. However, the identification of the radical trapped was cumbersome due to small a_H variations. Like EPPN, DEEPN and EPPyON failed to trap hydroxyl radical in aqueous environment but their superoxide adducts decayed less rapidly than most adducts previously synthesized, showing that the presence of a second electron-withdrawing ethoxycarbonyl group, and to a lesser extent the replacement of a phenyl ring by an

oxidopyridinium group, enhanced the stability of the superoxide spin adduct (Table 8). DEEPN is the most efficient derivative of the PBN series and could present interesting biological applications.[129] In view of these results, the nitrone *N*-[(1-oxidopyridin-1-ium-4-yl)-methylidene]-1,1-bis(ethoxycarbonyl)ethylamine *N*-oxide (DEEPyON) that bears an oxidopyridinium and two ethoxycarbonyl groups was then synthesized. DEEPyON was found to trap efficiently carbon-centered and superoxide radicals in aqueous media but the presence of a second ethoxycarbonyl group resulted in the decrease in the superoxide trapping rate, while an opposite effect was observed with cyclic nitrones.[82]

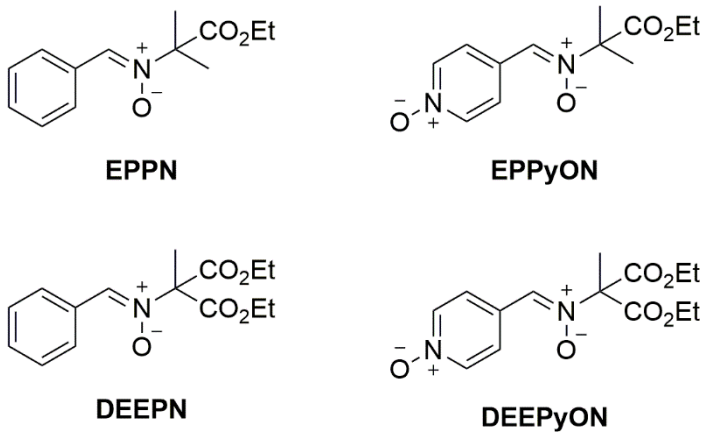

Figure 8. Chemical structure of EPPN, DEEPN, EPPyON and DEEPyON.

In order to optimize the structure of EPPN derivatives, Stolze *et al.* synthesized two series of analogues using the same synthetic route of EPPN. In the first series they replaced the ethoxy group by a propoxy (PPPN), *iso*-propoxy (*i*PPPN), *n*-butoxy (BPPN), *sec*-butoxy (*s*BPPN) and *tert*-butoxy moiety (*t*BPPN), increasing the lipophilicity (Figure 9). Unfortunately, these derivatives are not suitable for the detection of oxygen-centered radicals as their superoxide adducts are not stable enough (Table 8) and they failed to trap hydroxyl radicals.[130] In the second series the phenyl ring was replaced by 2-, 3-, and 4-pyridinyl substituents and the ethoxy group by propoxy, *iso*-propoxy and cyclopropylmethoxy moiety (Figure 9). All the derivatives formed stable superoxide with half-lives ranging from 4.6 to 10.7 min, which are more stable than the respective adducts of the phenyl derivatives. Only the superoxide adducts of EMPO and DEPMPO are more stable.[131]

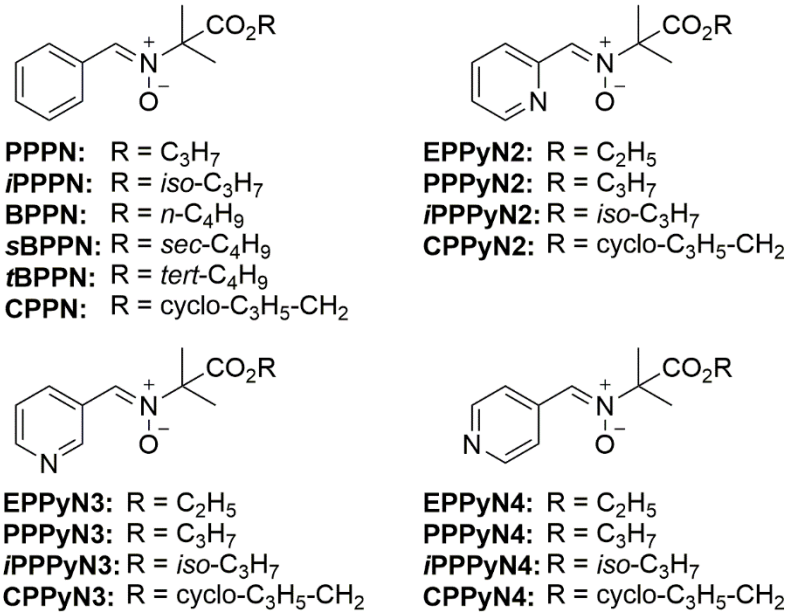

Figure 9. Chemical structure of EPPN-type spin traps.

Table 8. Octanol/Phosphate buffer partition coefficients K_p of EPPN-type nitrones and half-lives ($t_{1/2}$) of their superoxide adducts in aqueous media at pH 7.

Nitrone N	Lipophilicity	N-O_2H adduct[a]		Ref
	K_p	[N] (mmol.L^{-1})	$t_{1/2}$ (min)	
EPPN	29.8	10	5.3	128
DEEPN	4.8	10	15.8	129
EPPyON	0.33	10	6.2	129
PPPN	57	20	3.5	130
***i*PPPN**	60	20	5.4	130
BPPN	219	20	<1	130
***s*BPPN**	207	20	2.5	130
***t*BPPN**	145	20	≈ 1[b]	130
CPPN	72.6	20	4.1	131
EPPyN2	7.2	20	5.8	131
PPPyN2	23.2	20	4.6	131
***i*PPPyN2**	25.1	20	7.5	131
CPPyN2	19.4	20	8.5	131
EPPyN3	2.4	20	10.7	131
PPPyN3	7.9	20	10.1	131
***i*PPPyN3**	5.5	20	9.6	131
CPPyN3	10.0	20	10.2	131
EPPyN4	3.7	20	7.3	130
PPPyN4	12.7	20	6.1	131
***i*PPPyN4**	8.2	20	6.5	131
CPPyN4	11.9	20	6.4	131

[a] Superoxide was generated by the xanthine/xanthine oxidase system (Xa/XOD)
[b] Approximated value due to the formation of decomposition products.

3.2.4. Other PBN derivatives modified on the N-tert-butyl function

A series of PBN derivatives bearing one, two or three substituents (hydroxyl, ester, amide and carbamate) on the *N-tert*-butyl group (Figure 10) were synthesized by our group, offering an opportunity for conjugating the spin trap to target-specific ligands. These derivatives were obtained by the one-pot reduction/condensation of nitro precursors onto the commercially available benzaldehyde in the presence of Zn and AcOH. The substituent effect was demonstrated by a computational approach, where a positive increase of the nitronyl-C partial charge was observed for poly β-substituted compounds, suggesting better trapping of nucleophilic radicals. The *in vitro* cytoprotective activity of these derivatives against H_2O_2-induced cell death was measured on bovine aortic endothelial cells (BAEC). The most promising derivative of the series was PBN-CH_2NHAc, making the amide bond an efficient linker for further functionalization of PBN-type nitrones. This study confirmed that the choice of the substituent on the *N-tert*-butyl group is of high importance in the design of nitrones.[132]

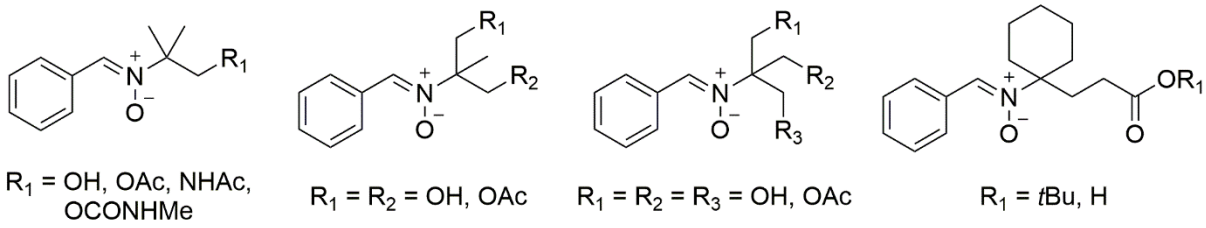

Figure 10. Chemical structure of mono-, di-, and tri-N-tert-butyl-substituted and N-cyclohexyl PBN derivatives.

Two bi-functional *N*-cyclohexylnitrones (Figure 10) were also synthesized with the expectation that the cycloaryl ring will enhance the lipophilicity of the molecule as well as the reactivity of the nitronyl function and the stability of the spin adducts formed due to restricted rotation and higher accessibility. Kinetics of superoxide-adduct decay showed that the presence of a cyclohexyl ring enhances the half-life of the $HO_2^{\bullet}$ adduct ($t_{1/2}$ = 5.5 and 6.7 min) compared to PBN ($t_{1/2}$ = 3.1 min).[133]

4. NITRONES AS NEUROPROTECTIVE AGENTS

4.1. Sulfophenyl substituted PBN

Two derivatives bearing sulfonate groups on the phenyl ring of the PBN have been developed to improve water solubility: an *ortho*-monosubstituted derivative called sodium 2-sulfophenyl-*N*-*tert*-butylnitrone (S-PBN) and a di-substituted derivative called disodium 2,4-disulfophenyl-*N*-*tert*-butylnitrone (NXY-059) (Figure 11). S-PBN and NXY-059 were able to trap oxygen- and carbon-centered radicals and to form stable adducts to allow EPR detection and characterization.[134] The derivative NXY-059 had the same efficacy as PBN in trapping radicals but it was more effective as an anti-ischemic agent. It also showed a much longer window of opportunity for administration after a stroke.[135] It has been shown to be a significantly efficient neuroprotective against stroke in both rat and primate models and it was the first neuroprotective compound to be examined clinically.[136] NXY-059 reached phase III clinical trials in the USA and two major studies were conducted, coded SAINT I[137] and SAINT II[17] respectively for Stroke-Acute Ischemic NXY Treatment. Unfortunately, in the SAINT II trail, it has been demonstrated that NXY-059 is ineffective for the treatment of acute ischemic stroke as no significant differences with the placebo group were observed.[18]

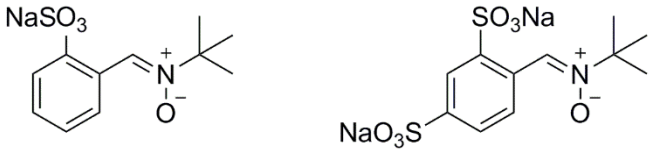

S-PBN **NXY-059**

Figure 11. Chemical structure of the derivatives S-PBN and NXY-059.

4.2. MDL-cyclic nitrones

The cyclic nitrone 3,4-dihydro-3,3-dimethyl-isoquinoline 2-oxide, called MDL 101,002, (Figure 12) was found to be 10-fold more active than PBN to inhibit lipid peroxidation,[138] and to be an effective neuroprotective agent in several models of focal ischemia.[139] A wide range of isoquinoline analogs were also synthesized such as aryl-substituted nitrones, related spiro compounds or derivatives with a more extended aromatic system (Figure 12). It was found

that their spin-trapping properties towards $HO^{\bullet}$ and $O_2^{\bullet-}$ radicals as well as their antioxidant activity in *in vitro* and *in vivo* models of oxidative stress-mediated diseases were significantly greater than that of PBN.[138,140–146] The therapeutic potential of 2-benzazepine compounds against age-related neurodegenerative disorders was studied and showed promising protection of dopaminergic neurons intoxicated with 6-hydroxydopamine, a toxin implicated in Parkinson's disease.[147,148]

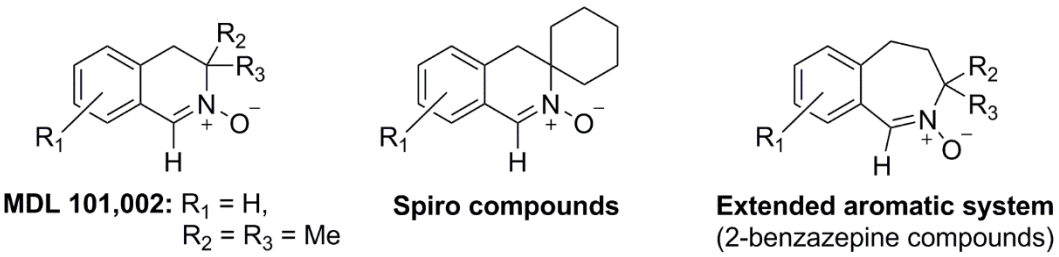

Figure 12. General structures of cyclic PBN derivatives, including the metabolites of MDL 101,002.

4.3. Imidazolyl nitrones

Nitrones with substituted imidazole moiety have been designed (Figure 13) with the expectation that a heterocyclic ring and extended conjugation would improve the bioavailability and reduce the toxicity. Imidazolyl nitrones with aromatic or heteroaromatic cycle substitutions proved to be better neuroprotective agents with less toxicity than PBN,[149] the activity being positively correlated with the lipophilicity. In addition, it was shown that the HOMO energy level of the nitrones also influenced the biological behavior with higher protection when the HOMO energy is higher. Among the derivatives, (*Z*)-α-[2-thiazol-2-yl)imidazol-4-yl]-*N*-*tert*-butylnitrone (S34176), bearing a trifluoro group in the *para* position of the phenylimidazolyl nitrone (Figure 13) was selected and its neuroprotective potential was studied in different *in vivo* paradigms of neuronal degeneration.[150] However, S34176 demonstrated a limited efficacy when administrated 3 h post-ischemia, indicating that S34176 may have a limited therapeutic benefit in the acute phase of cerebral ischemia.

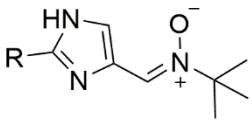

R = alkyl-, aryl-, or heteroaryl-substituent

S34176: R = 4-CF_3-Ph

Figure 13. General structure of Imidazolyl Nitrones.

Imidazolyl nitrones are also able to trap and stabilize carbon-centered radicals.[151] However, they poorly trapped oxygen or sulfur-centered radicals in polar media. EPR experiments have demonstrated that imidazoyl nitrones trap radicals on two sites: the $C_{(\alpha)}$ atom of the nitronyl function (alpha radical adduct) and the imidazoyl $C_{(5)}$ atom (5-radical adduct).

4.4. Thiadiazolyl and furaxanylnitrones

Porcal and co-workers synthesized in 2008 thiadiazolyl and furoxanylnitrones (Figure 14).[152] These derivatives combine in their structures a nitronyl function, an antioxidant fragment and a heterocyclic group able to stabilize the spin adduct formed. The neuroprotective activity of the derivatives was evaluated on a human neuroblastoma (SH-SY5Y) cells model. They were administered to the cells 1 h before the exposure to H_2O_2 as oxidative damaging agent. All the 1,2,4-thiadiazolylnitrones and the furoxanylnitrone FxBN protected similarly to or slightly higher than PBN. The activity of the 1,2,4-thiadiazolylnitrones depends on the substituent R_1 and 1,2,3-thiadiazolylnitrones did not show neuroprotective effects, indicating that there is an influence of the structure of the derivatives on the neuroprotective activity. 1,2,4-thiadiazolylnitrones and FxBN also showed excellent antioxidant properties, with an oxygen radical absorbance capacity (ORAC) ranging from 1.5- to 16.5- fold the value of PBN. Furthermore, EPR spectroscopy demonstrated the ability of these nitrones to directly trap and stabilize oxygen-, carbon-, sulfur- and nitrogen-centered free radicals. As the derivative FxBN showed optimum aqueous solubility, which is an advantage in biological experiments, its spin-trapping properties were thoroughly studied.[153] FxBN demonstrated excellent abilities to trap and stabilize hydroxyl and superoxide radicals in phosphate buffer (pH 7.4), with half-lives for FxBN-OH and FxBN-O_2H adducts being 126 and 27 min, respectively. Besides, FxBN-OH and FxBN-O_2H adducts exhibited distinct and characteristic EPR spectra. Finally, the ability of FxBN to act as spin trap in a specific biological system was confirmed and

showed that FxBN is a better spin trap than PBN or DMPO for oxygen radicals in biological systems.

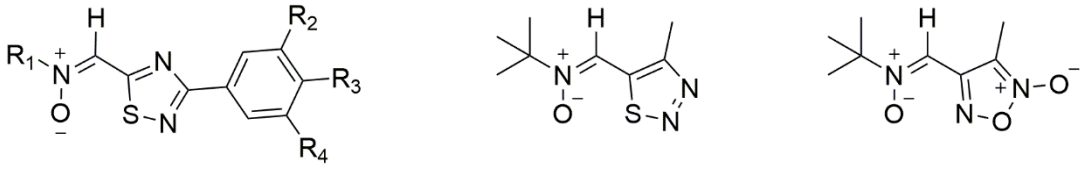

1,2,4-thiadiazolylnitrones (R_1 = *t*Bu, cyclohexyl or benzyl) | **1,2,3-thiadiazolylnitrones** | **furoxanylnitrones** (**FxBN**)

Figure 14. Chemical structure of thiadiazolylnitrones and furoxanylnitrones synthesized.

4.5. Quinolyl nitrones

More recently, Chioua and co-workers studied the influence of a quinolyl group on the neuroprotective activity of nitrones. High-level theoretical calculations indicated that these heteroaryl derivatives possess a high energy HOMO (highest occupied molecular orbital), and would therefore exhibit a good neuroprotection. This was confirmed in *in vitro* models of stroke. In particular, the quinolyl-derived nitrone named RP19 (Figure 15) was the best candidate found within this study, exhibiting the better neuroprotective effect in primary neuronal cultures exposed to oxygen-glucose deprivation (OGD).[154] It was found that RP19 at 50 µM was significantly more neuroprotective than NXY-059 on neuronal cultures subjected to OGD. RP19 also showed a significant *in vivo* neuroprotective activity at long-term recovery when administered between 24 and 72 h after ischemia.[155] In 2019, Chioua *et al.* reported the neuroprotective activity of 31 compounds comprising quinolyloximes, quinolylhydrazones, quinolylimines, quinolylnitrones and related heterocyclic azolylnitrones.[156] They showed that the incorporation of a phenyl ring or a methyl group in place of a *tert*-butyl or benzyl group on the nitrone moiety is deleterious for the neuroprotective activity. QN 23 (Figure 15), that showed neuroprotection in two *in vivo* models of cerebral ischemia, has recently entered preclinical studies for the treatment of stroke. Quinolylnitrones bearing the nitrone motif at C2, C3, C4 or C6 positions of the quinoline ring were also synthesized.[157] The most potent derivative was QN 6, bearing a *N*-*tert*-butyl group in a nitrone located at C4 position of the quinoline ring (Figure 15). It showed significant neuroprotection at 0.5 and 10 µM in an OGD model of primary neuronal cultures.

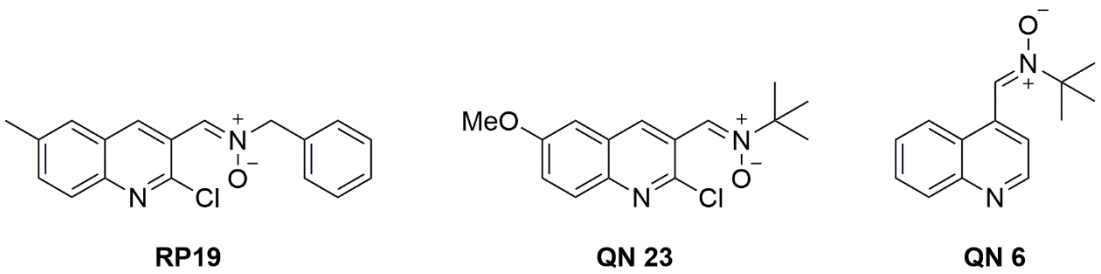

Figure 15. Chemical structure of the quinolylnitrones RP19, QN 23 and QN 6.

4.6. Tetramethylpyrazine-based nitrones

Sun *et al.* synthesized the compound TBN by conjugating the alkaloid tetramethylpyrazine (TMP) extracted from a traditional Chinese herb with a nitrone moiety.[158] The expectation was to combine the thrombolytic activity of the TMP group with the free radical-scavenging activity of the nitronyl function, a promising strategy for the treatment of ischemic stroke. TMP showed various pharmacological activities including inhibition of platelet aggregation, thrombolytic and anti-inflammation.[159,160] TMP showed significant protection in both transient and permanent rat middle cerebral artery occlusion (MCAO) models. The neuroprotection of TBN was demonstrated in *in vitro* and *in vivo* models of Parkinson disease[161] and ischemic stroke.[162] It has further been shown that TBN improves neurobehavioral functions and confers neuroprotection after traumatic brain injury.[163] TBN also readily crossed the blood brain barrier and had strong activity in neutralizing some of the most damaging radicals such as $HO^{\bullet}$, $O_2^{\bullet-}$ and $ONOO^-$.[164] Series of TBN derivatives were synthesized and their biological activities evaluated.[11,165] Among these new derivatives, the compound TN-2, armed with two nitrone moieties, showed the greatest neuroprotective activity in cultured cerebellar granule neurons and in rat MCAO model and was a promising agent for the treatment of ischemic stroke or Parkinson disease.[11,166]

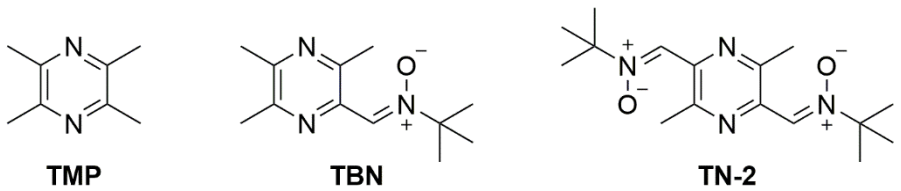

Figure 16. Chemical structure of TMP, TBN and TN-2.

5. CONCLUSION

Over the past decades, research has been notably focused on the development of DMPO and PBN derivatives in order to improve their spin-trapping and biological activities. Various synthetic methods are available to form the nitronyl group, involving oxidation reactions of imines, amines or hydroxylamines or non-oxidative reactions, such as condensation of aldehydes with hydroxylamines or alkylation of oximes. In order to understand the role played by reactive species in mediating a variety of pathological conditions, it is important to design nitrones able to detect and characterize free radicals in biological systems. Among these species, superoxide $O_2^{\bullet-}$ and hydroxyl $HO^{\bullet}$ radicals have received the most attention. Various nitrone derivatives have therefore been synthesized and studied. DMPO-type nitrones yielded distinct and characteristic spin adducts with $O_2^{\bullet-}$ and $HO^{\bullet}$ radicals. Greatly improvements of the stability of the superoxide spin adduct and of the reactivity towards $HO^{\bullet}$ have been observed compared to DMPO when an electron-withdrawing substituent (phosphoryl, alkoxycarbonyl, carbamoyl) was present at C-5 position. The persistence of the spin adducts can also be improved by the presence of bulky groups on the pyrroline ring. By introducing different substituents on the pyrroline ring of the nitrone, the octanol-water partition coefficient can be modulated, allowing the selection of the nitrone according to the type of radical we want to trap (lipid-soluble or water-soluble).

Linear PBN-type nitrones allow the possibility of rather easy functionalization, both on the aromatic ring and on the *N*-tert-butyl group and therefore provide more chemical versatility compared to cyclic DMPO-type nitrones. The introduction of various substituents in the *para*-position of the phenyl ring has shown that the electronic nature of the substituent influences the trapping rate of the nitrones towards various radicals. An electron-withdrawing group enhances the trapping rate of nucleophilic radicals whereas the presence of an electron-donating substituent increases the trapping rate of electrophilic radicals. The introduction of an electron-withdrawing group (phosphoryl, alkoxycarbonyl) in the α-position of the nitronyl function enhances the oxygen-centered radicals trapping in aqueous and organic media, with a better stability of the corresponding superoxide-adducts compared to PBN.

The chemical structure of the nitrone also plays a role in the protective activity of the nitrone in *in vitro* and *in vivo* models of diseases, with the notable example of the disulfonated derivative NXY-059. NXY-059 has been so far the most promising candidate for the

treatment of ischemic stroke. PBN-type nitrones are in general more lipophilic and can easily cross biomembranes. The derivatization of the *N*-*tert*-butyl group of the PBN offers opportunities for multifunctionalization of the nitrone for subcellar target specificity and controlled delivery in *in vitro* and *in vivo* systems. More recently, heteroaryl nitrones have been designed and studied. It has been shown that the presence of an heteroaromatic substituent on the nitrone double bond often improves the radical trapping and increases the stability of the spin adducts formed. In addition, the presence of a heterocycle allows the modulation of lipophilicity and solubility and therefore the crossing of biological membranes. Most of the heteroaryl nitrones studied have shown better biological activities than PBN on different models of neuroprotection.

REFERENCES

1 F. A. Villamena and J. L. Zweier, *Antioxid. Redox Signal.*, 2004, **6**, 619–629.
2 M. J. Davies, *Methods*, 2016, 21–30.
3 S. Pietri, M. Culcasi and P. J. Cozzone, *Eur. J. Biochem.*, 1989, **186**, 163–173.
4 H. M. Hughes, I. M. George, J. C. Evans, C. C. Rowlands, G. M. Powell and C. G. Curtis, *Biochem. J.*, 1991, **277**, 795–800.
5 M. B. Kadiiska, P. M. Hanna, S. J. Jordan and R. P. Mason, *Am. Soc. Pharmacol. Exp. Ther.*, 1993, **44**, 222–227.
6 H. D. Connor, W. Gao, S. Nukina, J. J. Lemasters, R. P. Mason and R. G. Thurman, *Transplantation*, 1992, **54**, 199–204.
7 F. A. Villamena, A. Das and K. M. Nash, *Future Med. Chem.*, 2012, **4**, 1171–1207.
8 G. P. Novelli, P. Angiolini, R. Tani, G. Consales and L. Bordi, *Free Radic. Res. Commun.*, 1986, **1**, 321–327.
9 G. P. Novelli, P. Angiolini, P. Livi and E. Paternostro, *Resuscitation*, 1989, **18**, 195–205.
10 R. A. Floyd, H. C. Castro Faria Neto, G. A. Zimmerman, K. Hensley and R. A. Towner, *Free Radic. Biol. Med.*, 2013, **62**, 145–156.
11 Y. Sun, G. Zhang, Z. Zhang, P. Yu, H. Zhong, J. Du and Y. Wang, *Bioorg. Med. Chem.*, 2012, **20**, 3939–3945.
12 S. A. Doggrell, *Curr. Opin. Investig. Drugs Lond. Engl. 2000*, 2006, **7**, 20–24.
13 P. L. Zamora and F. A. Villamena, *Future Med. Chem.*, 2013, **5**, 465–478.
14 M. N. A. Mandal, G. P. Moiseyev, M. H. Elliott, A. Kasus-Jacobi, X. Li, H. Chen, L. Zheng, O. Nikolaeva, R. A. Floyd, J. Ma and R. E. Anderson, *J. Biol. Chem.*, 2011, **286**, 32491–32501.
15 D. S. S. Costa, T. Martino, F. C. Magalhães, G. Justo, M. G. P. Coelho, J. C. F. Barcellos, V. B. Moura, P. R. R. Costa, K. C. C. Sabino and A. G. Dias, *Bioorg. Med. Chem.*, 2015, **23**, 2053–2061.
16 R. A. Floyd, *Aging Cell*, 2006, **5**, 51–57.
17 A. Shuaib, K. R. Lees, P. Lyden, J. Grotta, A. Davalos, S. M. Davis, H.-C. Diener, T. Ashwood, W. W. Wasiewski and U. Emeribe, *N. Engl. J. Med.*, 2007, **357**, 562–571.
18 H.-C. Diener, K. R. Lees, P. Lyden, J. Grotta, A. Davalos, S. M. Davis, A. Shuaib, T. Ashwood, W. Wasiewski, V. Alderfer, H.-G. Hardemark and L. Rodichok, *Stroke*, 2008, **39**, 1751–1758.
19 E. G. Janzen, J. L. Poyer, C. F. Schaefer, P. E. Downs and C. M. DuBose, *J. Biochem. Biophys. Methods*, 1995, **30**, 239–247.
20 R. A. Floyd, *Proc. Soc. Exp. Biol. Med.*, 1999, **222**, 236–245.
21 R. A. Floyd, *Free Radic. Biol. Med.*, 1999, **26**, 1346–1355.
22 H. Tomita, Y. Kotake and R. E. Anderson, *Invest. Ophthalmol. Vis. Sci.*, 2005, **46**, 427–434.
23 E. J. Locigno, J. L. Zweier and F. A. Villamena, *Org. Biomol. Chem.*, 2005, **3**, 3220-3227.
24 M. D. Croitoru, F. Ibolya, M. C. Pop, T. Dergez, B. Mitroi, M. T. Dogaru and B. Tőkés, *Nitric Oxide*, 2011, **25**, 309–315.

25 C. Frejaville, H. Karoui, B. Tuccio, F. Le Moigne, M. Culcasi, S. Pietri, R. Lauricella and P. Tordo, *J. Med. Chem.*, 1995, **38**, 258–265.
26 I. E. Blasig, S. Shuter, P. Garlick and T. Slater, *Free Radic. Biol. Med.*, 1994, **16**, 35–41.
27 M. Rosselin, B. Poeggeler and G. Durand, *Curr. Top. Med. Chem.*, 2017, **17**, 2006–2022.
28 D. R. Boyd, P. B. Coulter and J. W. Hamilton, *Tetrahedron Lett.*, 1984, **25**, 2287–2288.
29 D. R. Boyd, P. B. Coulter, N. D. Sharma, W. B. Jennings and V. E. Wilson, *Tetrahedron Lett.*, 1985, **26**, 1673–1676.
30 D. R. Boyd, P. B. Coulter, R. M. McGuckin and N. D. Sharma, *J. Chem. Soc. Perkin 1*, 1990, 301–306.
31 D. Christensen and K. A. Joergensen, *J. Org. Chem.*, 1989, **54**, 126–131.
32 N. Somasundaram and C. Srinivasan, *Tetrahedron Lett.*, 1998, **39**, 3547–3550.
33 G. Soldaini, F. Cardona and A. Goti, *Org. Lett.*, 2007, **9**, 473–476.
34 H. Mitsui, S. Zenki, T. Shiota and S.-I. Murahashi, *J. Chem. Soc. Chem. Commun.*, 1984, 874–875.
35 E. Marcantoni, M. Petrini and O. Polimanti, *Tetrahedron Lett.*, 1995, **36**, 3561–3562.
36 R. W. Murray, K. Iyanar, J. Chen and J. T. Wearing, *J. Org. Chem.*, 1996, **61**, 8099–8102.
37 A. Goti and L. Nannelli, *Tetrahedron Lett.*, 1996, **37**, 6025–6028.
38 V. B. Sharma, S. L. Jain and B. Sain, *Tetrahedron Lett.*, 2003, **44**, 3235–3237.
39 R. W. Murray and M. Singh, *J. Org. Chem.*, 1990, **55**, 2954–2957.
40 W. W. Zajac Jr, T. R. Walters and M. G. Darcy, *J. Org. Chem.*, 1988, **53**, 5856–5860.
41 C. Gella, È. Ferrer, R. Alibés, F. Busqué, P. de March, M. Figueredo and J. Font, *J. Org. Chem.*, 2009, **74**, 6365–6367.
42 S. Cicchi, M. Marradi, A. Goti and A. Brandi, *Tetrahedron Lett.*, 2001, **42**, 6503–6505.
43 S. Cicchi, F. Cardona, A. Brandi, M. Corsi and A. Goti, *Tetrahedron Lett.*, 1999, **40**, 1989–1992.
44 S. Cicchi, M. Corsi and A. Goti, *J. Org. Chem.*, 1999, **64**, 7243–7245.
45 S. Yudha S, I. Kusuma and N. Asao, *Tetrahedron*, 2015, **71**, 6459–6462.
46 E. G. Janzen and R. C. Zawalski, *J. Org. Chem.*, 1978, **43**, 1900–1903.
47 S. Franco, F. L. Merchán, P. Merino and T. Tejero, *Synth. Commun.*, 1995, **25**, 2275–2284.
48 A. Dondoni, S. Franco, F. Junquera, F. L. Merchán, P. Merino and T. Tejero, *Synth. Commun.*, 1994, **24**, 2537–2550.
49 R. Huie and W. R. Cherry, *J. Org. Chem.*, 1985, **50**, 1531–1532.
50 A. R. Katritzky, X. Cui, Q. Long, B. Yang, A. L. Wilcox and Y.-K. Zhang, *Org. Prep. Proced. Int.*, 2000, **32**, 175–183.
51 R. D. Hinton and E. G. Janzen, *J. Org. Chem.*, 1992, **57**, 2646–2651.
52 V. Gautheron-Chapoulaud, S. U. Pandya, P. Cividino, G. Masson, S. Py and Y. Vallée, *Synlett*, 2001, 1281–1283.
53 S. Morales, F. G. Guijarro, I. Alonso, J. L. García Ruano and M. B. Cid, *ACS Catal.*, 2016, **6**, 84–91.
54 E. Colacino, P. Nun, F. M. Colacino, J. Martinez and F. Lamaty, *Tetrahedron*, 2008, **64**, 5569–5576.
55 S. Yavuz, H. Ozkan, N. Colak and Y. Yildirir, *Molecules*, 2011, **16**, 6677–6683.
56 H. Valizadeh and L. Dinparast, *Heteroat. Chem.*, 2009, **20**, 177–181.

57 M. M. Andrade, M. T. Barros and R. C. Pinto, *Tetrahedron*, 2008, **64**, 10521–10530.
58 C. Chavarría, D. I. Perez, C. Pérez, J. A. Morales Garcia, S. Alonso-Gil, A. Pérez-Castillo, C. Gil, J. M. Souza and W. Porcal, *Eur. J. Med. Chem.*, 2012, **58**, 44–49.
59 E. Buehler, *J. Org. Chem.*, 1967, **32**, 261–265.
60 N. LeBel A. and N. Balasubramanian, *Tetrahedron Lett.*, 1985, **26**, 4331–4334.
61 F. Cardona, M. Bonanni, G. Soldaini and A. Goti, *ChemSusChem*, 2008, **1**, 327–332.
62 B. Singh, S. L. Jain, P. K. Khatri and B. Sain, *Green Chem.*, 2009, **11**, 1941-1944.
63 B. Singh, S. L. Jain, B. S. Rana, P. K. Khatri, A. K. Sinha and B. Sain, *ChemCatChem*, 2010, **2**, 1260–1264.
64 M. Mirza-Aghayan, M. Molaee Tavana and R. Boukherroub, *Tetrahedron Lett.*, 2014, **55**, 5471–5474.
65 A. P. Chavannavar, A. G. Oliver and B. L. Ashfeld, *Chem Commun*, 2014, **50**, 10853–10856.
66 R. Bonnett, R. F. C. Brown, V. M. Clark, I. O. Sutherland and A. Todd, *J Chem Soc*, 1959, 2094–2102.
67 H. Shechter, D. E. Ley and L. Zeldin, *J. Am. Chem. Soc.*, 1952, **74**, 3664–3668.
68 E. G. Janzen, L. T. Jandrisits, R. V. Shetty, D. Larry Haire and J. W. Hilborn, *Chem. Biol. Interact.*, 1989, **70**, 167–172.
69 L. Haire D., J. Hilborn W. and E. G. Janzen, *J. Org. Chem.*, 1986, **51**, 4298–4300.
70 C. Frejaville, H. Karoui, B. Tuccio, F. le Moigne, M. Culcasi, S. Pietri, R. Lauricella and P. Tordo, *J. Chem. Soc. Chem. Commun.*, 1994, 1793–1794.
71 B. Tuccio, R. Lauricella, C. Frejaville, J.-C. Bouteiller and P. Tordo, *J Chem Soc Perkin Trans 2*, 295–298.
72 S. Pietri, T. Liebgott, C. Fréjaville, P. Tordo and M. Culcasi, *FEBS J.*, 1998, **254**, 256–265.
73 V. Roubaud, A. Mercier, G. Olive, F. L. Moigne and P. Tordo, *J. Chem. Soc. Perkin Trans. 2*, 1997, 1827–1830.
74 G. Olive, F. Le Moigne, A. Mercier, A. Rockenbauer and P. Tordo, *J. Org. Chem.*, 1998, **63**, 9095–9099.
75 K. Stolze, N. Udilova and H. Nohl, *Free Radic. Biol. Med.*, 2000, **29**, 1005–1014.
76 H. Karoui, C. Nsanzumuhire, F. Le Moigne and P. Tordo, *J. Org. Chem.*, 1999, **64**, 1471–1477.
77 Y.-K. Xu, Z.-W. Chen, J. Sun, K. Liu, W. Chen, W. Shi, H.-M. Wang and Y. Liu, *J. Org. Chem.*, 2002, **67**, 7624–7630.
78 G. Olive, A. Mercier, F. Le Moigne, A. Rockenbauer and P. Tordo, *Free Radic. Biol. Med.*, 2000, **28**, 403–408.
79 F. A. Villamena, C. M. Hadad and J. L. Zweier, *J. Am. Chem. Soc.*, 2004, **126**, 1816–1829.
80 F. A. Villamena, C. M. Hadad and J. L. Zweier, *J. Phys. Chem. A*, 2003, **107**, 4407–4414.
81 H. Karoui, J.-L. Clément, A. Rockenbauer, D. Siri and P. Tordo, *Tetrahedron Lett.*, 2004, **45**, 149–152.
82 A. Allouch, V. Roubaud, R. Lauricella, J.-C. Bouteiller and B. Tuccio, *Org. Biomol. Chem.*, 2005, **3**, 2458–2462.

83 C. J. Traynham, S. R. Roof, H. Wang, R. A. Prosak, L. Tang, S. Viatchenko-Karpinski, H.-T. Ho, I. O. Racoma, D. J. Catalano, X. Huang, Y. Han, S.-U. Kim, S. Gyorke, G. E. Billman, F. A. Villamena and M. T. Ziolo, *PLoS ONE*, 2012, **7**, e52005.

84 H. Zhao, J. Joseph, H. Zhang, H. Karoui and B. Kalyanaraman, *Free Radic. Biol. Med.*, 2001, **31**, 599–606.

85 K. Stolze, N. Udilova and H. Nohl, *Biochem. Pharmacol.*, 2002, **63**, 1465–1470.

86 F. A. Villamena and J. L. Zweier, *J. Chem. Soc. Perkin Trans. 2*, 2002, 1340–1344.

87 P. Tsai, K. Ichikawa, C. Mailer, S. Pou, H. J. Halpern, B. H. Robinson, R. Nielsen and G. M. Rosen, *J. Org. Chem.*, 2003, **68**, 7811–7817.

88 K. Stolze, N. Udilova, T. Rosenau, A. Hofinger and H. Nohl, *Biol. Chem.*, 2003, **384**, 493–500.

89 N. Rohr-Udilova, K. Stolze, B. Marian and H. Nohl, *Bioorg. Med. Chem. Lett.*, 2006, **16**, 541–546.

90 K. Stolze, N. Udilova, T. Rosenau, A. Hofinger and H. Nohl, *Biochem. Pharmacol.*, 2005, **69**, 297–305.

91 K. Stolze, N. Rohr-Udilova, T. Rosenau, R. Stadtmüller and H. Nohl, *Biochem. Pharmacol.*, 2005, **69**, 1351–1361.

92 N. Rohr-Udilova, K. Stolze, S. Sagmeister, W. Parzefall, B. Marian, H. Nohl, R. Schulte-Hermann and B. Grasl-Kraupp, *Bioorg. Med. Chem. Lett.*, 2007, **17**, 5698–5703.

93 K. Stolze, N. Rohr-Udilova, T. Rosenau, A. Hofinger, D. Kolarich and H. Nohl, *Bioorg. Med. Chem.*, 2006, **14**, 3368–3376.

94 K. Stolze, N. Rohr-Udilova, T. Rosenau, A. Hofinger and H. Nohl, *Bioorg. Med. Chem.*, 2007, **15**, 2827–2836.

95 K. Stolze, N. Rohr-Udilova, A. Patel and T. Rosenau, *Bioorg. Med. Chem.*, 2011, **19**, 985–993.

96 F. A. Villamena, A. Rockenbauer, J. Gallucci, M. Velayutham, C. M. Hadad and J. L. Zweier, *J. Org. Chem.*, 2004, **69**, 7994–8004.

97 K. Anzai, T. Aikawa, Y. Furukawa, Y. Matsushima, S. Urano and T. Ozawa, *Arch. Biochem. Biophys.*, 2003, **415**, 251–256.

98 F. A. Villamena, S. Xia, J. K. Merle, R. Lauricella, B. Tuccio, C. M. Hadad and J. L. Zweier, *J. Am. Chem. Soc.*, 2007, **129**, 8177–8191.

99 F. A. Villamena, J. K. Merle, C. M. Hadad and J. L. Zweier, *J. Phys. Chem. A*, 2007, **111**, 9995–10001.

100 K. Stolze, N. Rohr-Udilova, A. Hofinger and T. Rosenau, *Bioorg. Med. Chem.*, 2008, **16**, 8082–8089.

101 K. Stolze, N. Rohr-Udilova, A. Hofinger and T. Rosenau, *Bioorg. Med. Chem.*, 2009, **17**, 7572–7584.

102 N. Sankuratri and E. G. Janzen, *Tetrahedron Lett.*, 1996, **37**, 5313–5316.

103 Y. Han, B. Tuccio, R. Lauricella, A. Rockenbauer, J. L. Zweier and F. A. Villamena, *J. Org. Chem.*, 2008, **73**, 2533–2541.

104 W. D. Emmons, *J. Am. Chem. Soc.*, 1957, **79**, 5739–5754.

105 E. G. Janzen, M. S. West, Y. Kotake and C. M. DuBose, *J. Biochem. Biophys. Methods*, 1996, **32**, 183–190.

106 D. F. Church, *J. Org. Chem.*, 1986, **51**, 1138–1140.
107 K. Pan, C.-R. Lin and T.-I. Ho, *Magn. Reson. Chem.*, 1993, **31**, 632–638.
108 G. Durand, F. Choteau, B. Pucci and F. A. Villamena, *J. Phys. Chem. A*, 2008, **112**, 12498–12509.
109 E. G. Janzen and C. A. Evans, *J. Am. Chem. Soc.*, 1973, **95**, 8205–8206.
110 E. G. Janzen, C. A. Evans and Y. Nishi, *J. Am. Chem. Soc.*, 1972, **94**, 8236–8238.
111 P. Schmid and K. U. Ingold, *J. Am. Chem. Soc.*, 1978, **100**, 2493–2500.
112 Y. Sueishi, D. Yoshioka, C. Yoshioka, S. Yamamoto and Y. Kotake, *Org. Biomol. Chem.*, 2006, **4**, 896–901.
113 C. L. Greenstock and R. H. Wiebe, *Can. J. Chem.*, 1982, **60**, 1560–1564.
114 M. Rosselin, B. Tuccio, P. Pério, Frederick. A. Villamena, P.-L. Fabre and G. Durand, *Electrochimica Acta*, 2016, **193**, 231–239.
115 Y. Sueishi, C. Yoshioka, C. Olea-Azar, L. A. Reinke and Y. Kotake, *Bull. Chem. Soc. Jpn.*, 2002, **75**, 2043–2047.
116 Y. Abe, S. Seno, K. Sakakibara and M. Hirota, *J. Chem. Soc. Perkin Trans. 2*, 1991, 897–903.
117 K. Murofushi, K. Abe and M. Hirota, *J. Chem. Soc. Perkin Trans. 2*, 1987, 1829–1833.
118 A. Zeghdaoui, B. Tuccio, J.-P. Finet, V. Cerri and P. Tordo, *J. Chem. Soc. Perkin Trans. 2*, 1995, 2087–2089.
119 B. Tuccio, A. Zeghdaoui, J.-P. Finet, V. Cerri and P. Tordo, *Res. Chem. Intermed.*, 1996, **22**, 393–404.
120 V. Roubaud, R. Lauricella, B. Tuccio, J.-C. Bouteiller and P. Tordo, *Res. Chem. Intermed.*, 1996, **22**, 405–416.
121 Y.-P. Liu, L.-F. Wang, Z. Nie, Y.-Q. Ji, Y. Liu, K.-J. Liu and Q. Tian, *J. Org. Chem.*, 2006, **71**, 7753–7762.
122 K. A. Petrov, V. A. Chauzov, L. V. Pastukhova and N. N. Bogdanov, *Zh Obshch Khim*, 1976, **46**, 1246–1250.
123 C. Rizzi, S. Marque, F. Belin, J.-C. Bouteiller, R. Lauricella, B. Tuccio, V. Cerri and P. Tordo, *J. Chem. Soc. Perkin Trans. 2*, 1997, 2513–2518.
124 E. Konorev, J. Baker and K. B, *Free Radic. Biol. Med.*, 1993, **14**, 127–137.
125 V. Roubaud, H. Dozol, C. Rizzi, R. Lauricella, J.-C. Bouteiller and B. Tuccio, *J. Chem. Soc. Perkin Trans. 2*, 2002, 958–964.
126 M. Cassien, C. Petrocchi, S. Thétiot-Laurent, M. Robin, E. Ricquebourg, C. Kandouli, A. Asteian, A. Rockenbauer, A. Mercier, M. Culcasi and S. Pietri, *Eur. J. Med. Chem.*, 2016, **119**, 197–217.
127 W. Kliegel, G. Lubkowitz, S. J. Rettig and J. Trotter, *Can. J. Chem.*, 1993, **71**, 2129–2138.
128 V. Roubaud, R. Lauricella, J.-C. Bouteiller and B. Tuccio, *Arch. Biochem. Biophys.*, 2002, **397**, 51–56.
129 A. Allouch, V. Roubaud, R. Lauricella, J.-C. Bouteiller and B. Tuccio, *Org. Biomol. Chem.*, 2003, **1**, 593–598.

130 K. Stolze, N. Udilova, T. Rosenau, A. Hofinger and H. Nohl, *Biochem. Pharmacol.*, 2003, **66**, 1717–1726.

131 K. Stolze, N. Udilova, T. Rosenau, A. Hofinger and H. Nohl, *Biochem. Pharmacol.*, 2004, **68**, 185–194.

132 M. Rosselin, F. Choteau, K. Zéamari, K. M. Nash, A. Das, R. Lauricella, E. Lojou, B. Tuccio, F. A. Villamena and G. Durand, *J. Org. Chem.*, 2014, **79**, 6615–6626.

133 G. Durand, M. Rosselin, P.-A. Klein, K. Zéamari, F. Choteau and B. Tuccio, *J. Org. Chem.*, 2017, **82**, 135–142.

134 K. R. Maples, F. Ma and Y.-K. Zhang, *Free Radic. Res.*, 2001, **34**, 417–426.

135 S. Kuroda, R. Tsuchidate, M.-L. Smith, K. R. Maples and B. K. Siesjo, *J Cereb Blood Flow Metab*, 1999, **19**, 778–787.

136 A. R. Green, T. Ashwood, T. Odergren and D. M. Jackson, *Pharmacol. Ther.*, 2003, **100**, 195–214.

137 K. R. Lees, J. A. Zivin, T. Ashwood, A. Davalos, S. M. Davis, H.-C. Diener, J. Grotta, P. Lyden, A. Shuaib and H.-G. H\a ardemark, *N. Engl. J. Med.*, 2006, **354**, 588–600.

138 C. E. Thomas, D. F. Ohlweiler and B. Kalyanaraman, *J. Biol. Chem.*, 1994, **269**, 28055–28061.

139 M. P. Johnson, D. R. McCarty, N. L. Velayo, C. G. Markgraf, P. A. Chmielewski, J. V. Ficorilli, H. C. Cheng and C. E. Thomas, *Life Sci.*, 1998, **63**, 241–253.

140 C. E. Thomas, J. M. Carney, R. C. Bernotas, D. A. Hay and A. A. Carr, *Ann. N. Y. Acad. Sci.*, 1994, **738**, 243–249.

141 J. F. French, C. E. Thomas, T. R. Downs, D. F. Ohlweiler, A. A. Carr and R. C. Dage, *Circ. Shock*, 1994, **43**, 130–136.

142 T. R. Downs, R. C. Dage and J. F. French, *Int. J. Immunopharmacol.*, 1995, **17**, 571–580.

143 R. C. Bernotas, C. E. Thomas, A. A. Carr, T. R. Nieduzak, G. Adams, D. F. Ohlweiler and D. A. Hay, *Bioorg. Med. Chem. Lett.*, 1996, **6**, 1105–1110.

144 T. L. Fevig, S. M. Bowen, D. A. Janowick, B. K. Jones, H. R. Munson, D. F. Ohlweiler and C. E. Thomas, *J. Med. Chem.*, 1996, **39**, 4988–4996.

145 C. E. Thomas, D. F. Ohlweiler, A. A. Carr, T. R. Nieduzak, D. A. Hay, G. Adams, R. Vaz and R. C. Bernotas, *J. Biol. Chem.*, 1996, **271**, 3097–3104.

146 C. E. Thomas, D. F. Ohlweiler, V. L. Taylor and C. J. Schmidt, *J. Neurochem.*, 1997, **68**, 1173–1182.

147 R. Soto-Otero, E. Méndez-Álvarez, S. Sánchez-Iglesias, F. I. Zubkov, L. G. Voskressensky, A. V. Varlamov, M. de Candia and C. Altomare, *Biochem. Pharmacol.*, 2008, **75**, 1526–1537.

148 R. Soto-Otero, E. Méndez-Álvarez, S. Sánchez-Iglesias, J. L. Labandeira-García, J. Rodríguez-Pallares, F. I. Zubkov, V. P. Zaytsev, L. G. Voskressensky, A. V. Varlamov, M. de Candia, F. Fiorella and C. Altomare, *Arch. Pharm. (Weinheim)*, 2012, **345**, 598–609.

149 A. Dhainaut, A. Tizot, E. Raimbaud, B. Lockhart, P. Lestage and S. Goldstein, *J. Med. Chem.*, 2000, **43**, 2165–2175.

150 B. Lockhart, A. Roger, N. Bonhomme, S. Goldstein and P. Lestage, *Eur. J. Pharmacol.*, 2005, **511**, 127–136.

151 K. Reybier, J. Boyer, V. Farines, F. Camus, J.-P. Souchard, M.-C. Monje, V. Bernardes-Genisson, S. Goldstein and F. Nepveu, *Free Radic. Res.*, 2006, **40**, 11–20.

152 W. Porcal, P. Hernández, M. González, A. Ferreira, C. Olea-Azar, H. Cerecetto and A. Castro, *J. Med. Chem.*, 2008, **51**, 6150–6159.

153 G. Barriga, C. Olea-Azar, E. Norambuena, A. Castro, W. Porcal, A. Gerpe, M. González and H. Cerecetto, *Bioorg. Med. Chem.*, 2010, **18**, 795–802.

154 M. Chioua, D. Sucunza, E. Soriano, D. Hadjipavlou-Litina, A. Alcázar, I. Ayuso, M. J. Oset-Gasque, M. P. González, L. Monjas, M. I. Rodríguez-Franco, J. Marco-Contelles and A. Samadi, *J. Med. Chem.*, 2012, **55**, 153–168.

155 M. I. Ayuso, E. Martínez-Alonso, M. Chioua, A. Escobar-Peso, R. Gonzalo-Gobernado, J. Montaner, J. Marco-Contelles and A. Alcázar, *ACS Chem. Neurosci.*, 2017, **8**, 2202–2213.

156 M. Chioua, E. Martínez-Alonso, R. Gonzalo-Gobernado, M. I. Ayuso, A. Escobar-Peso, L. Infantes, D. Hadjipavlou-Litina, J. J. Montoya, J. Montaner, A. Alcázar and J. Marco-Contelles, *J. Med. Chem.*, 2019, **62**, 2184–2201.

157 M. Chioua, M. Salgado-Ramos, D. Diez-Iriepa, A. Escobar-Peso, I. Iriepa, D. Hadjipavlou-Litina, E. Martínez-Alonso, A. Alcázar and J. Marco-Contelles, *ACS Chem. Neurosci.*, 2019, **10**, 2703–2706.

158 Y. Sun, J. Jiang, Z. Zhang, P. Yu, L. Wang, C. Xu, W. Liu and Y. Wang, *Bioorg. Med. Chem.*, 2008, **16**, 8868–8874.

159 S.-Y. Liu and D. M. Sylvester, *Thromb. Res.*, 1990, **58**, 129–140.

160 J.-Z. Hu, J.-H. Huang, Z.-M. Xiao, J.-H. Li, X.-M. Li and H.-B. Lu, *J. Neurol. Sci.*, 2013, **324**, 94–99.

161 B. Guo, D. Xu, H. Duan, J. Du, Z. Zhang, S. M. Lee and Y. Wang, *Biol. Pharm. Bull.*, 2014, **37**, 274–285.

162 Z. Zhang, G. Zhang, Y. Sun, S. S. W. Szeto, H. C. H. Law, Q. Quan, G. Li, P. Yu, E. Sho, M. K. W. Siu, S. M. Y. Lee, I. K. Chu and Y. Wang, *Sci. Rep.*, 2016, 37148.

163 G. Zhang, F. Zhang, T. Zhang, J. Gu, C. Li, Y. Sun, P. Yu, Z. Zhang and Y. Wang, *Neurochem. Res.*, 2016, **41**, 2948–2957.

164 Y. Sun, P. Yu, G. Zhang, L. Wang, H. Zhong, Z. Zhai, L. Wang and Y. Wang, *J. Neurosci. Res.*, 2012, **90**, 1662–1669.

165 H. Chen, G. Tan, J. Cao, G. Zhang, P. Yi, P. Yu, Y. Sun, Z. Zhang and Y. Wang, *Chem. Pharm. Bull.*, 2017, **65**, 56–65.

166 D.-P. Xu, K. Zhang, Z.-J. Zhang, Y.-W. Sun, B.-J. Guo, Y.-Q. Wang, P.-M. Hoi, Y.-F. Han and S. M.-Y. Lee, *Neurochem. Int.*, 2014, **78**, 76–85.

Chapitre 2

Reactivities of MeO-substituted PBN-type nitrones

Dans ce chapitre j'ai réalisé la synthèse des nitrones et leur caractérisation structurale ainsi que la détermination des coefficients de partition. J'ai réalisé les expériences de spin-trapping et l'analyse des données avec l'aide du Dr Kamal Zéamari en collaboration avec le Dr Béatrice Tuccio (ICR - UMR 7273, Marseille). J'ai également réalisé les expériences de voltampérométrie cyclique et l'analyse des données avec l'aide du Pr Paul-Louis Fabre (Pharma-Dec, UMR 152, Université Paul Sabatier – Toulouse III).

La détermination des charges partielles des nitrones et des potentiels d'ionisation a été réalisée par l'équipe du Pr Patrick Trouillas (INSERM, U1248 IPPRITT, Université de Limoges).

J'ai réalisé la rédaction du chapitre avec l'aide de mon directeur de thèse le Dr Grégory Durand.

Ce chapitre a été publié dans New Journal of Chemistry

Chapitre 2 - Reactivities of MeO-substituted PBN-type Nitrones

Table of contents

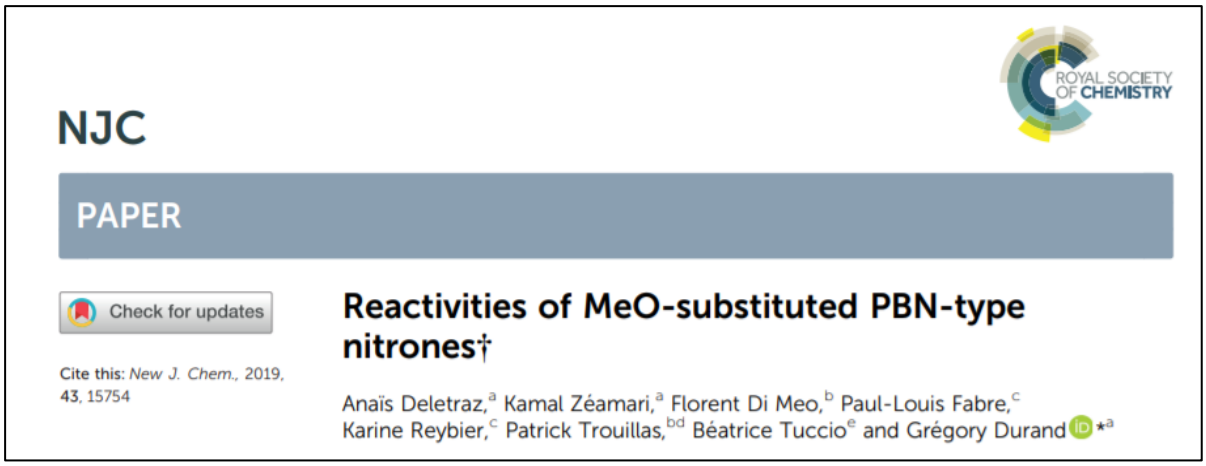

[a] Institut des Biomolécules Max Mousseron, UMR 5247 CNRS-Université Montpellier-ENSCM & Avignon Université, Equipe Chimie Bioorganique et Systèmes Amphiphiles, 301 rue Baruch de Spinoza, BP 21239, Avignon 84916 Cedex 9, France ;

[b] INSERM U1248 IPPRITT, Université de Limoges, Faculté de Médecine et Pharmacie, 2 rue du Professeur Descottes F-87000 Limoges, France ;

[c] Pharma-Dev, UMR 152, Université de Toulouse, IRD, UPS, 35 chemin des Maraîchers, 31400 Toulouse, France ;

[d] Regional Centre of Advanced Technologies and Materials, Palacký University, tr. 17 listopadu 12, 771 46 Olomouc, Czech Republic ;

[e] Aix-Marseille Université, CNRS, ICR UMR 7273, Avenue Escadrille Normandie Niemen, 13397 Marseille Cedex 20, France.

*Corresponding Author. Grégory Durand. E-mail: gregory.durand@univ-avignon.fr ; Phone: +33 (0)4 9014 4445.

ABSTRACT

In this work, α-phenyl-*N*-*tert*-butyl nitrone (PBN), *N*-benzylidene-1-diethoxyphosphoryl-1-methylethylamine *N*-oxide (PPN) and *N*-benzylidene-1-ethoxycarbonyl-1-methylethylamine *N*-oxide (EPPN) derivatives bearing methoxy groups (MeO-) on the phenyl ring were synthesized. Their electrochemical properties were studied by cyclic voltammetry and the results showed that the position and the number of methoxy substituents influence the redox potential of the nitronyl group. The spin-trapping ability of the derivatives was next investigated by electron paramagnetic resonance spectroscopy for the hydroxymethyl radical ($^{\bullet}CH_2OH$). The *ortho*, *meta* and *para* mono-substituted-PBN derivatives exhibited similar trapping rates to the parent PBN while surprisingly, nitrones with two MeO-substituents on the *ortho*-position failed to trap $^{\bullet}CH_2OH$. The trapping rates of the parent compounds were ranked as follows: PPN > EPPN > PBN, indicating that the presence of diethoxyphosphoryl and ethoxycarbonyl electron withdrawing groups on the *N*-*tert*-butyl group significantly enhanced the reactivity towards hydroxymethyl radicals. The effect of the substitutions on the atomic partial charges of the nitronyl-moiety and on the ionization potential was computationally rationalized and showed a strong correlation between the ionization potential and the experimentally measured oxidation potential.

KEYWORDS

Nitrones, Antioxidants, Electrochemistry, Electron Paramagnetic Resonance (EPR) Spectroscopy, Spin-Trapping.

1. INTRODUCTION

Nitrones were initially designed as probes for the indirect detection of free radical species in chemical and biological systems.[1] The addition of a free radical onto the nitronyl-carbon atom yields a persistent aminoxyl spin adduct, which can be detected and characterized in spin-trapping experiments by electron paramagnetic resonance (EPR) spectroscopy. This has allowed the identification of several carbon-, oxygen- or sulfur-centered biologically relevant free radicals.[2] The cyclic 5,5-dimethyl-1-pyrrolidine *N*-oxide (DMPO) and the linear α-phenyl-*N*-*tert*-butyl nitrone (PBN) have been the most commonly used spin traps. DMPO-type nitrones have shown better spin-trapping properties with more distinctive EPR spectra, faster kinetics of trapping and longer half-lives of their spin adducts whereas PBN-type nitrones exhibited a better distribution within tissues and cells and have been largely developed as very promising therapeutic agents.[3,4] Indeed, PBN-type nitrones have shown protective properties in animal models of neurodegenerative diseases,[5] stroke,[6] cardiovascular diseases[7] and cancer.[8] The PBN derivative, disodium [(*tert*-butylimino)methyl]-benzene-1,3-disulfonate *N*-oxide (NXY-059), was the first neuroprotective agent to reach phase III clinical trials in the USA for the treatment of acute stroke.[9,10]

In this context, several PBN derivatives have been synthesized and studied over the past few decades with the aim to improve their biological and/or spin-trapping activities.[11–19] With regards to the spin-trapping properties, excellent results have been obtained with *N*-benzylidene-1-diethoxyphosphoryl-1-methylethylamine *N*-oxide (PPN),[20–22] a phosphorylated analogue of PBN and with *N*-benzylidene-1-ethoxycarbonyl-1-methylethylamine *N*-oxide (EPPN),[13,23] an ester analogue of PBN. These derivatives, bearing an electron-withdrawing group in the α-position of the nitronyl function, have been shown to efficiently trap superoxide in aqueous media and to significantly increase the stability of the superoxide adduct. Our previous work on *para*-substituted PBNs identified 4-MeO-PBN as a potent nitrone derivative with a low oxidation potential and efficient trapping of phenyl radical.[24]

The current work aims at studying the influence of the electron-donating methoxy (MeO-) substituent on the reactivity of the nitronyl group of three classical nitrones, that is, α-phenyl-*N*-*tert*-butylnitrone (PBN), *N*-benzylidene-1-diethoxyphosphoryl-1-methylethylamine *N*-oxide (PPN), and *N*-benzylidene-1-ethoxycarbonyl-1-methylethylamine *N*-oxide (EPPN) (Figure 1). A series of methoxy-substituted phenyl nitrones was thus synthesized and their electrochemical properties were first studied. Using EPR competition kinetic experiments, the

relative rate constant of hydroxymethyl radical trapping was then determined. Finally, the effect of methoxy substituents on the nitronyl atomic charge densities and on the ionization potential (IP) was described, as supported by density functional theory (DFT) calculations.

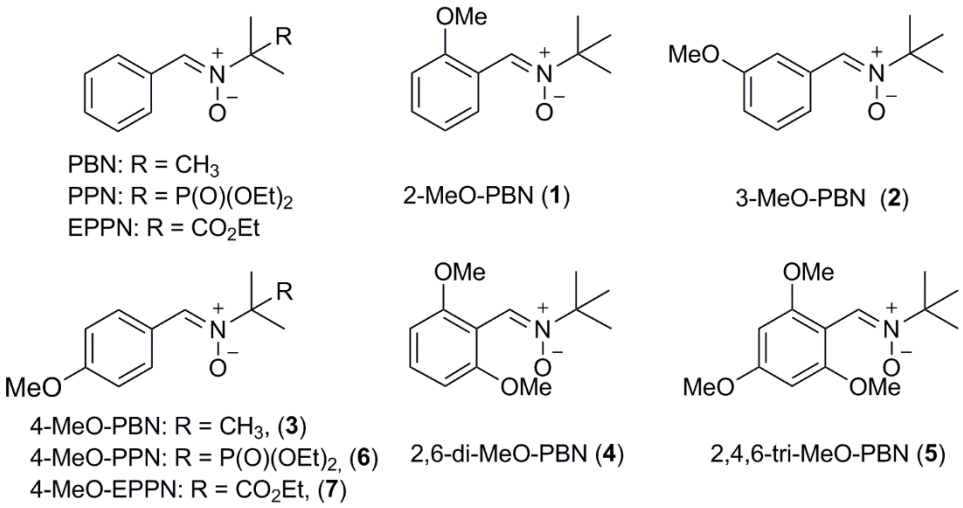

Figure 1. Chemical structures of nitrones used in this study.

2. RESULTS AND DISCUSSION

2.1. Synthesis

The MeO-PBN derivatives **1**-**4** were obtained by a one-pot reduction/condensation of 2-methyl-2-nitropropane onto the appropriate benzaldehyde in the presence of zinc powder,[25] as shown in Scheme 1. The 2,4,6-tri-MeO-PBN compound (**5**) was synthesized through direct condensation between 2,4,6-trimethoxybenzaldehyde and *N*-(*tert*butyl)hydroxylamine acetate in CH_2Cl_2, using pyrrolidine as a catalyst, following the procedure described by Morales *et al.*[26] PPN[21] and EPPN[23] were synthesized as previously described and the methoxy derivatives 4-MeO-PPN and 4-MeO-EPPN were obtained using similar synthetic routes. The 4-MeO-PPN compound (**6**) was prepared by condensing diethyl [1-(hydroxyamino)-1-methylethyl]phosphonate, which was obtained by the method described by Petrov *et al.*[27] with *p*-anisaldehyde in EtOH. For 4-MeO-EPPN (**7**), ethyl 2-methyl-2-nitropropanoate was first synthesized as previously reported[28] and was reduced *in situ* in hydroxylamine and condensed with *p*-anisaldehyde and NH_4Cl, following the procedure described by Stolze *et al.*[23]

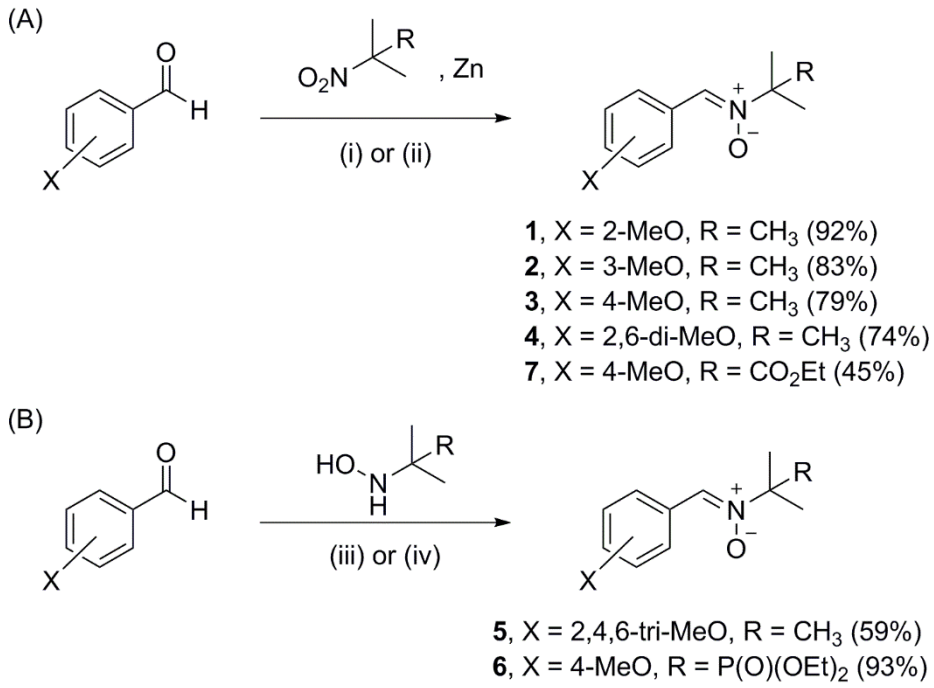

Scheme 1. Synthesis of nitrones by (A) a one-pot reduction/condensation of nitro-derivatives onto the appropriate benzaldehyde or by (B) direct condensation of N-substituted hydroxylamines with aromatic aldehydes.[a]

[a] *Reagents and conditions*: (i) AcOH, EtOH, 60 °C for compounds **1**-**4**; (ii) NH_4Cl, H_2O/MeOH (6/4, v/v), 60 °C for compound **7**; (iii) pyrrolidine, DCM, rt for compound **5**; (iv) EtOH, 60 °C for compound **6**.

The calculated octanol/water partition coefficient (*c* log *P*) of the nitrones was determined using ALOGPS 2.1 software and the values are listed in Table 1, along with the experimental values found in the literature. The introduction of a methoxy substituent on the phenyl ring decreases very slightly the lipophilicity compared to the parent nitrones (~ 0.10), with no influence of the position of the substituent. This is in good agreement with the experimental values found in the literature, where PBN, 3-MeO-PBN (**2**) and 4-MeO-PBN (**3**) exhibited similar log *P* values.[29] The polar effect of the methoxy groups on the lipophilicity seems to be additive with nitrones **4** and **5** being slightly less lipophilic than the monosubstituted derivatives **1**-**3**. This does not perfectly fit with the experimental value of nitrone **5** that was found to be similar to PBN.[29] With regards to PPN and EPPN, more pronounced differences were observed between the calculated and experimental values; they, however, remain within the same range.[13,21]

2.2. Cyclic Voltammetry

The electrochemical properties of the seven MeO-derivatives were investigated using cyclic voltammetry, and redox potentials are reported in Table 1. The experiments were performed in acetonitrile containing *tetra*-butylammonium perchlorate (TBAP) as the electrolyte. For the sake of comparison, the parent compounds were also analysed. PBN was oxidized through one-electron irreversible transfer and was reduced through a one-step two-electron reduction as previously reported,[30–32] the same behaviour being observed for the other derivatives.

Oxidation and reduction of nitrones were clearly observed, with values ranging from 1.21 to 1.68 V and from -2.56 to -1.95 V, respectively (Figure 2). The oxidation potentials measured for the MeO-derivatives were always lower than that of their parent compounds, showing that the presence of an electron-donating substituent facilitates the oxidation of the nitronyl group in agreement with the literature.[24,30–32] An opposite effect was noted for the reduction, with reduction potentials being higher than that of the parent compound, indicating harder reduction.

For the mono-substituted-PBNs, the *para* derivative (**3**) exhibited the lowest oxidation potential and the highest reduction potential while the *meta* derivative (**2**) exhibited the highest oxidation potential and the lowest reduction potential; however, the differences remained below 0.2 V. This indicates that the position of the substituent slightly influences the electrochemical properties of the nitrones. The effect was more pronounced when increasing the number of substituents. The oxidation and reduction potentials were respectively decreased and increased, suggesting an additive effect of the substituents. When compared to the parent compounds, the presence of the diethoxyphosphoryl or the ethoxycarbonyl electron-withdrawing groups facilitates reduction (~ 0.2 V) while slightly impairing oxidation (~ 0.05 V).

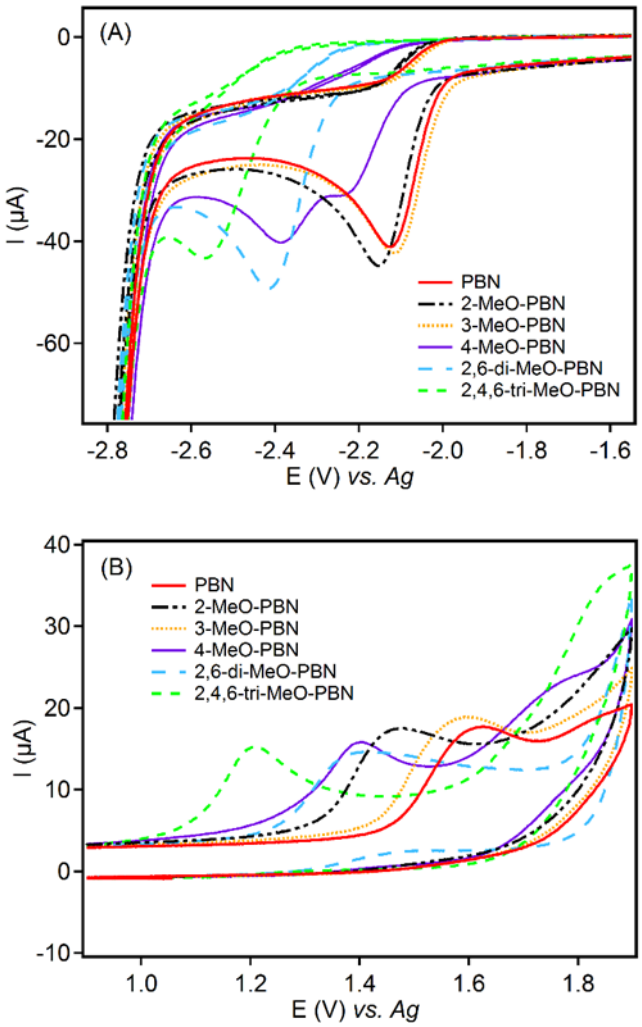

Figure 2. Cyclic voltammograms of PBN-derivatives in acetonitrile containing 0.1 M of TBAP at a GC electrode, potential scan rate υ = 0.1 V/s vs. Ag: (A) reduction and (B) oxidation.

Table 1 shows the values of the stability domains of the derivatives, which correspond to the differences between the oxidation and the reduction potentials, namely $E_p(a)$ - $E_p(c)$. These values represent the windows of electrochemical potential over which spin-trapping can be employed. This is of importance when detecting electrochemically generated radical species. Indeed, inverted spin–trapping may occur and lead to incorrect conclusions. In the inverted spin–trapping process,[33,34] the nitronyl group is oxidized to a radical cation or reduced to a radical anion, which can then react with a nucleophile or an electrophile, respectively, both yielding an aminoxyl radical that does not come from the radical addition onto the nitronyl group. For PBN, the stability domain value was 3.72 V, as previously reported.[24] The mono-substituted derivatives (**1**-**3**) exhibited a slightly smaller potential window whereas the stability domain of the di- and tri-substituted derivatives (**4** and **5**) was slightly larger. For both PPN and EPPN derivatives, the stability domain remains in the same range.

Table 1. Physicochemical, electrochemical and spin-trapping properties of MeO-derivatives.

			Voltammetry[f]			EPR spin-trapping			
	Lipophilicity		in CH_3CN[g], compound (1 mM)			$^{\bullet}CH_2OH$			
Compounds	*c*log*P*[a]	log*P*	$E_p(c)$ (V)	$E_p(a)$ (V)	Stability domain[h] (V)	a_N (G)	a_H (G)	a_P (G)	k_N/k_{PBN}[j]
PBN	2.67	1.2[b]	-2.12 (-2.12)[i]	1.60 (1.53)[i]	3.72	14.3	2.7	-	1
2-MeO-PBN (1)	2.57	nd[c]	-2.15	1.46	3.61	14.1	3.2	-	1.026
3-MeO-PBN (2)	2.57	1.4[b]	-2.11	1.57	3.68	14.0	3.2	-	0.935
4-MeO-PBN (3)	2.57	1.2	-2.22 (-2.23)[i]	1.40 (1.26)[i]	3.62	14.1	3.1	-	1.128 (0.832)[i]
2,6-di-MeO-PBN (4)	2.46	nd[c]	-2.41	1.39	3.80	nd[c,k]	nd[c,k]	-	nd[c,k]
2,4,6-tri-MeO-PBN (5)	2.36	1.2[b]	-2.56	1.21	3.77	nd[c,k]	nd[c,k]	-	nd[c,k]
PPN	3.01	1.0[d]	-1.96	1.64	3.60	13.5	2.7	38.5	6.369
4-MeO-PPN (6)	2.90	nd[c]	-2.08	1.44	3.52	13.5	2.9	38.8	5.882
EPPN	2.20	1.5[e]	-1.95	1.68	3.63	14.2	3.0	-	1.498
4-MeO-EPPN (7)	2.10	nd[c]	-2.11	1.46	3.57	13.7	3.0	-	0.891

[a] Calculated octanol/water partition coefficient values obtained using ALOGPS 2.1 software (http://www.vcclab.org/lab/alogps/).
[b] Data from Janzen *et al.*[29]
[c] Not determined.
[d] Data from Roubaud *et al.*[21]
[e] Data from Roubaud *et al.*[13]
[f] The peak potentials are given versus a silver wire electrode for a potential scan rate 0.1 V/s.
[g] Containing 0.1 M TBAP with reduction $E_p(c)$ and oxidation $E_p(a)$ at glassy carbon (GC) electrode.
[h] The stability domain is given as: $E_p(a)$-$E_p(c)$.
[i] Data from Rosselin *et al.*[24]
[j] Ratio of the second-order rate constants for the hydroxymethyl radical trapping by various nitrones (k_N) and by PBN (k_{PBN}) in methanol, calculated with a ratio k_{PBN}/k_{TN} = 0.069.
[k] The EPR signal of the adduct was too weak to allow a reliable determination of the ratio.

2.3. Hydroxymethyl radical trapping by electron paramagnetic resonance

The spin-trapping properties of the derivatives were studied by evaluating their capacity of trapping the hydroxymethyl radical ($^{\bullet}CH_2OH$), which is representative of the formation of alcohol-derived radicals during oxidative stress. Oxidative stress leads to overproduction of several reactive oxygen species ($O_2^{\bullet-}$, H_2O_2, $HO^{\bullet}$), which further react with sugars, proteins, lipids and DNA, thereby yielding carbon-centered radicals, like hydroxyalkyl radicals.[35] The $^{\bullet}CH_2OH$ radical was generated *in situ* by a standard Fenton system in the presence of the nitrone derivatives noted **N** and the competitive scavenger 1,3,5-tri[(*N*-(1-diethylphosphono)-1-methylethyl) *N*-oxy-aldimine] noted **TN**.[16] For 2,6-di-MeO-PBN (**4**) and 2,4,6-tri-MeO-PBN (**5**), only background noise was observed, indicating that these nitrones did not efficiently trap the hydroxymethyl radicals. Although we have no strong evidence to discard side-reactions between $^{\bullet}OH$ or $^{\bullet}CH_2OH$ radicals with the methoxy groups of these nitrones, the steric hindrance due to the *ortho* substituents very likely explains the inefficiency of (**4**) and (**5**) to act as spin traps. The five mono-substituted derivatives gave rise to a standard six-line EPR spectrum due to hyperfine couplings of the unpaired electron with nitrogen and β-hydrogen nuclei. For PPN and 4-MeO-PPN (**6**), additional lines due to the coupling with the phosphorous atom were observed. The hyperfine coupling constants (hfcc) are reported in Table 1 and are consistent with PBN-type spin adducts.[36]

The $^{\bullet}CH_2OH$ spin-trapping rate was assessed by measuring the relative intensity (as the signal area) of the EPR signals of the **N**-CH_2OH and **TN**-CH_2OH adducts (Figure 3). PPN and 4-MeO-PPN (**6**) were directly tested *versus* PBN instead of **TN**. The standard kinetic competition model described by Roubaud *et al.*[16] was employed (eqn (1)):

$$R/r = 1 + k_{\mathrm{N}}[\mathrm{N}]/k_{\mathrm{TN}}[\mathrm{TN}] \qquad (1)$$

k_N and k_{TN} correspond to the second-order rate constants for $^{\bullet}CH_2OH$ trapping by the nitrones **N** and **TN**, respectively while *R* and *r* represent the trapping rate by both **TN** and **N**, and by **TN** only, respectively.

By plotting the *R*/*r* ratio as a function of [**N**]/[**TN**] ratio, a straight line was obtained for each derivative (Figure 3) and five different [**N**]/[**TN**] ratios kept between 2 and 5 were used. In order to compare the spin-trapping of MeO-derivatives with PBN for nitrones **1**-**3**, EPPN and

nitrone **7**, a k_{PBN}/k_{TN} ratio of 0.069 was determined using commercially available PBN instead of **N**. From these results, the k_N/k_{PBN} ratio was calculated and the values obtained are reported in Table 1.

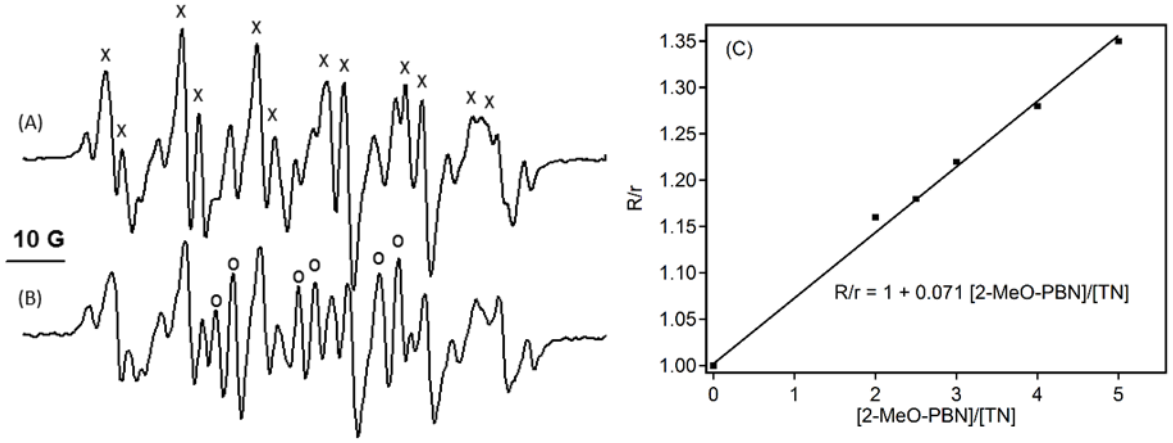

Figure 3. (A)-(B) EPR signals of TN and 2-MeO-PBN (**1**) hydroxymethyl radical adducts, respectively. Hydroxymethyl radical was generated by a Fenton system and the ratio of [**1**]/[TN] was: (A) [**1**]/[TN] = 2; (B) [**1**]/[TN] = 5. The peaks topped by a cross (×) correspond to the hydroxymethyl radical adduct of TN and those topped by a round (○) correspond to the hydroxymethyl radical adduct of **1**. (C) Determination of the relative rate constant k_N/k_{TN} of $^{\bullet}CH_2OH$ trapping by nitrone **1** (R^2 = 0.999).

All the derivatives tested exhibited lower $^{\bullet}CH_2OH$ radical trapping efficiency than **TN**, which bears three nitronyl groups. For derivatives **1-3**, k_N/k_{PBN} values ranged from 0.935 to 1.128, indicating similar rates of trapping to PBN. This suggests that for a given nitrone, the position of the MeO-substituent on the phenyl ring has no significant effect on the trapping of $^{\bullet}CH_2OH$. With regards to the α-substituted derivatives, EPPN trapped $^{\bullet}CH_2OH$ radicals 1.5 times faster than PBN, while PPN exhibited even more improved reactivity, that is, 6.4 times faster trapping. This demonstrates that the introduction of an electron-withdrawing group in the α-position of the nitronyl function improves the spin-trapping properties.

2.4. Calculated nitronyl atomic partial charge and ionization potentials

The electronic population analysis within the natural bond orbital (NBO) framework[37,38] on the nitronyl atoms (H, C, N and O) and the IPs of PBN derivatives were calculated in water using the DFT formalism (Table 2). The electronic densities on the nitronyl atoms depend on

the position and on the number of MeO substituents as well as on the presence of an electron-withdrawing group in the α-position of the nitronyl function. Therefore, two electronic effects are operatively affecting the nitronyl atomic partial charges of the derivatives, the inductive effect of the diethoxyphosphoryl and carbonyl groups at the α-position and the mesomeric effect of the methoxy substituents. Using ^{1}H NMR spectroscopy, the chemical shifts of the nitronyl-H in $CDCl_3$ were measured and showed a good correlation with the nitronyl-H atomic partial charges (Figure 4A). It is worth mentioning that only 2,6-di-MeO-PBN (**4**) and 2,4,6-tri-MeO-PBN (**5**) were out of the correlation. This correlation confirms the polar effect of the substituents both on the aromatic ring and in the α-position of the nitronyl function, however with subtler effects in case of poly-substitution likely due to the compensation of each electronic effect over the whole charge delocalization.

Table 2. Calculated atomic partial charges of the nitronyl atoms and ionization potentials of MeO-derivatives at the (CPCM)/M06-2X/6-31+g(d,p) level of theory.

	Atomic partial charges of the nitronyl atoms (*e*)				
Compounds	H	C	N	O	IP (eV)
PBN	0.254	0.019	0.080	-0.636	6.0
2-MeO-PBN (1)	0.262	0.009	0.084	-0.633	5.6
3-MeO-PBN (2)	0.255	0.021	0.081	-0.635	6.0
4-MeO-PBN (3)	0.253	0.028	0.069	-0.651	5.7
2,6-di-MeO-PBN (4)	0.261	0.018	0.085	-0.638	5.7
2,4,6-tri-MeO-PBN (5)	0.259	0.036	0.075	-0.644	5.4
PPN	0.258	0.033	0.073	-0.628	6.0
4-MeO-PPN (6)	0.254	0.056	0.056	-0.644	5.6
EPPN	0.250	0.020	0.084	-0.610	6.0
4-MeO-EPPN (7)	0.248	0.031	0.072	-0.626	5.7

Since nitrones have a similar reactivity to carbonyl groups allowing nucleophilic addition reactions, the electronic population of the nitronyl-carbon provides hints about the reactivity of the nitronyl function. For the *ortho*-derivative (**1**), the nitronyl-C atomic partial charge is close to zero, being the lowest over the series. This suggests that this position would be mildly reactive toward a nucleophilic attack. Conversely, for 4-MeO-PPN (**6**), both the *para* electron-donating MeO substituent and α-position electron-withdrawing diethoxyphosphoryl group lead to synergistic electronic effects. This suggests that it would be highly reactive toward a nucleophilic attack, as shown by the nitronyl-C atomic partial charge, which was the most positive of the series. While plotting the relative rate constants of $^{\bullet}CH_2OH$ addition to

nitrones *versus* the nitronyl-C atomic partial charge (Figure 4B), a good correlation for PBN, PPN and EPPN was observed (R^2 = 0.9996), the more positive the nitronyl-C atomic partial charge, the faster the addition reaction. Our experimental values therefore indicate that an electron withdrawing inductive effect on the *N-tert* butyl group increases the reactivity of the nitronyl group towards the $^{\bullet}CH_2OH$ radical. This is supported by the nucleophilic nature of the $^{\bullet}CH_2OH$ radical.[39] However, when adding the MeO-derivatives, the positive mesomeric effects on the aromatic ring tend to decrease the reactivity and no correlation with the nitronyl-C atomic partial charge was observed, suggesting that not only electronic factors are involved in the trapping reaction of $^{\bullet}CH_2OH$ with the nitronyl group. This highlights the need for further studies to determine how these two effects alter the reactivity of the nitronyl group and which of the two is more prominent.

Given the chemical accuracy of IP calculations at the DFT level of theory (*ca.* 0.1 eV), the following ranking was obtained (See Table 2): 2,4,6-tri-MeO-PBN (**5**) < 4-MeO-PPN (**6**) ≈ 2-MeO-PBN (**1**) ≈ 4-MeO-PBN (**3**) ≈ 2,6-di-MeO-PBN (**4**) ≈ 4-MeO-EPPN (**7**) < PBN ≈ EPPN ≈ PPN ≈ 3-MeO-PBN (**2**). This ranking is in excellent agreement with the experimentally observed oxidation potentials (See Figure 4C); the lower the IP, the lower the oxidation potential. For instance, the highest calculated IP value was observed for EPPN, which also exhibits the highest oxidation potential. Such strong correlation between IP and oxidation potential (R^2 = 0.926, Figure 4C) clearly suggests that a computational approach could (i) predict the electrochemical properties of nitrones but also (ii) provide hints in order to tune oxidation properties of nitronyl derivatives. For example, the presence of an electron-withdrawing group in the α-position of the nitronyl moiety does not modify the stability of the radical cation formed after the electron transfer event, as depicted by the similar spin density distributions (Figure 5). Likewise, *meta*-substitution by donating moieties (*e.g.*, MeO) does not stabilize the radical cation forms. However, the significant increase of π-delocalization over the aromatic ring strongly stabilizes the radical cation, wich in turn decreases IP and thus the oxidation potential.

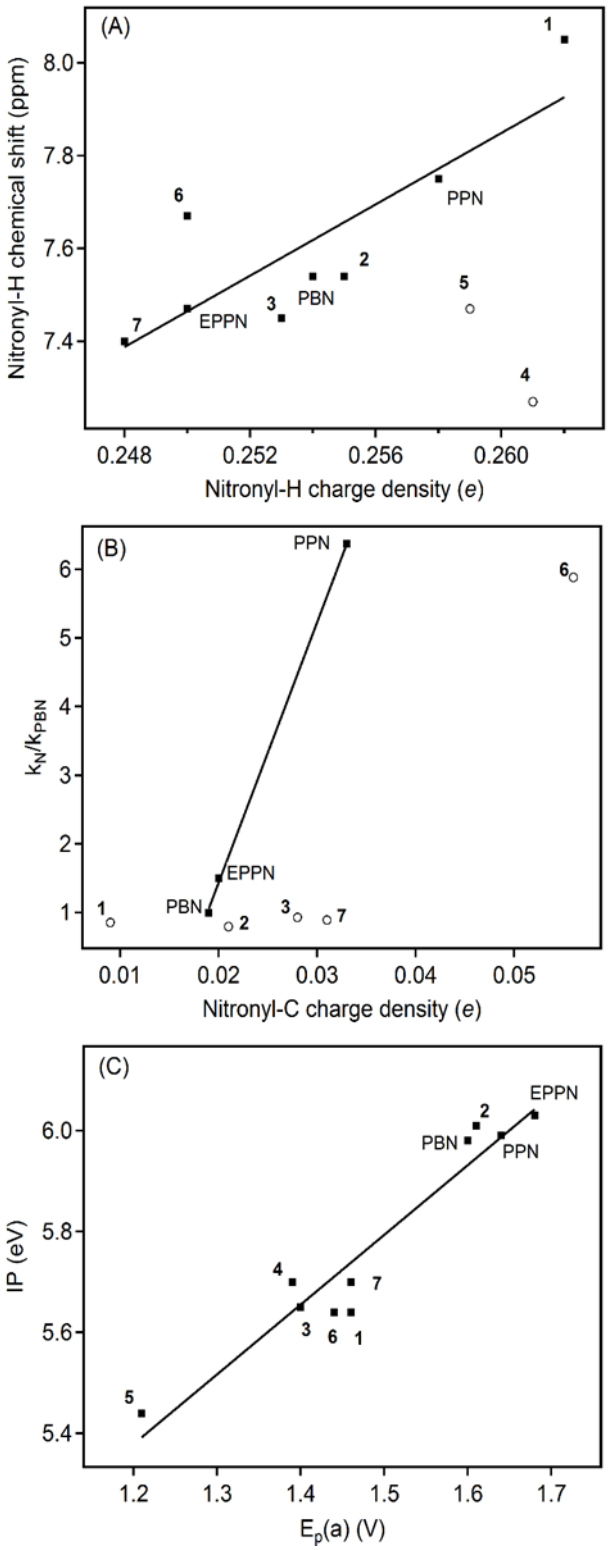

Figure 4. (A) Correlation of nitronyl-H chemical shifts with nitronyl-H charge densities (R^2 = 0.852 excluding the outliers 2,6-di-MeO-PBN and 2,4,6-tri-MeO-PBN marked as (○)); (B) Plots of experimental relative rate constants of hydroxymethyl addition to nitrones with nitronyl-C charge density; (C) Correlation of ionization potential with oxidation potential of nitrones (R^2 = 0.926).

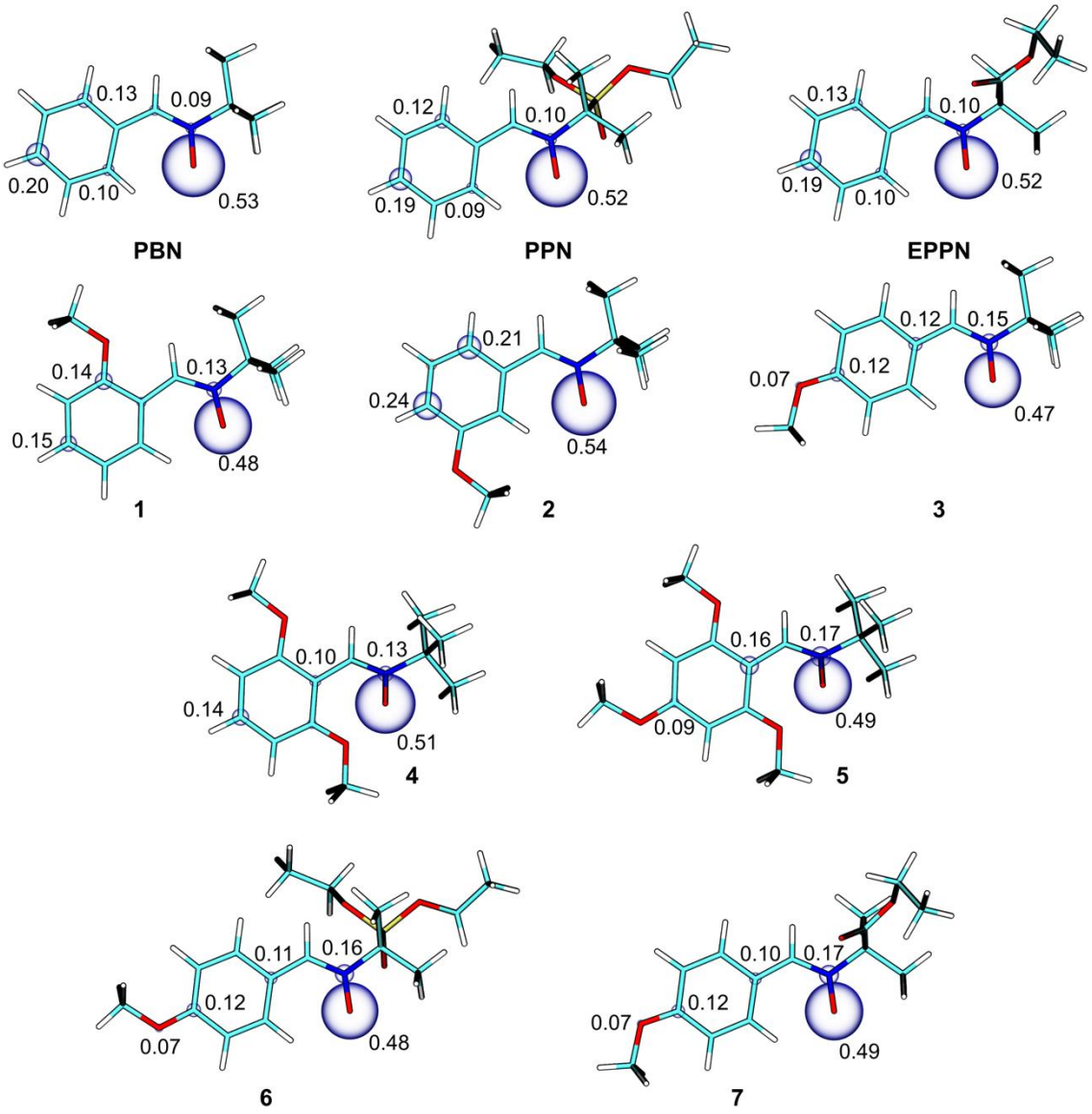

Figure 5. Mulliken spin density distribution of the radical cations formed after single electron abstractions.

3. CONCLUSION

In this work, we have studied the effect of the position and the number of electron-donating MeO-substituents on the reactivity of phenyl nitrones. A series of mono-substituted (*ortho*-, *meta*- and *para*-) and di- and tri-substituted derivatives of PBN was synthesized as well as the

4-MeO-derivatives of PPN and EPPN. The substituent effect was demonstrated by a computational approach, from which a correlation between ^{1}H NMR chemical shifts and nitronyl-H atomic partial charges of the derivatives was obtained. Cyclic voltammetry experiments showed that the redox potentials depend on the position and on the number of substituents. While electron-donating groups on the phenyl ring tend to favour oxidation compared to unsubstituted derivatives, electron-withdrawing groups in the α-position of the nitronyl function slightly impair oxidation. An opposite trend was obviously demonstrated for the reduction of the nitronyl function. With regard to the number of substituents, the electronic effects appeared to be additive. The computed ionization potentials were found to correlate with the experimental oxidation potentials, suggesting that a computational approach may predict the electrochemical properties of nitrones. The reactivity towards $^{\bullet}CH_2OH$ radical trapping was correlated with the electron-withdrawing nature of the substituent in the α-position of the nitronyl function, with PPN being the most efficient trap, supporting the nucleophilic nature of $^{\bullet}CH_2OH$. However, when adding MeO-substituents, the rates of trapping were significantly lowered, with an absence of correlation with the nitronyl-C atomic partial charges. In addition, with the di-*ortho* substituted derivatives, no trapping was observed. This suggests that not only electronic factors are involved in the spin-trapping reaction and therefore this warrants further investigation.

EXPERIMENTAL SECTION

Synthesis. All reagents were obtained from commercial sources and were used as received. All solvents were distilled and dried according to standard procedures. The TLC analysis was performed on aluminium sheets coated with silica gel (40−63 μm). Compound detection was achieved either by exposure to UV light (254 nm) and/or by spraying a 5% sulfuric acid solution in ethanol or a 2% ninhydrin solution in ethanol and then by heating up to ~ 150 °C. Flash column chromatography was carried out on silica gel (40−63 μm). Melting points have not been corrected. NMR spectra were recorded on a Bruker AC400 at 400, 100 and 162 MHz for ^{1}H, ^{13}C and ^{31}P experiments, respectively. Chemical shifts are given in ppm relative to the solvent residual peak as a heteronuclear reference for ^{1}H and ^{13}C. Abbreviations used for signal patterns are as follows: s, singlet; d, doublet; dd, doublet of doublets; t, triplet; td,

triplet of doublets; q, quartet; m, multiplet. HR-MS spectra were recorded on a mass spectrometer equipped with a TOF analyzer for ESI+ experiments.

***N-tert*-butyl-α-(2-methoxy)phenylnitrone (1).** In an argon atmosphere and under stirring, o-anisaldehyde (1.22 g, 9.0 mmol, 1.0 equiv), 2-methyl-2-nitropropane (1.9 mL, 17.9 mmol, 2.0 equiv) and AcOH (3.1 mL, 54.0 mmol, 6.0 equiv) were dissolved in dry EtOH. The mixture was cooled down to 0 °C, then zinc powder (2.4 g, 36.0 mmol, 4.0 equiv) was slowly added in order to keep the temperature below 15 °C. The mixture was stirred at room temperature for 30 min then heated at 60 °C in the dark for 22 h in the presence of molecular sieves (4Å). The reaction mixture was filtered off through a pad of Celite, and the solvent was removed under vacuum. The crude mixture was purified by flash chromatography (EtOAc/cyclohexane, 2/8) followed by two successive crystallisations from EtOAc/*n*-hexane to afford 1.70 g of the title compound (8.2 mmol, yield 92%) as a white powder. R_f (EtOAc/cyclohexane, 2/8) = 0.16. ^{1}H NMR (400 MHz, $CDCl_3$,) δ 9.36 (1H, dd, *J* = 8.0 and 1.2 Hz), 8.05 (1H, s), 7.35 (1H, td, *J* = 8.4 and 2.0 Hz), 7.02 (1H, t, *J* = 7.6 Hz), 6.88 (1H, d, *J* = 8.2 Hz), 3.86 (3H, s), 1.61 (9H, s); ^{13}C NMR (100 MHz, $CDCl_3$) δ 157.2, 131.3, 128.8, 124.5, 120.9, 120.2, 109.7, 71.1, 55.7, 28.5. The spectral data was in agreement with the literature.[40]

***N-tert*-butyl-α-(3-methoxy)phenylnitrone (2).** The synthetic procedure was essentially the same as for compound **1**. m-anisaldehyde (1.39 g, 10.2 mmol) and 2-methyl-2-nitropropane (2.2 mL, 20.4 mmol) were used as starting materials. The reaction time was 24 h. The crude mixture was purified by flash chromatography (EtOAc/cyclohexane, 4/6) followed by two successive crystallisations from EtOAc/*n*-hexane to afford 1.76 g of the title compound (8.5 mmol, yield 83%) as a white powder. R_f (EtOAc/cyclohexane, 4/6) = 0.28. ^{1}H NMR (400 MHz, $CDCl_3$,) δ 8.34 (1H, s), 7.54 (1H, s), 7.48 (1H, d, *J* = 7.6 Hz), 7.31 (1H, t, *J* = 8.0 Hz), 6.97 (1H, dd, *J* = 8.0 and 2.4 Hz), 3.86 (3H, s), 1.62 (9H, s); ^{13}C NMR (100 MHz, $CDCl_3$) δ 159.7, 132.4, 130.3, 129.3, 122.1, 117.6, 112.3, 71.1, 55.5, 28.5. The spectral data were in agreement with the literature.[41]

***N-tert*-butyl-α-(4-methoxy)phenylnitrone (3).** The synthetic procedure was essentially the same as for compound **1**. p-anisaldehyde (1.42 g, 10.4 mmol) and 2-methyl-2-nitropropane (2.3 mL, 20.8 mmol) were used as starting materials. The reaction time was 26 h. The crude mixture was purified by flash chromatography (EtOAc/cyclohexane, 5/5) followed by two

successive crystallisations from EtOAc/*n*-hexane to afford 1.70 g of the title compound (8.2 mmol, yield 79%) as a white powder. R_f (EtOAc/cyclohexane, 5/5) = 0.18. ^{1}H NMR (400 MHz, $CDCl_3$,) δ 8.27 (2H, d, *J* = 9.2 Hz), 7.45 (1H, s), 6.91 (2H, d, *J* = 8.0 Hz), 3.83 (3H, s), 1.59 (9H, s); ^{13}C NMR (100 MHz, $CDCl_3$) δ 160.9, 130.8, 129.5, 124.2, 113.8, 70.2, 55.4, 28.4. The spectral data were in agreement with the literature.[40]

***N*-*tert*-butyl-α-(2,6-dimethoxy)phenylnitrone (4).** The synthetic procedure was essentially the same as for compound **1**. 2,6-dimethoxybenzaldehyde (890 mg, 5.36 mmol) and 2-methyl-2-nitropropane (1.2 mL, 10.72 mmol) were used as starting materials. The reaction time was 21 h. The crude mixture was purified by flash chromatography (EtOAc/MeOH, 98/2) followed by two successive crystallisations from EtOAc/*n*-hexane to afford 944 mg of the title compound (3.98 mmol, yield 74%) as a white powder. R_f (EtOAc/MeOH, 95/5) = 0.32. ^{1}H NMR (400 MHz, $CDCl_3$,) δ 7.54 (1H, s), 7.27 (1H, t, *J* = 8.4 Hz), 6.55 (2H, d, *J* = 8.4 Hz), 3.82 (6H, s), 1.61 (9H, s); ^{13}C NMR (100 MHz, $CDCl_3$) δ 158.9, 130.7, 124.9, 109.1, 104.0, 70.1, 56.1, 28.5. HR-MS (ESI+, m/z) calcd for $C_{13}H_{20}NO_3$ $[(M + H)^+]$ 238.1443, found 238.1449.

***N*-*tert*-butyl-α-(2,4,6-trimethoxy)phenylnitrone (5).** Under an argon atmosphere and stirring, 2,4,6-trimethoxybenzaldehyde (1.01 g, 5.17 mmol, 1.0 equiv) and *N*-(*tert*-butyl)hydroxylamine acetate (770 mg, 5.17 mmol, 1.0 equiv) were dissolved in dry DCM (0.33 M). Pyrrolidine (0.5 mL, 6.20 mmol, 1.2 equiv) was added and the mixture was stirred at room temperature for 1 h. The solvent was removed under vacuum and the crude mixture was purified by flash chromatography (EtOAc/MeOH, 95/5) followed by two successive crystallisations from EtOAc/*n*-hexane to afford 0.81 g of the title compound (3.03 mmol, yield 59%) as a white powder. R_f (EtOAc/MeOH, 95/5) = 0.26. ^{1}H NMR (400 MHz, $CDCl_3$,) δ 7.47 (1H, s), 6.12 (2H, s), 3.81 (3H, s), 3.80 (6H, s), 1.59 (9H, s); ^{13}C NMR (100 MHz, $CDCl_3$) δ 162.6, 159.7, 124.7, 102.4, 91.0, 69.8, 56.0, 55.6, 28.6. The spectral data were in agreement with the literature.[42]

***N*-2-(diethoxyphosphoryl-propyl)-α-(4-methoxy)phenylnitrone (6).** Under an argon atmosphere and stirring, *p*-anisaldehyde (565 mg, 4.15 mmol, 1.0 equiv) and diethyl [1-(hydroxyamino)-1-methylethyl]phosphonate[20] (876 mg, 4.15 mmol, 1.0 equiv) were dissolved in dry EtOH. The mixture was stirred at 60 °C for 22 h. The solvent was removed under vacuum and the crude mixture was purified by flash chromatography (EtOAc/cyclohexane,

9/1) to afford 1.27 g of the title compound (3.86 mmol, yield 93%) as a colorless oil. R_f (EtOAc/cyclohexane, 9/1) = 0.22. ^{1}H NMR (400 MHz, $CDCl_3$,) δ 8.27 (2H, d, *J* = 8.8 Hz), 7.67 (1H, d, *J* = 2.8 Hz), 6.92 (2H, d, *J* = 9.2 Hz), 4.23-4.19 (4H, m), 3.84 (3H, s), 1.82 (6H, d, *J* = 14.8 Hz), 1.32 (6H, t, *J* = 7.2 Hz); ^{13}C NMR (100 MHz, $CDCl_3$) δ 161.3, 133.1 (d, *J* = 4 Hz), 131.2, 123.9 (d, *J* = 2 Hz), 113.9, 72.3 (d, *J* = 153 Hz), 63.4 (d, *J* = 7 Hz), 55.5, 23.4, 16.6 (d, *J* = 6 Hz); ^{31}P NMR (162 MHz, $CDCl_3$) δ 23.38. HR-MS (ESI+, m/z) calcd for $C_{15}H_{25}NO_5P$ $[(M + H)^+]$ 330.1470, found 330.1469.

***N*-2-(ethoxycarbonyl-propyl)-α-(4-methoxy)phenylnitrone (7).** Under an argon atmosphere and stirring, ethyl 2-methyl-2-nitropropanoate[23] (2.00 g, 12.42 mmol, 1.0 equiv), *p*-anisaldehyde (1.8 mL, 14.90 mmol, 1.2 equiv) and NH_4Cl (930 mg, 17.39 mmol, 1.4 equiv) were dissolved in H_2O/MeOH (6/4, v/v). The mixture was cooled down to 0 °C, then zinc powder (1.61 g, 24.84 mmol, 2.0 equiv) was slowly added to keep the temperature below 15 °C. The mixture was stirred at room temperature for 1h then heated at 60 °C in the dark for 18 h. The reaction mixture was filtered off through a pad of Celite, and the solvent was removed under vacuum. The crude mixture was purified by flash chromatography (EtOAc/cyclohexane, 5/5) followed by two successive crystallisations from EtOAc/*n*-hexane to afford 1.49 g of the title compound (5.62 mmol, yield 45%) as a white powder. R_f (EtOAc/cyclohexane, 5/5) = 0.26. ^{1}H NMR (400 MHz, $CDCl_3$,) δ 8.27 (2H, d, *J* = 8.8 Hz), 7.40 (1H, s), δ 6.93 (2H, d, *J* = 8.8 Hz), 4.25 (2H, q, *J* = 7.2 Hz), 3.85 (3H, s), 1.81 (6H, s), 1.27 (3H, t, *J* = 7.2 Hz); ^{13}C NMR (100 MHz, $CDCl_3$) δ 170.8, 161.4, 131.2, 131.0, 123.5, 114.0, 76.5, 62.2, 55.5, 24.6, 14.1. HR-MS (ESI+, m/z) calcd for $C_{14}H_{20}NO_4$ $[(M + H)^+]$ 266.1392, found 266.1398.

Determination of *c* log *P* values. The partition coefficient octanol/water (*c* log *P*) was determined by using ALOGPS 2.1 software, which is available at www.vcclab.org/lab/alogps/.

Cyclic voltammetric measurements. The electrochemical experiments were carried out using a three-electrode cell under a dry argon atmosphere at room temperature. A silver wire electrode was used as the reference electrode and a platinum wire was used as the auxiliary

electrode. The working electrode (glassy carbon) was polished prior to each experiment using a 0.04 μm aqueous alumina slurry on a wetted polishing cloth.

EPR measurements and spin-trapping kinetics. EPR measurements were carried out using a Bruker EMX spectrometer operating at the X-band with 100 kHz modulation frequency. The general instrument settings used for spectral acquisition were as follows: microwave power, 20 mW; modulation amplitude, 1 G; received gains, 9×10^1 to 9×10^2; scan time, 5 s; sweep width, 100 G. The spectra were recorded at room temperature, and measurements were performed using a capillary tube. The spectrum simulation was carried out using the WINSIM program,[43] available as free software from Public Electron Paramagnetic Resonance Software Tools (http://www.niehs.nih.gov/research/resources/software/tox-pharm/tools/). The solvents were of the highest purity grade and used without further purification. Trinitrone TN was synthesized and purified as previously described.[16] To generate the hydroxymethyl ($^{\bullet}CH_2OH$) radical, nitrone (100 mM) was dissolved in a Fenton system containing hydrogen peroxide (6%) and iron (II) sulfate (6 mM) in methanol. The method of kinetic competition permitted us to evaluate the ratio of the second-order rate constants for the trapping of $^{\bullet}CH_2OH$ by one of the nitrone N of interest (k_N, corresponding to the compounds **1**–**7**) and TN (k_{TN}) or PBN (k_{PBN}) used as competitive inhibitors. Then, the commercially available PBN was tested *versus* TN to determine the ratio of the rate constants for the trapping of $^{\bullet}CH_2OH$ by PBN and by TN: *i.e.*, k_{PBN}/k_{TN} for nitrones **1**-**5** and **7**. The concentrations of the various nitrones were varied to keep the [N]/[TN] ratio between 2 and 5. For each nitrone, at least five experiments were repeated twice. In each case, a series of 10 EPR spectra was then recorded (scan time for a single spectrum; 20 s). The signal-to-noise ratio was improved using an SVD procedure, as described elsewhere.[44] The signal recorded exactly 2 min after the beginning of the reaction was then simulated using the WinSim software to determine the relative areas of the **N**-CH_2OH and **TN**-CH_2OH adducts. In this approach, the *R/r* ratio was evaluated as follows:

$$\frac{R}{r} = \frac{area\ of\ N\text{-}R\ signal + area\ of\ TN\text{-}R\ signal}{area\ of\ TN\text{-}R\ signal} \qquad (2)$$

General computational methods. Geometries and energies were optimized using the DFT formalism with the hybrid meta-GGA (Generalized Gradient Approximation) M06-2X

functional and the 6-31+G(d,p) basis set. Three other hybrid functionals were tested on PBN, taken as a reference compound, namely B3LYP, B3P86 and PBE1PBE (data not shown). No differences were observed in terms of atomic charges, one of the major parameters under scrutiny in this work, hence the M06-2X functional was chosen for all compounds, as a good standard.[45] The use of a larger basis set (namely 6-311+g(2d,3pd)) did not exhibit significant differences in terms of atomic charges with respect to 6-31+G(d,p), suggesting the absence of a basis set effect owing to the relatively small molecular size of the series. Therefore, the 6-31+G(d,p) basis set was used for all compounds. A frequency analysis was systematically performed at 298 K and 1 atm, at the M06-2X/6-31+G(d,p) level of theory, confirming the optimized geometries at the potential energy surface minimum owing to the absence of any imaginary frequency. Solvent (water) effects were considered by using the C-PCM (conductor-like polarizable continuum model) solvation model.[46,47] In continuum models, the solute is embedded into a shape-adapted cavity surrounded by a dielectric continuum characterized by its dielectric constant. Calculations were performed in water ($\varepsilon = 78.35$). The atomic charge analysis was performed using the natural population analysis (NPA) within the NBO (Natural Bond Orbital) framework. The IP was calculated as follows:

$$IP = E(ArNO^{\bullet+}) - E(ArNO),$$

where $ArNO^{\bullet+}$ is the radical cation obtained after electron withdraw from the neutral form of the PBN derivatives, named here as ArNO. It is worth mentioning that IP corresponds to the adiabatic energy of electron withdrawal energy, *i.e.*, considering the radical cation energy using the neutral form geometry. All calculations were performed with Gaussian 09 Rev. A2.[48]

CONFLICTS OF INTEREST

There are no conflicts to declare.

ACKNOWLEDGEMENTS

Anaïs Deletraz was the recipient of a fellowship from the “Région Provence Alpes Côte d’Azur”. We thank the company Neuro-Sys (www.neuro-sys.com) for supporting this work. Thanks are also due: to Fédération RENARD IR-RPE CNRS 3443 for providing funds for the EPR studies; to CALI for computational facilities and the National Program of Sustainability I from the Ministry-of-Youth, Education and Sports of the Czech Republic (LO1305); and to Miss Jamila Chetouani for her excellent technical assistance in acquiring computational data. This study was conducted with the financial support of the European Regional Development Fund, the French Government, the “Région Provence Alpes Côte d'Azur”, the Departmental Council of Vaucluse and the Urban Community of Avignon.

NOTES AND REFERENCES

1 F. A. Villamena and J. L. Zweier, *Antioxid. Redox Signal.*, 2004, **6**, 619–629.
2 M. J. Davies, *Methods*, 2016, 21–30.
3 R. A. Floyd, R. D. Kopke, C.-H. Choi, S. B. Foster, S. Doblas and R. A. Towner, *Free Radic. Biol. Med.*, 2008, **45**, 1361–1374.
4 F. A. Villamena, A. Das and K. M. Nash, *Future Med. Chem.*, 2012, **9**, 1171–1207.
5 R. A. Floyd, H. C. Castro Faria Neto, G. A. Zimmerman, K. Hensley and R. A. Towner, *Free Radic. Biol. Med.*, 2013, **62**, 145–156.
6 Y. Sun, G. Zhang, Z. Zhang, P. Yu, H. Zhong, J. Du and Y. Wang, *Bioorg. Med. Chem.*, 2012, **20**, 3939–3945.
7 P. L. Zamora and F. A. Villamena, *Future Med. Chem.*, 2013, **5**, 465–478.
8 D. S. S. Costa, T. Martino, F. C. Magalhães, G. Justo, M. G. P. Coelho, J. C. F. Barcellos, V. B. Moura, P. R. R. Costa, K. C. C. Sabino and A. G. Dias, *Bioorg. Med. Chem.*, 2015, **23**, 2053–2061.
9 A. Shuaib, K. R. Lees, P. Lyden, J. Grotta, A. Davalos, S. M. Davis, H.-C. Diener, T. Ashwood, W. W. Wasiewski and U. Emeribe, *N. Engl. J. Med.*, 2007, **357**, 562–571.
10 H.-C. Diener, K. R. Lees, P. Lyden, J. Grotta, A. Davalos, S. M. Davis, A. Shuaib, T. Ashwood, W. Wasiewski, V. Alderfer, H.-G. Hardemark and L. Rodichok, *Stroke*, 2008, **39**, 1751–1758.
11 D. F. Church, *J. Org. Chem.*, 1986, **51**, 1138–1140.
12 K. Murofushi, K. Abe and M. Hirota, *J. Chem. Soc. Perkin Trans. 2*, 1987, 1829–1833.
13 V. Roubaud, R. Lauricella, J.-C. Bouteiller and B. Tuccio, *Arch. Biochem. Biophys.*, 2002, **397**, 51–56.
14 A. Allouch, V. Roubaud, R. Lauricella, J.-C. Bouteiller and B. Tuccio, *Org. Biomol. Chem.*, 2005, **3**, 2458–2462.
15 C. Rizzi, S. Marque, F. Belin, J.-C. Bouteiller, R. Lauricella, B. Tuccio, V. Cerri and P. Tordo, *J. Chem. Soc. Perkin Trans. 2*, 1997, 2513–2518.
16 V. Roubaud, H. Dozol, C. Rizzi, R. Lauricella, J.-C. Bouteiller and B. Tuccio, *J. Chem. Soc. Perkin Trans. 2*, 2002, 958–964.
17 S. Kim, G. V. M. de A. Vilela, J. Bouajila, A. G. Dias, F. Z. G. A. Cyrino, E. Bouskela, P. R. R. Costa and F. Nepveu, *Bioorg. Med. Chem.*, 2007, **15**, 3572–3578.
18 M. Rosselin, F. Choteau, K. Zéamari, K. M. Nash, A. Das, R. Lauricella, E. Lojou, B. Tuccio, F. A. Villamena and G. Durand, *J. Org. Chem.*, 2014, **79**, 6615–6626.
19 M. Stiles, G. P. Moiseyev, M. L. Budda, A. Linens, R. S. Brush, H. Qi, G. L. White, R. F. Wolf, J. Ma, R. Floyd and others, *PLOS One*, 2015, **10**, e0145305.
20 A. Zeghdaoui, B. Tuccio, J.-P. Finet, V. Cerri and P. Tordo, *J. Chem. Soc. Perkin Trans. 2*, 1995, 2087–2089.
21 V. Roubaud, R. Lauricella, B. Tuccio, J.-C. Bouteiller and P. Tordo, *Res. Chem. Intermed.*, 1996, **22**, 405–416.
22 B. Tuccio, A. Zeghdaoui, J.-P. Finet, V. Cerri and P. Tordo, *Res. Chem. Intermed.*, 1996, **22**, 393–404.

23 K. Stolze, N. Udilova, T. Rosenau, A. Hofinger and H. Nohl, *Biochem. Pharmacol.*, 2003, **66**, 1717–1726.
24 M. Rosselin, B. Tuccio, P. Pério, Frederick. A. Villamena, P.-L. Fabre and G. Durand, *Electrochimica Acta*, 2016, **193**, 231–239.
25 R. Huie and W. R. Cherry, *J. Org. Chem.*, 1985, **50**, 1531–1532.
26 S. Morales, F. G. Guijarro, I. Alonso, J. L. García Ruano and M. B. Cid, *ACS Catal.*, 2016, **6**, 84–91.
27 K. A. Petrov, V. A. Chauzov, L. V. Pastukhova and N. N. Bogdanov, *Zh Obshch Khim*, 1976, **46**, 1246–1250.
28 M. Ito, H. Okui, H. Nakagawa, S. Mio, T. Iwasaki and J. Iwabuchi, *Heterocycles*, 2002, **67**, 881–884.
29 E. G. Janzen, M. S. West, Y. Kotake and C. M. DuBose, *J. Biochem. Biophys. Methods*, 1996, **32**, 183–190.
30 G. L. McIntire, H. N. Blount, H. J. Stronks, R. V. Shetty and E. G. Janzen, *J. Phys. Chem.*, 1980, **84**, 916–921.
31 B. J. Acken, D. E. Gallis, J. A. Warshaw and D. R. Crist, *Can. J. Chem.*, 1992, **70**, 2076–2080.
32 B. Tuccio, P. Bianco, J. C. Bouteiller and P. Tordo, *Electrochimica Acta*, 1999, **44**, 4631–4634.
33 L. Eberson, *J. Chem. Soc. Perkin Trans. 2*, 1992, 1807–1813.
34 L. Eberson, *J. Chem. Soc. Perkin Trans. 2*, 1994, 171–176.
35 A. Phaniendra, D. B. Jestadi and L. Periyasamy, *Indian J. Clin. Biochem.*, 2015, **30**, 11–26.
36 G. R. Buettner, *Free Radic. Biol. Med.*, 1987, **3**, 259–303.
37 J. P. Foster and F. Weinhold, *J. Am. Chem. Soc.*, 1980, **102**, 7211–7218.
38 A. E. Reed and F. Weinhold, *J. Chem. Phys.*, 1985, **83**, 1736–1740.
39 F. De Vleeschouwer, V. Van Speybroeck, M. Waroquier, P. Geerlings and F. De Proft, *Org. Lett.*, 2007, **9**, 2721–2724.
40 D. Christensen, K. A. Jørgensen and R. G. Hazell, *J Chem Soc Perkin Trans 1*, 1990, 2391–2397.
41 R. D. Hinton and E. G. Janzen, *J. Org. Chem.*, 1992, **57**, 2646–2651.
42 G. K. S. Prakash, Z. Zhang, F. Wang, M. Rahm, C. Ni, M. Iuliucci, R. Haiges and G. A. Olah, *Chem. - Eur. J.*, 2014, **20**, 831–838.
43 D. R. Duling, *J. Magn. Reson. 1969*, 1994, 105–110.
44 R. Lauricella, A. Allouch, V. Roubaud, J.-C. Bouteiller and B. Tuccio, *Org. Biomol. Chem.*, 2004, **2**, 1304–1309.
45 Y. Zhao and D. G. Truhlar, *Theor. Chem. Acc.*, 2008, **120**, 215–241.
46 V. Barone and M. Cossi, *J. Phys. Chem. A*, 1998, **102**, 1995–2001.
47 M. Cossi, N. Rega, G. Scalmani and V. Barone, *J. Comput. Chem.*, 2003, **24**, 669–681.
48 Gaussian 09, Revision A.02, M. J. Frisch, G. W. Trucks, H. B. Schlegel, G. E. Scuseria, M. A. Robb, J. R. Cheeseman, G. Scalmani, V. Barone, G. A. Petersson, H. Nakatsuji, X. Li, M. Caricato, A. Marenich, J. Bloino, B. G. Janesko, R. Gomperts, B. Mennucci, H. P.

Hratchian, J. V. Ortiz, A. F. Izmaylov, J. L. Sonnenberg, D. Williams-Young, F. Ding, F. Lipparini, F. Egidi, J. Goings, B. Peng, A. Petrone, T. Henderson, D. Ranasinghe, V. G. Zakrzewski, J. Gao, N. Rega, G. Zheng, W. Liang, M. Hada, M. Ehara, K. Toyota, R. Fukuda, J. Hasegawa, M. Ishida, T. Nakajima, Y. Honda, O. Kitao, H. Nakai, T. Vreven, K. Throssell, J. A. Montgomery, Jr., J. E. Peralta, F. Ogliaro, M. Bearpark, J. J. Heyd, E. Brothers, K. N. Kudin, V. N. Staroverov, T. Keith, R. Kobayashi, J. Normand, K. Raghavachari, A. Rendell, J. C. Burant, S. S. Iyengar, J. Tomasi, M. Cossi, J. M. Millam, M. Klene, C. Adamo, R. Cammi, J. W. Ochterski, R. L. Martin, K. Morokuma, O. Farkas, J. B. Foresman, and D. J. Fox, Gaussian, Inc., Wallingford CT, 2016.

Supporting Information For

Reactivities of MeO-substituted PBN-type Nitrones

Anaïs Deletraz,[a] Kamal Zéamari,[a] Florent Di Meo,[b] Paul-Louis Fabre,[c] Karine Reybier,[c] Patrick Trouillas,[b,d] Béatrice Tuccio,[e] and Grégory Durand[a*]

[a] Institut des Biomolécules Max Mousseron, UMR 5247 CNRS-Université Montpellier-ENSCM & Avignon Université, Equipe Chimie Bioorganique et Systèmes Amphiphiles, 301 rue Baruch de Spinoza, BP 21239, Avignon 84916 Cedex 9, France ;
[b] INSERM U1248 IPPRITT, Université de Limoges, Faculté de Médecine et Pharmacie, 2 rue du Professeur Descottes F-87000 Limoges, France ;
[c] Pharma-Dev, UMR 152, Université de Toulouse, IRD, UPS, 35 chemin des Maraîchers, 31400 Toulouse, France ;
[d] Regional Centre of Advanced Technologies and Materials, Palacký University, tr. 17 listopadu 12, 771 46 Olomouc, Czech Republic ;
[e] Aix-Marseille Université, CNRS, ICR UMR 7273, Avenue Escadrille Normandie Niemen, 13397 Marseille Cedex 20, France.
*Corresponding Author. Grégory Durand. E-mail: gregory.durand@univ-avignon.fr; Phone: +33 (0)4 9014 4445.

Table of contents

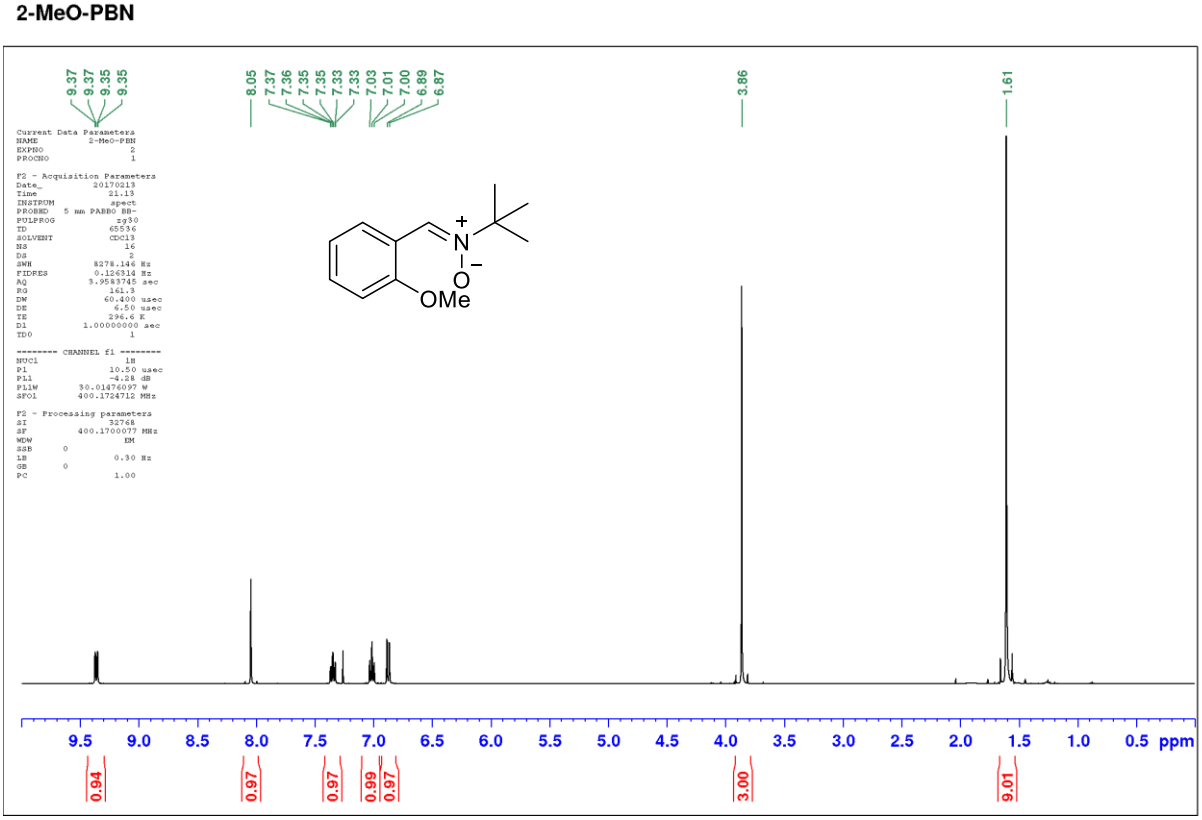

Figure S1. ^{1}H NMR spectrum of compound **1** in $CDCl_3$.

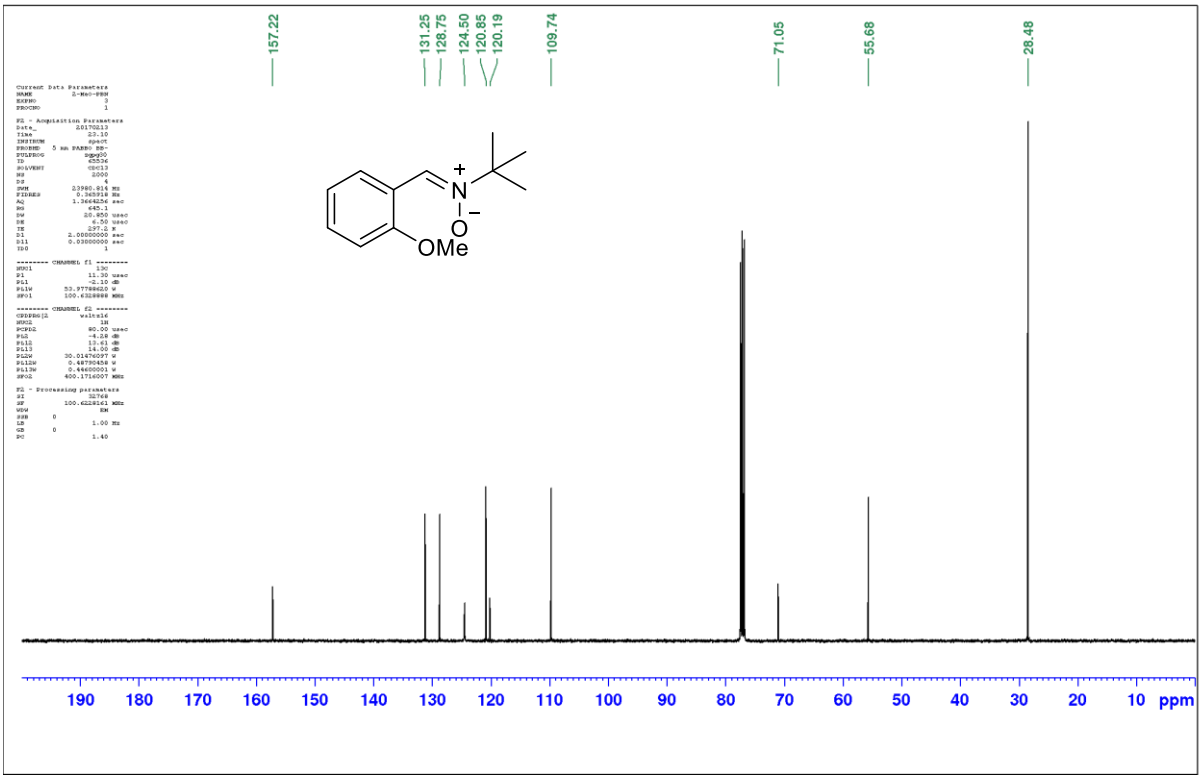

Figure S2. ^{13}C NMR spectrum of compound **1** in $CDCl_3$.

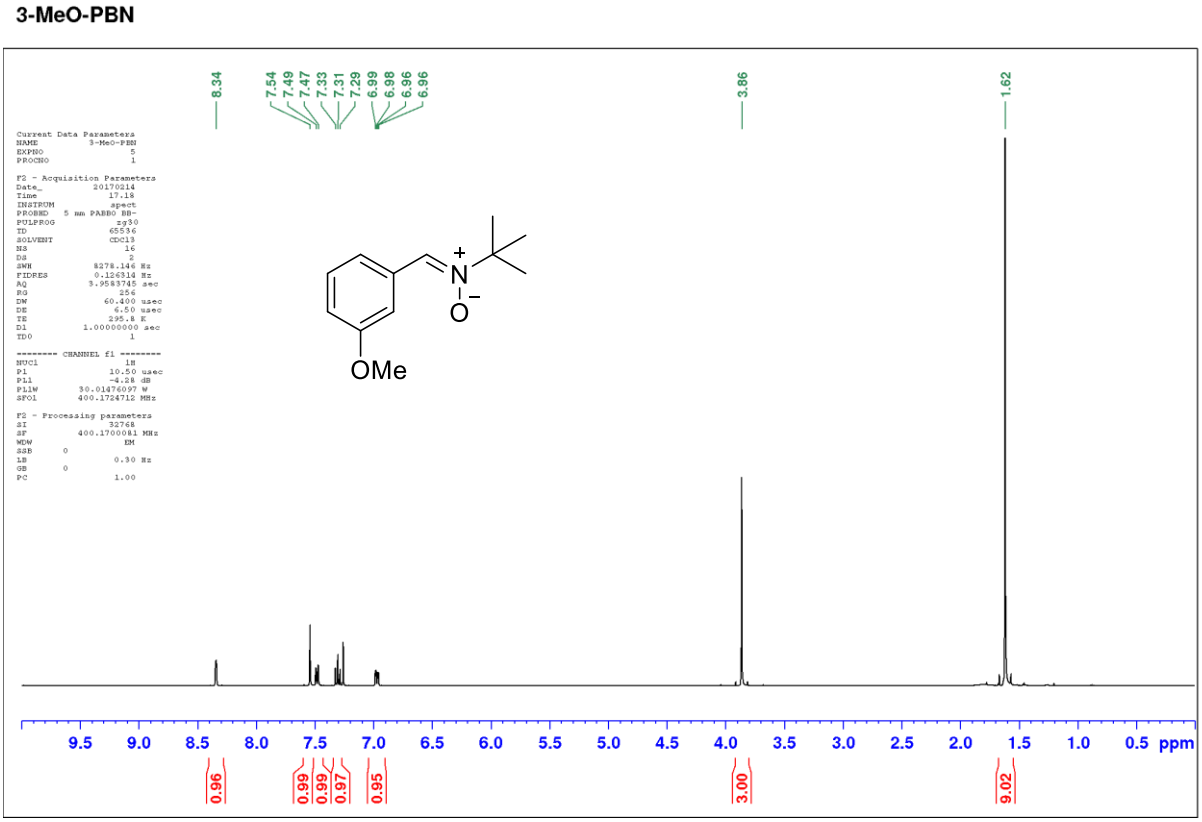

Figure S3. ^{1}H NMR spectrum of compound **2** in $CDCl_3$.

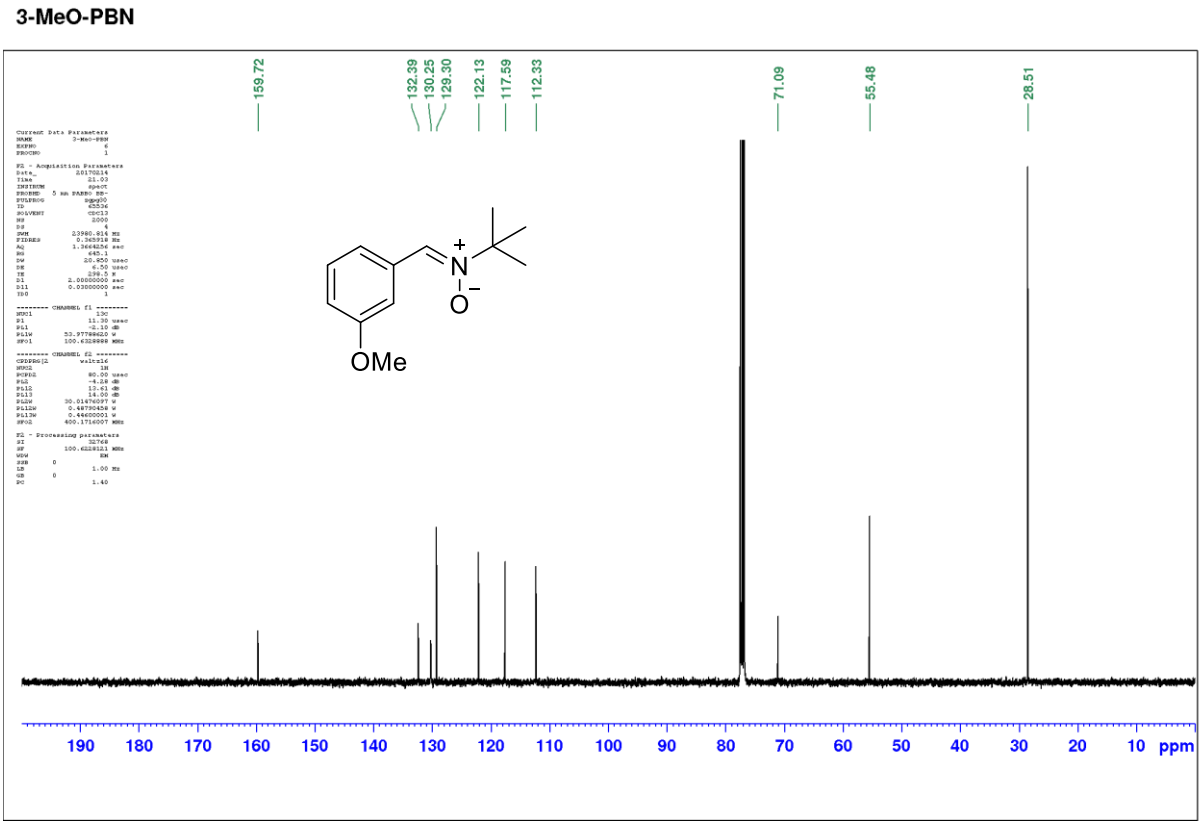

Figure S4. ^{13}C NMR spectrum of compound **2** in $CDCl_3$.

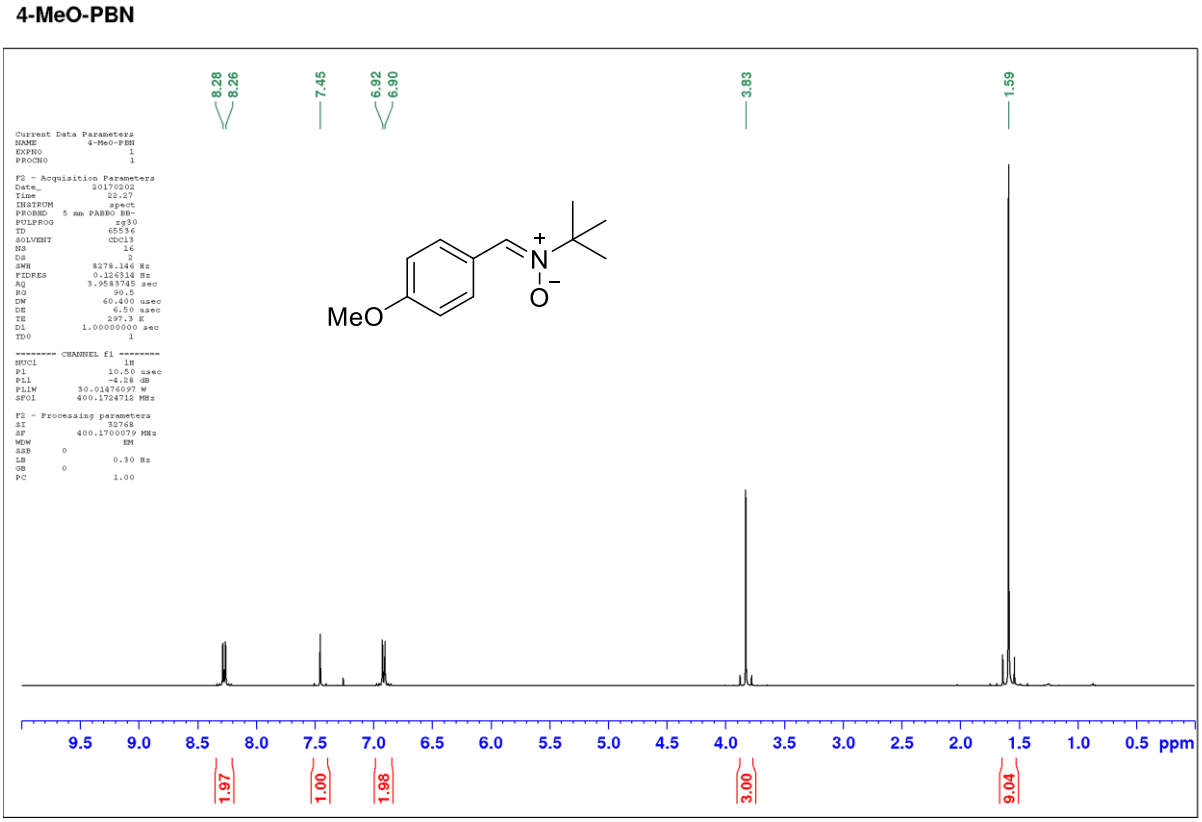

Figure S5. ^{1}H NMR spectrum of compound **3** in $CDCl_3$.

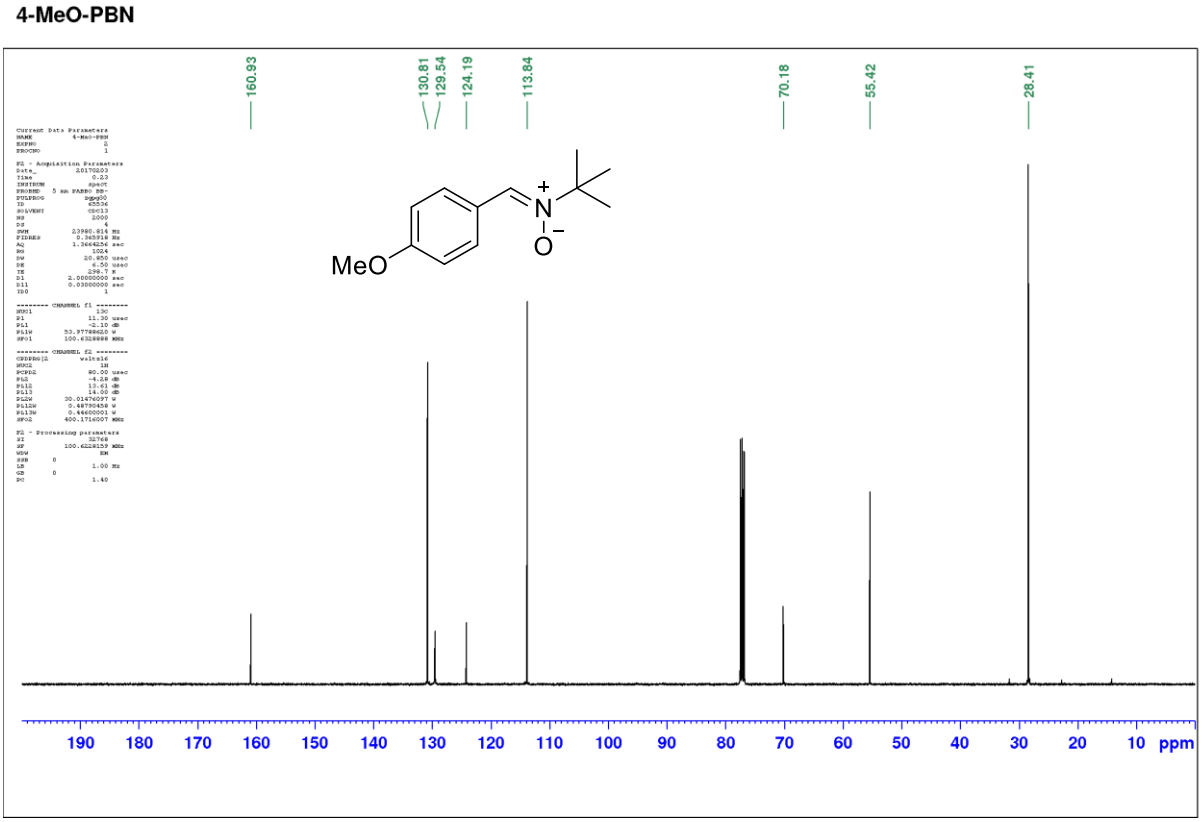

Figure S6. ^{13}C NMR spectrum of compound **3** in $CDCl_3$.

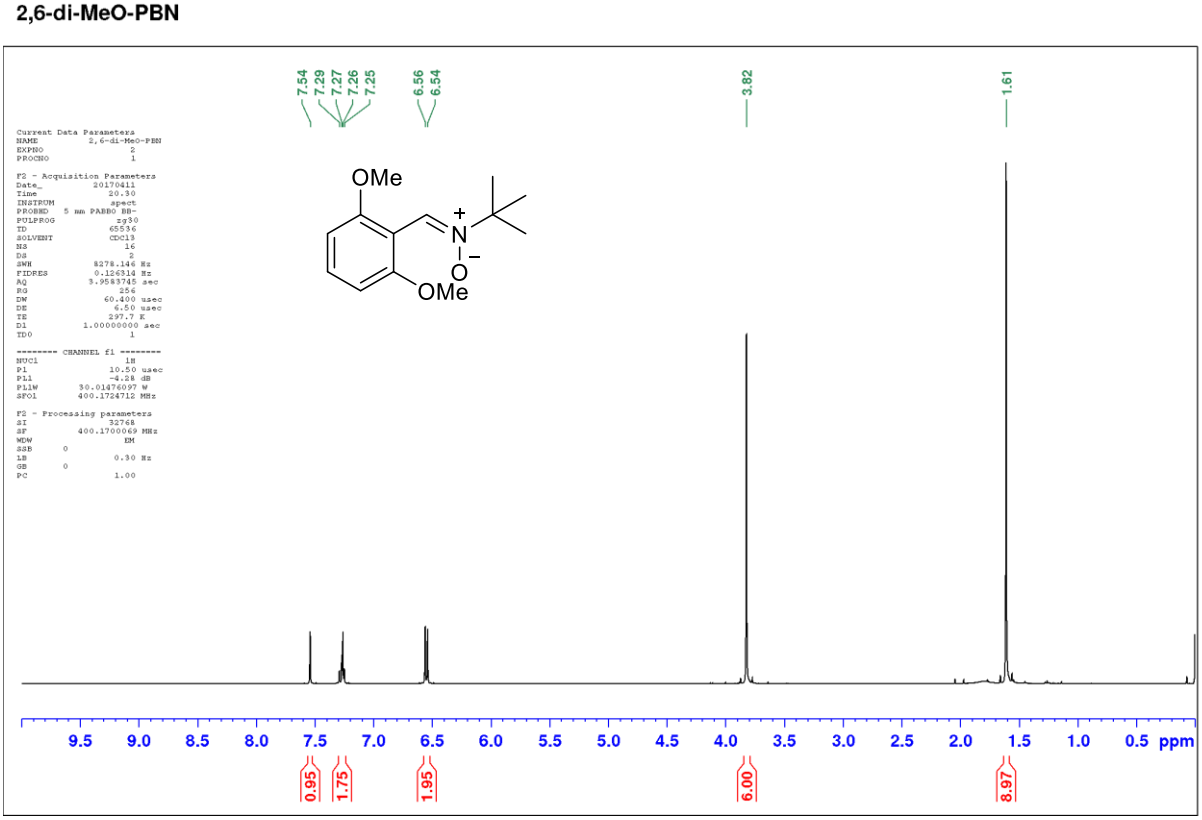

Figure S7. ^{1}H NMR spectrum of compound **4** in $CDCl_3$.

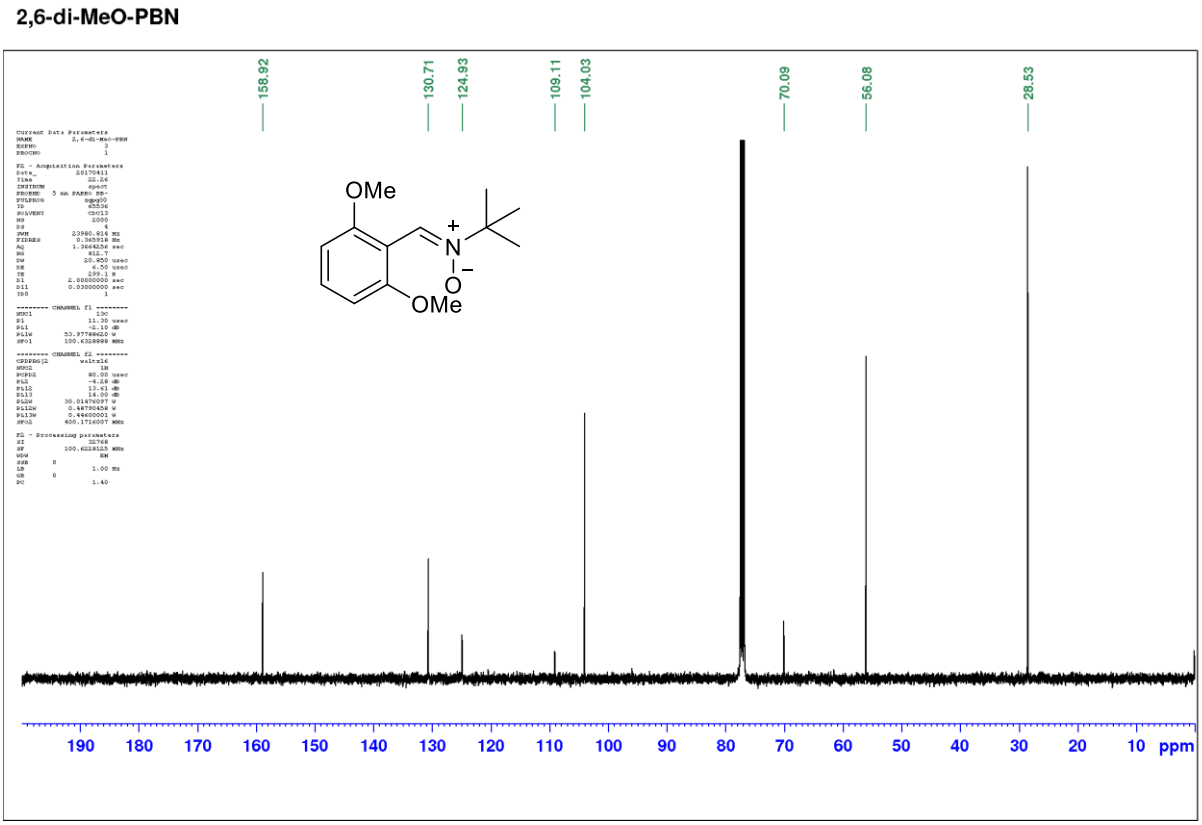

Figure S8. ^{13}C NMR spectrum of compound **4** in $CDCl_3$.

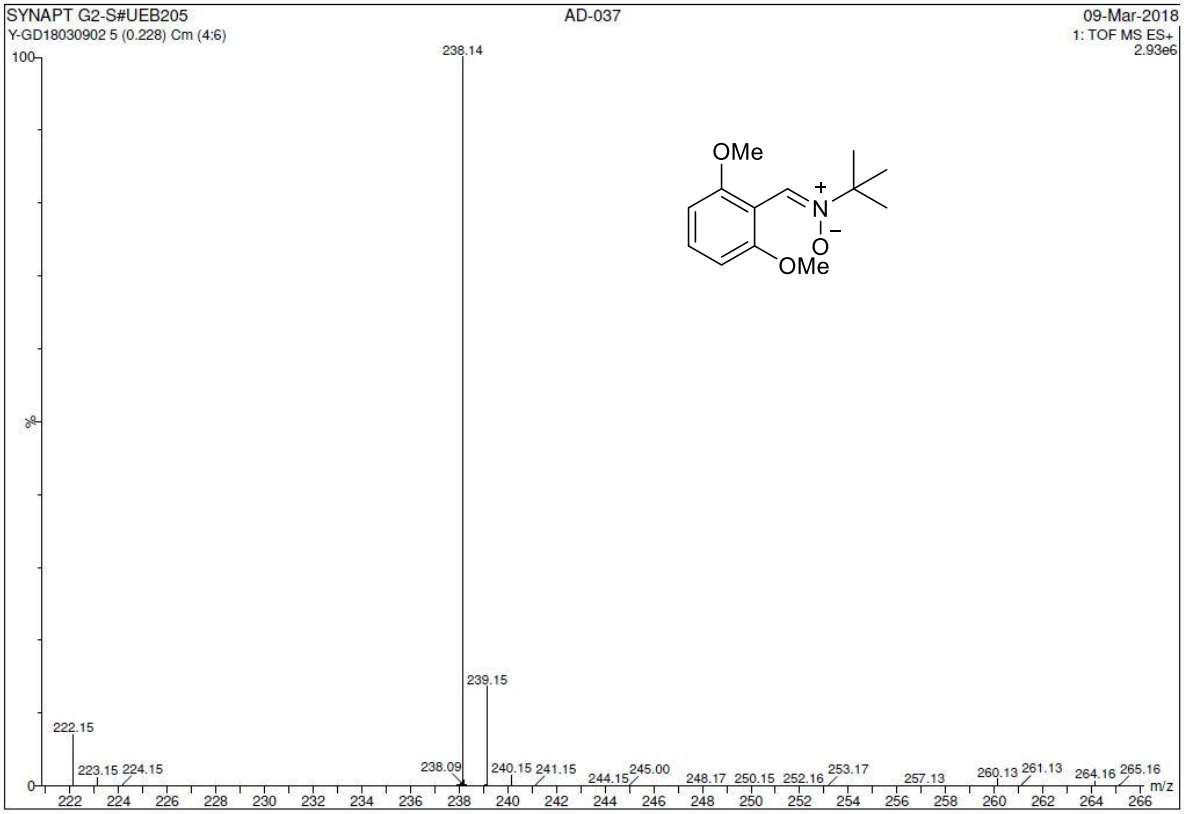

Figure S9. High-resolution mass spectrum of compound **4**.

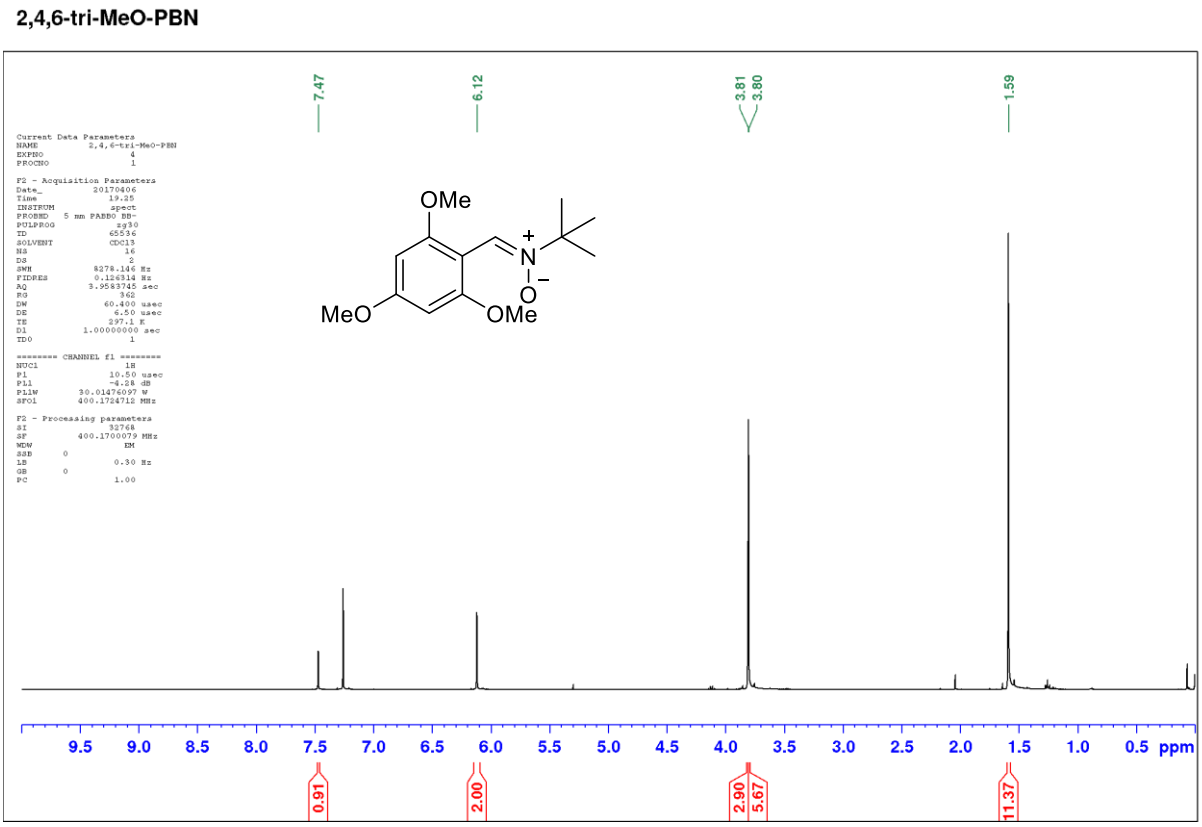

Figure S10. ^{1}H NMR spectrum of compound **5** in $CDCl_3$.

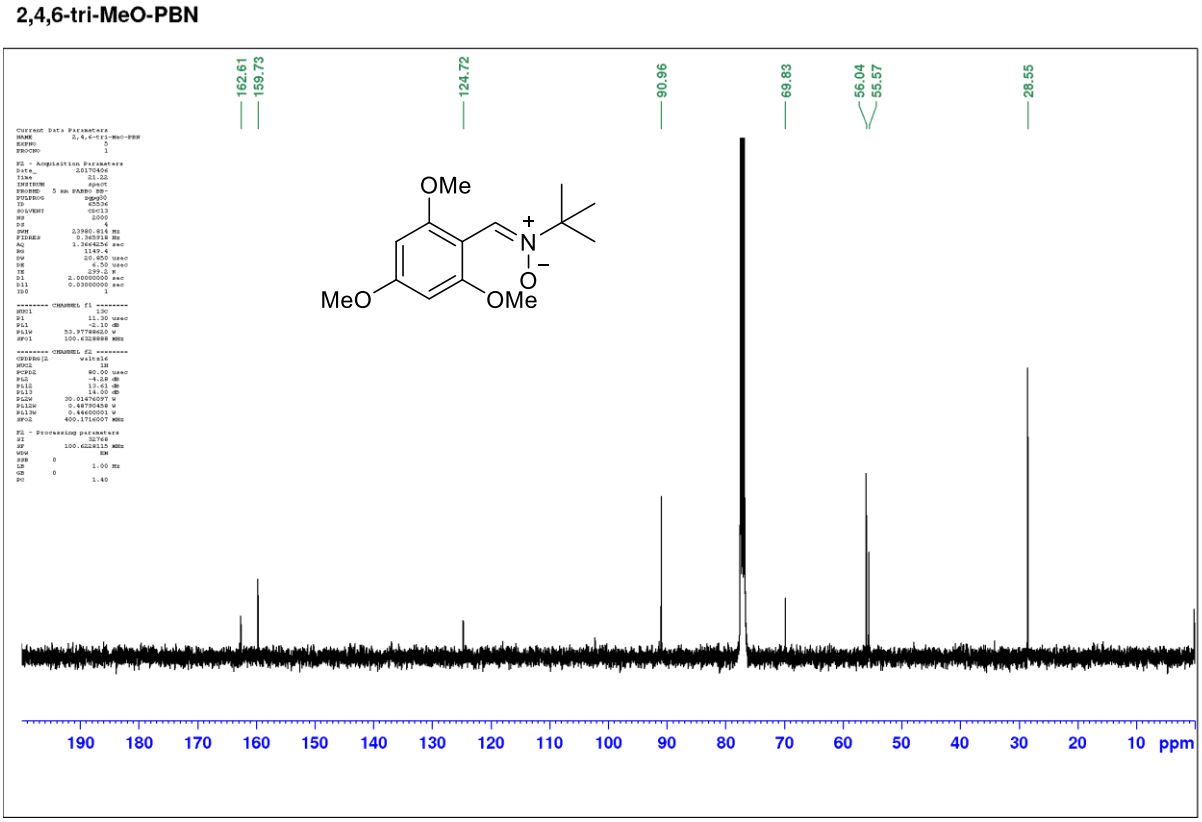

Figure S11. ^{13}C NMR spectrum of compound **5** in $CDCl_3$.

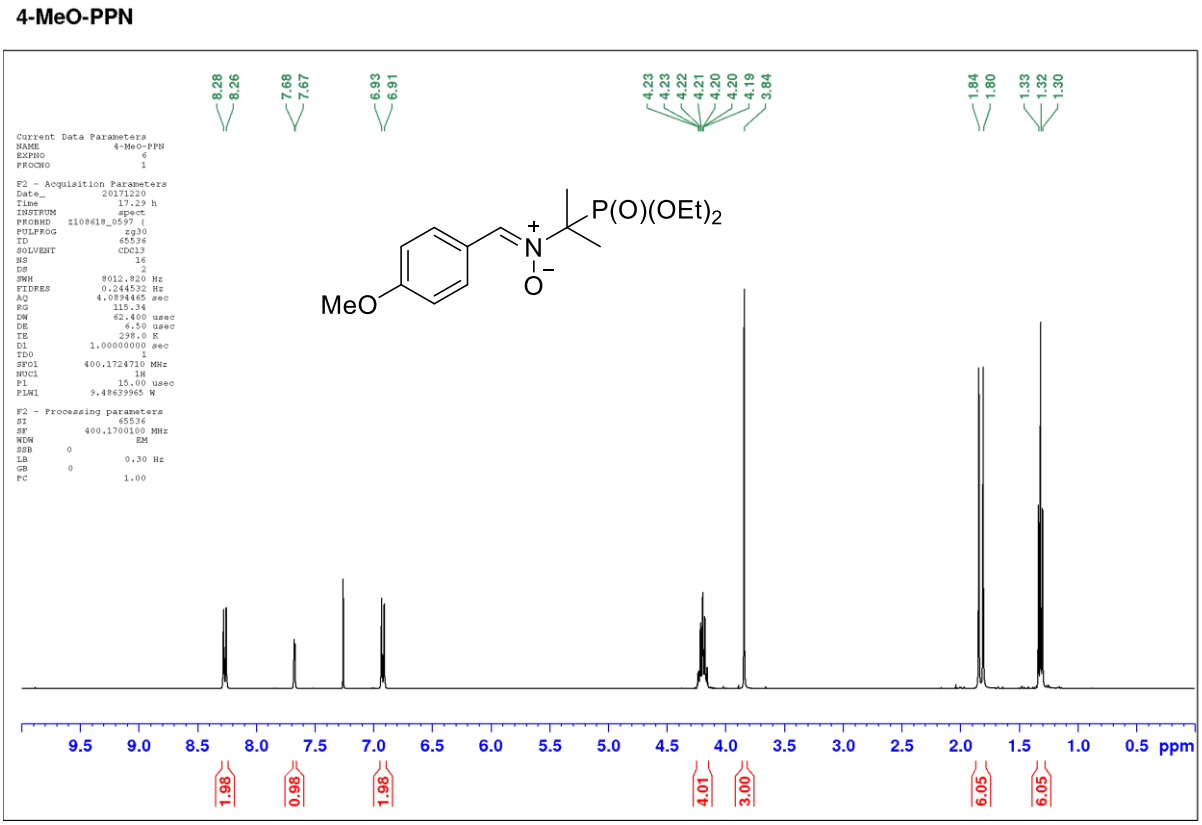

Figure S12. ^{1}H NMR spectrum of compound **6** in $CDCl_3$.

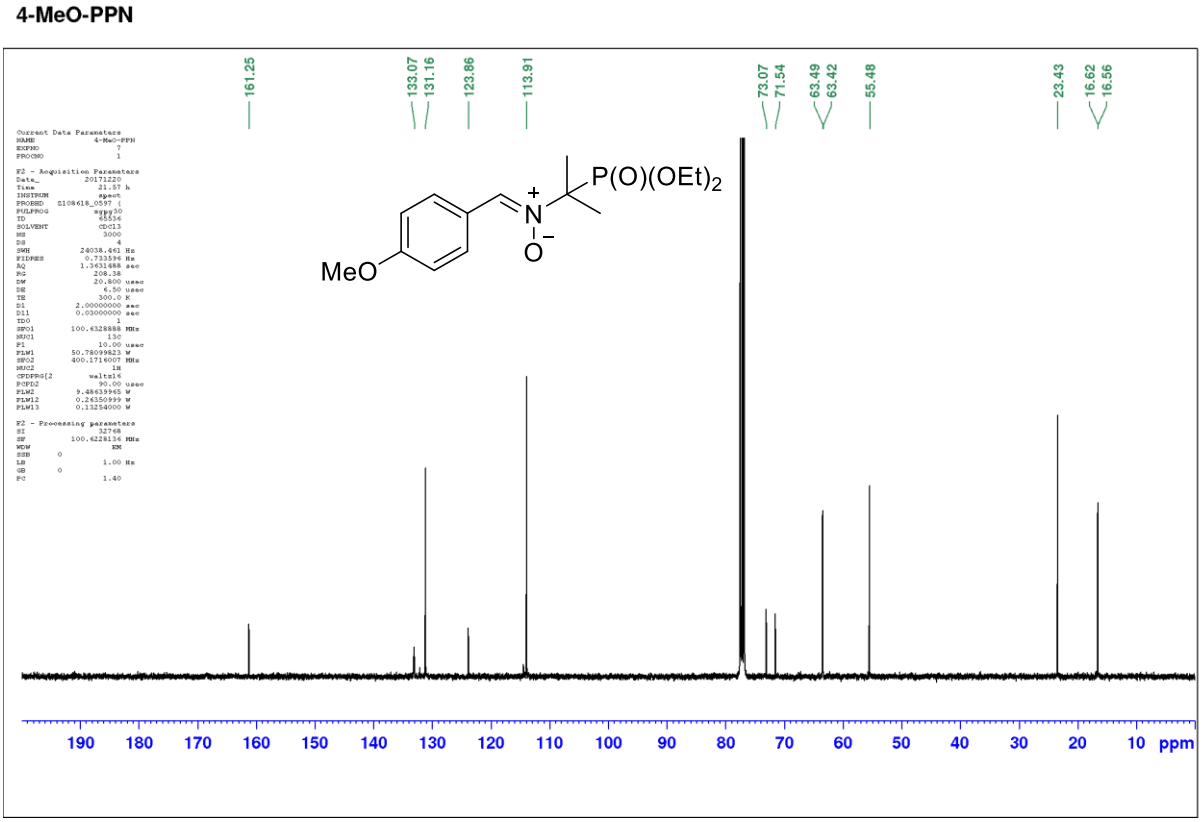

Figure S13. ^{13}C NMR spectrum of compound **6** in $CDCl_3$.

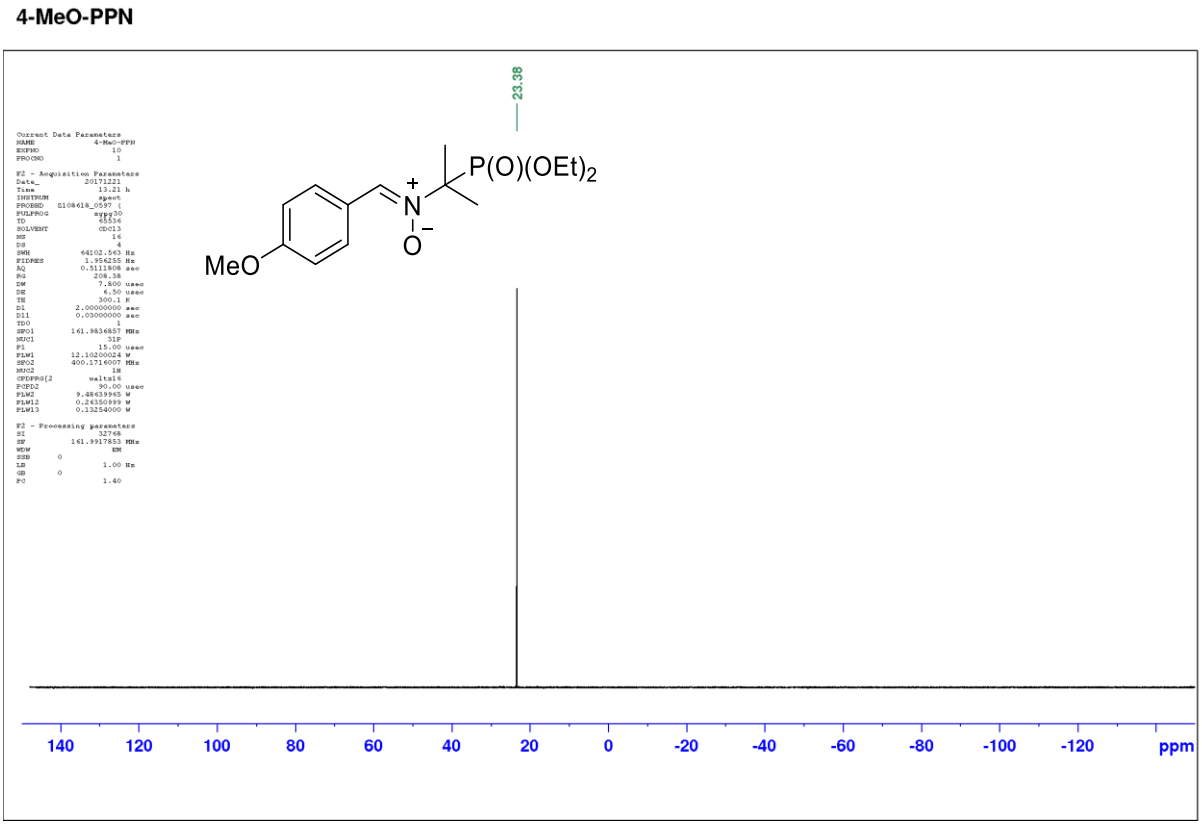

Figure S14. ^{31}P NMR spectrum of compound **6** in $CDCl_3$.

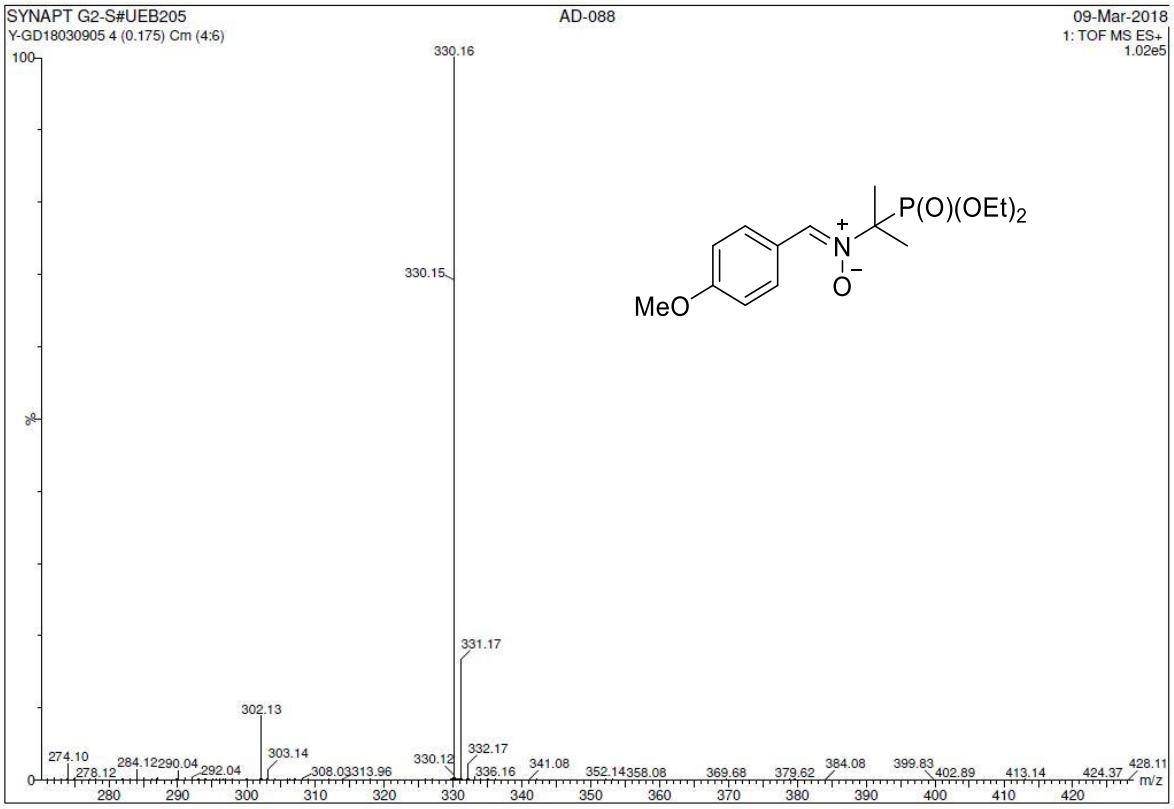

Figure S15. High-resolution mass spectrum of compound **6**.

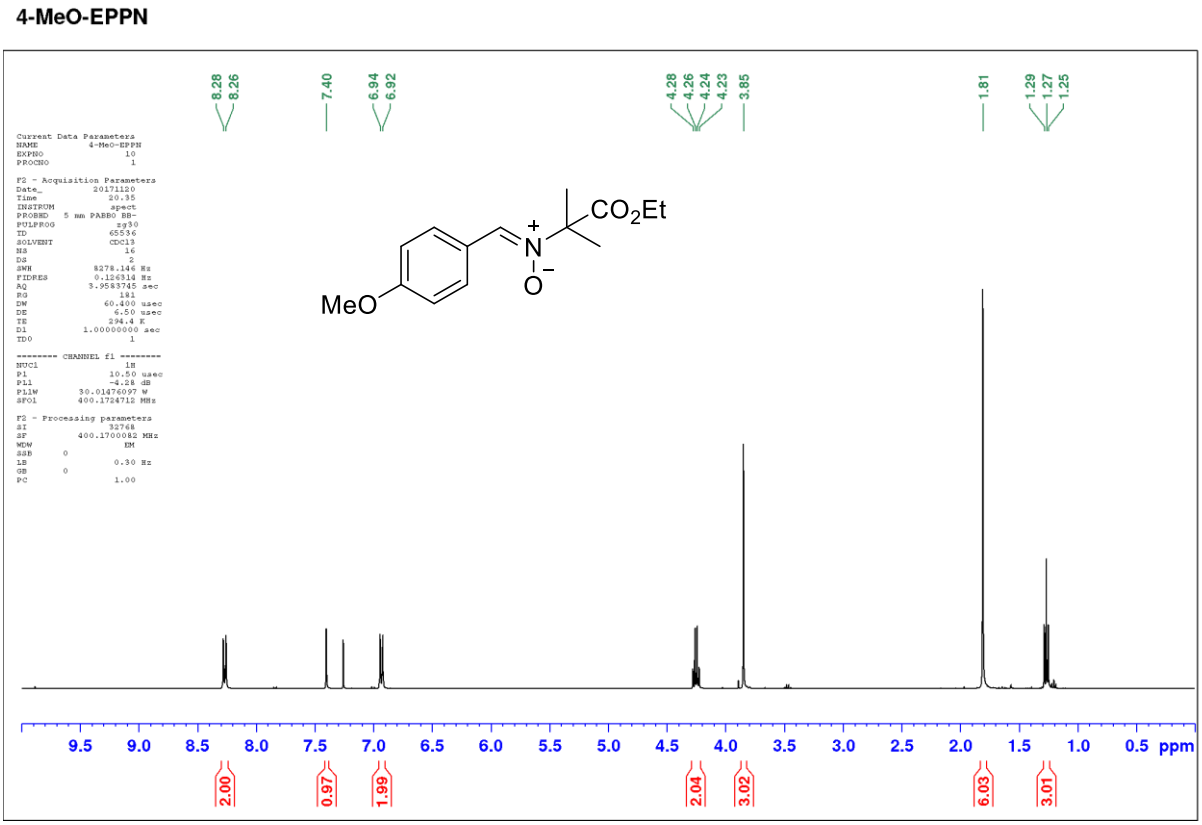

Figure S16. ^{1}H NMR spectrum of compound **7** in $CDCl_3$.

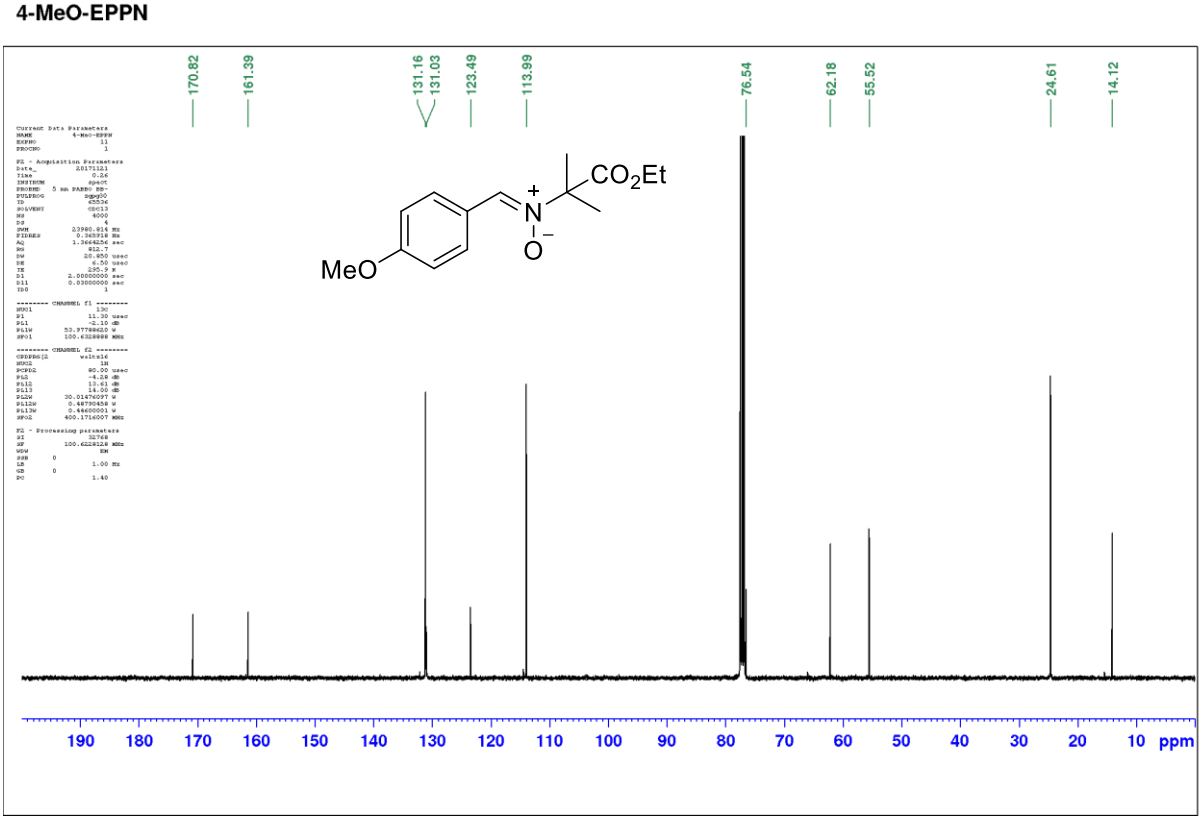

Figure S17. ^{13}C NMR spectrum of compound **7** in $CDCl_3$.

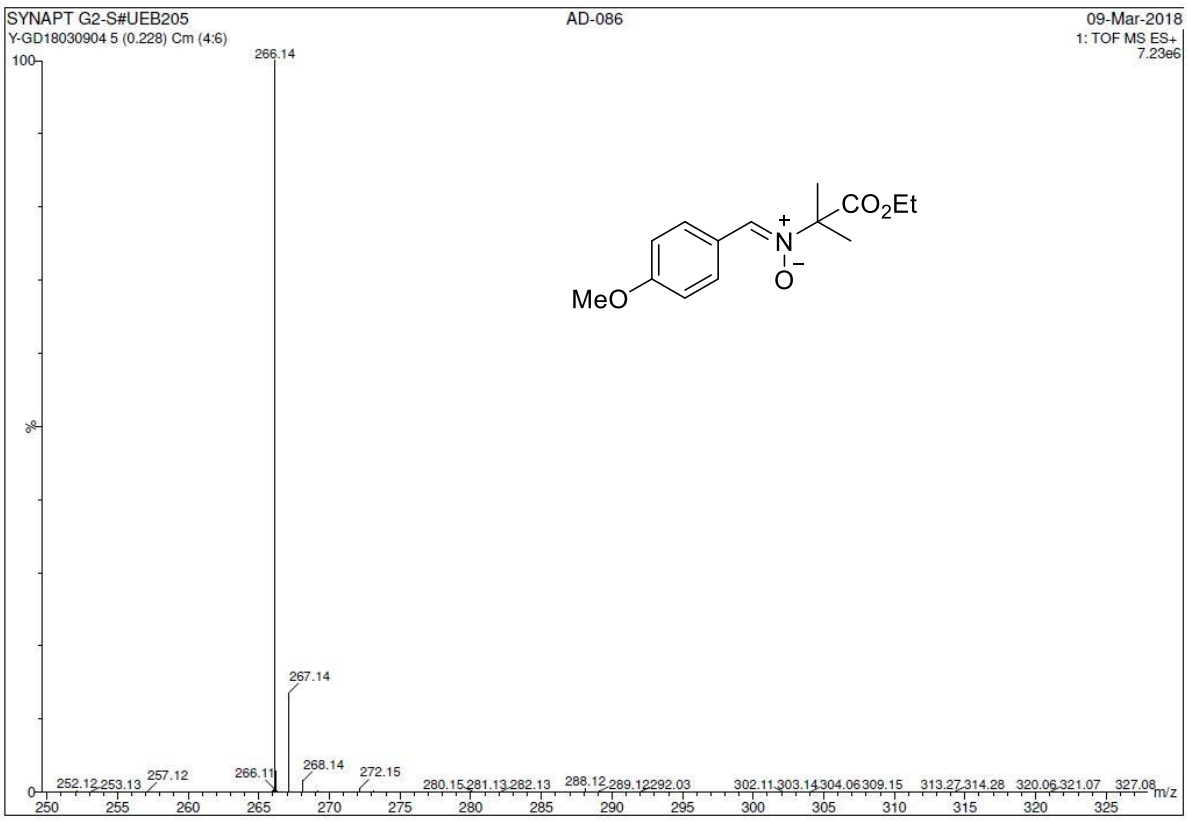

Figure S18. High-resolution mass spectrum of compound **7**.

Chapitre 3

Para-substituted α-Phenyl-*N*-*tert*-butyl Nitrones: Spin-Trapping and Electrochemical and Neuroprotective Properties

Dans ce chapitre j'ai réalisé la synthèse des nitrones et leur caractérisation structurale. J'ai réalisé les expériences de spin-trapping et l'analyse des données avec l'aide du Dr Béatrice Tuccio (ICR, UMR 7273, Marseille). J'ai également réalisé les expériences de voltampérométrie cyclique et l'analyse des données avec l'aide du Pr Paul-Louis Fabre (Pharma-Dec, UMR 152, Université Paul Sabatier – Toulouse III).

La détermination des charges partielles des nitrones et des potentiels d'ionisation a été réalisée par l'équipe du Pr Patrick Trouillas (INSERM, U1248 IPPRITT, Université de Limoges).

La détermination des effets neuroprotecteurs a été réalisée par l'équipe du Pr Michel Vignes (IBMM – UMR 5247, Montpellier) et par la société Neuro-Sys (Gardanne).

J'ai réalisé la rédaction du chapitre avec l'aide de mon directeur de thèse le Dr Grégory Durand.

Ce chapitre sera soumis très prochainement à Organic & Biomolecular Chemistry

Chapitre 3 - *Para*-substituted α-Phenyl-*N*-*tert*-butyl Nitrones: Spin-Trapping and Electrochemical and Neuroprotective Properties

Table of contents

ABSTRACT

In this work, a series of *para*-substituted α-phenyl-*N*-tert-butyl nitrones (PBN) was studied. Their radical trapping properties were evaluated by electron paramagnetic resonance, with 4-CF_3-PBN being the fastest derivative to trap hydroxymethyl radical ($^{\bullet}CH_2OH$). The electrochemical properties of the nitrones were further investigated by cyclic voltammetry and 4-CF_3-PBN bearing an electron-withdrawing group was the easiest to reduce, with the lowest cathodic peak potential in the series, while 4-iPr-PBN exhibited the highest reduction potential due to its electron-donating group. An opposite trend was observed for the oxidation and very good correlations between the redox potentials, the Hammett constants (σ_p) and computationally determined ionization potentials were observed. Finally, the neuroprotective effect of these derivatives was studied using two different *in vitro* models of oxidative stress on cortical neurons and glial cells. Out of the thirteen derivatives studied, eight nitrones showed good protective effects on at least one of the two models.

KEYWORDS

Nitrones, Oxidative Stress, Antioxidants, Spin-Trapping, Electrochemistry, Electron Paramagnetic Resonance (EPR) Spectroscopy, Neuroprotection.

1. INTRODUCTION

An exposure to an important oxidative stress leads to the production of reactive oxygen species (ROS), mostly free radicals such as superoxide ion $O_2^{\bullet-}$ or hydroxyl radical $HO^{\bullet}$ to name but a few, as well as reactive nitrogen species (RNS) and reactive sulphur species (RSS). Some of these reactive species are beneficial to the living organisms as they intervene as modulators of cellular function, signalling and immune response but when they are present in high levels they lead to cellular injury.[1,2] Oxidative stress is often associated to several pathologies like cardiovascular diseases, stroke, cancer, neurodegenerative diseases and aging.[1,3] To prevent oxidative damage, synthetic antioxidants have been developed and nitrones are promising agents with considerable potential as therapeutics.[4–6] Nitrones have also been widely used as spin traps for the detection and characterization of free radicals by electron paramagnetic resonance (EPR) spectroscopy. In the spin-trapping technique, free radicals react with the nitronyl function to form stable and EPR-identifiable aminoxyl radicals.[7,8] Two families of nitrones have been developed, the cyclic ones derived from 5,5-dimethyl-1-pyrroline *N*-oxide (DMPO) and the linear ones derived from α-phenyl-*N*-tert-butyl nitrone (PBN).

Over the past decades, several analogues of DMPO and PBN have been designed in order to increase their spin-trapping properties and their biological activities.[6,9,10] When used as spin traps, it is important to design nitrones with a high rate constant of free radical trapping as well as a great stability of the corresponding aminoxyl spin adduct to ensure efficient detection. In general, cyclic nitrones lead to more persistent adducts than linear ones and analogues of DMPO with a great potential have been designed. One can cite the phosphorylated analogue 5-diethoxyphosphoryl-5-methyl-1-pyrrolidine *N*-oxide (DEPMPO),[11] the ester derivative 5-ethoxycarbonyl-5-methyl-1-pyrrolidine *N*-oxide (EMPO)[12] and the amido analogue 5-carbamoyl-5-methyl-1-pyrrolidine *N*-oxide (AMPO).[13,14] AMPO was reported to have the highest rate constant of superoxide trapping, followed by EMPO and then DEPMPO. Linear nitrones have been also employed successfully in spin-trapping experiments but are generally less efficient than cyclic ones.[15–17] However, PBN and its derivatives exhibited a better distribution within tissues and cells and have therefore been widely used in *ex vivo* and *in vivo* studies of radical production in whole animals.[18–20] Linear nitrones are usually easier to synthesize and purify as they are often solid at room temperature and can be recrystallized to afford paramagnetic impurity free samples. Moreover, linear

PBN-type nitrones allow the possibility of rather easy functionalization both on the aromatic ring and on the *N*-tert-butyl group and therefore provide more chemical versatility. Considering their antioxidant activity, nitrones have exhibited protective properties against brain injury,[21] renal injury,[22] visual loss,[23,24] neuronal damage[25] and other age-related diseases.[26] The PBN derivative called 2,4-disulfophenyl-*N*-*tert*-butyl nitrone (NXY-059) was the first neuroprotective agent to reach phase III clinical trials in the USA.[27,28]

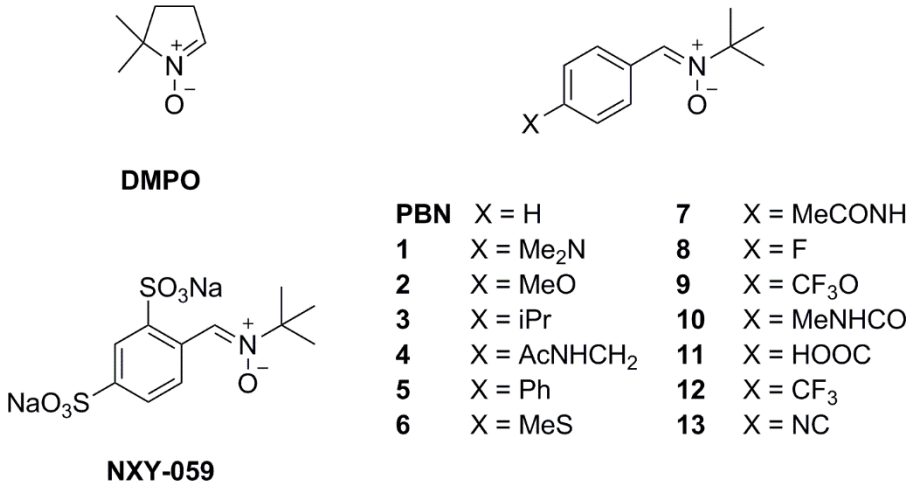

Figure 1. Chemical structure of DMPO, PBN, NXY-059 and the X-PBNs studied in this work.

Nitrones have a very broad activity that depends on the nature and the position of the substituents on the nitronyl function. Therefore, the choice of substituents is very important and depend on the properties to be improved such as: water-solubility,[29,30] lipophilicity,[30,31] rate constant of radical trapping,[32–34] adduct stability,[35,36] bioactivity,[24,37] as well as the possibility of cellular or tissue targeting thanks to the ligation to specific molecular targets.[38–43] Over the past years, the reactivity of *para*-substituted derivatives of PBN has been explored in order to identify the most promising substituent for improved and optimal reactivity towards free radicals. It has been shown that the electronic nature of the substituents influences the rate of radical trapping on the nitronyl function. The presence of an electron-withdrawing group on the *para*-position of the phenyl ring increased the reactivity towards nucleophilic addition reactions.[32–34,44] On the contrary, nitrones with an electron-donating group exhibited high reactivity towards electrophilic radicals.[45,46] The polar effect of the substituents has been also correlated with the electrochemical properties of the nitronyl function, the derivatives bearing an electron-withdrawing group being more easily reduced and more hardly oxidized than those bearing an electron-donating group.[34]

In this work, we studied the spin-trapping properties of *para*-substituted nitrones (4-iPr-PBN, 4-Ph-PBN, 4-MeS-PBN, 4-MeCONH-PBN, 4-F-PBN, 4-CF_3O-PBN and 4-CF_3-PBN) as well as their electrochemical properties. The electrochemical properties were correlated to computationally determined ionization potentials. Finally, the *in vitro* neuroprotection of all the derivatives was investigated in two paradigms of oxidative stress.

2. RESULTS AND DISCUSSION

2.1. EPR study of hydroxymethyl radical trapping

To evaluate the ability to scavenge carbon-centered radicals, the relative rate constant of trapping of hydroxymethyl radical ($^{\bullet}CH_2OH$) by 4-iPr-PBN, 4-Ph-PBN, 4-MeS-PBN, 4-MeCONH-PBN, 4-F-PBN, 4-CF_3O-PBN and 4-CF_3-PBN was measured. α-hydroxycarbon-centered radicals can be produced during oxidative stress by an attack of $HO^{\bullet}$ on alcohols and are therefore of interest when evaluating nitrone antioxidant activities.[47] The Fenton reaction was used to produce *in situ* $^{\bullet}CH_2OH$ radicals in the presence of methanol. Under these conditions, all the generated spin adducts of $^{\bullet}CH_2OH$ radical (noted **N**-CH_2OH) gave rise to a standard six-line EPR spectrum, a triplet of doublets (nitrogen (a_N) and β-hydrogen (a_H) couplings), characteristic of nitroxide adducts.[48] The EPR hyperfine splitting constants (hfsc's) a_N and a_H of the simulated $^{\bullet}CH_2OH$ adducts are reported in Table 1. All the derivatives present similar nitrogen hfsc (~ 15.3 G) except 4-Ph-PBN (14.0 G), probably due to the higher resonance of the phenyl substituent.

In order to evaluate the spin-trapping kinetics of the derivatives compared to that of PBN, a method based on the competition between the nitrone **N** and the 1,3,5-tri[(N-(1-diethylphosphono)-1-methylethyl) *N*-oxy-aldimine] **TN** scavenger was used by generating the $^{\bullet}CH_2OH$ radical in the presence of **N** and **TN**. The $^{\bullet}CH_2OH$ spin-trapping rate was determined by measuring the intensity (as the signal area) of the corresponding adducts at different [**N**]/[**TN**] ratio (Figure 2). For each nitrone, plotting the *R*/*r* ratio *vs* [**N**]/[**TN**] (where *R* and *r* represent the trapping rate constant by both **TN** and **N**, and by **TN** only, respectively) gave a straight-line which slope value was equal to the k_N/k_{TN} ratio (Figure 2C). To compare the spin-trapping of the derivatives with PBN, the k_{PBN}/k_{TN} ratio was also determined using commercially available PBN instead of **N** and from this the k_N/k_{PBN} ratio was calculated for the whole series with values ranging from 0.25 to 3.18 (Table 1).

Table 1. Physicochemical and spin-trapping properties of PBN derivatives.

		EPR		
		$^{\bullet}CH_2OH$		
Nitrones	σ_p [a]	a_N (G)	a_H (G)	k_N/k_{PBN} [b] (± 0.05)
4-iPr-PBN (3)	-0.15	15.4	3.8	0.25
4-Ph-PBN (5)	-0.01	14.0	3.0	0.78
4-MeS-PBN (6)	0	15.4	3.5	0.33
PBN	0	15.3	3.8	1.00
4-MeCONH-PBN (7)	0	15.3	3.6	0.58
4-F-PBN (8)	0.06	15.4	3.4	1.72
4-CF_3O-PBN (9)	0.35	15.3	3.3	1.84
4-CF_3-PBN (12)	0.54	15.2	3.3	3.18

[a] Data from Hansch *et al.*[49]
[b] Ratio of the second-order rate constants for the hydroxymethyl radical trapping by various nitrones (k_N) and by PBN (k_{PBN}) in methanol, calculated with a ratio k_{PBN}/k_{TN} = 0.057.

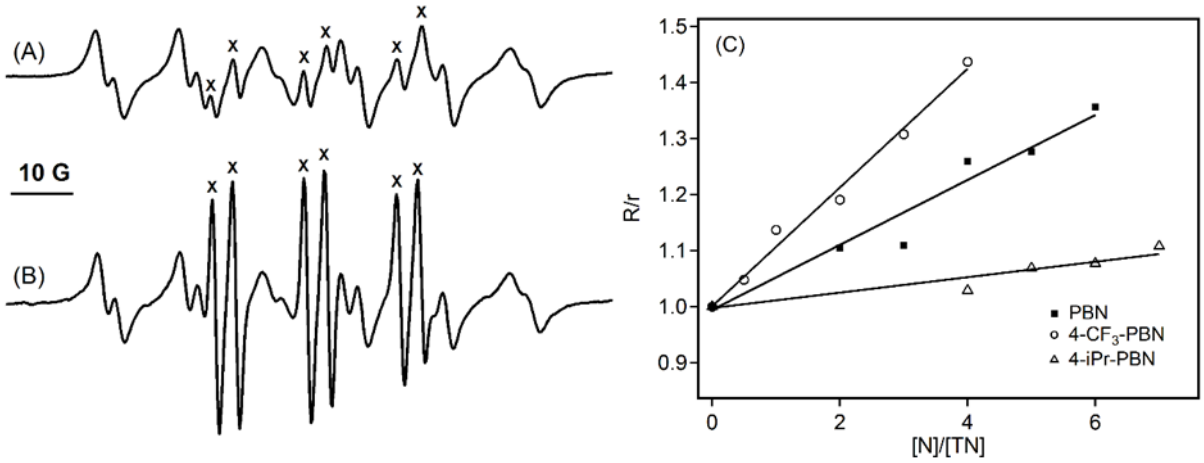

Figure 2. EPR signals of TN and **N** hydroxymethyl radical adducts, respectively. (A): **N** = PBN and (B): **N** = 4-CF_3-PBN. Hydroxymethyl radical was generated by a Fenton system and the concentration ratio [**N**]/[TN] = 4. The peaks topped by a cross (×) correspond to the hydroxymethyl radical adduct of **N**. (C) Determination of the relative rate constants k_N/k_{TN} of $^{\bullet}CH_2OH$ trapping by PBN, 4-CF_3-PBN and 4-iPr-PBN.

4-iPr-PBN, 4-MeS-PBN, 4-MeCONH-PBN and 4-Ph-PBN trapped $^{\bullet}CH_2OH$ slower than PBN while 4-F-PBN and 4-CF_3O-PBN trapped $^{\bullet}CH_2OH$ 1.7 and 1.8 times faster than PBN, respectively. With a spin-trapping rate 3.2 times higher than that observed for PBN, 4-CF_3-PBN, which bears a strong electron-withdrawing substituent, was the most potent of the series even including the *para*-PBN derivatives previously studied.[34,50] The two very potent PBN-

type nitrones that have been previously used as spin traps, PPN and EPPN,[51,52] exhibit k_N/k_{PBN} values of 6.4 and 1.5, respectively.[50] This indicates the high efficiency of the fluorinated derivatives 4-F-PBN, 4-CF_3O-PBN and 4-CF_3-PBN.

The plot of the rate constants by the different nitrones versus the Hammett values of their substituents showed a very good correlation (Figure 3A, R^2 = 0.86). A positive value of the slope ρ, as observed, is indicative of the nucleophilic nature of the addition of the radical on the nitronyl function, which agrees with the work of De Vleeschouwer *et al.* who classified hydroxymethyl radical as a strong nucleophile.[53] Moreover, it has been already shown that an electron-withdrawing substituent in PBN-type derivatives increases the reactivity of the nitronyl function for nucleophilic radical addition,[14,54] further supporting our observation.

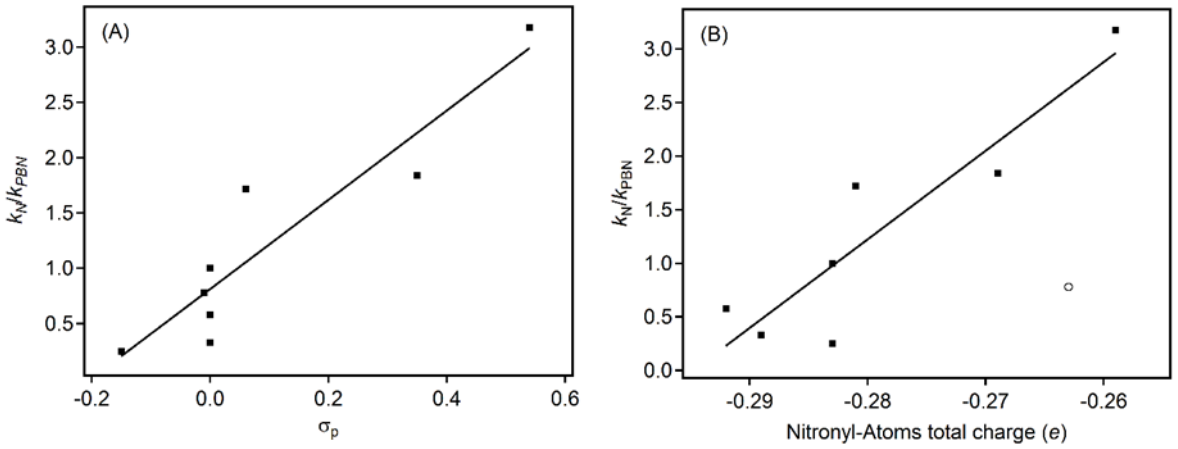

Figure 3. Correlation of relative rate constants (k_N/k_{PBN}) of $^{\bullet}CH_2OH$ addition to nitrones with (A)**:** Hammett constants (σ_p) (R^2 = 0.86) and with (B): atomic total charge of the nitronyl moiety (R^2 = 0.83, excluding the outlier 4-Ph-PBN marked as ○).

The atomic partial charges of the nitronyl atoms (H, C, N and O) and the atomic total charge of the nitronyl moiety were calculated for all the derivatives using the natural population analysis (NPA) within the natural bond orbital (NBO) framework and are reported in Table S1.[55,56] A positive correlation between the rate constants of $^{\bullet}CH_2OH$ addition to nitrones with the atomic total charge of the nitronyl moiety was observed (Figure 3B) as well as a good correlation between the atomic total charge of the nitronyl atoms of all the series and the Hammett constants (σ_p)[49] of the substituents (Figure S1). This confirms again that the $^{\bullet}CH_2OH$ free radical scavenging occurs through nucleophilic radical addition requiring

electron withdrawing groups in the nitrones, which directly impact on the partial charges of the nitronyl moiety, where the nucleophilic addition is expected to occur.[44]

2.2. Cyclic Voltammetry

The electrochemical properties of 4-iPr-PBN, 4-Ph-PBN, 4-MeS-PBN, 4-MeCONH-PBN, 4-F-PBN, 4-CF_3O-PBN and 4-CF_3-PBN were investigated using cyclic voltammetry and the redox potentials are reported in Table 2. The experiments were carried out in acetonitrile containing *tetra*-butylammonium perchlorate (TBAP) as electrolyte. Reduction and oxidation potentials of all the nitrones have been observed in the electroactivity domain of the solvent (Figure 4 and Figures S2 and S3). As expected, the peak currents are linearly related to the square root of the potential scan rate (Figures S4-S6), demonstrating that the process is diffusion-controlled.[57,58] By calibrating the current *vs.* ferrocene, the number of electrons involved in the reduction or the oxidation processes can be deduced.[59] PBN, 4-iPr-PBN, 4-Ph-PBN, 4-F-PBN and 4-CF_3O-PBN were reduced through two successive two-electron transfers in agreement with previous observations on other PBN-type nitrones.[34,60–62] For derivatives 4-MeCONH-PBN and 4-CF_3-PBN, an additional electron transfer was also observed as shown in Figure 4. This is likely due to the reduction of trifluoromethyl substituent of 4-CF_3-PBN while this corresponds to the reduction of the carbonyl group for 4-MeCONH-PBN. 4-MeS-PBN, which possesses a thiomethyl substituent, underwent a one-step, two-electron reduction. For all the derivatives except 4-Ph-PBN, the reduction appeared irreversible as no associated backward peaks were observed. The reduction of the nitronyl group into a radical nitroxide anion corresponds to the first peak obtained, with values ranging from -2.21 to -1.83 V.

Considering the anodic behavior, PBN and derivatives 4-iPr-PBN, 4-Ph-PBN and 4-CF_3-PBN were oxidized through an irreversible one-electron transfer whereas 4-MeS-PBN, 4-MeCONH-PBN, 4-F-PBN and 4-CF_3O-PBN possess two oxidation peaks. The first peak observed corresponds to the oxidation of the nitronyl function with values ranging from 1.41 to 1.89 V, except for 4-MeS-PBN where the first peak would correspond to the oxidation of the thiomethyl group.

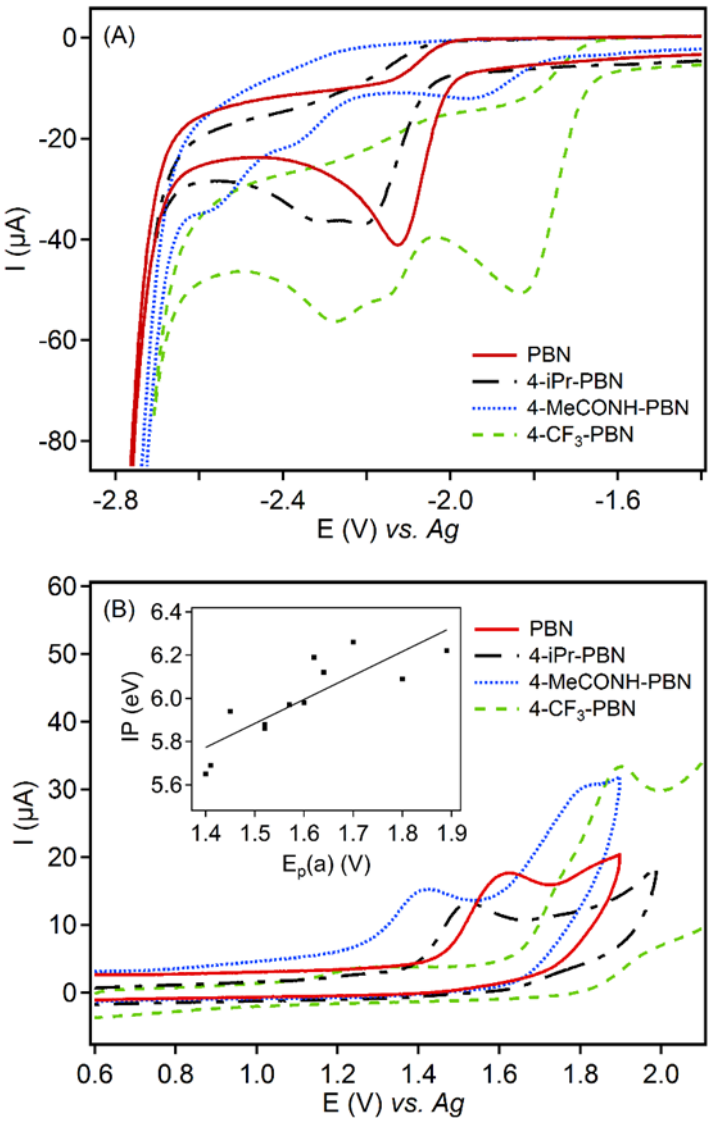

Figure 4. Cyclic voltammograms of PBN, 4-iPr-PBN, 4-MeCONH-PBN and 4-CF_3-PBN in acetonitrile containing 0.1 M of TBAP at a GC electrode, potential scan rate υ = 0.1 V/s: (A) reduction and (B) oxidation. Inset: correlation of ionization potential with oxidation potential of nitrones (R^2 = 0.71), excluding the outlier 4-MeS-PBN for which more complex oxidation process was observed. The correlation includes previous nitrones from Rosselin *et al.*[34]

4-CF_3-PBN bearing an electron-withdrawing group is the easiest to reduce, with the lowest cathodic peak potential in the series and the hardest to oxidize. On the contrary, the derivative with the highest reduction potential was 4-iPr-PBN which has an electron-donating group and very good correlations between the Hammett constants (σ_p)[49] and the redox potentials were observed (Figure S7). The ionization potentials (IPs) were also computationally determined (Table 2) and a good correlation between IP and the oxidation potential (R^2 = 0.71, Figure 4) was also observed.

Table 2. Electrochemical[a] properties and calculated ionization potentials[b] of 4-X-PBN derivatives.

	in CH_3CN[c], compound (1 mM)						
	E_p(c) (V)			E_p(a) (V)		Stability	IP
Nitrones	1st peak	2nd peak	3rd peak	1st peak	2nd peak	domain (V)[d]	(eV)
4-iPr-PBN (3)	-2.21	-2.30		1.52		3.73	5.9
4-Ph-PBN (5)	-1.96	-2.56 (r)		1.52		3.48	5.9
4-MeS-PBN (6)	-2.06			1.32	1.62	3.38	7.0
PBN	-2.12	-2.27		1.60		3.72	6.0
4-MeCONH-PBN (7)	-1.93	-2.35	-2.56	1.41	1.80	3.34	5.7
4-F-PBN (8)	-2.10	-2.19		1.57	1.78	3.67	6.0
4-CF_3O-PBN (9)	-2.02	-2.13		1.64	1.86	3.66	6.1
4-CF_3-PBN (12)	-1.83	-2.13	-2.27	1.89		3.72	6.2

[a] The peak potentials are given versus a silver wire electrode for a potential scan rate 0.1 V/s; in general, the electron transfers appeared irreversible (no backward peak observed) except for nitrone 4-Ph-PBN noted (r).
[b] The IPs were calculated at the (CPCM)/M06-2X/6-31+g(d,p) level of theory.
[c] Containing 0.1 M of TBAP with reduction E_p(c) and oxidation E_p(a) at glassy carbon (GC) electrode.
[d] The stability domain is given as: E_p(a) - E_p(c).

In connection with spin-trapping applications, the stability domain of the derivatives was calculated and is reported in Table 2. It represents the potential window where the spin-trapping technique can be safely applied with electrochemically-generated radicals with no risk of inverted spin-trapping process.[63,64] It is calculated between the least positive E_p(a) and the least negative E_p(c). 4-iPr-PBN, 4-F-PBN, 4-CF_3O-PBN and 4-CF_3-PBN have similar stability domain than PBN (~ 3.70 V) whereas 4-Ph-PBN, 4-MeS-PBN and 4-MeCONH-PBN present a stability domain slightly slower (~ 3.40 V). Therefore, all the spin traps exhibit potential windows broad enough to be used in electrochemical investigations.[62,65]

2.3. Cell culture and viability studies

The *in vitro* cytoprotective effect of the derivatives was next evaluated on two types of assays. In the first test, nitrones at 10 µM were pre-incubated with glial cells for 24 h before excitotoxic tBuOOH exposure (300 µM) and the cell survival was evaluated by a MTT assay (Figure 5). 4-Me_2N-PBN, 4-MeS-PBN, 4-MeCONH, 4-F-PBN and 4-CF_3-PBN exhibited significant protection on this first model. It has also been demonstrated that the derivatives 4-

F-PBN and 4-CF_3-PBN protected the rat retina from light damage when administered intraperitoneal.[24] These two derivatives therefore exhibit interesting therapeutic activities.

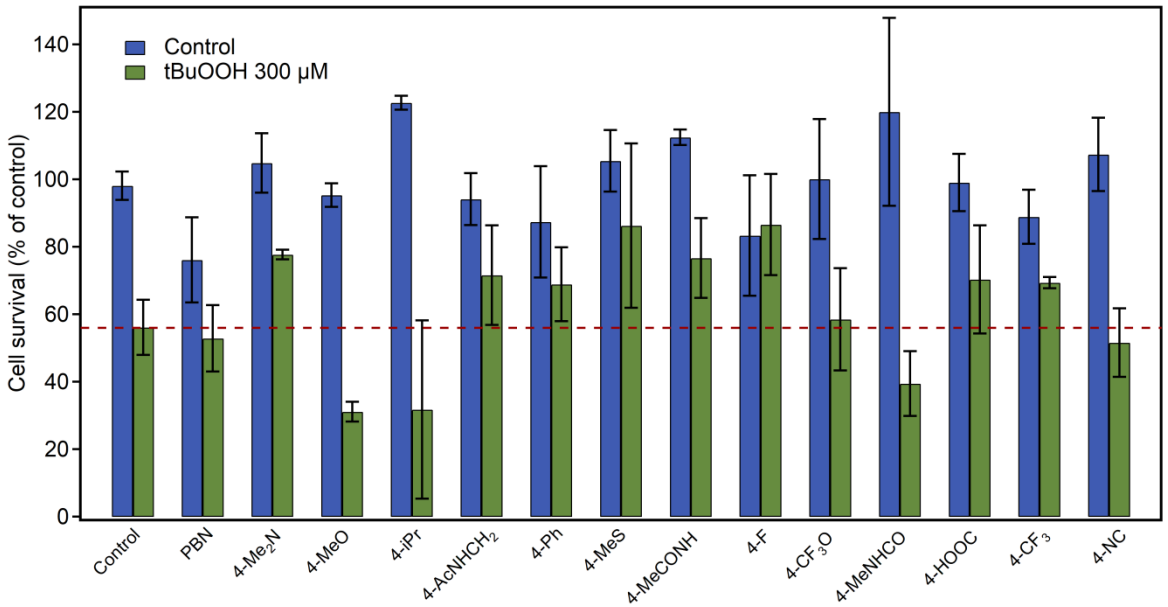

Figure 5. Antioxidant effect of PBN derivatives at 10 µM on glial cells injured tBuOOH (300 µM, 24 h), after 24 h of incubation with nitrones. Cell survival evaluation: MTT assay.

In the second assay, the nitrones at different concentrations (0.1, 1 and 10 µM) were pre-incubated with primary cortical neurons for 1 h before excitotoxic glutamate exposure (20 µmol/L for 20 min followed by a wash-out). 48 h after the glutamate wash-out, the cell survival was evaluated by MTT assay (Figure 6). Glutamate excitotoxicity is one of the well-accepted pathophysiological mechanisms behind many neurodegenerative diseases like amyotrophic lateral sclerosis (ALS), Alzheimer's, and Huntington's disease. It causes the generation of reactive oxygen species ROS and NOS that result in oxidative and nitrosative stress. At 10 µM, 4-HOOC-PBN, 4-NC-PBN, 4-Me_2N-PBN and 4-MeNHCO-PBN showed significant neuroprotection against the glutamate injury. At lower concentration, only 4-HOOC-PBN was neuroprotective and the best cell protection was observed at 0.1 µM. This may indicate toxicity at high concentration and suggests that 4-HOOC-PBN could be a good candidate for neuroprotection at low concentration. Previous studies showed that, *in vitro*, PBN protected rat cerebellar neurons against an excitotoxic glutamate exposure (100 µM) with an half-maximal effective concentration (EC_{50}) of 2.7 mM.[66] Only 4-Me_2N-PBN was also neuroprotective according to the first assay, showing that the cell protection of a compound depends on the type of toxicity induced. It can also depend on the type of cells studied and on the pre-incubation time with the compounds.

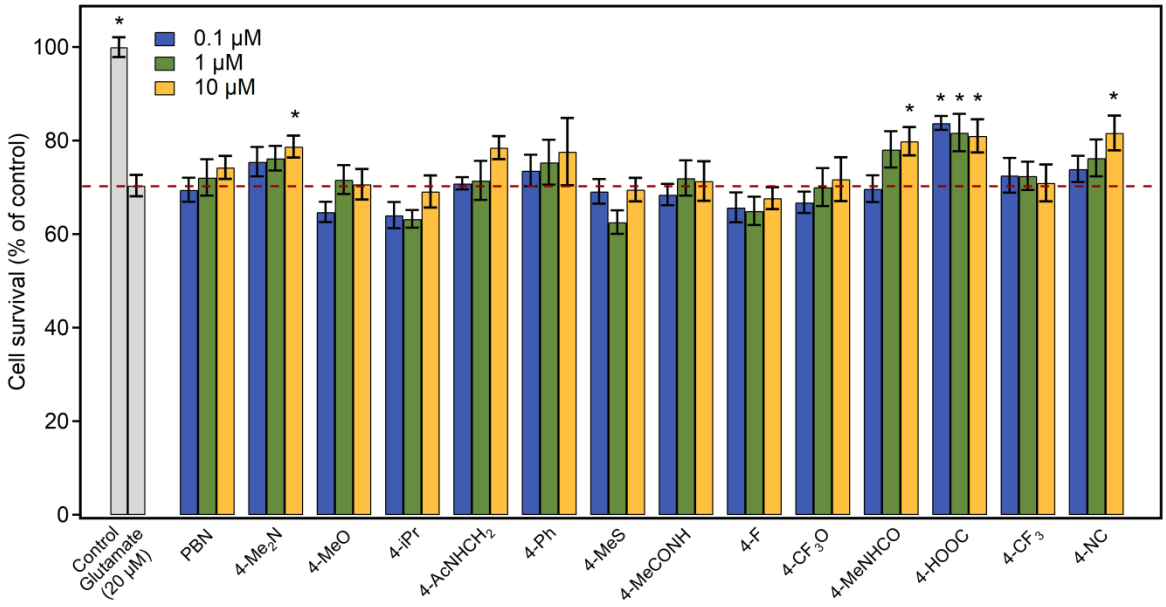

Figure 6. Neuroprotective effect of PBN derivatives at 0.1 µM, 1 µM and 10 µM on primary cortical neurons injured by glutamate (20 µM, 20 min, evaluation performed 48 h after glutamate wash-out), after 1 h of incubation with nitrones. Cell survival evaluation: MTT assay. Significance was accepted with * $p < 0.05$ vs glutamate condition, by one-way ANOVA followed by PLSD Fisher's test.

3. CONCLUSION

A series of *para*-substituted PBN nitrones was studied to investigate the influence of the nature of the substituent on the spin-trapping and neuroprotective activities of the nitronyl function. The spin-trapping ability towards hydroxymethyl radical showed that the presence of an electron-withdrawing group on the *para* position significantly increased the trapping rate. The derivative 4-CF_3-PBN gave the best spin-trapping activity with a trapping rate 3.2 times higher than PBN and it is therefore a potential candidate for spin-trapping experiments. The spin-trapping rate was positively correlated with the atomic total charge of the nitronyl function, the higher the charge, the faster the reaction.

The electrochemical properties of the derivatives were studied and the polar effect of *para*-substituents was confirmed. With a strong electron-withdrawing CF_3 group, the 4-CF_3-PBN was more easily reduced and more hardly oxidized while an opposite trend was observed with 4-iPr-PBN. Some nitrones showed neuroprotective activities in *in vitro* models, however, no correlation between the electronic nature of the substituents and their neuroprotective properties was determined. The best results were obtained with the derivative 4-HOOC-PBN

that protected well cortical neurons after a glutamate intoxication, even at a very low concentration of 0.1 µM suggesting it may be used as a neuroprotectant. To further improve its activity, the synthesis of 4-HOOC-PBN derivatives is currently being developed by our team.

EXPERIMENTAL SECTION

Synthesis. The derivatives 4-iPr-PBN, 4-Ph-PBN, 4-MeS-PBN, 4-F-PBN, 4-CF_3O-PBN and 4-CF_3-PBN were obtained by the "one-pot" reduction/condensation of 2-methyl-2-nitropropane onto the appropriate benzaldehyde in the presence of zinc powder and AcOH.[67,68] 4-MeCONH-PBN was obtained by direct condensation of 4-acetamidobenzaldehyde with *N*-(*tert*-butyl)hydroxylamine acetate using pyrrolidine as catalyst according to the methodology developed by Morales *et al*.[69] with a few modifications. The final compounds were purified by flash chromatography and two successive crystallizations, to ensure high purity and the spectral data were in agreement with the literature.[70–73] Details are given in supporting information.

EPR Measurements and hydroxymethyl spin-trapping kinetics. EPR measurements were carried out on a Bruker EMX spectrometer operating at X-band with 100 kHz modulation frequency. The general instrument settings used for spectral acquisition were as follows: microwave power, 20 mW; modulation amplitude, 1 G; received gains, 5×10^4 to 1×10^6; scan time, 5 s; sweep width, 100 G. Spectra were recorded at room temperature, and measurements were performed using a capillary tube. The spectrum simulation was carried out using the WINSIM program,[74] available as free software from Public Electron Paramagnetic Resonance Software Tools (http://www.niehs.nih.gov/research/resources/software/tox-pharm/tools/). The solvents were of the highest purity grade and used without further purification. The trinitrone TN was synthesized and purified as previously described.[17] To generate the hydroxymethyl ($^{\bullet}CH_2OH$) radical, nitrone (100 mM) was dissolved in a Fenton system containing hydrogen peroxide (6%) and iron (II) sulfate (6 mM) in methanol. The method of kinetic competition described by Roubaud *et al*.[17] was used to evaluate the ratio of the second-order rate constants (k_N/k_{PBN}) for the trapping of $^{\bullet}CH_2OH$ by one of the nitrone **N** of interest and **TN** used as competitive inhibitor. This method yielded equation 1 in which k_N and k_{TN} represent the rate constants of

$^{\bullet}CH_2OH$ trapping by the nitrone **N** under consideration and by **TN**, respectively. *R* and *r* represent the rate constant by both **TN** and **N**, and by **TN** only, respectively.

$$R/r = 1 + k_{\mathrm{N}}[\mathrm{N}]/k_{\mathrm{TN}}[\mathrm{TN}] \quad (1)$$

Then, the commercially available PBN was also tested versus **TN** in order to determine the ratio of the rate constants for the trapping of $^{\bullet}CH_2OH$ by PBN and by **TN**: *i.e.*, $k_{\mathrm{PBN}}/k_{\mathrm{TN}}$. The concentrations of the various nitrones were varied to keep the [**N**]/[**TN**] ratio between 2 and 7. For each nitrone, at least five experiments were repeated twice. In each case, a series of 10 EPR spectra was then recorded (scan time for a single spectrum: 20 s). The signal-to-noise ratio was improved using a SVD procedure, as described elsewhere.[75] The signal recorded exactly 2 min after the beginning of the reaction was then simulated using the WinSim software in order to determine the relative areas of the adducts **N**-CH_2OH and **TN**-CH_2OH. In this approach, the ratio R/r was evaluated as follows:

$$\frac{R}{r} = \frac{area\ of\ N-R\ signal + area\ of\ TN-R\ signal}{area\ of\ TN-R\ signal} \quad (2)$$

General computational methods. Geometries and energies were optimized using DFT formalism with the hybrid meta-GGA (Generalized Gradient Approximation) M06-2X[76] functional and the 6-31+G(d,p) basis set. The frequency analysis was systematically performed at 298 K and 1 atm, at the M06-2X/6-31+G(d,p) level of theory confirming that optimized geometries at in a potential energy surface minimum owing to the absence of any imaginary frequency. Solvent (water) effects were considered by using the C-PCM (conductor-like polarizable continuum model) solvation model,[77,78] in which the solute is embedded into a shape-adapted cavity surrounded by a dielectric continuum characterized by its dielectric constant ε. Calculations were performed in water (ε = 78.35). The atomic charge analysis was performed using the natural population analysis (NPA) within the NBO (Natural Bond Orbital) framework. The IP was calculated as follows: IP = $E(ArNO^{\bullet+})$ – E(ArNO), where $ArNO^{\bullet+}$ is the radical cation obtained after electron withdraw from the neutral form of the PBN derivatives, named here ArNO. It is worth mentioning that IP corresponds to the adiabatic energy of electron withdraw energy, i.e., considering the radical cation energy using the neutral form geometry. All calculations were performed with Gaussian 09 Rev. A2.[79]

Cyclic voltammetric measurements. The electrochemical experiments were carried out at room temperature in acetonitrile containing 100 mM of TBAB, using VersaSTAT 4. A

conventional cell with three electrodes was used: (i) a silver electrode wire as the reference electrode, (ii) a platinum electrode wire as the auxiliary electrode and (iii) a glassy carbon disk as the working electrode. The working electrode was polished prior to each experiment using a 0.04 μm aqueous alumina slurry on a wetted polishing cloth. The potentials are reported versus the silver wire electrode, Ag. All solutions were deoxygenated by argon bubbling through the solution for 10 min and a blanket of argon was maintained over the solution during the experiment. The voltamperograms were recorded for a nitrone concentration equal to 1 mM. Ferrocene was used in order to calibrate the electron transfers.[59]

***In vitro* neuroprotective measurements.**

Glial cells model. C6 cells (rat gliomas) were seeded in 24-well culture plates (500 μL volume) containing DMEM medium (Dulbecco's modified Eagle medium) supplemented with 10% fetal calf serum. They were left in an incubator at 37 °C on 5% CO_2 until reaching 80% of confluence. Then, the culture medium was replaced by serum-free DMEM medium containing the nitrones to be tested. The cells were returned to the incubator for 24 h. The oxidative stress was then induced by treating the cells with *t*BuOOH (100 to 500 μM) for 24 h. Finally, the measurement of cell survival was performed using the MTT test. For this, the medium of each culture well was first replaced by 100 μL of Krebs-Ringer extracellular medium containing: 125 mM NaCl, 3.5 mM KCl, 25 mM $NaHCO_3$, 1.25 mM KH_2PO_4, 1.5 mM, $CaCl_2$, 1.25 mM $MgSO_4$, 10mM d-glucose, and 10mM Hepes (pH 7.4), heated to 33 °C and bubbled with carbogen (95% O_2; 5% CO_2) for 15 min. 10 μL of a solution of MTT (2.5 mg /mL in PBS) were added and the cells were then returned to the incubator for 45 min to allow the transformation of MTT into formazan. The MTT solution was removed and 50 μL of DMSO were added per well to dissolve the formazan crystals. 50 μL more of DMSO were added to dilute the resulting solution. Finally, the optical density (DO) was assessed by spectrophotometer at 570 nm wavelength (LT-4000, LabTech). The DO was corresponding to the cell survival in each culture well.

Primary cortical cells model. Rat cortical neurons were cultured as described by Singer *et al.* and Callizot *et al.*[80,81] Briefly, pregnant females (Wistar; JanvierLabs) at 15 days of gestation were killed by cervical dislocation. Fetuses were collected and immediately placed in ice-cold L15 Leibovitz medium (Pan Biotech) with a 2% penicillin (10,000 U/ml) and streptomycin (10 mg/ml) solution (PS) and 1% bovine serum albumin (BSA). Cortexes was treated for 20 min at 37 °C with a trypsin-EDTA (Pan Biotech) solution at a final concentration of 0.05%

trypsin and 0.02% EDTA. The dissociation was stopped by addition of Dulbecco's modified Eagle's medium (DMEM) with 4.5 g/liter of glucose (Pan Biotech,), containing DNAse I grade II (final concentration 0.5 mg/ml; Pan Biotech) and 10% fetal calf serum (FCS; Invitrogen). Cells were mechanically dissociated by three forced passages through the tip of a 10-ml pipette. Cells were then centrifuged at 515 g for 10 min at 4 °C. The supernatant was discarded, and the pellet was resuspended in a defined serum-free culture medium consisting of Neurobasal medium (Invitrogen) with a 2% solution of B27 supplement (Invitrogen), 2 mmol/liter of L-glutamine (Pan Biotech), 2% of PS solution, and 10 ng/ml of brain-derived neurotrophic factor (BDNF; Pan Biotech). Viable cells were counted in a Neubauer cytometer, using the trypan blue exclusion test. The cells were seeded at a density of 25,000 per well in 96-well plates precoated with poly-L-lysine and were cultured at 37 °C in an air (95%)-CO_2 (5%) incubator. The medium was changed every 2 days. ***Viability studies.*** On day 13 of culture, BDNF (50 ng/ml) or test compounds (at 0.1, 1 and 10 µM) were pre-incubated with primary cortical neurons for 1 h before glutamate exposure. Then, glutamate (Sigma) was added in the cell culture to a final concentration of 20 µM diluted in control medium in presence of BDNF or test compounds for 20 min. After 20 min, glutamate was washed and fresh culture medium with BDNF or test compounds was added for additional 48 h. Test compounds were tested on one culture in 96 well plates (6 wells per conditions). After 48 h of glutamate intoxication (on day 15 of culture), the MTT assay was performed using CellTiter 96® Aqueous One Solution Cell Proliferation Assay (Promega, USA). Briefly, 20 µL of tetrazolium compound was added directly in culture well for 3 h. The optic density (DO) was assessed by spectrophotometer at 450 nm wavelength by Glomax apparatus (Promega). The DO was corresponding to the cell survival in each culture well. Data were expressed in percentage of control conditions (no intoxication, no glutamate = 100 %) in order to express the glutamate injury. All values were expressed as mean +/- SEM (s.e.mean) of the culture (n = 5-6 wells per condition per culture). Statistical analyses on the different conditions were performed (ANOVA followed by PLSD Fisher's test when allowed, using PADPRISM software version 5.0).

ACKNOWLEDGEMENTS

Anaïs Deletraz was the recipient of a fellowship from the "Région Provence Alpes Côte d'Azur". We thank: Fédération RENARD IR-RPE CNRS 3443 for providing funds for the

EPR studies; CALI for computational facilities and the National Program of Sustainability I from the Ministry-of-Youth, Education and Sports of the Czech Republic (LO1305); and Miss Jamila Chetouani for her excellent technical assistance in acquiring computational data. This study was conducted with the financial support of the European Regional Development Fund, the French Government, the "Région Provence Alpes Côte d'Azur", the Departmental Council of Vaucluse and the Urban Community of Avignon.

SUPPORTING INFORMATION

Octanol-water partition coefficients (*c* log *P*) and Calculated atomic partial charges of the nitronyl atoms and ionization potentials of 4-X-PBN derivatives; Correlation of the σ_p values with atomic total charge of nitrones; Cyclic voltammograms of 4-F-PBN, 4-CF_3O-PBN, 4-MeS-PBN and 4-Ph-PBN; Normalized cyclic voltammograms ($I/\upsilon^{1/2} = f(E)$) of PBN and 4-MeS-PBN as a function of potential scan rate υ; Linear regressions corresponding to potential scan rate variations on PBN, 4-CF_3-PBN, 4-iPr-PBN and 4-MeCONH-PBN; General procedure for the synthesis of 4-iPr-PBN, 4-Ph-PBN, 4-MeS-PBN, 4-MeCONH-PBN, 4-F-PBN, 4-CF_3O-PBN and 4-CF_3-PBN and ^1H and ^{13}C NMR spectra of the compounds.

REFERENCES

1 B. Halliwell and J. M. C. Gutteridge, *Free Radicals in Biology and Medicine*, Oxford University Press, 2015.
2 T. Finkel and N. J. Holbrook, *Nature*, 2000, **408**, 239–247.
3 F. A. Villamena, *Reactive Species Detection in Biology: From Fluorescence to Electron Paramagnetic Resonance Spectroscopy*, Elsevier., 2017.
4 R. A. Floyd, R. D. Kopke, C.-H. Choi, S. B. Foster, S. Doblas and R. A. Towner, *Free Radic. Biol. Med.*, 2008, **45**, 1361–1374.
5 F. A. Villamena, A. Das and K. M. Nash, *Future Med. Chem.*, 2012, **9**, 1171–1207.
6 M. Rosselin, B. Poeggeler and G. Durand, *Curr. Top. Med. Chem.*, 2017, **17**, 2006–2022.
7 F. A. Villamena and J. L. Zweier, *Antioxid. Redox Signal.*, 2004, **6**, 619–629.
8 C. L. Hawkins and M. J. Davies, *Biochim. Biophys. Acta BBA - Gen. Subj.*, 2014, **1840**, 708–721.
9 S. Goldstein and P. Lestage, *Curr. Med. Chem.*, 2000, **7**, 1255–1267.
10 F. A. Villamena, in *Reactive Species Detection in Biology*, Elsevier, 2017, 163–202.
11 C. Frejaville, H. Karoui, B. Tuccio, F. Le Moigne, M. Culcasi, S. Pietri, R. Lauricella and P. Tordo, *J. Med. Chem.*, 1995, **38**, 258–265.
12 G. Olive, A. Mercier, F. Le Moigne, A. Rockenbauer and P. Tordo, *Free Radic. Biol. Med.*, 2000, **28**, 403–408.
13 F. A. Villamena, A. Rockenbauer, J. Gallucci, M. Velayutham, C. M. Hadad and J. L. Zweier, *J. Org. Chem.*, 2004, **69**, 7994–8004.
14 F. A. Villamena, S. Xia, J. K. Merle, R. Lauricella, B. Tuccio, C. M. Hadad and J. L. Zweier, *J. Am. Chem. Soc.*, 2007, **129**, 8177–8191.
15 A. Allouch, V. Roubaud, R. Lauricella, J.-C. Bouteiller and B. Tuccio, *Org. Biomol. Chem.*, 2003, **1**, 593–598.
16 A. Allouch, V. Roubaud, R. Lauricella, J.-C. Bouteiller and B. Tuccio, *Org. Biomol. Chem.*, 2005, **3**, 2458–2462.
17 V. Roubaud, H. Dozol, C. Rizzi, R. Lauricella, J.-C. Bouteiller and B. Tuccio, *J. Chem. Soc. Perkin Trans. 2*, 2002, 958–964.
18 H. M. Hughes, I. M. George, J. C. Evans, C. C. Rowlands, G. M. Powell and C. G. Curtis, *Biochem. J.*, 1991, **277**, 795–800.
19 M. B. Kadiiska, P. M. Hanna, S. J. Jordan and R. P. Mason, *Am. Soc. Pharmacol. Exp. Ther.*, 1993, **44**, 222–227.
20 H. D. Connor, W. Gao, S. Nukina, J. J. Lemasters, R. P. Mason and R. G. Thurman, *Transplantation*, 1992, **54**, 199–204.
21 K. R. Maples, A. R. Green and R. A. Floyd, *CNS Drugs*, 2004, **18**, 1071–1084.
22 P. K. Datta, S. Reddy, M. Sharma and E. A. Lianos, *Nephron Exp. Nephrol.*, 2006, **103**, e131–e138.
23 M. N. A. Mandal, G. P. Moiseyev, M. H. Elliott, A. Kasus-Jacobi, X. Li, H. Chen, L. Zheng, O. Nikolaeva, R. A. Floyd, J. Ma and R. E. Anderson, *J. Biol. Chem.*, 2011, **286**, 32491–32501.

24 M. Stiles, G. P. Moiseyev, M. L. Budda, A. Linens, R. S. Brush, H. Qi, G. L. White, R. F. Wolf, J. Ma, R. Floyd and others, *PLOS One*, 2015, **10**, e0145305.
25 C. L. Willis and D. E. Ray, *NeuroToxicology*, 2007, **28**, 161–167.
26 R. A. Floyd, *Aging Cell*, 2006, **5**, 51–57.
27 A. Shuaib, K. R. Lees, P. Lyden, J. Grotta, A. Davalos, S. M. Davis, H.-C. Diener, T. Ashwood, W. W. Wasiewski and U. Emeribe, *N. Engl. J. Med.*, 2007, **357**, 562–571.
28 H.-C. Diener, K. R. Lees, P. Lyden, J. Grotta, A. Davalos, S. M. Davis, A. Shuaib, T. Ashwood, W. Wasiewski, V. Alderfer, H.-G. Hardemark and L. Rodichok, *Stroke*, 2008, **39**, 1751–1758.
29 E. G. Janzen and R. C. Zawalski, *J. Org. Chem.*, 1978, **43**, 1900–1903.
30 E. G. Janzen, M. S. West, Y. Kotake and C. M. DuBose, *J. Biochem. Biophys. Methods*, 1996, **32**, 183–190.
31 G. T. Balogh, Z. Szántó, E. Forrai, W. Győrffy and A. Lopata, *J. Pharm. Biomed. Anal.*, 2005, **39**, 1057–1062.
32 C. L. Greenstock and R. H. Wiebe, *Can. J. Chem.*, 1982, **60**, 1560–1564.
33 Y. Sueishi, C. Yoshioka, C. Olea-Azar, L. A. Reinke and Y. Kotake, *Bull. Chem. Soc. Jpn.*, 2002, **75**, 2043–2047.
34 M. Rosselin, B. Tuccio, P. Pério, Frederick. A. Villamena, P.-L. Fabre and G. Durand, *Electrochimica Acta*, 2016, **193**, 231–239.
35 V. Roubaud, R. Lauricella, B. Tuccio, J.-C. Bouteiller and P. Tordo, *Res. Chem. Intermed.*, 1996, **22**, 405–416.
36 K. Stolze, N. Udilova, T. Rosenau, A. Hofinger and H. Nohl, *Biochem. Pharmacol.*, 2004, **68**, 185–194.
37 S. Kim, G. V. M. de A. Vilela, J. Bouajila, A. G. Dias, F. Z. G. A. Cyrino, E. Bouskela, P. R. R. Costa and F. Nepveu, *Bioorg. Med. Chem.*, 2007, **15**, 3572–3578.
38 C. Quin, J. Trnka, A. Hay, M. P. Murphy and R. C. Hartley, *Tetrahedron*, 2009, **65**, 8154–8160.
39 L. Robertson and R. C. Hartley, *Tetrahedron*, 2009, **65**, 5284–5292.
40 Y. Han, Y. Liu, A. Rockenbauer, J. L. Zweier, G. Durand and F. A. Villamena, *J. Org. Chem.*, 2009, **74**, 5369–5380.
41 K. Abbas, M. Hardy, F. Poulhès, H. Karoui, P. Tordo, O. Ouari and F. Peyrot, *Free Radic. Biol. Med.*, 2014, **71**, 281–290.
42 M. Hardy, F. Poulhés, E. Rizzato, A. Rockenbauer, K. Banaszak, H. Karoui, M. Lopez, J. Zielonka, J. Vasquez-Vivar, S. Sethumadhavan, B. Kalyanaraman, P. Tordo and O. Ouari, *Chem. Res. Toxicol.*, 2014, **27**, 1155–1165.
43 L. Socrier, M. Rosselin, F. Choteau, G. Durand and S. Morandat, *Biochim. Biophys. Acta BBA - Biomembr.*, 2017, **1859**, 2495–2504.
44 G. Durand, F. Choteau, B. Pucci and F. A. Villamena, *J. Phys. Chem. A*, 2008, **112**, 12498–12509.
45 K. Murofushi, K. Abe and M. Hirota, *J. Chem. Soc. Perkin Trans. 2*, 1987, 1829–1833.
46 Y. Abe, S. Seno, K. Sakakibara and M. Hirota, *J. Chem. Soc. Perkin Trans. 2*, 1991, 897–903.
47 A. Phaniendra, D. B. Jestadi and L. Periyasamy, *Indian J. Clin. Biochem.*, 2015, **30**, 11–26.

48 G. R. Buettner, *Free Radic. Biol. Med.*, 1987, **3**, 259–303.
49 C. Hansch, A. Leo and R. W. Taft, *Chem. Rev.*, 1991, **91**, 165–195.
50 A. Deletraz, K. Zéamari, F. Di Meo, P.-L. Fabre, K. Reybier, P. Trouillas, B. Tuccio and G. Durand, *New J. Chem.*, 2019, **43**, 15754–15762.
51 A. Zeghdaoui, B. Tuccio, J.-P. Finet, V. Cerri and P. Tordo, *J. Chem. Soc. Perkin Trans. 2*, 1995, 2087–2089.
52 V. Roubaud, R. Lauricella, J.-C. Bouteiller and B. Tuccio, *Arch. Biochem. Biophys.*, 2002, **397**, 51–56.
53 F. De Vleeschouwer, V. Van Speybroeck, M. Waroquier, P. Geerlings and F. De Proft, *Org. Lett.*, 2007, **9**, 2721–2724.
54 Y. Sueishi, D. Yoshioka, C. Yoshioka, S. Yamamoto and Y. Kotake, *Org. Biomol. Chem.*, 2006, **4**, 896-901.
55 J. P. Foster and F. Weinhold, *J. Am. Chem. Soc.*, 1980, **102**, 7211–7218.
56 A. E. Reed and F. Weinhold, *J. Chem. Phys.*, 1985, **83**, 1736–1740.
57 V. Suryanarayanan, S. Yoshihara and T. Shirakashi, *Electrochimica Acta*, 2005, **51**, 991–999.
58 K. Nakahara, S. Iwasa, J. Iriyama, Y. Morioka, M. Suguro, M. Satoh and E. J. Cairns, *Electrochimica Acta*, 2006, **52**, 921–927.
59 C. Amatore, M. Azzabi, P. Calas, A. Jutand, C. Lefrou and Y. Rollin, *J. Electroanal. Chem. Interfacial Electrochem.*, 1990, **288**, 45–63.
60 G. L. McIntire, H. N. Blount, H. J. Stronks, R. V. Shetty and E. G. Janzen, *J. Phys. Chem.*, 1980, **84**, 916–921.
61 B. Tuccio, P. Bianco, J. C. Bouteiller and P. Tordo, *Electrochimica Acta*, 1999, **44**, 4631–4634.
62 B. J. Acken, D. E. Gallis, J. A. Warshaw and D. R. Crist, *Can. J. Chem.*, 1992, **70**, 2076–2080.
63 L. Eberson, *J. Chem. Soc. Perkin Trans. 2*, 1992, 1807–1813.
64 L. Eberson, *J. Chem. Soc. Perkin Trans. 2*, 1994, 171–176.
65 T. H. Walter, E. E. Bancroft, G. L. McIntire, E. R. Davis, L. M. Gierasch and H. N. Blount, *Can. J. Chem.*, 1982, **60**, 1621–1636.
66 T.-L. Yue, J.-L. Gu, P. G. Lysko, H.-Y. Cheng, F. C. Barone and G. Feuerstein, *Brain Res.*, 1992, **574**, 193–197.
67 R. Huie and W. R. Cherry, *J. Org. Chem.*, 1985, **50**, 1531–1532.
68 F. Choteau, B. Tuccio, F. A. Villamena, L. Charles, B. Pucci and G. Durand, *J. Org. Chem.*, 2012, **77**, 938–948.
69 S. Morales, F. G. Guijarro, I. Alonso, J. L. García Ruano and M. B. Cid, *ACS Catal.*, 2016, **6**, 84–91.
70 R. D. Hinton and E. G. Janzen, *J. Org. Chem.*, 1992, **57**, 2646–2651.
71 K. Ikeda, T. Tatsumo, H. Ogo, S. Masumoto, T. Fujibayashi, R. Nagata, U.S. Patent, 6,194,461 B1, 2001.
72 M. Kelly, J. Kincaid and S. Janagani, U.S. Patent, 0,182,060 A1, 2005.73 X. Song, Y. Qian, R. Ben, X. Lu, H.-L. Zhu, H. Chao and J. Zhao, *J. Med. Chem.*, 2013, **56**, 6531–6535.

74 D. R. Duling, *J. Magn. Reson.*, 1994, 105–110.
75 R. Lauricella, A. Allouch, V. Roubaud, J.-C. Bouteiller and B. Tuccio, *Org. Biomol. Chem.*, 2004, **2**, 1304–1309.
76 Y. Zhao and D. G. Truhlar, *Theor. Chem. Acc.*, 2008, **120**, 215–241.
77 V. Barone and M. Cossi, *J. Phys. Chem. A*, 1998, **102**, 1995–2001.
78 M. Cossi, N. Rega, G. Scalmani and V. Barone, *J. Comput. Chem.*, 2003, **24**, 669–681.
79 Gaussian 09, Revision A.02, M. J. Frisch, G. W. Trucks, H. B. Schlegel, G. E. Scuseria, M. A. Robb, J. R. Cheeseman, G. Scalmani, V. Barone, G. A. Petersson, H. Nakatsuji, X. Li, M. Caricato, A. Marenich, J. Bloino, B. G. Janesko, R. Gomperts, B. Mennucci, H. P. Hratchian, J. V. Ortiz, A. F. Izmaylov, J. L. Sonnenberg, D. Williams-Young, F. Ding, F. Lipparini, F. Egidi, J. Goings, B. Peng, A. Petrone, T. Henderson, D. Ranasinghe, V. G. Zakrzewski, J. Gao, N. Rega, G. Zheng, W. Liang, M. Hada, M. Ehara, K. Toyota, R. Fukuda, J. Hasegawa, M. Ishida, T. Nakajima, Y. Honda, O. Kitao, H. Nakai, T. Vreven, K. Throssell, J. A. Montgomery, Jr., J. E. Peralta, F. Ogliaro, M. Bearpark, J. J. Heyd, E. Brothers, K. N. Kudin, V. N. Staroverov, T. Keith, R. Kobayashi, J. Normand, K. Raghavachari, A. Rendell, J. C. Burant, S. S. Iyengar, J. Tomasi, M. Cossi, J. M. Millam, M. Klene, C. Adamo, R. Cammi, J. W. Ochterski, R. L. Martin, K. Morokuma, O. Farkas, J. B. Foresman, and D. J. Fox, Gaussian, Inc., Wallingford CT, 2016.
80 C. A. Singer, X. A. Figueroa-Masot, R. H. Batchelor and D. M. Dorsa, *J. Neurosci.*, 1999, **19**, 2455–2463.
81 N. Callizot, M. Combes, R. Steinschneider and P. Poindron, *J. Neurosci. Res.*, 2013, **91**, 706–716.

Supporting Information For

Para-substituted α-Phenyl-*N*-*tert*-butyl Nitrones: Spin-Trapping and Electrochemical and Neuroprotective Properties

Table of contents

Table S1. Octanol-water partition coefficients (*c log P*) and calculated atomic partial charges of the nitronyl atoms and ionization potentials of 4-X-PBN derivatives at the (CPCM)/M06-2X/6-31+g(d,p) Level of Theory.

			Atomic partial charges of the nitronyl atoms (*e*)					
Compounds	σ_p [a]	c*log P* [b]	H	C	N	O	Total	IP (eV)
4-Me_2N-PBN (1)	-0.83	2.67	0.251	0.034	0.056	-0.666	-0.325	5.1
4-MeO-PBN (2)	-0.27	2.57	0.253	0.028	0.069	-0.651	-0.301	5.7
4-iPr-PBN (3)	-0.15	3.76	0.260	0.023	0.076	-0.642	-0.283	5.9
4-AcNHCH_2-PBN (4)	-0.05	2.06	0.255	0.020	0.080	-0.637	-0.282	5.9
4-Ph-PBN (5)	-0.01	4.35	0.248	0.003	0.098	-0.612	-0.263	5.9
4-MeS-PBN (6)	0	3.17	0.255	0.021	0.076	-0.641	-0.289	7.0
PBN	0	2.67	0.254	0.019	0.080	-0.636	-0.283	6.0
4-MeCONH-PBN (7)	0	2.28	0.254	0.023	0.075	-0.644	-0.292	5.7
4-F-PBN (8)	0.06	2.73	0.256	0.020	0.080	-0.637	-0.281	6.0
4-CF_3O-PBN (9)	0.35	3.50	0.257	0.014	0.087	-0.627	-0.269	6.1
4-MeNHCO-PBN (10)	0.36	2.17	0.258	0.012	0.088	-0.590	-0.232	6.1
4-HOOC-PBN (11)	0.45	2.19	0.258	0.006	0.094	-0.615	-0.257	6.2
4-CF_3-PBN (12)	0.54	3.43	0.258	0.008	0.093	-0.618	-0.259	6.2
4-NC-PBN (13)	0.66	2.48	0.259	0.003	0.097	-0.611	-0.252	6.3

[a]Data from Hansch et al.[1]
[b]Calculated octanol/water partition coefficient values obtained using ALOGPS 2.1 software (http://www.vcclab.org/lab/alogps/).

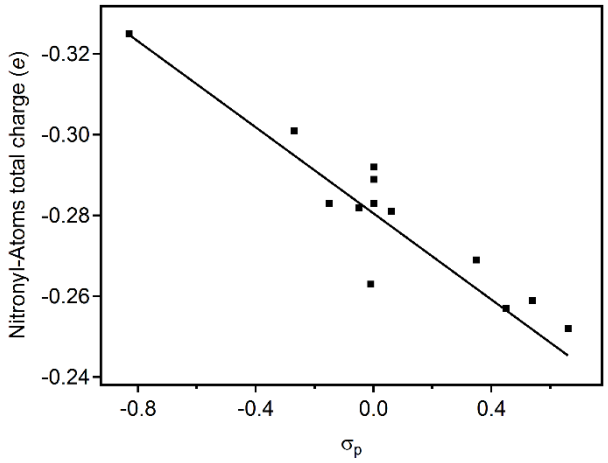

Figure S1. Correlation of atomic total charge of the nitronyl moiety with Hammett constants σ_p (R^2 = 0.77).

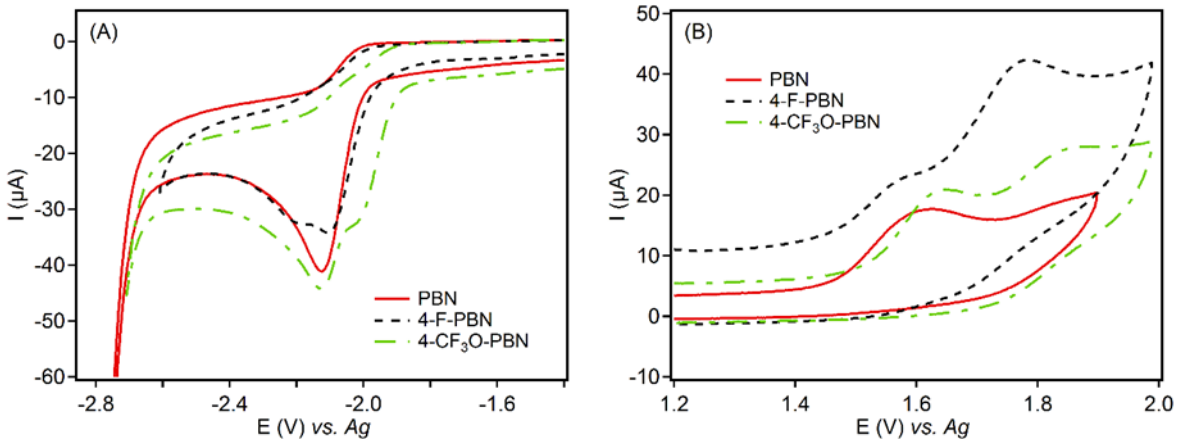

Figure S2. Cyclic voltammograms of PBN, 4-F-PBN and 4-CF_3O-PBN, reduction (A) and oxidation (B) in acetonitrile containing 0.1 M of TBAB at a GC electrode, potential scan rate υ = 0.1 V/s.

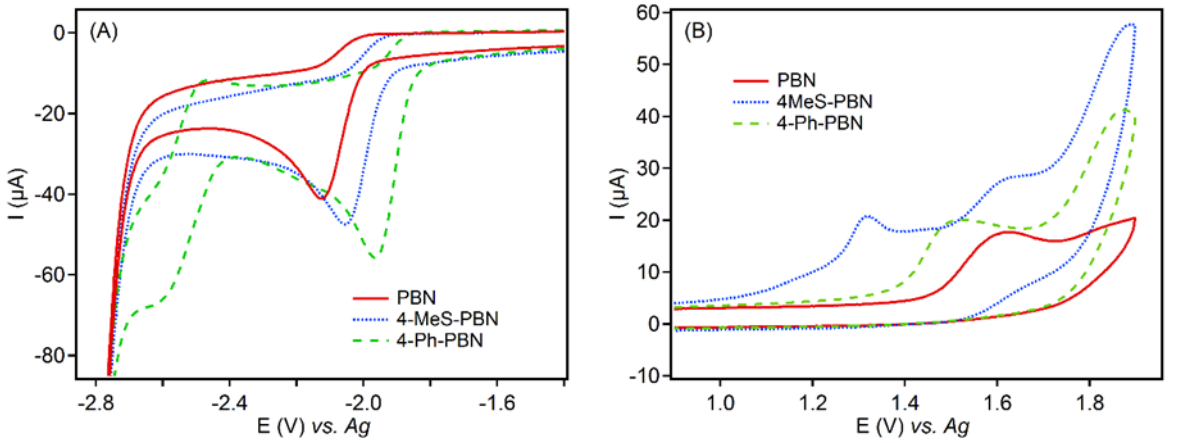

Figure S3. Cyclic voltammograms of PBN, 4-MeS-PBN and 4-Ph-PBN, reduction (A) and oxidation (B) in acetonitrile containing 0.1 M of TBAB at a GC electrode, potential scan rate υ = 0.1 V/s.

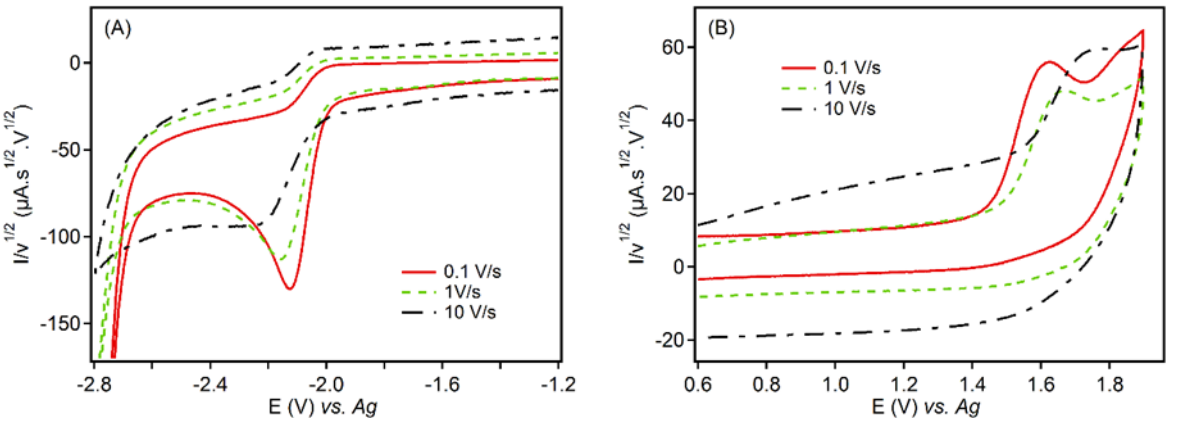

Figure S4. Normalized cyclic voltammograms ($I/\upsilon^{1/2}$ = f(E)) of PBN, reduction (A) and oxidation (B) in acetonitrile containing 0.1 M of TBAB at a GC electrode as a function of potential scan rate υ.

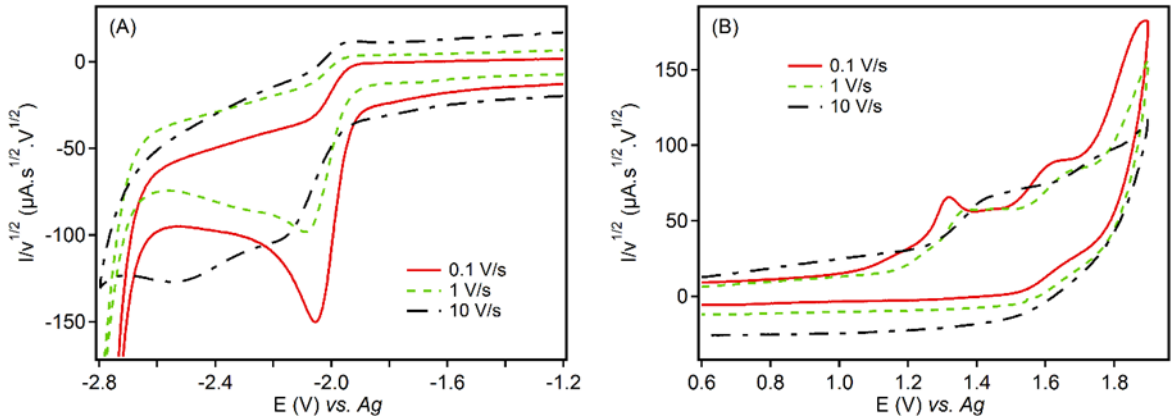

Figure S5. Normalized cyclic voltammograms ($I/\upsilon^{1/2}$ = f(E)) of 4-MeS-PBN, reduction (A) and oxidation (B) in acetonitrile containing 0.1 M of TBAB at a GC electrode as a function of potential scan rate υ.

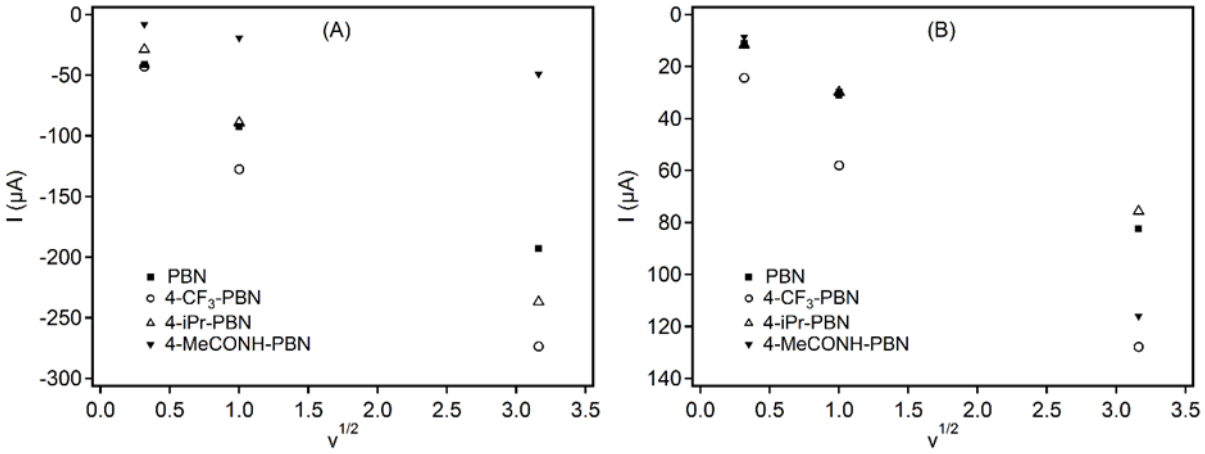

Figure S6. Linear regressions corresponding to potential scan rate variations on PBN, 4-CF_3-PBN, 4-iPr-PBN and 4-MeCONH-PBN, reduction (A) and oxidation (B) in acetonitrile containing 0.1 M of TBAP at potential scan rate ranging from 0.1 to 10 V/s.

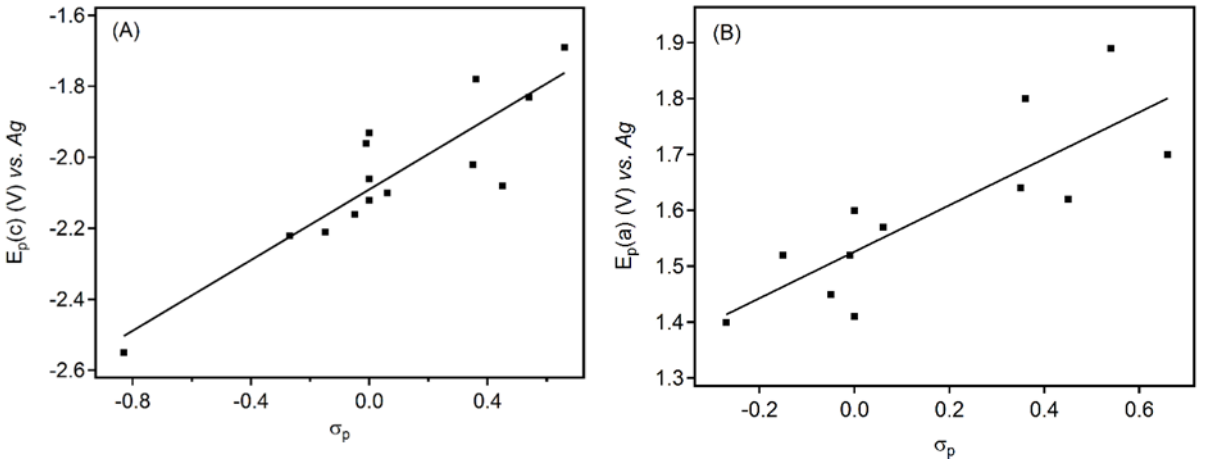

Figure S7. Correlation of Hammett constants (σ_p) with (A): the reduction peak potential (R^2 = 0.78) and with (B): the oxidation peak potential of the nitronyl function (R^2 = 0.68), excluding the outlier 4-MeS-PBN for which more complex oxidation process was observed.

Synthesis. All reagents were from commercial sources and were used as received. All solvents were distilled and dried according to standard procedures. Reaction courses and product mixtures were routinely monitored by TLC on silica gel (60 F_{254} Merck plates). Compound detection was achieved either by exposure to UV light (254 nm) and/or by spraying a 5% sulfuric acid solution in ethanol or a 2% ninhydrin solution in ethanol and then heating to ~150 °C. Flash column chromatography was carried out on silica gel (40−63 μm) with a CombiFlash system. NMR spectra were recorded on a Bruker AC400 at 400 and 100 MHz for ^{1}H and ^{13}C experiments, respectively. Chemical shifts are given in ppm relative to the solvent residual peak as a heteronuclear reference for ^{1}H and ^{13}C. Abbreviations used for signal patterns are as follows: bs, broad singlet; s, singlet; d, doublet; t, triplet; m, multiplet. HR-MS spectra were recorded on a Synapt G2-S (Waters) mass spectrometer equipped with a TOF analyzer for ESI+ experiments.

General procedure for the synthesis of 4-X-PBNs (except 4-MeCONH-PBN). Under an argon atmosphere and under stirring, the corresponding benzaldehyde (1.0 equiv), 2-methyl-2-nitropropane (2.0 equiv) and AcOH (6.0 equiv) were dissolved in dry EtOH. The mixture was cooled down to 0 °C then zinc powder (4.0 equiv) was slowly added in order to keep the temperature below 15 °C. The mixture was stirred at room temperature for 30 min then heated at 60 °C in the dark overnight in the presence of molecular sieves (4Å). The reaction mixture was filtered through a pad of Celite, and the solvent was removed under vacuum. The crude mixture was purified by flash chromatography (EtOAc/cyclohexane) followed by two successive crystallizations from EtOAc/*n*-hexane.

***N*-*tert*-butyl-α-(4-isopropyl)phenylnitrone (3).** Flash chromatography (EtOAc/cyclohexane, 2:8 v/v). Yield 60%. White powder. R_f (EtOAc/cyclohexane, 2:8 v/v) = 0.18. Elemental analysis calculated for $C_{14}H_{21}NO$: C, 76.7; H, 9.7; N, 6.4; found: C, 77.2; H, 9.5; N, 5.9%. ^{1}H NMR (400 MHz, $CDCl_3$) δ 8.22 (2H, d, *J* = 8.4 Hz), 7.51 (1H, s), 7.27 (2H, d, *J* = 8.4 Hz), 2.98-2.89 (1H, m), 1.61 (9H, s), 1.25 (6H, d, *J* = 6.8 Hz); $^{13}C\{1H\}$ NMR (100 MHz, $CDCl_3$) δ 151.5, 129.9, 129.1, 128.9, 126.6, 70.6, 34.3, 28.5, 23.9. The spectral data were in agreement with the literature.[2]

***N*-*tert*-butyl-α-(4-phenyl)phenylnitrone (5).** Flash chromatography (EtOAc/cyclohexane, 2:8 v/v). Yield 57%. White powder. R_f (EtOAc/cyclohexane, 3:7 v/v) = 0.32. Elemental analysis calculated for $C_{17}H_{19}NO$: C, 80.6; H, 7.6; N, 5.5; found: C, 80.8; H, 7.3; N, 5.4%. ^{1}H NMR (400 MHz, $CDCl_3$) δ 8.37 (2H, d, *J* = 8.4 Hz), 7.68-7.63 (4H, m), 7.59 (1H, s), 7.47-

7.43 (2H, m), 7.38-7.36 (1H, m), 1.63 (9H, s); $^{13}C\{1H\}$ NMR (100 MHz, $CDCl_3$) δ 142.7, 140.4, 130.2, 129.7, 129.4, 129.0, 127.9, 127.2, 127.1, 70.9, 28.5. The spectral data were in agreement with the literature.[2]

***N-tert*-butyl-α-(4-methylthio)phenylnitrone (6).** Flash chromatography (EtOAc/cyclohexane 3:7 v/v). Yield 39%. White powder. R_f (EtOAc/cyclohexane, 3:7 v/v) = 0.20. Elemental analysis calculated for $C_{12}H_{17}NOS$: C, 64.5; H, 7.7; N, 6.3; found: C, 64.0; H, 7.8; N, 5.8%. ^1H NMR (400 MHz, $CDCl_3$) δ 8.22 (2H, d, *J* = 8.4 Hz), 7.49 (1H, s), 7.25 (2H, d, *J* = 8.4 Hz), 2.51 (3H, s), 1.61 (9H, s); $^{13}C\{1H\}$ NMR (100 MHz, $CDCl_3$) δ 141.5, 129.5, 129.2, 127.8, 125.6, 70.7, 28.5, 15.3. The spectral data were in agreement with the literature.[3]

***N-tert*-butyl-α-(4-fluoro)phenylnitrone (8).** Flash chromatography (EtOAc/cyclohexane, 3:7 v/v). Yield 55%. White powder. R_f (EtOAc/cyclohexane, 3:7 v/v) = 0.25. Elemental analysis calculated for $C_{11}H_{14}FNO$: C, 67.7; H, 7.2; N, 7.2; found: C, 68.0; H, 7.0; N, 7.3%. ^1H NMR (400 MHz, $CDCl_3$) δ 8.35-8.32 (2H, m), 7.53 (1H, s), 7.10 (2H, t, *J* = 8.8 Hz), 1.61 (9H, s); $^{13}C\{1H\}$ NMR (100 MHz, $CDCl_3$) δ 163.4 (d, *J* = 251 Hz), 131.1 (d, *J* = 8 Hz), 128.9, 127.6 (d, *J* = 3 Hz), 115.6 (d, *J* = 21 Hz), 70.9, 28.5. The spectral data were in agreement with the literature.[2]

***N-tert*-butyl-α-(4-trifluoromethoxy)phenylnitrone (9).** Flash chromatography (EtOAc/cyclohexane, 2:8 v/v). Yield 54%. White powder. R_f (EtOAc/cyclohexane, 2:8 v/v) = 0.19. Elemental analysis calculated for $C_{12}H_{14}F_3NO_2$: C, 55.2; H, 5.4; N, 5.4; found: C, 55.5; H, 5.3; N, 5.1%. ^1H NMR (400 MHz, $CDCl_3$) δ 8.36 (2H, d, *J* = 8.8 Hz), 7.56 (1H, s), 7.25 (2H, d, *J* = 8.8 Hz), 1.62 (9H, s); $^{13}C\{1H\}$ NMR (100 MHz, $CDCl_3$) δ 149.8, 130.4, 129.8, 128.5, 120.7, 120.5 (d, *J* = 256 Hz), 71.3, 28.5. The spectral data were in agreement with the literature.[4]

***N-tert*-butyl-α-(4-trifluoromethyl)phenylnitrone (12).** Flash chromatography (EtOAc/cyclohexane, 2:8 v/v). Yield 84%. White powder. R_f (EtOAc/cyclohexane, 1:9 v/v) = 0.13. Elemental analysis calculated for $C_{12}H_{14}F_3NO$: C, 58.8; H, 5.8; N, 5.7; found: C, 59.1; H, 5.5; N, 5.6%. ^1H NMR (400 MHz, $CDCl_3$) δ 8.39 (2H, d, *J* = 8.4 Hz), 7.65 (2H, d, *J* = 8.4 Hz), 7.62 (1H, s), 1.63 (9H, s); $^{13}C\{1H\}$ NMR (100 MHz, $CDCl_3$) δ 134.3, 131.3 (d, *J* = 32 Hz), 128.8, 128.6, 125.5-125.3 (m), 124.0 (d, *J* = 269 Hz), 71.8, 28.5. The spectral data were in agreement with the literature.[2]

***N*-*tert*-butyl-α-(4-acetamido)phenylnitrone (7).** Under an argon atmosphere and under stirring, 4-acetamidobenzaldehyde (1.0 equiv) and *N*-(*tert*-butyl)hydroxylamine acetate (1.0 equiv) were dissolved in dry DCM. Pyrrolidine (1.2 equiv) was added and the mixture was stirred at room temperature for 18 h. The solvent was removed under vacuum and the crude mixture was purified by flash chromatography (EtOAc/cyclohexane, 9:1 v/v) followed by two successive crystallizations from MeOH/Et_2O to afford 500 mg of the title compound (2.14 mmol, 53%) as a white powder. R_f (EtOAc/cyclohexane, 8:2 v/v) = 0.10. Elemental analysis calculated for $C_{13}H_{18}N_2O_2$: C, 66.6; H, 7.7; N, 12.0; found: C, 64.9; H, 7.6; N, 11.1%. ^{1}H NMR (400 MHz, $CDCl_3$) δ 8.24 (2H, d, *J* = 8.8 Hz), 7.97 (1H, bs), 7.58 (2H, d, *J* = 8.8 Hz), 7.50 (1H, s), 2.16 (3H, s), 1.59 (9H, s); ^{13}C{1H} NMR (100 MHz, $CDCl_3$) δ 168.7, 139.8, 130.0, 129.8, 126.9, 119.2, 70.6, 28.4, 24.8. The spectral data were in agreement with the literature.[5]

Determination of *c* log *P* Values. The partition coefficient octanol/water (*c* log *P*) was determined using ALOGPS 2.1 software, which is available at www.vcclab.org/lab/alogps/.

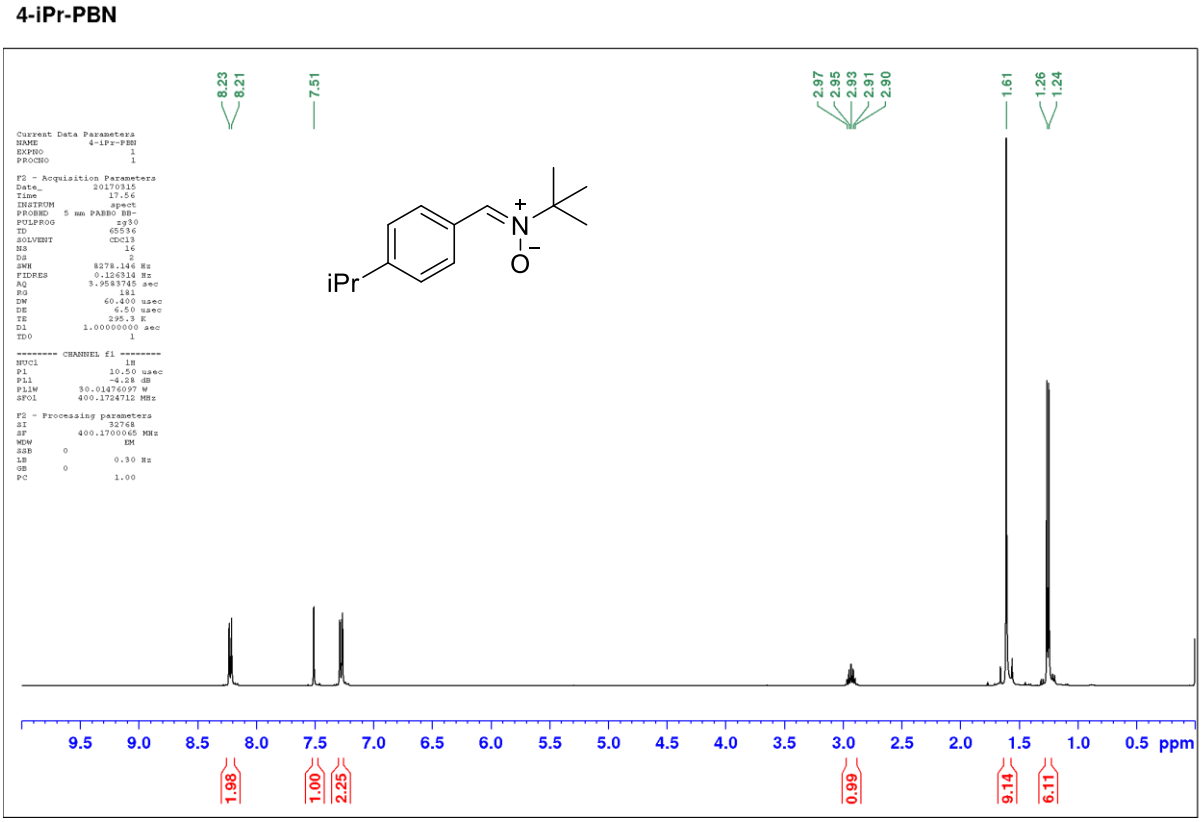

Figure S8. ^{1}H NMR spectrum of 4-iPr-PBN in $CDCl_3$.

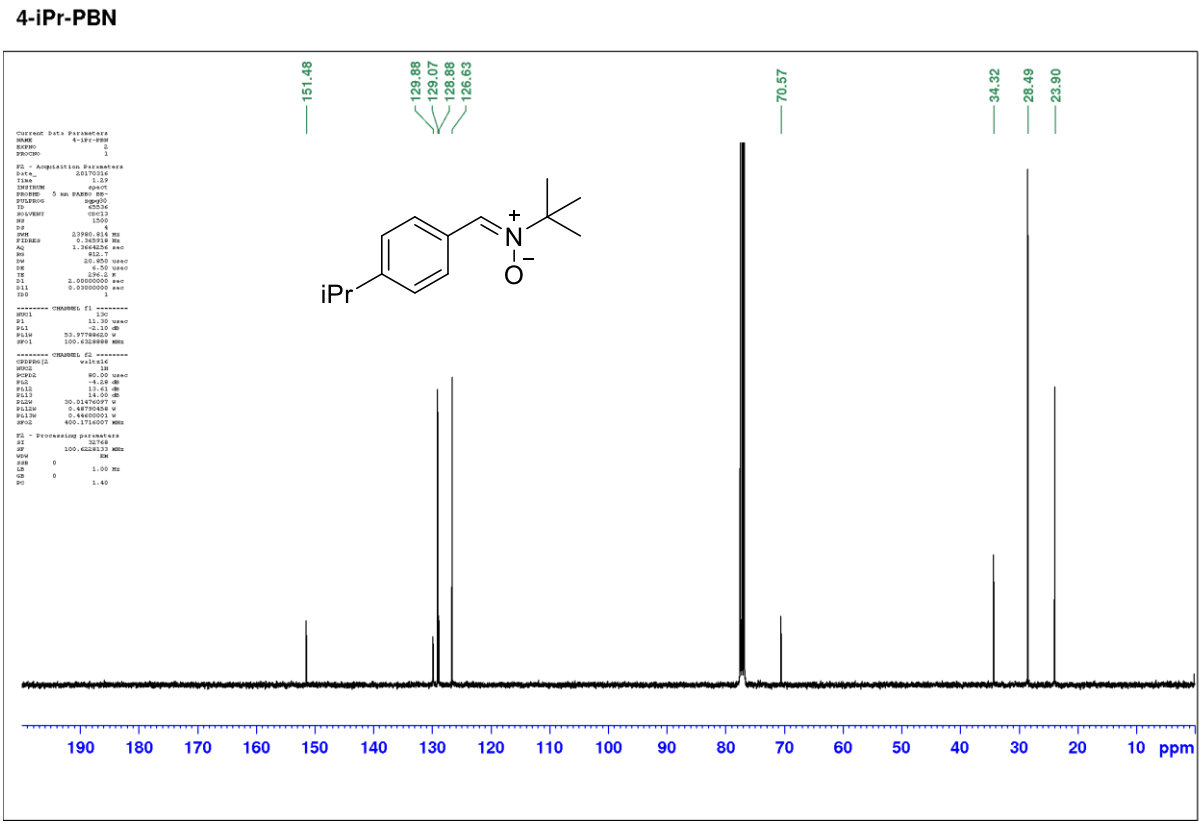

Figure S9. ^{13}C NMR spectrum of 4-iPr-PBN in $CDCl_3$.

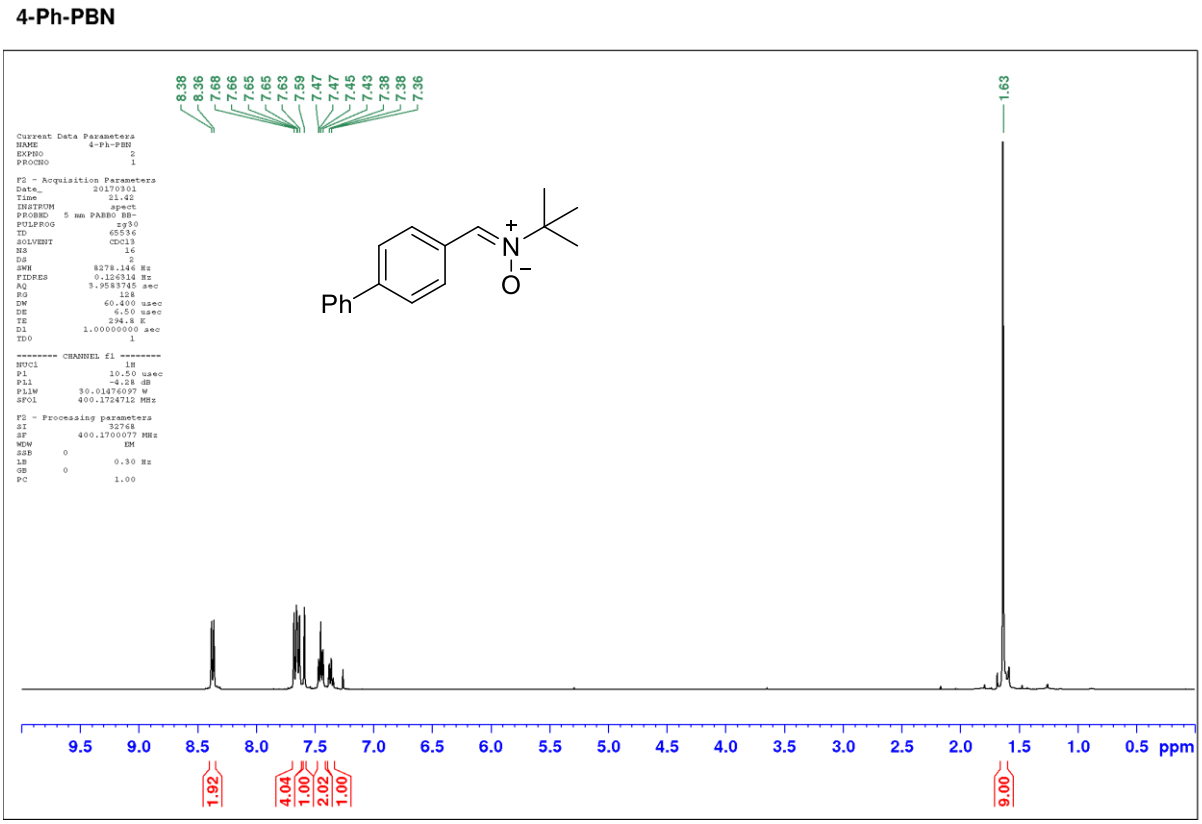

Figure S10. ^{1}H NMR spectrum of 4-Ph-PBN in $CDCl_3$.

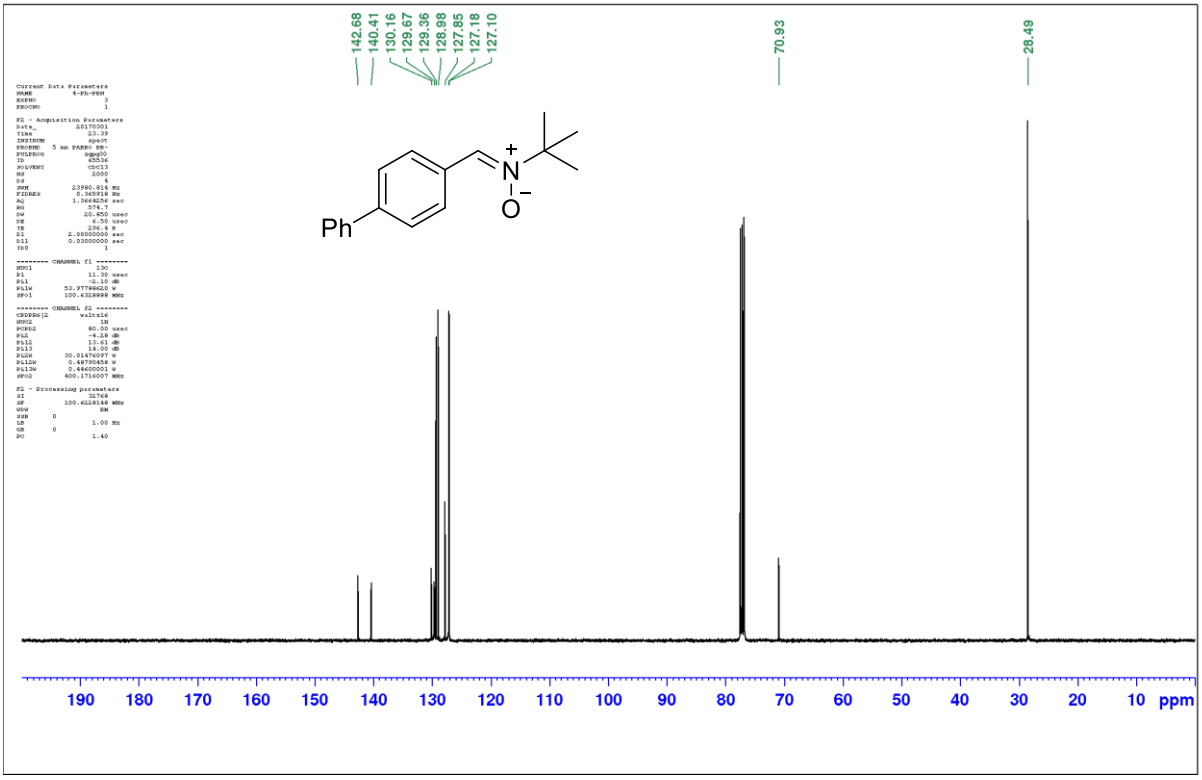

Figure S11. ^{13}C NMR spectrum of 4-Ph-PBN in $CDCl_3$.

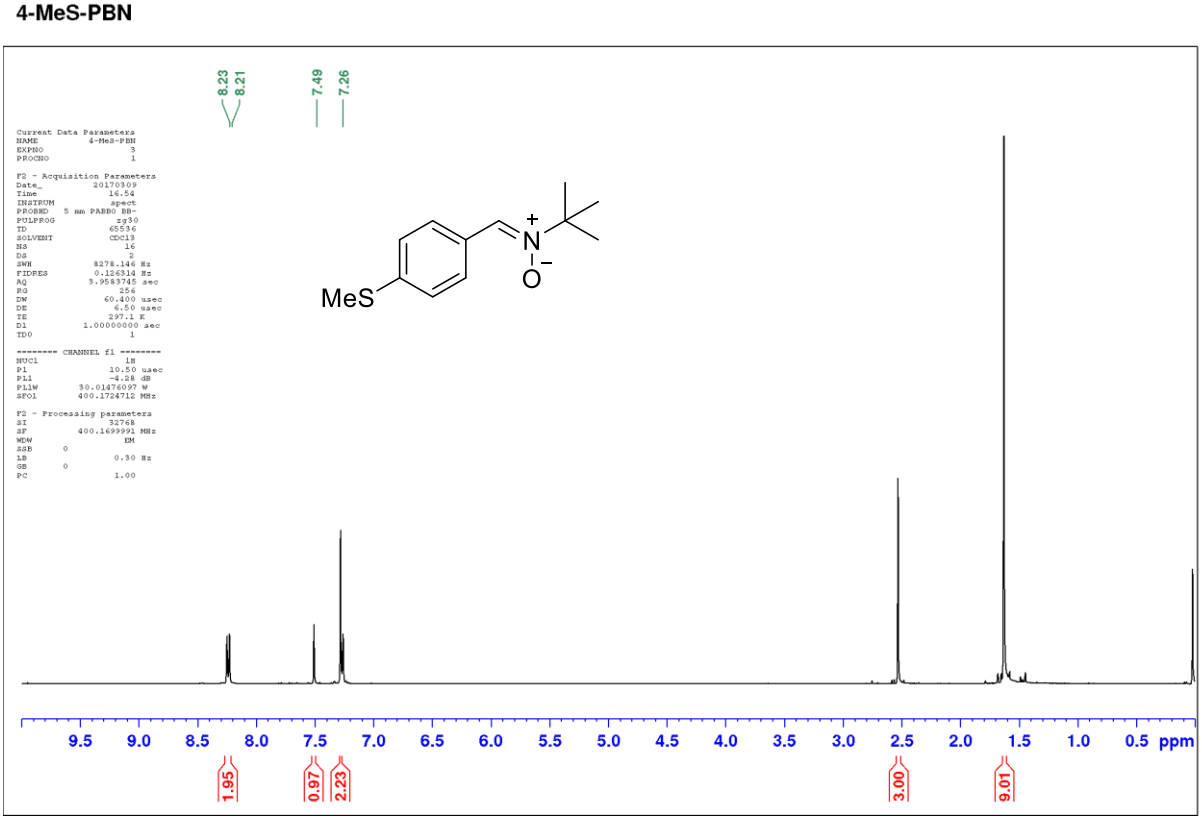

Figure S12. ^{1}H NMR spectrum of 4-MeS-PBN in $CDCl_3$.

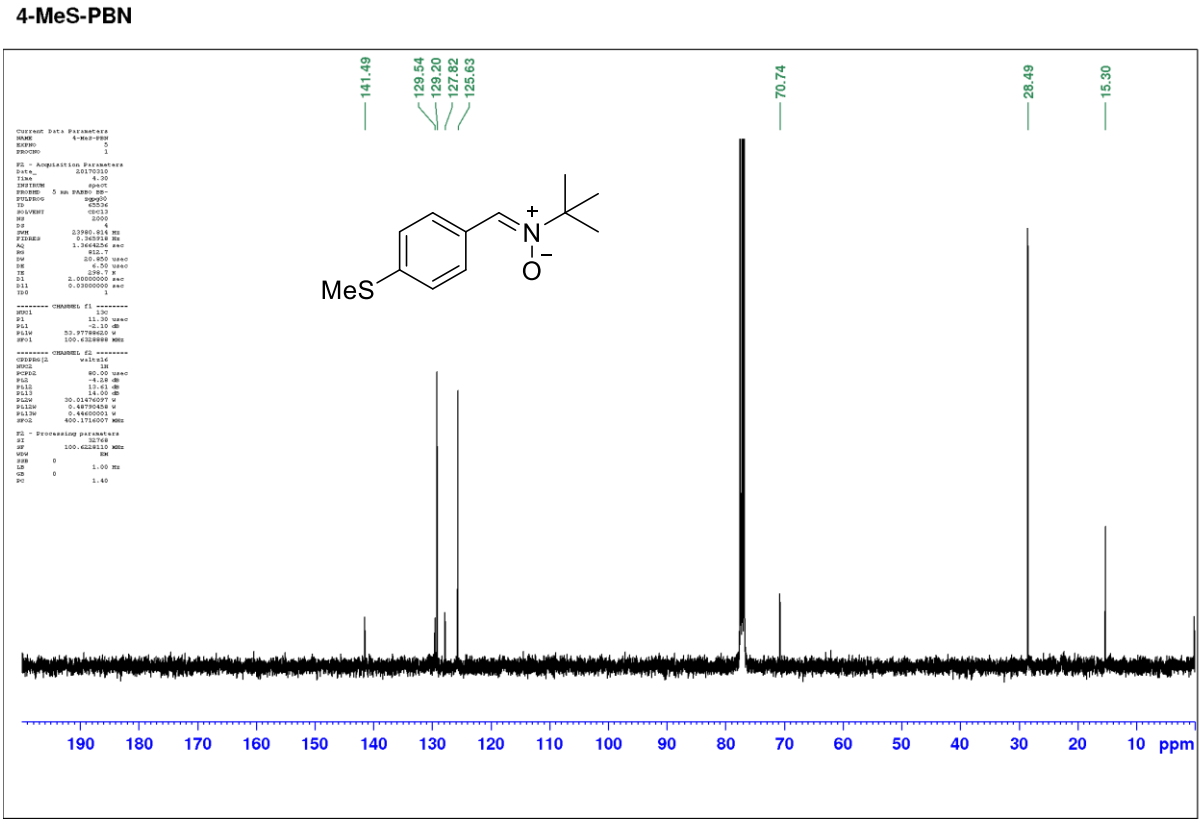

Figure S13. ^{13}C NMR spectrum of 4-MeS-PBN in $CDCl_3$.

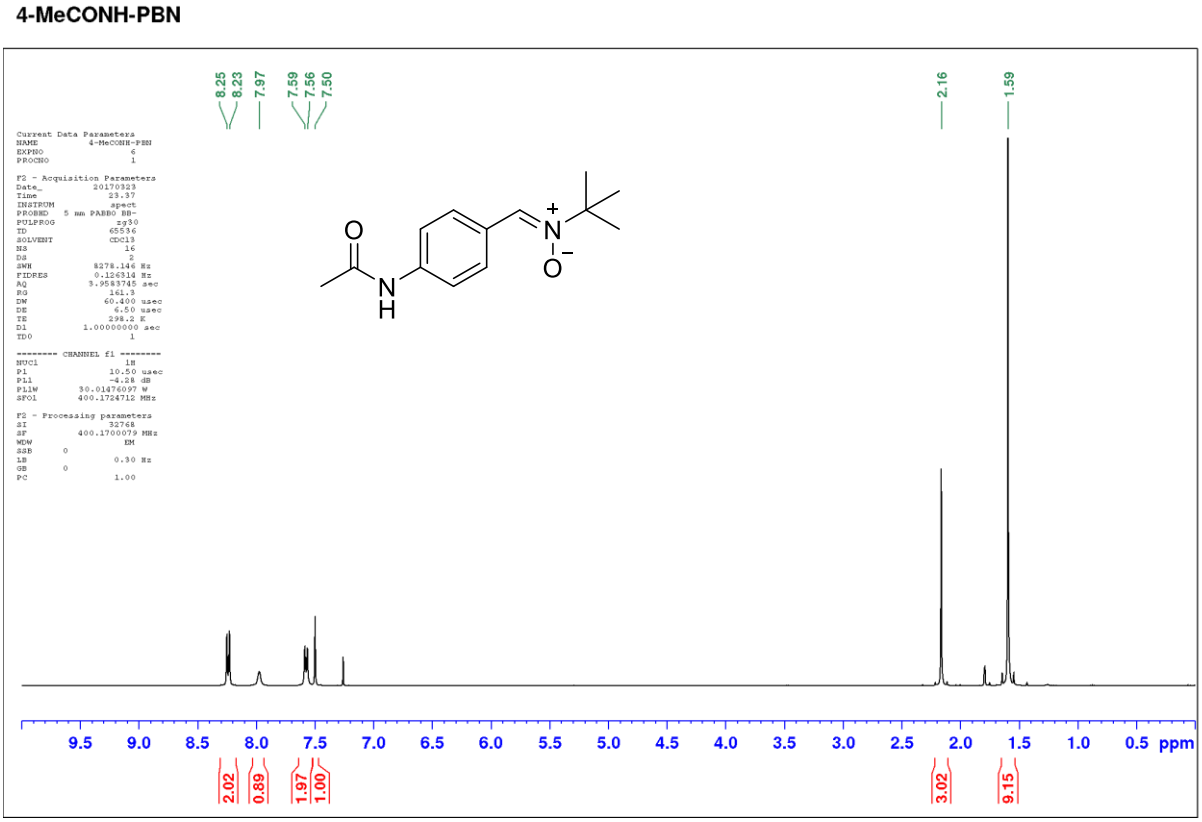

Figure S14. ^{1}H NMR spectrum of 4-MeCONH-PBN in $CDCl_3$.

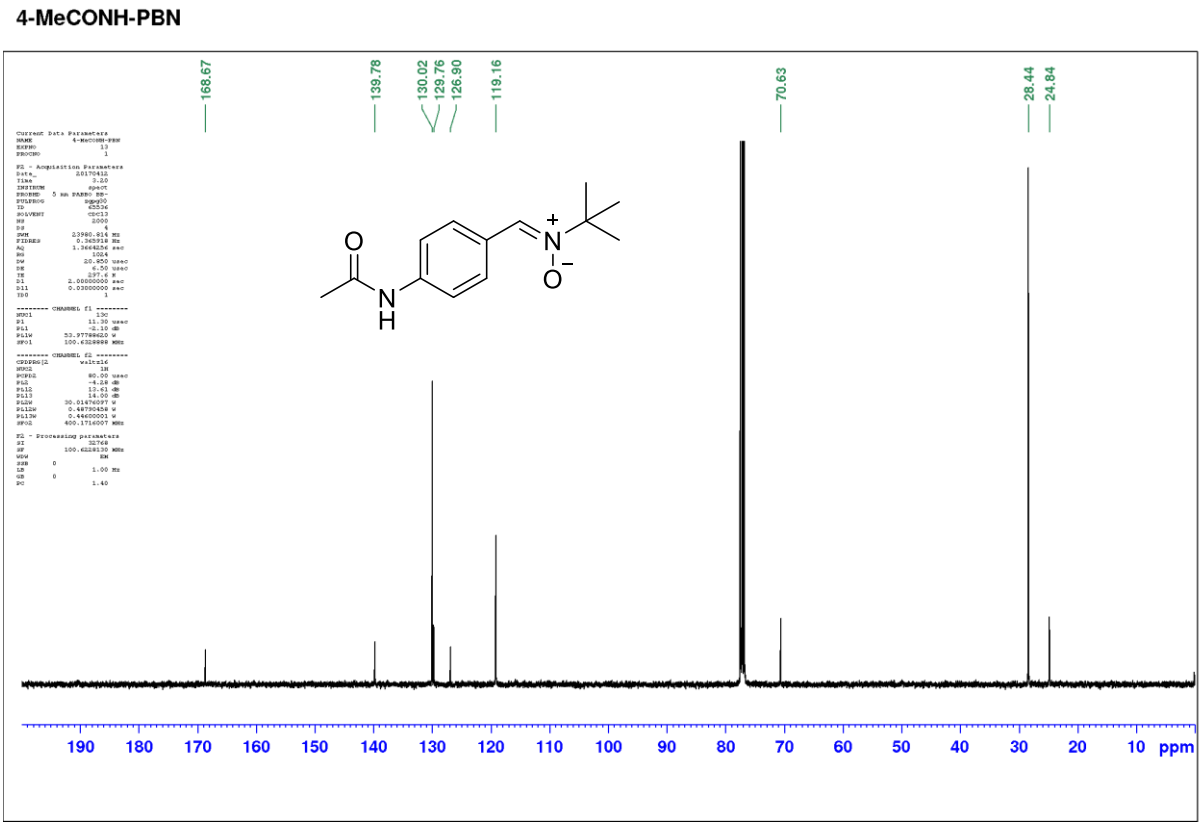

Figure S15. ^{13}C NMR spectrum of 4-MeCONH-PBN in $CDCl_3$.

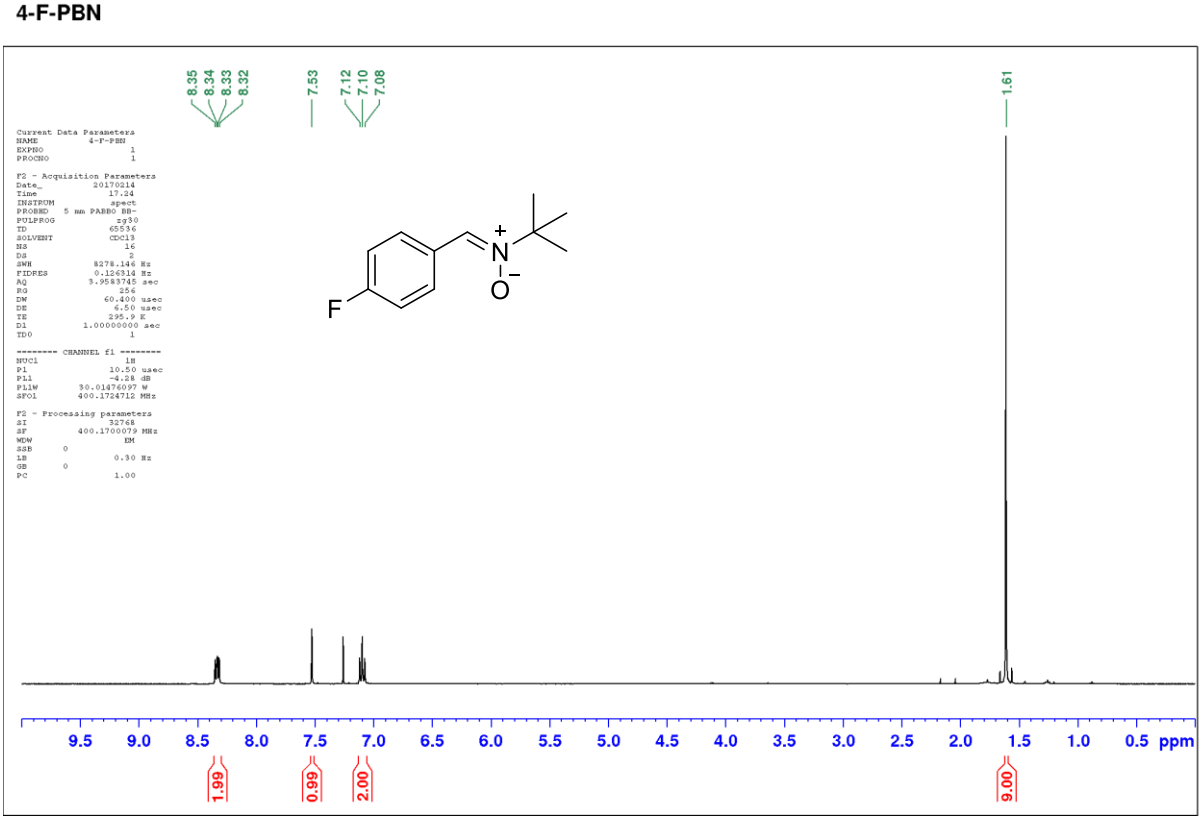

Figure S16. ^{1}H NMR spectrum of 4-F-PBN in $CDCl_3$.

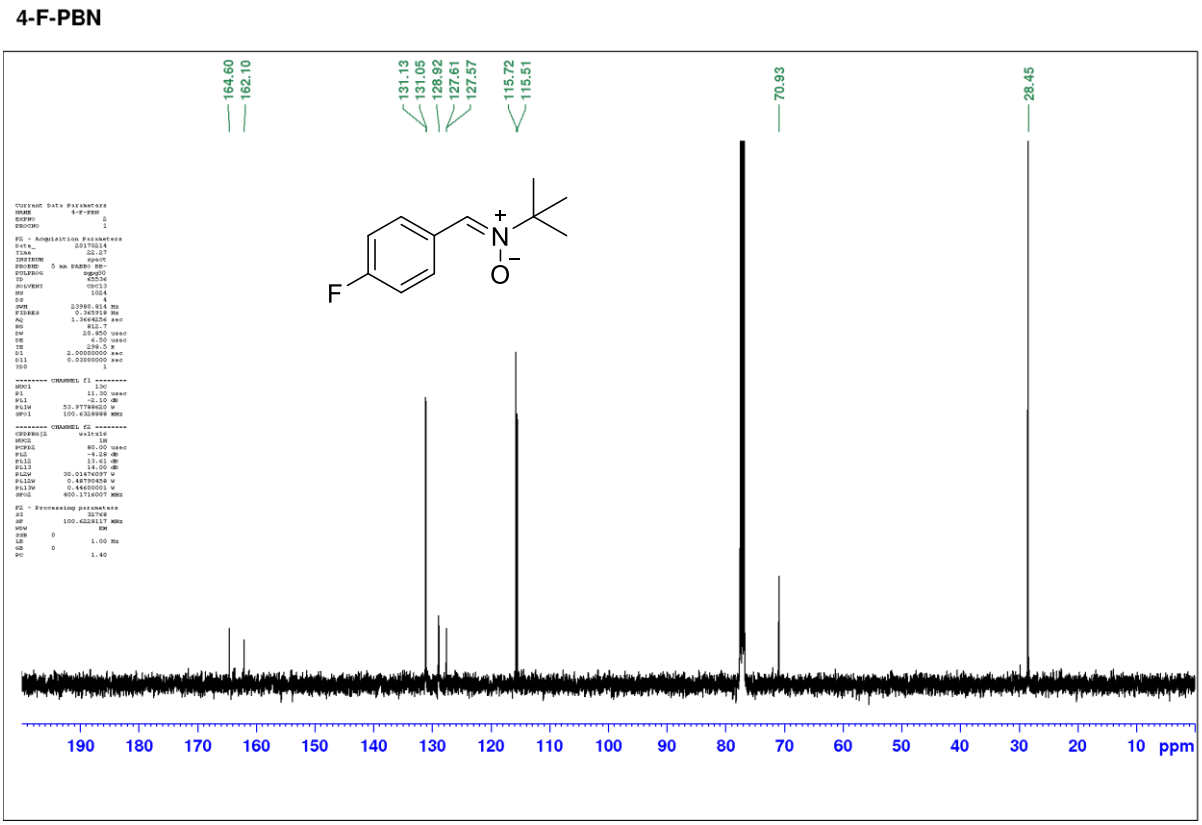

Figure S17. ^{13}C NMR spectrum of 4-F-PBN in $CDCl_3$.

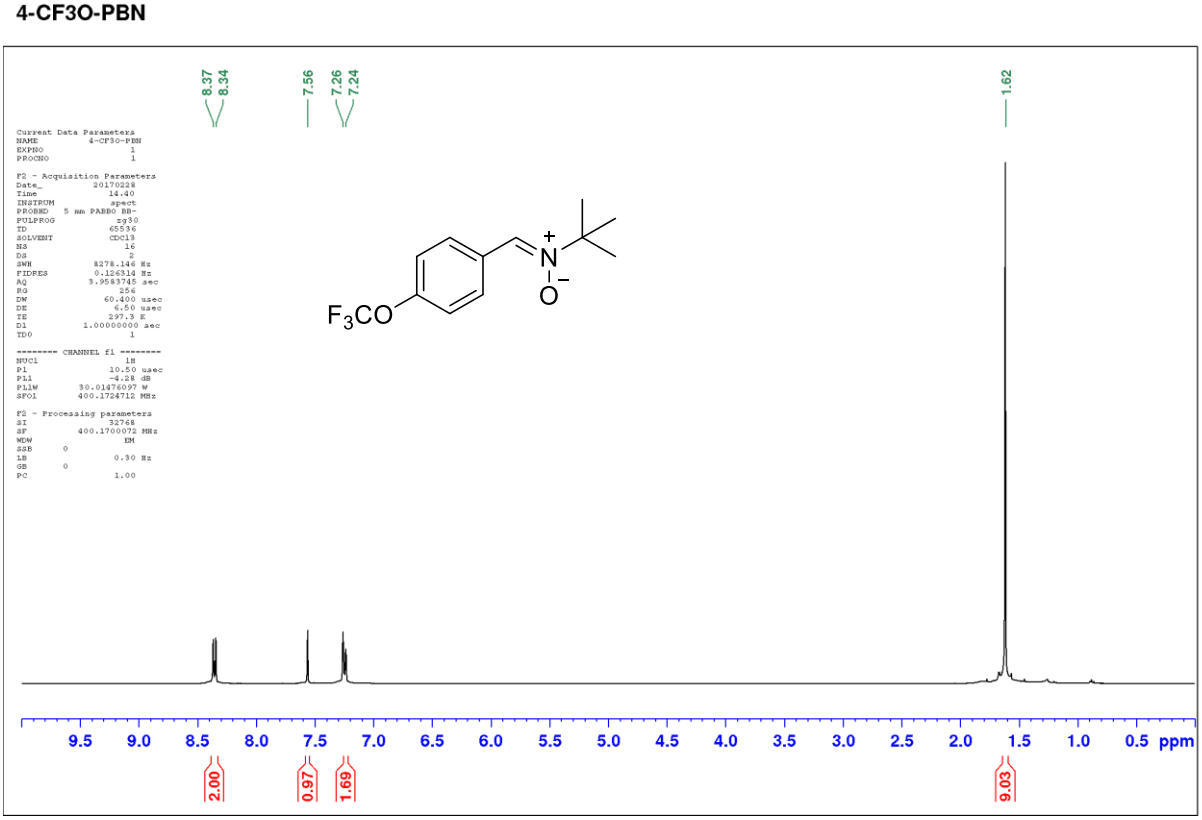

Figure S18. ^{1}H NMR spectrum of 4-CF_3O-PBN in $CDCl_3$.

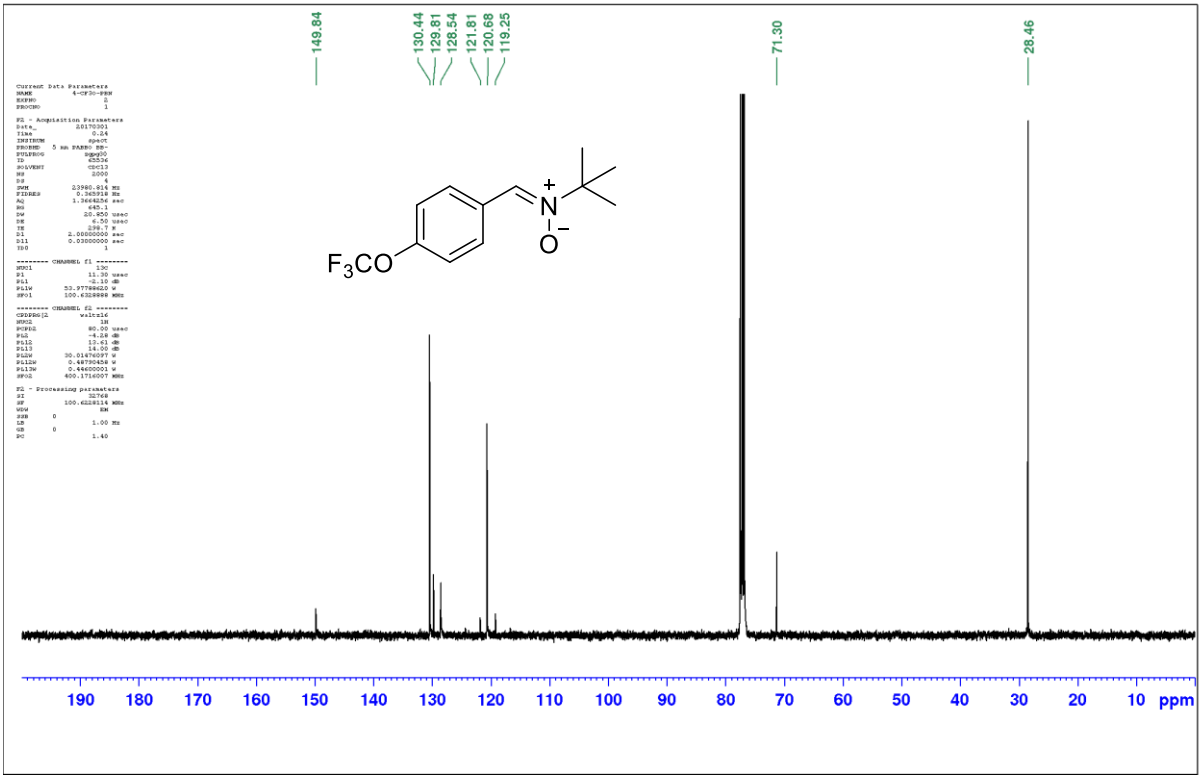

Figure S19. ^{13}C NMR spectrum of 4-CF_3O-PBN in $CDCl_3$.

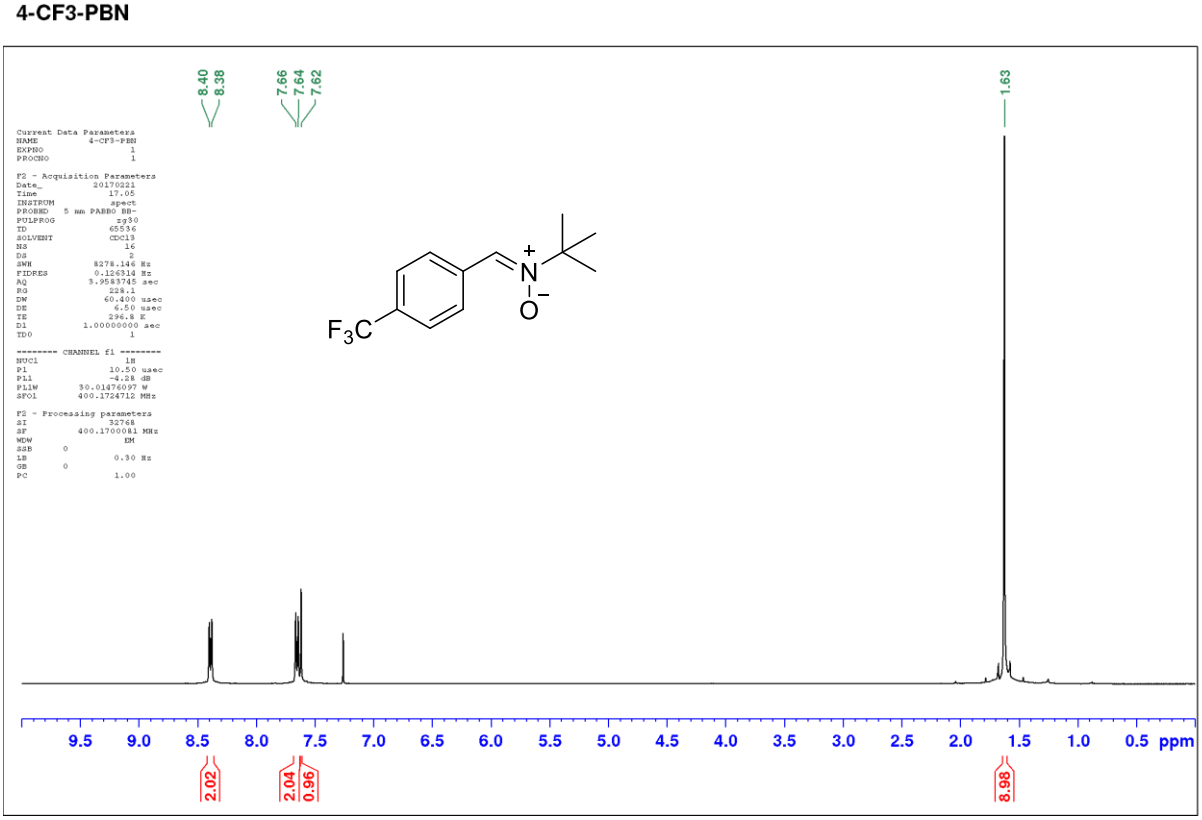

Figure S20. ^{1}H NMR spectrum of 4-CF_3-PBN in $CDCl_3$.

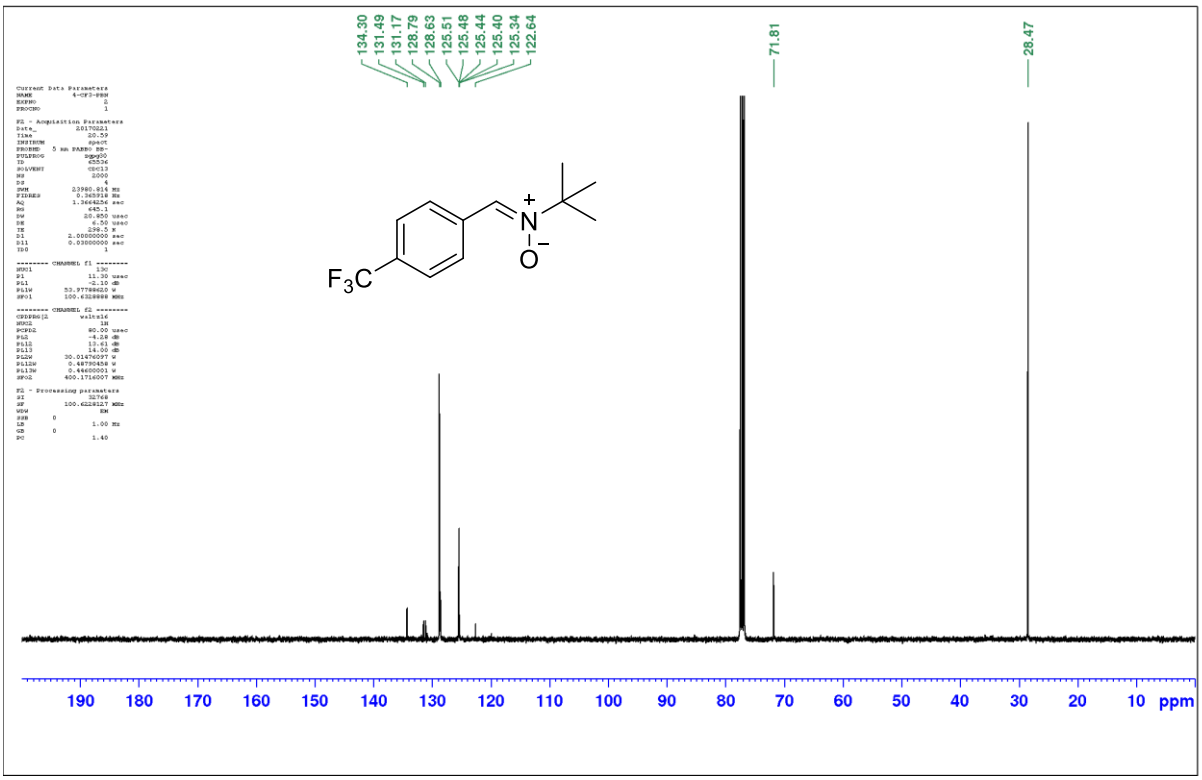

Figure S21. ^{13}C NMR spectrum of 4-CF_3-PBN in $CDCl_3$.

REFERENCES

1 C. Hansch, A. Leo and R. W. Taft, *Chem. Rev.*, 1991, **91**, 165–195.
2 X. Song, Y. Qian, R. Ben, X. Lu, H.-L. Zhu, H. Chao and J. Zhao, *J. Med. Chem.*, 2013, **56**, 6531–6535.
3 M. Kelly, J. Kincaid and S. Janagani, U.S. Patent, 0,182,060 A1, 2005.
4 K. Ikeda, T. Tatsumo, H. Ogo, S. Masumoto, T. Fujibayashi, R. Nagata, U.S. Patent, 6,194,461 B1, 2001.
5 R. D. Hinton and E. G. Janzen, *J. Org. Chem.*, 1992, **57**, 2646–2651.

Chapitre 4

Substituted α-Phenyl and α-Naphthlyl-*N*-*tert*-butyl Nitrones: Synthesis, Spin-Trapping and Neuroprotection Evaluation

Dans ce chapitre j'ai réalisé la synthèse des nitrones et leur caractérisation structurale ainsi que la détermination des coefficients de partition. J'ai réalisé les expériences de spin-trapping et l'analyse des données avec l'aide du Dr Kamal Zéamari en collaboration avec le Dr Béatrice Tuccio (ICR - UMR 7273, Marseille). J'ai également réalisé les expériences de voltampérométrie cyclique et l'analyse des données.

La détermination des effets neuroprotecteurs a été réalisé par l'équipe du Pr Michel Vignes (IBMM – UMR 5247, Montpellier) et par la société Neuro-Sys (Gardanne).

Actuellement, le Dr Frederick Villamena (Ohio State University) travaille sur la détermination des charges partielles des nitrones et de potentiel d'ionisation ainsi que sur la thermodynamique d'addition du radical hydroxymethyl.

J'ai réalisé la rédaction du chapitre avec l'aide de mon directeur de thèse le Dr Grégory Durand.

Ce chapitre sera soumis prochainement à Journal of Organic Chemistry

Chapitre 4 - Substituted α-Phenyl and α-Naphthlyl-*N*-*tert*-butyl Nitrones: Synthesis and Spin-Trapping and Neuroprotection Evaluation

Table of contents

ABSTRACT

In this work, a series of new functionalized derivatives of α-phenyl-*N*-*tert*-butyl nitrone (PBN) bearing a hydroxyl, an acetate or an acetamide substituent on the *N*-*tert*-butyl moiety and *para*-substituted phenyl or naphthlyl moieties were synthesized. Their ability to trap hydroxymethyl radical was evaluated by electron paramagnetic resonance spectroscopy using a kinetic competition method. The presence of two electron-withdrawing substituents on both sides of the nitronyl function improves the spin-trapping properties, with the derivatives 4-HOOC-PBN-CH_2OAc and 4-HOOC-PBN-CH_2NHAc being ~4x more reactive than PBN. The electrochemical properties of the derivatives were further investigated by cyclic voltammetry and showed that the redox potentials of the nitrones is largely influenced by the nature of the substituents both on the aromatic ring and on the *N*-*tert*-butyl function. The derivatives with an acetamide group on the *N*-*tert*-butyl function, PBN-CH_2NHAc, 4-AcNHCH$_2$-PBN-CH_2NHAc and 4-MeO-PBN-CH_2NHAc, were the easiest to oxidize. Finally, the neuroprotection of the derivatives was evaluated in *in vitro* models of oxidative stress and cellular injury on cortical neurons and glial cells, respectively. Out of the thirteen derivatives tested, eight showed good protective effects in at least one of the two models, with the derivatives PBN-CH_2NHAc and 4-HOOC-PBN being the most promising.

KEYWORDS

Nitrones, Oxidative Stress, Antioxidants, Spin-Trapping, Electrochemistry, Electron Paramagnetic Resonance (EPR) Spectroscopy, Neuroprotection.

1. INTRODUCTION

Oxidative stress is defined as an imbalance between the cellular production of reactive oxygen and nitrogen species (ROS/RNS) and their elimination by the antioxidant defences (*e.g.* superoxide dismutase, catalase, vitamins E and C, polyphenols, carotenoids). ROS include free radicals (*e.g.* superoxide ($O_2^{\bullet}$) or hydroxyl radicals ($HO^{\bullet}$)) and non-radical oxidants (*e.g.* hydrogen peroxide (H_2O_2) or peroxynitrite ($ONOO^-$)).[1,2] At low to moderate concentrations, these reactive species are important in maintaining normal physiological functions and are beneficial to the living organisms but in unregulated high concentrations could lead to oxidative stress and, ultimately, to cell death.[3] Oxidative stress is, therefore, involved in many human pathologies such as cardiovascular diseases, stroke, cancer, neurodegenerative diseases and aging.[1,4] In this context, the design and the synthesis of antioxidant molecules to regulate oxidative stress-related diseases has become an important area of research in the field of medicinal chemistry.

Among the synthetic antioxidants known, nitrone spin traps are of particular interest due to their ability to react with free radicals to form a persistent aminoxyl spin adduct, making them an efficient analytical tool for the detection and identification of short-lived radicals using electron paramagnetic resonance (EPR) spectroscopy.[5–7] This technique called spin-trapping has allowed the identification of several carbon-, oxygen- or sulfur-centered relevant free radicals and has been used to study the radical processes occurring in chemical or biochemical environments.[8] The linear *α*-phenyl-*N*-tert-butyl nitrone (PBN) and the cyclic 5,5-dimethyl-1-pyrroline *N*-oxide (DMPO) have been the most commonly used spin traps. DMPO and its derivatives have shown better spin-trapping properties than PBN-type nitrones due to longer half-lives and more distinctive EPR spectra of their radical adducts.[4] However, PBN and its derivatives exhibited a better distribution within tissues and cells and have therefore been widely used in *ex vivo* and *in vivo* studies of radical production in whole animals,[9–11] and as antioxidant agents in several biological models.[12,13] They have shown protective properties in animal models of neurodegenerative diseases,[14] stroke,[15] cardiovascular diseases[16] and cancer.[17] The PBN derivative called 2,4-disulfophenyl-*N*-*tert*-butyl nitrone (NXY-059) was the first neuroprotective agent to reach phase III clinical trials in the USA.[18,19] Linear nitrones synthesis is facile due to their final solid form at room temperature making their purification simple where they can be recrystallized to afford products free of paramagnetic impurities.

Moreover, linear nitrones could be easily functionalized both on the aromatic ring and on the *N*-tert-butyl group and, therefore, provides more versatility for derivatization.

Over the past years, several *para*-substituted nitrones have been studied by our group and others, showing that the reactivity of the nitronyl function depends on the nature of the substituents.[20–23] Among the *para*-substituted PBNs derivatives previously tested by our team, we identified 4-HOOC-PBN as a potent PBN analogue with good spin-trapping properties and a significant neuroprotective activity (Chapter 3).[22,23] Several *N-tert*-butyl substituted PBN-type nitrones have also been synthesized in order to improve the reactivity of the nitronyl function. One can cite the phosphorylated analogue *N*-benzylidene-1-diethoxyphosphoryl-1-methylethylamine *N*-oxide (PPN),[24–26] and the ester derivative *N*-benzylidene-1-ethoxycarbonyl-1-methylethylamine *N*-oxide (EPPN).[27,28] These derivatives, bearing an electron-withdrawing group in the α-position of the nitronyl function, have been shown to efficiently trap superoxide in aqueous environment and to significantly increase the stability of the superoxide adduct formed. The electronic effect of various substituents in the β-position of the nitronyl function on the reactivity of nitrones had also been studied, such as hydroxyl (PBN-CH_2OH), acetate (PBN-CH_2OAc), acetamide (PBN-CH_2NHAc) and carbamate (PBN-$CH_2OCONHMe$) groups.[29] Among the derivatives tested, PBN-CH_2NHAc gave the best results that are low oxidation potential, good trapping properties, and cytoprotective activity, making the amide bond an efficient linker for *N-tert*-butyl functionalization of PBN-type nitrones.

To optimize nitrone reactivity to radicals for improved radical detection and pharmacological property, several bi-functionalized nitrones with modifications on both the aromatic ring and the β-position from the nitronyl group were synthesized. We hypothesize that both inductive and resonance effects of substituents on the *tert*-butyl and phenyl groups, respectively, would have a synergistic property on nitrone reactivity. The first series of nitrones were synthesized having a carboxylic acid group in the *para*-position with a hydroxyl, an acetate or an acetamide substituent in the β-position of the nitronyl function (**5**-**7**), as shown in Figure 1. We also synthesized a series of β-acetamide derivatives (4-X-PBN-CH_2NHAc) bearing an electron-withdrawing (**7**), a neutral (**8**) or an electron-donating (**9**) substituent in the *para*-position of the phenyl ring. A series of naphthalene derivatives bearing various substituents in the β-position (H, OH, OAc, NHAc) were finally synthesized (**10**-**13**), as shown in Figure 1. Using EPR competition kinetic experiments, the relative rate constant of hydroxymethyl radical trapping was determined for each of the derivatives. The electrochemical properties of

the bi-functionalized nitrones were studied by cyclic voltammetry and compared to the mono-functionalized nitrones PBN-CH_2OH, PBN-CH_2OAc, PBN-CH_2NHAc and 4-HOOC-PBN previously synthesized by our team.[22,29] Finally, to test the relationship of nitrone redox properties with their antioxidant property, the *in vitro* neuroprotective activity of all the derivatives was investigated on two models of oxidative stress.

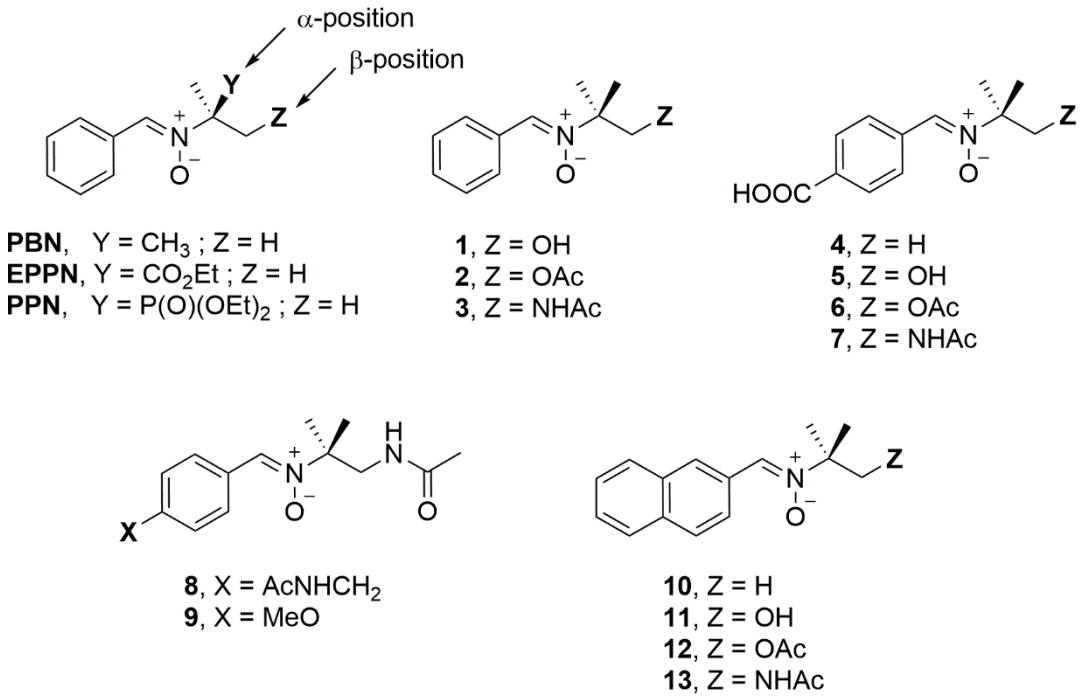

Figure 1. Chemical structure of PBN derivatives.

2. RESULTS AND DISCUSSION

2.1. Synthesis

General methods for the preparation of nitrones have been described elsewhere,[30] through condensation of *N*-substituted hydroxylamines with aromatic aldehydes or ketones[31] as the most common and direct approach to synthesize PBN-type nitrones. Although this method is widely used to synthesize PBN-type nitrones, it is limited by the poor commercial availability and stability of the hydroxylamines. This problem can be overcome by using the "one-pot" synthesis method developed by Huie *et al.*[32] This method involves generating the hydroxylamine *in situ* through reduction of the nitro precursor which is more available and therefore, is preferable in linear nitrone synthesis.

However, the synthesis of 4-HOOC-PBN-CH_2Y derivatives through one-pot reduction/condensation of nitro precursors failed probably due to the sensitivity of the carbonyl substituent under these conditions, as previously noticed.[30] These derivatives were, therefore, obtained by direct condensation of the appropriate hydroxylamine with commercially available 4-carboxybenzaldehyde, as shown in Scheme 1. First, the precursors hydroxylamines **14** and **18** were synthesized by reducing 2-methyl-2-nitropropanol and *N*-(2-methyl-2-nitropropyl)acetamide (**17**), respectively, with zinc powder in the presence of NH_4Cl. *N*-(2-methyl-2-nitropropyl)acetamide (**17**) was prepared in four steps from 2-methyl-2-nitropropanol, according to a previously published procedure.[29] After purification by flash chromatography, the hydroxylamines **14** and **18** were condensed with 4-carboxybenzaldehyde to give 4-HOOC-PBN-CH_2OH (**5**) and 4-HOOC-PBN-CH_2NHAc (**7**) in 67 and 58% yields. The failure to obtain 4-HOOC-PBN-CH_2OAc (**6**) by direct acetylation of 4-HOOC-PBN-CH_2OH with a 1:1 v/v mixture of pyridine and Ac_2O was probably due to the formation of a pyridinium benzoate salt by an acid-base reaction between the carboxylic acid group of 4-HOOC-PBN-CH_2OH and the pyridine thus preventing the acetylation of 4-HOOC-PBN-CH_2OH. Eventually, 4-HOOC-PBN-CH_2OAc was obtained through an alternative route, that is, the nitro acetyl compound **15** was first synthesized in 87% yield by acetylation of 2-methyl-2-nitropropanol. Reduction of **15** gave hydroxylamine **16** in only 12% yield. Hydroxylamine **16** was found to be volatile during the evaporation of the solvents under vacuum. In addition, it is unstable at room temperature as evidenced by the formation of several side-products as observed through ^1H NMR and TLC. Nevertheless, 4-HOOC-PBN-CH_2OAc was obtained in 49% yield by direct condensation of hydroxylamine **16** with 4-carboxybenzaldehyde in dry EtOH.

Following the same synthetic procedure, 4-$AcNHCH_2$-PBN-CH_2NHAc (**9**) was synthesized in 37% yield by direct condensation of hydroxylamine **18** and *N*-(4-formylbenzyl)acetamide, as prepared following our previously reported procedure.[22] 4-MeO-PBN-CH_2NHAc (**8**) was obtained through one pot reduction/condensation of *N*-(2-methyl-2-nitropropyl)acetamide[29] (**17**) with *p*-anisaldehyde in 66% yield.

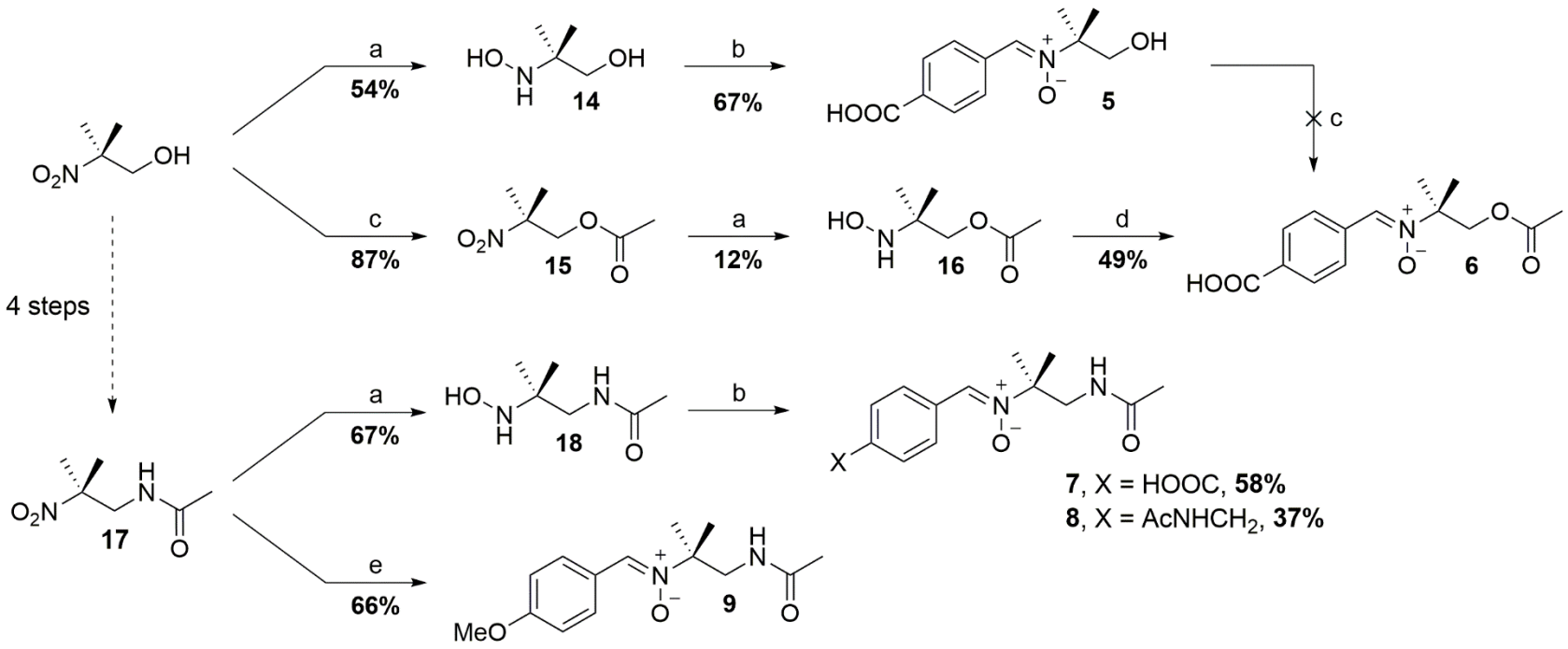

Scheme 1. Synthesis of 4-HOOC-PBN-CH_2Y and 4-X-PBN-CH_2NHAc derivatives.[a]

[a]*Reagents and conditions:* (a) NH_4Cl, zinc powder, THF/H_2O (3:1 v/v), rt or 50 °C for compound **14**; (b) 4-carboxybenzaldehyde for compounds **5** and **7** or *N*-(4-formylbenzyl)acetamide[22] for compound **8**, THF/AcOH (3:2 v/v), 60 °C, 4Å molecular sieves; (c) Pyridine/Ac_2O (1:1 v/v), rt; (d) 4-carboxybenzaldehyde, dry EtOH, 60 °C; (e) *p*-anisaldehyde, zinc powder, AcOH, dry EtOH, 60 °C, 4Å molecular sieves.

NBN (**10**), NBN-CH_2OH (**11**) and NBN-CH_2NHAc (**13**) were also successfully synthesized *via* one-pot reduction/condensation of nitro precursors from commercially available 2-naphthaldehyde in the presence of zinc powder and AcOH in dry EtOH, as shown in Scheme 2. The reactions were carried out overnight under argon and in the absence of light to avoid possible degradation of the hydroxylamine. Molecular sieves were added to the mixture in order to increase reaction efficiency. NBN[33] and NBN-CH_2OH were synthesized in 39% and 70% yields from commercially available 2-methyl-2-nitropropane and 2-methyl-2-nitropropanol, respectively. NBN-CH_2NHAc was synthesized in 66% yield from *N*-(2-methyl-2-nitropropyl)acetamide (**17**).[29] The acetylation of NBN-CH_2OH by a 1:1 v/v mixture of pyridine and Ac_2O gave NBN-CH_2OAc (**12**) in 57% yield. All the final nitrone products were purified by flash chromatography along with two successive crystallizations to ensure high purity.

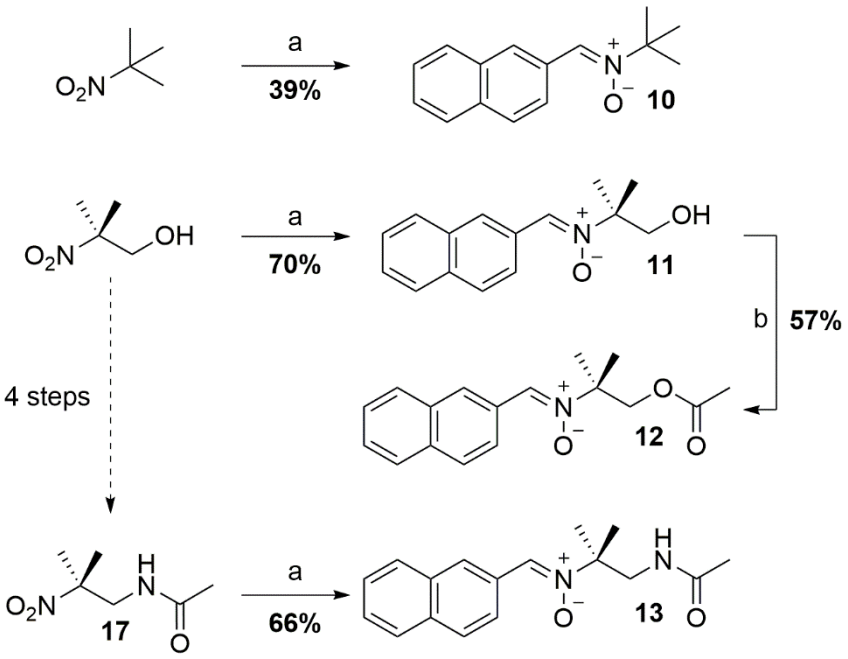

Scheme 2. Synthesis of NBN-CH_2Y derivatives.[a]

[a]*Reagents and conditions*: (a) 2-naphthaldehyde, zinc powder, AcOH, dry EtOH, 60 °C, 4Å molecular sieves; (b) Pyridine/Ac_2O (1:1 v/v), rt.

The calculated octanol/water partition coefficient (*c* log *P*) of the nitrones was determined using ALOGPS 2.1 software and the values are reported in Table 1. The results show that the lipophilicity of the nitrones can be modulated by introducing substituents of different polarity in the *para*-position of the phenyl ring and/or in the β-position of the nitronyl function. The introduction of a polar hydroxyl or acetamide group in the β-position of the nitronyl function

(PBN-CH_2OH, PBN-CH_2NHAc) decreases the lipophilicity of the nitrones compared to PBN. The presence of an acetate group (PBN-CH_2OAc) also decreases the *c* log *P* but to a lesser extent. The lipophilicity is even lower when the polar carboxylic acid function is present in the *para*-position of the phenyl ring, with the derivatives 4-HOOC-PBN-CH_2OH, 4-HOOC-PBN-CH_2OAc and 4-HOOC-PBN-CH_2NHAc having lower *c* log *P* than PBN-CH_2OH, PBN-CH_2OAc and PBN-CH_2NHAc, respectively. On the contrary, the introduction of a polycyclic naphthalene group increases the lipophilicity of the nitrones compared to PBN; NBN being the most lipophilic derivative of the series.

2.2. EPR study of hydroxymethyl radical trapping

Nitrones are widely used as probes for the indirect detection and characterization of short-lived free radical species by electron paramagnetic resonance (EPR) spectroscopy. An ideal spin trap is characterized by its high rate of free radical trapping as well as a high stability of the corresponding aminoxyl spin adduct formed for efficient free radical detection. To evaluate the spin-trapping ability of the PBN derivatives, we chose to study the trapping of hydroxymethyl radical ($^{\bullet}CH_2OH$), an alcohol-derived radicals formed during oxidative stress.[10,11] During oxidative stress, the reactive oxygen species ($O_2^{\bullet-}$, H_2O_2, $HO^{\bullet}$) produced react with lipids, proteins, sugars and DNA yielding carbon-centered radicals such as hydroxyalkyl and methyl radicals.[34] The $^{\bullet}CH_2OH$ radical was generated *in situ* by a Fenton reaction in the presence of methanol. All the nitrones tested gave rise to a standard six-line EPR spectrum, *i.e.*, a triplet of doublets with nitrogen (a_N) and β-hydrogen (a_H) couplings, characteristic of nitroxide adducts. The EPR hyperfine splitting constants (hfsc's) a_N and a_H of the simulated $^{\bullet}CH_2OH$ adducts are reported in Table 1 and are consistent with PBN-type spin adducts.[35]

Table 1. Octanol-water partition coefficients (*c*log*P*) and spin-trapping properties of PBN derivatives.

	Lipophilicity	EPR spin-trapping ($^{\bullet}CH_2OH$)		
Compounds	*c*log*P*[a]	a_N (G)	a_H (G)	k_N/k_{PBN}[b] (± 0.05)
PBN	2.67	14.3	2.7	1.00
PBN-CH_2OH (1)	1.72	14.3	3.3	2.38
PBN-CH_2OAc (2)	2.20	13.9	2.7	1.46
PBN-CH_2NHAc (3)	1.74	14.1	3.1	3.15
4-HOOC-PBN (4)	2.19	14.3	2.7	1.44[c]
4-HOOC-PBN-CH_2OH (5)	1.24	14.0	2.5	1.48
4-HOOC-PBN-CH_2OAc (6)	1.73	14.1	2.8	3.55
4-HOOC-PBN-CH_2NHAc (7)	1.26	14.3	3.0	3.75
4-$AcNHCH_2$-PBN-CH_2NHAc (8)	1.13	14.1	2.8	1.28
4-MeO-PBN-CH_2NHAc (9)	1.63	14.0	2.8	0.62
NBN (10)	3.85	14.4	3.1	0.59
NBN-CH_2OH (11)	2.90	14.2	3.0	1.32
NBN-CH_2OAc (12)	3.39	14.0	2.8	1.31
NBN-CH_2NHAc (13)	3.05	14.1	3.0	1.36

[a]Calculated octanol/water partition coefficient values obtained using ALOGPS 2.1 software (http://www.vcclab.org/lab/alogps/).
[b] Ratio of the second-order rate constants for the hydroxymethyl radical trapping by various nitrones (k_N) and by PBN (k_{PBN}) in methanol.
[c] Data from Rosselin *et al.*[23]

In order to determine the rate constant of $^{\bullet}CH_2OH$ trapping by each PBN derivative, a kinetic method based on the competition between the studied nitrone noted **N** and the 1,3,5-tri[(*N*-(1-diethylphosphono)-1-methylethyl) *N*-oxy-aldimine] scavenger noted **TN** was used by generating the $^{\bullet}CH_2OH$ radical in the presence of **N** and **TN**. The $^{\bullet}CH_2OH$ spin-trapping rate was determined by measuring the intensity (as the signal area) of the corresponding adducts at different [**N**]/[**TN**] ratio (Figure 2). For each nitrone, plotting the *R/r* ratio *vs* [**N**]/[**TN**] (where *R* and *r* represent the trapping rate constant by both **TN** and **N**, and by **TN** only, respectively) gave a straight-line which slope value was equal to the ratio k_N/k_{TN} (Figure 2C). To compare the spin-trapping of the derivatives with PBN, the k_{PBN}/k_{TN} ratio was calculated using commercially available PBN instead of **N**. From these results, the k_N/k_{PBN} ratio was determined for the derivatives with values ranging from 0.59 to 3.75 (Table 1).

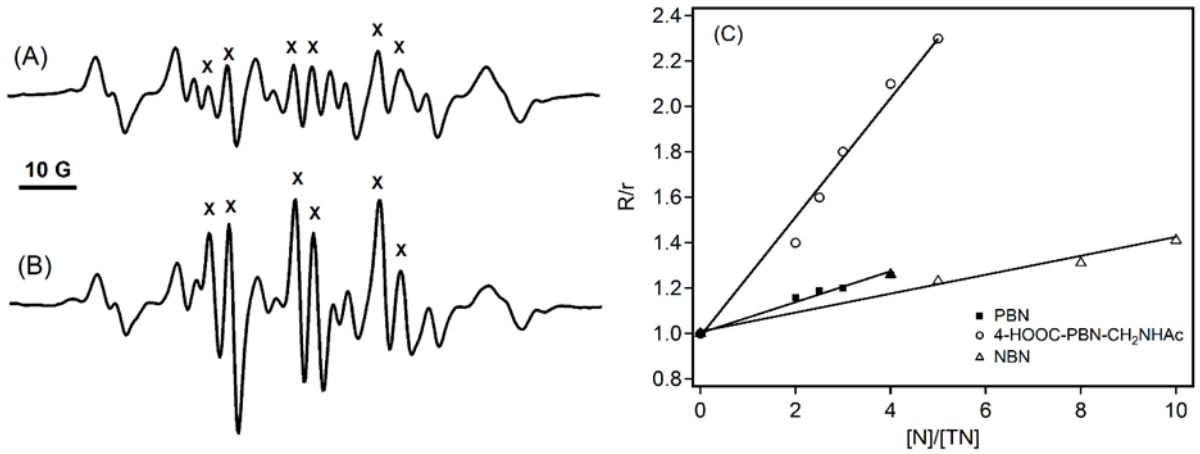

Figure 2. (A)-(B) EPR signals of **TN** and 4-HOOC-PBN-CH_2NHAc hydroxymethyl radical adducts. Hydroxymethyl radical was generated by a Fenton system and the ratio [**N**]/[**TN**] was: (A) [**N**]/[**TN**] = 2; (B) [**N**]/[**TN**] = 5. The peaks topped by a cross (×) correspond to the hydroxymethyl radical adduct of 4-HOOC-PBN-CH_2NHAc. (C) Determination of the relative rate constant k_N/k_{TN} of $^{\bullet}CH_2OH$ trapping by PBN, 4-HOOC-PBN-CH_2NHAc and NBN.

Only NBN and 4-MeO-PBN-CH_2NHAc exhibited trapping rates slower than that of PBN. Regarding the polar effect of the *N-tert*-butyl substituents (compounds **1**-**3**) on the reactivity of the nitronyl function, the following order of increasing spin-trapping activity was observed: PBN < PBN-CH_2OAc < PBN-CH_2OH < PBN-CH_2NHAc, showing that the introduction of an electron-withdrawing group in the β-position of the nitronyl function improves the reactivity of the nitrone towards $^{\bullet}CH_2OH$ radical.

With regards to the 4-HOOC-PBN-CH_2Y series (compounds **4**-**7**), the most efficient spin traps were 4-HOOC-PBN-CH_2NHAc and 4-HOOC-PBN-CH_2OAc being 3.8 and 3.6 times more reactive than PBN, respectively. This shows that the combination of electron-withdrawing groups both in the *para*-position of the phenyl ring and in the β-position of the nitronyl function increases the spin-trapping properties of PBN-type nitrones. Their trapping rates are lower than that of the very efficient PBN-type nitrone PPN, bearing a diethoxyphosphoryl group in the α-position of the nitronyl function[36] but their synthesis and purification are much simpler.

For the derivative 4-HOOC-PBN-CH_2OH, the presence in small quantities of an oxazolidine-*N*-oxyl compound was observed by EPR. This compound very likely originates from intramolecular nucleophilic addition of the hydroxyl group onto the nitronyl-carbon followed by fast autoxidation of the hydroxylamine (Forrester-Hepburn mechanism), as already observed for trihydroxylated nitrones.[37] The formation of this cyclic nitroxide could explain

why 4-HOOC-PBN-CH_2OH has similar reactivity towards $^{\bullet}CH_2OH$ radical than 4-HOOC-PBN, despite the presence of an electron-withdrawing group in the β-position of the nitronyl function.

PBN-CH_2NHAc also showed improved spin-trapping properties with a k_N/k_{PBN} value of 3.15 but when an electron-donating substituent was introduced in the *para*-position of the phenyl ring (4-MeO-PBN-CH_2NHAc), the rate constant of $^{\bullet}CH_2OH$ trapping significantly decreased (k_N/k_{PBN} = 0.62). This confirms our previous results obtained on MeO-substituted PBN-type nitrones.[36] The rate constant of $^{\bullet}CH_2OH$ trapping also decreased with the derivative 4-$AcNHCH_2$-PBN-CH_2NHAc bearing two acetamide groups on both sides of the nitronyl function. On the contrary, the presence of an electron-withdrawing group in the *para*-position of the phenyl ring (4-HOOC-PBN-CH_2NHAc) slightly increased the spin-trapping reactivity of the nitronyl function, as already reported in the literature for *para*-substituted PBN derivatives towards nucleophilic radicals such as $^{\bullet}CH_2OH$.[20–23,38]

Regarding the NBN-CH_2Y series, the presence of a polycyclic aromatic naphthalene group (nitrones **10**-**13**) decreased the rate constant of $^{\bullet}CH_2OH$ trapping compared to the respective PBN-CH_2Y derivatives. This could be explained by the ability of naphthalene to react with $^{\bullet}OH$, as reported in the literature.[39] The $^{\bullet}OH$ radicals produced by the Fenton reaction could react with the naphthalene group of the derivatives causing the formation of naphthol and preventing the trapping of $^{\bullet}CH_2OH$ radicals. However, the presence of an electron-withdrawing substituent in the β-position increased the reactivity of the nitronyl function but no difference was noted among the substituent ($k_N/k_{PBN} \approx 1.3$).

2.3. Cyclic Voltammetry

The electrochemical behavior of the bi-functionalized PBN derivatives was investigated using cyclic voltammetry and the redox potentials are reported in Table 2. The experiments were performed in acetonitrile containing *tetra*-butylammonium perchlorate (TBAP) as electrolyte. All the derivatives exhibited two reduction potentials, as shown in Figure 3 and Figures S1-S2, and as already observed in the literature for β-substituted nitrones.[29,40] The first peak corresponds to the reduction of the nitronyl function with values ranging from -2.35 V to -1.87, except for 4-HOOC-PBN-CH_2OH and 4-HOOC-PBN-CH_2OAc where a slight peak was observed. Only for the derivatives NBN-CH_2OAc, 4-HOOC-PBN-CH_2OH, 4-HOOC-PBN-CH_2OAc and 4-HOOC-PBN-CH_2NHAc, the reduction of the nitronyl function

appeared reversible as associated backward peaks were observed. This reflects a greater stability of the radical nitroxide anion formed. Regarding the series of 4-HOOC-PBN-CH_2Y derivatives, when comparing to 4-HOOC-PBN, the reduction of the nitronyl group was more difficult in the presence of an acetamide substituent whereas it was slightly easier in the presence of a hydroxyl group and with no effect of the acetate group. With regards to the 4-X-PBN-CH_2NHAc series, the reduction of the nitronyl function became slightly easier with the presence of an electron-withdrawing group in the *para*-position whereas it became much harder with an electron-donating substituent, as already observed.[23,41,42] The presence of a polycyclic naphthalene group (NBN) slightly decreased the reduction potential compared to PBN. For this series of derivatives, the highest reduction potential observed was also that of the acetamide derivative NBN-CH_2NHAc followed by the acetate derivative NBN-CH_2OAc and NBN, which has no substituent in the β-position. The derivative NBN-CH_2OH, bearing a hydroxyl function, had the lowest reduction potential of the series.

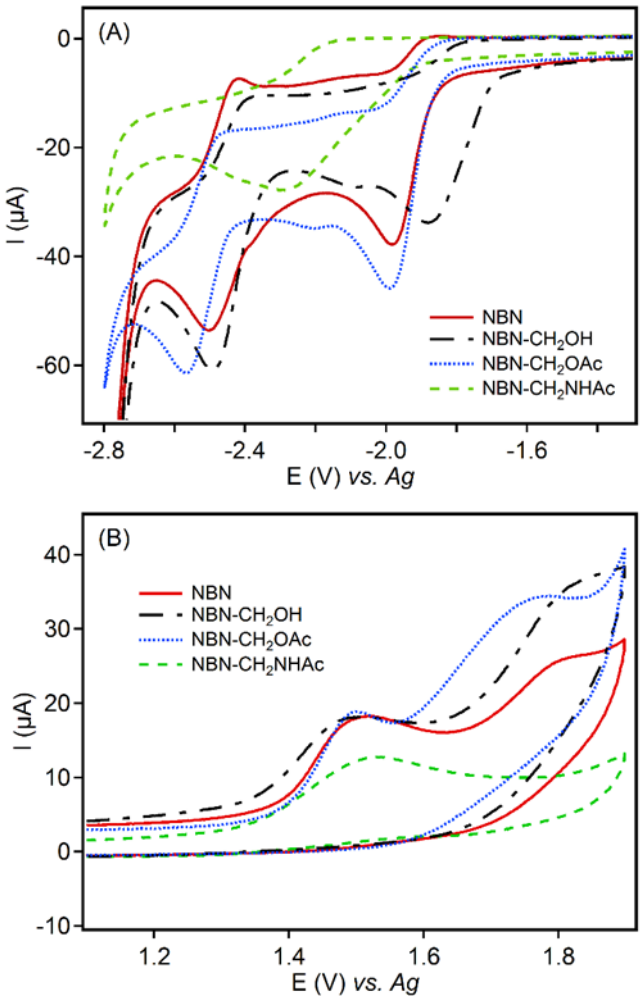

Figure 3. Cyclic voltammograms of NBN-CH_2Y derivatives in acetonitrile containing 0.1 M of TBAP at a GC electrode, potential scan rate υ = 0.1 V/s: (A) reduction and (B) oxidation.

Considering the anodic behavior, PBN, mono β-substituted derivatives, NBN-CH_2NHAc, 4-HOOC-PBN-CH_2OH, 4-HOOC-PBN-CH_2NHAc and 4-$AcNHCH_2$-PBN-CH_2NHAc were oxidized through an irreversible one-electron transfer whereas NBN, NBN-CH_2OH, NBN-CH_2OAc, 4-HOOC-PBN, 4-HOOC-PBN-CH_2OAc and 4-MeO-PBN-CH_2NHAc possess two oxidation peaks, as shown in Figure 3 and Figures S1-S2. The first peak corresponds to the oxidation of the nitronyl function with values ranging from 1.40 to 1.78 V. Regarding the 4-HOOC-PBN-CH_2Y series, 4-HOOC-PBN-CH_2OH presented similar oxidation potential than 4-HOOC-PBN, showing that the presence of a hydroxyl group in the β-position has no influence on the oxidation of the nitronyl function. In contrast, the presence of the acetate group tends to increase the oxidation potential whereas the acetamide group tends to decrease it. The same observation was made for the mono-substituted derivatives. With regards to the 4-X-PBN-CH_2NHAc series, 4-HOOC-PBN-CH_2NHAc, bearing an electron-withdrawing group in the *para*-position, exhibited a lower oxidation potential than that of PBN-CH_2NHAc while 4-HOOC-PBN-CH_2NHAc and 4-$AcNHCH_2$-PBN-CH_2NHAc had similar oxidation potentials than PBN-CH_2NHAc. The presence of a polycyclic naphthalene group (NBN) slightly decreased the oxidation potential compared to PBN and all the NBN-CH_2Y derivatives exhibited similar oxidation potentials (~ 1.51 V).

To assess spin trap stability for biological spin-trapping applications, the stability domain of the derivatives was calculated and is reported in Table 2. It represents the potential window over which spin-trapping technique can be safely applied without the risk of inverted spin-trapping process.[43,44] All the nitrones studied have stability domain of 3 V or more, and would be therefore suitable for electrochemical spin-trapping experiments.[42,45] For PBN, the stability domain value was 3.72 V, as previously reported[23] and for all the functionalized nitrones the stability domain ranges from 2.97 V for 4-HOOC-PBN-CH_2OH to 3.82 V for NBN-CH_2NHAc.

Table 2. Electrochemical[a] properties of PBN derivatives.

	in CH_3CN[b], compound (1 mM)				
	E_p(c) (V)		E_p(a) (V)		Stability domain[f](V)
Compounds	1st peak	2nd peak	1st peak	2nd peak	
PBN	-2.12	-2.27	1.60		3.72
PBN-CH_2OH (1)	-1.92[c]	-2.12[c]	1.57[c]		3.49
PBN-CH_2OAc (2)	-2.03[c]	-2.40[c]	1.67[c]		3.70
PBN-CH_2NHAc (3)	-1.99 (-1.97)[c]	-2.10 (-2.15)[c]	1.41 (1.44)[c]		3.40
4-HOOC-PBN (4)	-2.08[d]	-2.21[d]	1.62[d]	1.91[d]	3.70
4-HOOC-PBN-CH_2OH (5)	-1.37[e]	-2.00 (r)	1.60		2.97
4-HOOC-PBN-CH_2OAc (6)	-1.55[e]	-2.08 (r)	1.78	1.93	3.33
4-HOOC-PBN-CH_2NHAc (7)	-1.94 (r)	-2.25	1.54		3.48
4-AcNHCH$_2$-PBN-CH_2NHAc (8)	-2.03	-2.17	1.40		3.43
4-MeO-PBN-CH_2NHAc (9)	-2.35	-2.59	1.42	2.01	3.77
NBN (10)	-1.98	-2.50 (r)	1.51	1.80	3.49
NBN-CH_2OH (11)	-1.87	-2.49 (r)	1.48	1.82	3.35
NBN-CH_2OAc (12)	-1.99 (r)	-2.56 (r)	1.50	1.77	3.49
NBN-CH_2NHAc (13)	-2.29	-2.89 (r)	1.53		3.82

[a] The peak potentials are given versus a silver wire electrode for a potential scan rate 0.1 V/s; in general, the electron transfers appeared irreversible (no backward peak observed) except for a few reversible couples noted (r).

[b] Containing 0.1 M of TBAP with reduction E_p(c) and oxidation E_p(a) at glassy carbon (GC) electrode.

[c] Data from Rosselin *et al.*[29]

[d] Data from Rosselin *et al.*[23]

[e] A slight peak was observed.

[f] The stability domain is given as: E_p(a) - E_p(c)

2.4. Cell culture and viability studies

Excitotoxicity and oxidative stress are well known to play a significant role in the pathogenesis of neurodegeneratives diseases. While they refer to different mechanisms, excitotoxicity and oxidative stress may cooperate in inducing neuron cell death.[46,47] The cytoprotective properties of the nitrones were evaluated *in vitro* using two different models. In the first assay, the nitrones at 10 µM were pre-incubated with glial cells for 24 h and were challenged for 24 h with tBuOOH (300 µM). Degree of cytoprotection was measured using [3-(4,5-dimethylthiazol-2-yl)-2-5diphenyltetrazolium-bromide] (MTT) assay and the results are presented in Figure 4. Neither PBN nor any β-substituted PBN derivatives showed cytoprotective effect with PBN-CH_2OAc and PBN-CH_2NHAc being even slightly toxic. For the NBN-CH_2Y series, no significant protection was observed. On the contrary, 4-HOOC-PBN exhibited more pronounced cytoprotection and the addition of a hydroxyl or an acetamide substituent in the β-position of the nitronyl function (4-HOOC-PBN-CH_2OH and 4-HOOC-PBN-CH_2NHAc) improved this protection, with these two derivatives being the most protective agents overall.

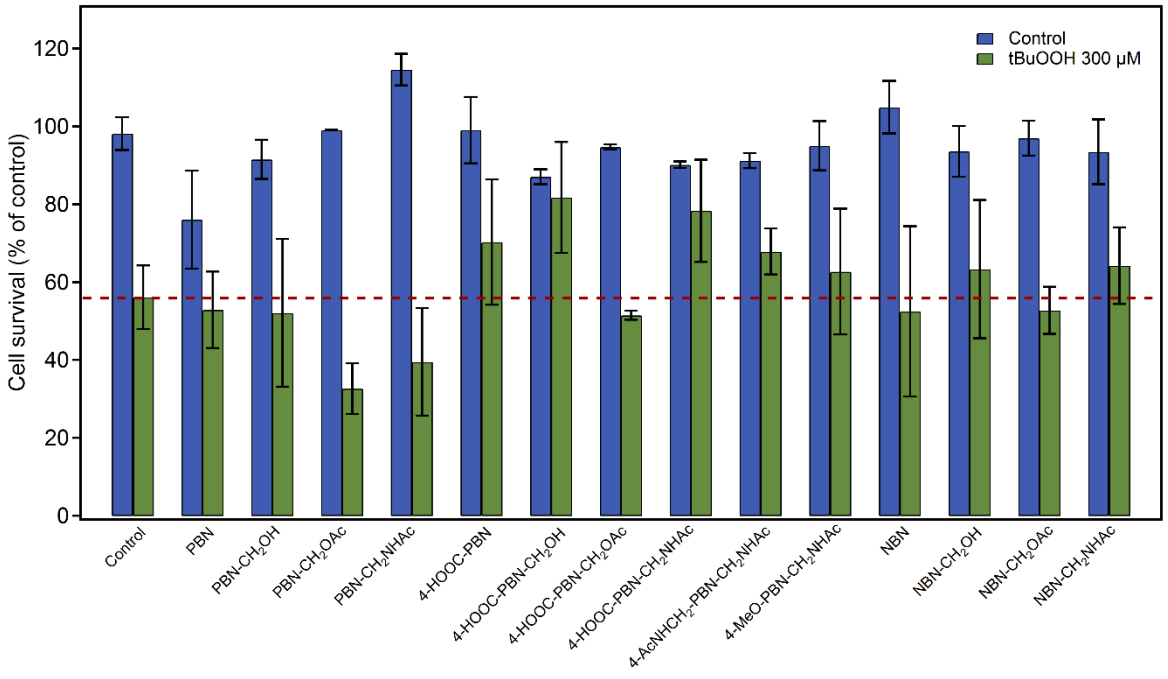

Figure 4. Antioxidant effect of PBN derivatives at 10 µM on glial cells injured tBuOOH (300 µM, 24 h), after 24 h of incubation with nitrones. Cell survival evaluation: MTT assay.

In the second assay, the nitrones at different concentrations (0.1, 1 and 10 µM) were pre-incubated with primary cortical neurons for 1 h before excitotoxic glutamate exposure (20 µmol/L for 20 min followed by a wash-out). MTT assay was carried out 48 h after the glutamate wash-out and the results are presented in Figure 5. Glutamate plays a fundamental role in neural transmission, development, differentiation and plasticity but excess of glutamate can lead to neuronal death by a mixed form of necrosis and apoptosis. With regards to the PBN-CH_2Y series, the acetate and acetamide derivatives showed significant neuroprotection at 10 µM but the activity was lost at lower concentrations suggesting a dose dependent protection. Regarding the 4-HOOC-PBN-CH_2Y series, 4-HOOC-PBN showed significant neuroprotection at 0.1, 1 and 10 µM. However, when a hydroxyl, acetate or acetamide substituent was introduced in the β-position of the nitronyl function, the neuroprotective activity was lost. Among the NBN series, only NBN and its hydroxyl derivative exhibited neuroprotection. These results show that the effects of the substituents in the *para*-position of the phenyl ring and in the β-position of the nitronyl function are not additives. Indeed, 4-HOOC-PBN and PBN-CH_2NHAc were neuroprotective at 10 µM whereas when combining the two substituents on the same nitrone, 4-HOOC-PBN-CH_2NHAc is not. NBN showed neuroprotection at 0.1 µM but at higher concentration a decrease of cell survival was observed, which may indicate a slight toxicity that might be due to the naphthalene group. Further, it has been reported that the metabolites of naphthalene can cause acute hemolysis.[48,49]

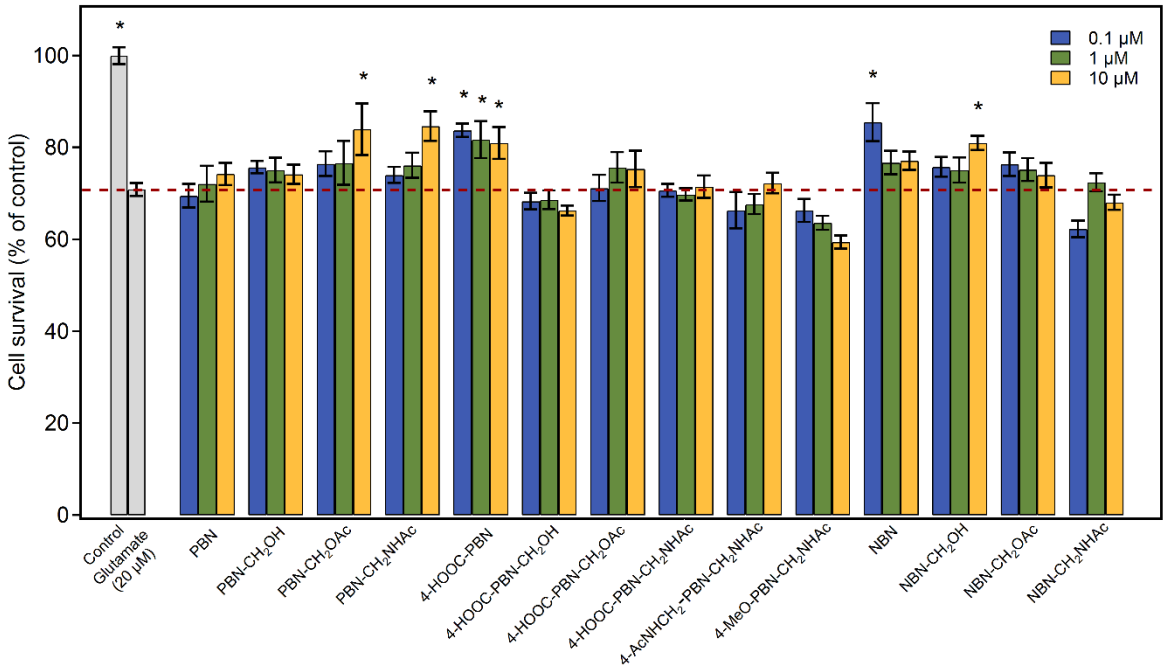

Figure 5. Neuroprotective effect of PBN derivatives at 0.1 µM, 1 µM and 10 µM on primary cortical neurons injured by glutamate (20 µM, 20 min, evaluation performed 48 h after glutamate wash-out), after 1 h of incubation with nitrones. Cell survival evaluation: MTT assay. Significance was accepted with * $p < 0.05$ vs glutamate condition, by one-way ANOVA followed by PLSD Fisher's test.

The ability of PBN to alleviate glutamate neurotoxicity had already been demonstrated *in vivo* however this was attributed to the free radical scavenging mechanism of PBN.[50] The extreme low concentration of nitrones used in this assay clearly supports that other mechanisms than direct free radical scavenging are involved in cytoprotection with 4-HOOC-PBN and NBN affording efficient protection at only 0.1 µM. Moreover, no correlation between the rate of spin-trapping of the derivatives and their neuroprotective activity was observed, with for example 4-HOOC-PBN being significantly neuroprotective but having a slightly higher rate of trapping than that of PBN while, on the contrary, 4-HOOC-PBN-CH_2OAc proved to be one of the best spin traps of the series but showed no cytoprotection. The absence of correlation between the redox properties of the derivatives –both experimental and calculated– and their cytoprotection also suggest it is not mediated by an antioxidant mechanism. Finally, we demonstrated it was possible to combine in one molecule the two properties. PBN-CH_2NHAc and 4-HOOC-PBN-CH_2NHAc are indeed the only derivatives to have both good radical scavenging property and cytoprotection.

3. CONCLUSION

In this work, new bi-functionalized PBN-type nitrones were synthesized and the combined effects of modifications both on the phenyl ring and on the *N-tert*-butyl group on the reactivity of the nitronyl function were studied. We also synthesized a naphthalene-based series where the phenyl ring was replaced by a naphthlyl group. The spin-trapping properties of the new derivatives towards hydroxymethyl radical were investigated and showed that the introduction of an electron-withdrawing group in the β-position of the nitronyl function significantly increased the trapping rate, especially with the derivatives PBN-CH_2OH and PBN-CH_2NHAc being 2.4 and 3.2 times more efficient than PBN, respectively. Excellent spin-trapping properties were observed for the bi-functionalized derivatives 4-HOOC-PBN-CH_2OAc and 4-HOOC-PBN-CH_2NHAc, having a trapping rate 3.6 and 3.8 times higher than that of PBN, respectively. When the phenyl group was substituted by a bicyclic naphthalene group, the trapping rates were decreased indicating a deactivating contribution of the naphthlyl towards hydroxymethyl radical trapping.

Cyclic voltammetry experiments showed that the redox potentials of the nitrones are influenced by the nature of the substituents both on the aromatic ring and on the *N-tert*-butyl group. All the nitrones showed stability domain equal or superior to 3 V which make them therefore suitable for electrochemical spin-trapping experiments. For the oxidation potential, the presence of an acetate group increased it whereas an acetamide substituent decreased it, except for the naphthalene series where all the derivatives exhibited similar oxidation potentials. Finally, the neuroprotection of the derivatives in two *in vitro* models of oxidative stress and cellular injury on glial cells and cortical neurons, respectively, showed interesting activities on at least one model. On the first model of oxidative stress, 4-HOOC-PBN-CH_2OH and 4-HOOC-PBN-CH_2NHAc were the most potent whereas PBN-CH_2OAc, PBN-CH_2NHAc, NBN, NBN-CH_2OH and 4-HOOC-PBN showed high neuroprotection on the second model. Taken together, PBN-CH_2NHAc, 4-HOOC-PBN and 4-HOOC-PBN-CH_2NHAc appear as the most promising nitrones with both good trapping properties and neuroprotection.

EXPERIMENTAL SECTION

Synthesis. All reagents were from commercial sources and were used as received. All solvents were distilled and dried according to standard procedures. Reaction courses and product mixtures were routinely monitored by TLC on silica gel (60 F_{254} Merck plates). Compound detection was achieved either by exposure to UV light (254 nm) and/or by spraying a 5% sulfuric acid solution in ethanol or a 2% ninhydrin solution in ethanol and then heating to ~150 °C. Flash column chromatography was carried out on silica gel (40−63 μm) with a CombiFlash system. NMR spectra were recorded on a Bruker AC400 at 400 and 100 MHz for ^{1}H and ^{13}C experiments, respectively. Chemical shifts are given in ppm relative to the solvent residual peak as a heteronuclear reference for ^{1}H and ^{13}C. Abbreviations used for signal patterns are as follows: bs, broad singlet; s, singlet; d, doublet; m, multiplet. HR-MS spectra were recorded on a Synapt G2-S (Waters) mass spectrometer equipped with a TOF analyzer for ESI+ experiments.

***N*-(2-(hydroxyamino)-2-methylpropan-1-ol (14).** 2-methyl-2-nitropropanol (2.38 g, 20.0 mmol, 1.0 equiv) and NH_4Cl (1.61 g, 30.0 mmol, 1.5 equiv) were dissolved in a THF/H_2O (3:1 v/v) mixture at room temperature. The mixture was cooled down to 0 °C then zinc powder (2.60 g, 40.0 mmol, 2.0 equiv) was slowly added in order to keep the temperature below 15 °C. The mixture was stirred at room temperature for 17 h and then heated at 50 °C for 5 h. The reaction mixture was filtered through a pad of Celite, washed with MeOH and the solvents were removed under vacuum. The crude mixture was purified by flash chromatography (EtOAc/MeOH, 95:5 v/v) to afford 1.13 g of the title compound (10.8 mmol, 54%) as a white powder. R_f (EtOAc/MeOH, 95:5 v/v) = 0.18. ^{1}H NMR (400 MHz, DMSO-d_6) 3.21 (2H, s), 0.88 (6H, s). $^{13}C\{1H\}$ NMR (100 MHz, DMSO-d_6) 65.3, 57.5, 21.5. This compound was found unstable at room temperature and was directly used without further purification and characterization.

α-(4-carboxy)phenyl-*N*-(2-methyl-1-hydroxyl-2-propyl)nitrone (5). Under an argon atmosphere and under stirring, 4-carboxybenzaldehyde (1.14 g, 7.6 mmol, 1.0 equiv) and hydroxylamine **14** (1.09 g, 10.4 mmol, 1.4 equiv) were dissolved in a THF/AcOH (3:2 v/v) mixture. The mixture was stirred at 60 °C in the dark for 18 h in the presence of molecular sieves (4Å). The reaction mixture was filtered through a pad of Celite, and the solvents were removed under vacuum. The crude mixture was purified by flash chromatography (EtOAc/MeOH, 95:5 v/v) followed by two successive crystallizations from MeOH/Et_2O to

afford 1.21 g of the title compound (5.1 mmol, 67%) as a white powder. R_f (EtOAc/MeOH, 95:5 v/v) = 0.12. Mp > degradation temperature. Anal. Calcd for $C_{12}H_{15}NO_4$: C, 60.8; H, 6.4; N, 5.9; Found: C, 60.9; H, 6.5; N, 5.7. ^{1}H NMR (400 MHz, MeOD) 8.41 (2H, d, *J* = 8.4 Hz), 8.07 (2H, d, *J* = 8.4 Hz), 7.93 (1H, s), 3.79 (2H, s), 1.57 (6H, s). ^{13}C{1H} NMR (100 MHz, MeOD) 169.0, 135.9, 135.2, 133.4, 130.6, 130.4, 76.0, 68.4, 23.4. HR-MS (ESI/Q-TOF) *m/z*: $[M+H]^+$ calcd for $C_{12}H_{16}NO_4$ 238.1079; Found 238.1078.

2-methyl-2-nitropropyl acetate (15). Under stirring, 2-methyl-2-nitropropanol (5.18 g, 43.53 mmol) was dissolved in a pyridine/Ac_2O (1:1 v/v) mixture at 0 °C. After 5 h of stirring at room temperature, the mixture was poured into cold 3N HCl and extracted with DCM (3×). The organic layer was washed with brine, dried over $MgSO_4$ and concentrated under vacuum. The crude mixture was purified by flash chromatography (EtOAc/cyclohexane, 1:9 v/v) to afford 6.07 g of the title compound (37.7 mmol, 87%) as a colorless liquid. R_f (EtOAc/cyclohexane, 1:9 v/v) = 0.28. ^{1}H NMR (400 MHz, $CDCl_3$) 4.36 (2H, s), 2.03 (3H, s), 1.58 (6H, s). ^{13}C{1H} NMR (100 MHz, $CDCl_3$) 170.1, 86.2, 68.3, 23.1, 20.6. The spectral data were in agreement with the literature.[51]

***N*-(2-(hydroxyamino)-2-methylpropyl acetate (16).** The synthetic procedure was essentially the same as for compound **14**. Compound **15** (2.97 g, 18.5 mmol) was used as starting material. The mixture was stirred at room temperature for 2 h. The crude mixture was purified by flash chromatography (EtOAc/cyclohexane, 8:2 v/v) to afford 318 mg of the title compound (2.16 mmol, 12%) as a blue oil. R_f (EtOAc/cyclohexane, 8:2 v/v) = 0.25. ^{1}H NMR (400 MHz, MeOD) 4.01 (2H, s), 2.07 (3H, s), 1.95 (1H, bs), 1.07 (6H, s). ^{13}C{1H} NMR (100 MHz, MeOD) 172.9, 68.4, 57.8, 21.7, 20.7. This compound was found volatile and unstable at room temperature and was directly used without further purification and characterization.

α-(4-carboxy)phenyl-*N*-(2-methyl-1-acetate-2-propyl)nitrone (6). Under an argon atmosphere and under stirring, 4-carboxybenzaldehyde (311 mg, 2.07 mmol, 1.0 equiv) and hydroxylamine **16** (304 mg, 2.07 mmol, 1.0 equiv) were dissolved in dry EtOH. The mixture was stirred at 60 °C in the dark for 1 h, and the solvent was removed under vacuum. The crude mixture was purified by flash chromatography (EtOAc/cyclohexane, 8:2 v/v) followed by two successive crystallizations from EtOAc/*n*-hexane to afford 276 mg of the title compound (0.99 mmol, 49%) as a white powder. Mp: 138.7-140.6 °C. R_f (EtOAc/cyclohexane, 8:2 v/v) = 0.14. Anal. Calcd for $C_{14}H_{17}NO_5$: C, 60.2; H, 6.1; N, 5.0; Found: C, 59.2; H, 5.8; N, 4.8. ^{1}H NMR (400 MHz, $CDCl_3$) 8.38 (2H, d, *J* = 8.4 Hz), 8.15 (2H, d, *J* = 8.4 Hz), 7.61 (1H, s), 4.44 (2H, s), 2.04 (3H, s), 1.65 (6H, s). ^{13}C{1H} NMR (100

MHz, $CDCl_3$) 170.6, 170.5, 135.3, 131.0, 130.5, 128.8, 73.1, 68.4, 23.8, 20.9. HR-MS (ESI/Q-TOF) *m/z*: $[M+H]^+$ calcd for $C_{14}H_{18}NO_5$ 280.1185; Found 280.1184.

***N*-(2-(hydroxyamino)-2-methylpropyl)acetamide (18).** The synthetic procedure was essentially the same as for compound **14**. *N*-(2-methyl-2-nitropropyl)acetamide[29] (2.53 g, 15.8 mmol) was used as starting material. The mixture was stirred at room temperature for 20 h. The crude mixture was purified by flash chromatography (EtOAc/MeOH, 9:1 v/v) to afford 1.54 g of the title compound (10.6 mmol, 67%) as a blue oil. R_f (EtOAc/MeOH, 9:1 v/v) = 0.28. ^{1}H NMR (400 MHz, DMSO-*d6*) 7.59 (1H, bs), 6.90 (1H, bs), 5.22 (1H, bs), 3.02 (2H, d, *J* = 6.4 Hz), 1.83 (3H, s), 0.88 (6H, s). ^{13}C{1H} NMR (100 MHz, DMSO-d_6) 169.6, 56.8, 44.6, 22.6, 22.5. This compound was found unstable at room temperature and was directly used without further purification and characterization.

α-(4-carboxy)phenyl-*N*-(2-methyl-1-acetamide-2-propyl)nitrone (7). The synthetic procedure was essentially the same as for compound **5**. 4-carboxybenzaldehyde (1.09 g, 7.3 mmol) and hydroxylamine **18** (1.49 g, 10.2 mmol) were used as starting materials. Reaction time was 23 h. The crude mixture was purified by flash chromatography (EtOAc/MeOH, 9:1 v/v) followed by two successive crystallizations from MeOH/Et_2O to afford 1.17 g of the title compound (4.2 mmol, 58%) as a yellow powder. R_f (EtOAc/MeOH, 9:1 v/v) = 0.14. Mp > degradation temperature. Anal. Calcd for $C_{14}H_{18}N_2O_4$: C, 60.4; H, 6.5; N, 10.1; Found: C, 59.9; H, 6.8; N, 9.7. ^{1}H NMR (400 MHz, MeOD) 8.42 (2H, d, *J* = 8.4 Hz), 8.07 (2H, d, *J* = 8.4 Hz), 7.94 (1H, s), 3.68 (2H, s), 1.94 (3H, s), 1.58 (6H, s). ^{13}C{1H} NMR (100 MHz, MeOD) 173.8, 169.1, 135.9, 134.6, 133.5, 130.6, 130.4, 75.7, 47.6, 24.7, 22.5. HR-MS (ESI/Q-TOF) *m/z*: $[M+H]^+$ calcd for $C_{14}H_{19}N_2O_4$ 279.1345; Found 279.1346.

α-(4-acetamido)phenyl-*N*-(2-methyl-1-acetamide-2-propyl)nitrone (8). The synthetic procedure was essentially the same as for compound **5**. *N*-(4-formylbenzyl)acetamide[22] (904 mg, 5.11 mmol) and hydroxylamine **18** (1.05 g, 7.19 mmol) were used as starting materials. Reaction time was 18 h. The crude mixture was purified by flash chromatography (EtOAc/MeOH, 85:15 v/v) followed by two successive crystallizations from MeOH/Et_2O to afford 571 mg of the title compound (1.87 mmol, 37%) as a brown powder. R_f (EtOAc/MeOH, 85:15 v/v) = 0.19. Mp: 144.0-146.2 °C. Anal. Calcd for $C_{16}H_{23}N_3O_3$: C, 62.9; H, 7.6; N, 13.8; Found: C, 62.8; H, 7.8; N, 13.6. ^{1}H NMR (400 MHz, MeOD) 8.52 (1H, bs), 8.32 (2H, d, *J* = 8.4 Hz), 7.94 (1H, bs), 7.85 (1H, s), 7.38 (2H, d, *J* = 8.4 Hz), 4.41 (2H, d, *J* = 6.4 Hz), 3.67 (2H, d, *J* = 6.4 Hz), 2.01 (3H, s), 1.93 (3H, s), 1.56 (6H, s). ^{13}C{1H} NMR (100

MHz, MeOD) 173.7, 173.2, 143.4, 135.9, 131.1, 130.7, 128.4, 75.0, 47.5, 43.9, 24.7, 22.5. HR-MS (ESI/Q-TOF) *m/z*: $[M+H]^+$ calcd for $C_{16}H_{24}N_3O_3$ 306.1818; Found 306.1821.

α-(4-methoxy)phenyl-*N*-(2-methyl-1-acetamide-2-propyl)nitrone (9). Under an argon atmosphere and under stirring, *p*-anisaldehyde (792 mg, 5.8 mmol, 1.0 equiv), *N*-(2-methyl-2-nitropropyl)acetamide[29] (1.40 g, 8.7 mmol, 1.5 equiv) and AcOH (2.0 mL, 34.8 mmol, 6.0 equiv) were dissolved in dry EtOH. The mixture was cooled down to 0 °C then zinc powder (1.52 g, 23.2 mmol, 4.0 equiv) was slowly added in order to keep the temperature below 15 °C. The mixture was stirred at room temperature for 1 h then heated at 60 °C in the dark for 21 h in the presence of molecular sieves (4Å). The reaction mixture was filtered through a pad of Celite, and the solvents were removed under vacuum. The crude mixture was purified by flash chromatography (EtOAc) followed by two successive crystallizations from EtOAc/*n*-hexane to afford 1.01 g of the title compound (3.8 mmol, 66%) as a white powder. R_f (EtOAc/MeOH, 95:5 v/v) = 0.30. Mp: 114.7-116.2 °C. Anal. Calcd for $C_{14}H_{20}N_2O_3$: C, 63.6; H, 7.6; N, 10.6; Found: C, 63.8; H, 7.7; N, 10.4. ^{1}H NMR (400 MHz, $CDCl_3$) 8.25 (2H, d, *J* = 8.8 Hz), 7.42 (1H, s), 6.95 (2H, d, *J* = 8.8 Hz), 6.66 (1H, bs), 3.86 (3H, s), 3.67 (2H, d, *J* = 6.4 Hz), 1.98 (3H, s), 1.58 (6H, s). ^{13}C{1H} NMR (100 MHz, $CDCl_3$) 170.6, 161.5, 131.5, 131.2, 123.5, 114.1, 72.7, 55.5, 47.6, 25.2, 23.5. HR-MS (ESI/Q-TOF) *m/z*: $[M+H]^+$ calcd for $C_{14}H_{21}N_2O_3$ 265.1552; Found 265.1554.

***N-tert*-butyl-α-(naphthalen-2-yl)nitrone (10).** The synthetic procedure was essentially the same as for compound **9**. 2-naphthaldehyde (780 mg, 5.0 mmol) and 2-methyl-2-nitropropane (1.03 g, 10.0 mmol) were used as starting materials. Reaction time was 17 h. The crude mixture was purified by flash chromatography (EtOAc/cyclohexane, 2:8 v/v) to afford 440 mg of the title compound (1.94 mmol, 39%) as a yellow oil. R_f (EtOAc/cyclohexane, 2:8 v/v) = 0.18. Anal. Calcd for $C_{15}H_{17}NO$: C, 79.26; H, 7.54; N, 6.16; Found: C 79.24; H, 7.40; N, 5.91. ^{1}H NMR (400 MHz, $CDCl_3$) δ 9.43 (1H, s), 7.93-7.91 (1H, m), 7.84-7.80 (3H, m), 7.71 (1H, s), 7.52-7.48 (2H, m), 1.67 (9H, s). ^{13}C{1H} NMR (100 MHz, $CDCl_3$) δ 134.2, 133.4, 130.4, 129.5, 128.7, 128.2, 127.9, 127.6, 127.3, 126.6, 126.5, 71.1, 28.5. HR-MS (ESI/Q-TOF) *m/z*: $[M+H]^+$ calcd for $C_{15}H_{18}NO$ 228.1388; Found 228.1396. The spectral data was in agreement with the literature.[52]

α-(naphthalen-2-yl)-*N*-(2-methyl-1-hydroxy-2-propyl)nitrone (11). The synthetic procedure was essentially the same as for compound **9**. 2-naphthaldehyde (1.15 g, 7.4 mmol) and 2-methyl-2-nitropropanol (1.75 g, 14.7 mmol) were used as starting materials. Reaction time was 40 h. The crude mixture was purified by flash chromatography

(EtOAc/cyclohexane, 6:4 v/v) followed by two successive crystallizations from EtOAc/*n*-hexane to afford 1.26 g of the title compound (5.2 mmol, 70%) as a yellow powder. R_f (EtOAc/cyclohexane, 6:4 v/v) = 0.21. Mp: 121.8-122.7 °C. Anal. Calcd for $C_{15}H_{17}NO_2$: C, 74.05; H, 7.04; N, 5.76; Found: C 73.79; H, 6.84; N, 5.39. ^{1}H NMR (400 MHz, $CDCl_3$) δ 9.26 (1H, s), 7.94-7.80 (4H, m), 7.64 (1H, s), 7.56-7.49 (2H, m), 3.84 (2H, s), 1.64 (6H, s). ^{13}C{1H} NMR (100 MHz, $CDCl_3$) δ 134.4, 133.2, 132.5, 129.5, 129.4, 128.1, 127.7, 127.6, 127.6, 126.7, 126.5, 73.2, 70.0, 24.0. HR-MS (ESI/Q-TOF) *m/z*: $[M+H]^+$ calcd for $C_{15}H_{18}NO_2$ 244.1338; Found 244.1338.

α-(naphthalen-2-yl)-*N*-(2-methyl-1-acetate-2-propyl)nitrone (12). Under stirring, nitrone **11** was dissolved in a pyridine/Ac_2O (1:1 v/v) mixture at 0 °C. After 4 h of stirring at room temperature, the mixture was poured into cold 3N HCl and extracted with DCM (3x). The organic layer was washed with brine, dried over $MgSO_4$ and concentrated under vacuum. The crude mixture was purified by flash chromatography (EtOAc/cyclohexane, 3:7 v/v) followed by two successive crystallizations from EtOAc/*n*-hexane to afford 834 mg of the title compound (2.93 mmol, 57%) as a white powder. R_f (EtOAc/cyclohexane, 4:6 v/v) = 0.26. Mp: 104.2-105.2 °C. Anal. Calcd for $C_{17}H_{19}NO_3$: C, 71.56; H, 6.71; N, 4.91; Found: C 71.40; H, 6.27; N, 4.66. ^{1}H NMR (400 MHz, $CDCl_3$) δ 9.40 (1H, s), 7.95-7.81 (4H, m), 7.68 (1H, s), 7.56-7.48 (2H, m), 4.48 (2H, s), 2.04 (3H, s), 1.68 (6H, s). ^{13}C{1H} NMR (100 MHz, $CDCl_3$) δ 170.6, 134.4, 133.4, 132.5, 129.5, 129.3, 128.1, 127.7, 127.6, 126.7, 126.6, 72.3, 68.4, 23.9, 20.9. HR-MS (ESI/Q-TOF) *m/z*: $[M+H]^+$ calcd for $C_{17}H_{20}NO_3$ 286.1443; Found 286.1443.

α-(naphthalen-2-yl)-*N*-(2-methyl-1-acetamide-2-propyl)nitrone (13). The synthetic procedure was essentially the same as for compound **9**. 2-naphthaldehyde (753 mg, 4.83 mmol) and *N*-(2-methyl-2-nitropropyl)acetamide[29] (1.55 g, 9.66 mmol) were used as starting materials. Reaction time was 42 h. The crude mixture was purified by flash chromatography (EtOAc) followed by two successive crystallizations from EtOAc/*n*-hexane to afford 900 mg of the title compound (3.17 mmol, 66%) as a yellow powder. R_f (EtOAc) = 0.17. Mp: 107.1-107.9 °C. Anal. Calcd for $C_{15}H_{20}N_2O_2$: C, 71.81; H, 7.09; N, 9.85; Found: C 70.38; H, 6.27; N, 9.58. ^{1}H NMR (400 MHz, $CDCl_3$) δ 9.30 (1H, s), 7.94-7.82 (4H, m), 7.66 (1H, s), 7.57-7.50 (2H, m), 6.60 (1H, bs), 3.74 (2H, d, *J* = 6.4 Hz), 2.00 (3H, s), 1.65 (6H, s). ^{13}C{1H} NMR (100 MHz, $CDCl_3$) δ 170.6, 134.4, 133.3, 132.2, 129.4, 129.2, 128.2, 127.7, 127.7, 127.6, 126.8, 126.4, 73.7, 47.5, 25.3, 23.5. HR-MS (ESI/Q-TOF) *m/z*: $[M+H]^+$ calcd for $C_{17}H_{21}N_2O_2$ 285.1603; Found 285.1605.

Determination of *c* log *P* Values. The partition coefficient octanol/water (*c* log *P*) was determined using ALOGPS 2.1 software, which is available at www.vcclab.org/lab/alogps/.

EPR measurements and hydroxymethyl spin-trapping kinetics. EPR measurements were carried out on a Bruker EMX plus spectrometer operating at X-band with 100 kHz modulation frequency. The general instrument settings used for spectral acquisition were as follows: microwave power, 20 mW; modulation amplitude, 1 G; received gains 5×10^4 to 1×10^6; scan time, 5 s; sweep width, 100 G. Spectra were recorded at room temperature, and measurements were performed using a capillary tube. The spectrum simulation was carried out using the WINSIM program,[53] available as free software from Public Electron Paramagnetic Resonance Software Tools (http://www.niehs.nih.gov/research/resources/software/tox-pharm/tools/). The solvents were of the highest purity grade and used without further purification. The trinitrone TN was synthesized and purified as previously described.[54] To generate the hydroxymethyl ($^{\bullet}CH_2OH$) radical, nitrone (100 mM) was dissolved in a Fenton system containing hydrogen peroxide (6%) and iron (II) sulfate (6 mM) in methanol. The method of kinetic competition described by Roubaud *et al.*[54] was used to evaluate the ratio of the second-order rate constants (k_N/k_{PBN}) for the trapping of $^{\bullet}CH_2OH$ by one of the nitrone **N** of interest and **TN** used as competitive inhibitor. This method yielded equation 1 in which k_N and k_{TN} represent the rate constants of $^{\bullet}CH_2OH$ trapping by the nitrone **N** under consideration and by **TN**, respectively. *R* and *r* represent the rate constant by both **TN** and **N**, and by **TN** only, respectively.

$$R/r = 1 + k_N[N]/k_{TN}[TN] \quad (1)$$

Then, the commercially available PBN was also tested versus **TN** in order to determine the ratio of the rate constants for the trapping of $^{\bullet}CH_2OH$ by PBN and by **TN**: *i.e.*, k_{PBN}/k_{TN}. The concentrations of the various nitrones were varied to keep the [**N**]/[**TN**] ratio between 2 and 10. For each nitrone, at least five experiments were repeated twice. In each case, a series of 10 EPR spectra was then recorded (scan time for a single spectrum: 20 s). The signal-to-noise ratio was improved using a SVD procedure, as described elsewhere.[55] The signal recorded exactly 2 min after the beginning of the reaction was then simulated using the WinSim software in order to determine the relative areas of the adducts **N**-CH_2OH and **TN**-CH_2OH. In this approach, the ratio R/r was evaluated as follows:

$$\frac{R}{r} = \frac{area\ of\ N-R\ signal + area\ of\ TN-R\ signal}{area\ of\ TN-R\ signal} \quad (2)$$

Cyclic voltammetric measurements. The electrochemical experiments were carried out at room temperature in acetonitrile containing 100 mM of TBAB, using VersaSTAT 4. A conventional cell with three electrodes was used: (i) a silver electrode wire as the reference electrode, (ii) a platinum electrode wire as the auxiliary electrode and (iii) a glassy carbon disk as the working electrode. The working electrode was polished prior to each experiment using a 0.04 μm aqueous alumina slurry on a wetted polishing cloth. The potentials are reported versus the silver wire electrode, Ag. All solutions were deoxygenated by argon bubbling through the solution for 10 min and a blanket of argon was maintained over the solution during the experiment. The voltamperograms were recorded for a nitrone concentration equal to 1 mM. Ferrocene was used in order to calibrate the electron transfers.[56]

***In vitro* neuroprotective measurements.**

Glial cells model. C6 cells (rat gliomas) were seeded in 24-well culture plates (500 μL volume) containing DMEM medium (Dulbecco's modified Eagle medium) supplemented with 10% fetal calf serum. They were left in an incubator at 37 °C on 5% CO_2 until reaching 80% of confluence. Then, the culture medium was replaced by serum-free DMEM medium containing the nitrones to be tested. The cells were returned to the incubator for 24 h. The oxidative stress was then induced by treating the cells with *t*BuOOH (100 to 500 μM) for 24 h. Finally, the measurement of cell survival was performed using the MTT test. For this, the medium of each culture well was first replaced by 100 μL of Krebs-Ringer extracellular medium containing: 125 mM NaCl, 3.5 mM KCl, 25 mM $NaHCO_3$, 1.25 mM KH_2PO_4, 1.5 mM, $CaCl_2$, 1.25 mM $MgSO_4$, 10mM d-glucose, and 10mM Hepes (pH 7.4), heated to 33 °C and bubbled with carbogen (95% O_2; 5% CO_2) for 15 min. 10 μL of a solution of MTT (2.5 mg /mL in PBS) were added and the cells were then returned to the incubator for 45 min to allow the transformation of MTT into formazan. The MTT solution was removed and 50 μL of DMSO were added per well to dissolve the formazan crystals. 50 μL more of DMSO were added to dilute the resulting solution. Finally, the optical density (DO) was assessed by spectrophotometer at 570 nm wavelength (LT-4000, LabTech). The DO was corresponding to the cell survival in each culture well.

Primary cortical cells model. Rat cortical neurons were cultured as described by Singer *et al*. and Callizot *et al*.[57,58] Briefly, pregnant females (Wistar; JanvierLabs) at 15 days of gestation were killed by cervical dislocation. Fetuses were collected and immediately placed in ice-cold L15 Leibovitz medium (Pan Biotech) with a 2% penicillin (10,000 U/ml) and streptomycin (10 mg/ml) solution (PS) and 1% bovine serum albumin (BSA). Cortexes was treated for 20 min at 37 °C with a trypsin-EDTA (Pan Biotech) solution at a final concentration of 0.05% trypsin and 0.02% EDTA. The dissociation was stopped by addition of Dulbecco's modified Eagle's medium (DMEM) with 4.5 g/liter of glucose (Pan Biotech,), containing DNAse I grade II (final concentration 0.5 mg/ml; Pan Biotech) and 10% fetal calf serum (FCS; Invitrogen). Cells were mechanically dissociated by three forced passages through the tip of a 10-ml pipette. Cells were then centrifuged at 515 g for 10 min at 4 °C. The supernatant was discarded, and the pellet was resuspended in a defined serum-free culture medium consisting of Neurobasal medium (Invitrogen) with a 2% solution of B27 supplement (Invitrogen), 2 mmol/liter of L-glutamine (Pan Biotech), 2% of PS solution, and 10 ng/ml of brain-derived neurotrophic factor (BDNF; Pan Biotech). Viable cells were counted in a Neubauer cytometer, using the trypan blue exclusion test. The cells were seeded at a density of 25,000 per well in 96-well plates precoated with poly-L-lysine and were cultured at 37 °C in an air (95%)-CO_2 (5%) incubator. The medium was changed every 2 days. ***Viability studies.*** On day 13 of culture, BDNF (50 ng/ml) or test compounds (at 0.1, 1 and 10 µM) were pre-incubated with primary cortical neurons for 1 h before glutamate exposure. Then, glutamate (Sigma) was added in the cell culture to a final concentration of 20 µM diluted in control medium in presence of BDNF or test compounds for 20 min. After 20 min, glutamate was washed and fresh culture medium with BDNF or test compounds was added for additional 48 h. Test compounds were tested on one culture in 96 well plates (6 wells per conditions). After 48 h of glutamate intoxication (on day 15 of culture), the MTT assay was performed using CellTiter 96® Aqueous One Solution Cell Proliferation Assay (Promega, USA). Briefly, 20 µL of tetrazolium compound was added directly in culture well for 3 h. The optic density (DO) was assessed by spectrophotometer at 450 nm wavelength by Glomax apparatus (Promega). The DO was corresponding to the cell survival in each culture well. Data were expressed in percentage of control conditions (no intoxication, no glutamate = 100 %) in order to express the glutamate injury. All values were expressed as mean +/- SEM (s.e.mean) of the culture (n = 5-6 wells per condition per culture). Statistical analyses on the different conditions were performed (ANOVA followed by PLSD Fisher's test when allowed, using PADPRISM software version 5.0).

ACKNOWLEDGEMENTS

Anaïs Deletraz was the recipient of a fellowship from the “Région Provence Alpes Côte d’Azur”. We thank: Fédération RENARD IR-RPE CNRS 3443 for providing funds for the EPR studies. This study was conducted with the financial support of the European Regional Development Fund, the French Government, the “Région Provence Alpes Côte d'Azur”, the Departmental Council of Vaucluse and the Urban Community of Avignon.

SUPPORTING INFORMATION

Cyclic voltammograms of 4-HOOC-PBN-CH_2Y and X-PBN-CH_2NHAc derivatives in acetonitrile containing 0.1 M of TBAP at a GC electrode, potential scan rate υ = 0.1 V/s; ^{1}H and ^{13}C NMR spectra of nitrones **5**-**13** and intermediates **14**-**16** and **18**; HRMS spectra of nitrones **5**-**13**.

REFERENCES

1 B. Halliwell and J. M. C. Gutteridge, *Free Radicals in Biology and Medicine*, Oxford University Press, 2015.
2 H. Sies, *Redox Biol.*, 2015, **4**, 180–183.
3 C. Espinosa-Diez, V. Miguel, D. Mennerich, T. Kietzmann, P. Sánchez-Pérez, S. Cadenas and S. Lamas, *Redox Biol.*, 2015, **6**, 183–197.
4 F. A. Villamena, *Reactive Species Detection in Biology: From Fluorescence to Electron Paramagnetic Resonance Spectroscopy*, Elsevier., 2017.
5 G. M. Rosen, B. E. Britigan, H. J. Halpern and S. Pou, *Free Radicals: Biology and Detection by Spin Trapping*, Oxford University Press, 1999.
6 F. A. Villamena and J. L. Zweier, *Antioxid. Redox Signal.*, 2004, **6**, 619–629.
7 C. L. Hawkins and M. J. Davies, *Biochim. Biophys. Acta BBA - Gen. Subj.*, 2014, **1840**, 708–721.
8 M. J. Davies, *Methods*, 2016, 21–30.
9 H. M. Hughes, I. M. George, J. C. Evans, C. C. Rowlands, G. M. Powell and C. G. Curtis, *Biochem. J.*, 1991, **277**, 795–800.
10 M. B. Kadiiska, P. M. Hanna, S. J. Jordan and R. P. Mason, *Am. Soc. Pharmacol. Exp. Ther.*, 1993, **44**, 222–227.
11 H. D. Connor, W. Gao, S. Nukina, J. J. Lemasters, R. P. Mason and R. G. Thurman, *Transplantation*, 1992, **54**, 199–204.
12 R. A. Floyd, R. D. Kopke, C.-H. Choi, S. B. Foster, S. Doblas and R. A. Towner, *Free Radic. Biol. Med.*, 2008, **45**, 1361–1374.
13 F. A. Villamena, A. Das and K. M. Nash, *Future Med. Chem.*, 2012, **9**, 1171–1207.
14 R. A. Floyd, H. C. Castro Faria Neto, G. A. Zimmerman, K. Hensley and R. A. Towner, *Free Radic. Biol. Med.*, 2013, **62**, 145–156.
15 Y. Sun, G. Zhang, Z. Zhang, P. Yu, H. Zhong, J. Du and Y. Wang, *Bioorg. Med. Chem.*, 2012, **20**, 3939–3945.
16 P. L. Zamora and F. A. Villamena, *Future Med. Chem.*, 2013, **5**, 465–478.
17 D. S. S. Costa, T. Martino, F. C. Magalhães, G. Justo, M. G. P. Coelho, J. C. F. Barcellos, V. B. Moura, P. R. R. Costa, K. C. C. Sabino and A. G. Dias, *Bioorg. Med. Chem.*, 2015, **23**, 2053–2061.
18 A. Shuaib, K. R. Lees, P. Lyden, J. Grotta, A. Davalos, S. M. Davis, H.-C. Diener, T. Ashwood, W. W. Wasiewski and U. Emeribe, *N. Engl. J. Med.*, 2007, **357**, 562–571.
19 H.-C. Diener, K. R. Lees, P. Lyden, J. Grotta, A. Davalos, S. M. Davis, A. Shuaib, T. Ashwood, W. Wasiewski, V. Alderfer, H.-G. Hardemark and L. Rodichok, *Stroke*, 2008, **39**, 1751–1758.
20 C. L. Greenstock and R. H. Wiebe, *Can. J. Chem.*, 1982, **60**, 1560–1564.
21 Y. Sueishi, C. Yoshioka, C. Olea-Azar, L. A. Reinke and Y. Kotake, *Bull. Chem. Soc. Jpn.*, 2002, **75**, 2043–2047.
22 G. Durand, F. Choteau, B. Pucci and F. A. Villamena, *J. Phys. Chem. A*, 2008, **112**, 12498–12509.
23 M. Rosselin, B. Tuccio, P. Pério, Frederick. A. Villamena, P.-L. Fabre and G. Durand, *Electrochimica Acta*, 2016, **193**, 231–239.

24 A. Zeghdaoui, B. Tuccio, J.-P. Finet, V. Cerri and P. Tordo, *J. Chem. Soc. Perkin Trans. 2*, 1995, 2087–2089.
25 V. Roubaud, R. Lauricella, B. Tuccio, J.-C. Bouteiller and P. Tordo, *Res. Chem. Intermed.*, 1996, **22**, 405–416.
26 B. Tuccio, A. Zeghdaoui, J.-P. Finet, V. Cerri and P. Tordo, *Res. Chem. Intermed.*, 1996, **22**, 393–404.
27 V. Roubaud, R. Lauricella, J.-C. Bouteiller and B. Tuccio, *Arch. Biochem. Biophys.*, 2002, **397**, 51–56.
28 K. Stolze, N. Udilova, T. Rosenau, A. Hofinger and H. Nohl, *Biochem. Pharmacol.*, 2003, **66**, 1717–1726.
29 M. Rosselin, F. Choteau, K. Zéamari, K. M. Nash, A. Das, R. Lauricella, E. Lojou, B. Tuccio, F. A. Villamena and G. Durand, *J. Org. Chem.*, 2014, **79**, 6615–6626.
30 R. D. Hinton and E. G. Janzen, *J. Org. Chem.*, 1992, **57**, 2646–2651.
31 E. G. Janzen and R. C. Zawalski, *J. Org. Chem.*, 1978, **43**, 1900–1903.
32 R. Huie and W. R. Cherry, *J. Org. Chem.*, 1985, **50**, 1531–1532.
33 X. Song, Y. Qian, R. Ben, X. Lu, H.-L. Zhu, H. Chao and J. Zhao, *J. Med. Chem.*, 2013, **56**, 6531–6535.
34 A. Phaniendra, D. B. Jestadi and L. Periyasamy, *Indian J. Clin. Biochem.*, 2015, **30**, 11–26.
35 G. R. Buettner, *Free Radic. Biol. Med.*, 1987, **3**, 259–303.
36 A. Deletraz, K. Zéamari, F. Di Meo, P.-L. Fabre, K. Reybier, P. Trouillas, B. Tuccio and G. Durand, *New J. Chem.*, 2019, **43**, 15754–15762.
37 F. Choteau, B. Tuccio, F. A. Villamena, L. Charles, B. Pucci and G. Durand, *J. Org. Chem.*, 2012, **77**, 938–948.
38 F. De Vleeschouwer, V. Van Speybroeck, M. Waroquier, P. Geerlings and F. De Proft, *Org. Lett.*, 2007, **9**, 2721–2724.
39 N. J. Bunce, L. Liu, J. Zhu and D. A. Lane, *Environ. Sci. Technol.*, 1997, **31**, 2252–2259.
40 B. Tuccio, P. Bianco, J. C. Bouteiller and P. Tordo, *Electrochimica Acta*, 1999, **44**, 4631–4634.
41 G. L. McIntire, H. N. Blount, H. J. Stronks, R. V. Shetty and E. G. Janzen, *J. Phys. Chem.*, 1980, **84**, 916–921.
42 B. J. Acken, D. E. Gallis, J. A. Warshaw and D. R. Crist, *Can. J. Chem.*, 1992, **70**, 2076–2080.
43 L. Eberson, *J. Chem. Soc. Perkin Trans. 2*, 1992, 1807–1813.
44 L. Eberson, *J. Chem. Soc. Perkin Trans. 2*, 1994, 171–176.
45 T. H. Walter, E. E. Bancroft, G. L. McIntire, E. R. Davis, L. M. Gierasch and H. N. Blount, *Can. J. Chem.*, 1982, **60**, 1621–1636.
46 M. F. Beal, *FASEB J.*, 1992, **6**, 3338–3344.
47 S. C. Bondy and C. P. LeBel, *Free Radic. Biol. Med.*, 1993, **14**, 633–642.
48 J. V. Mackell, F. Rieders, H. Brieger and E. L. Bauer, *Pediatrics*, 1951, **7**, 722–728.
49 T. Valaes, S. A. Doxiadis and P. Fessas, *J. Pediatr.*, 1963, **63**, 904–915.
50 E. Lancelot, M.-L. Revaud, R. G. Boulu, M. Plotkine and J. Callebert, *Free Radic. Biol. Med.*, 1997, **23**, 1031–1034.
51 K. Ikeda, T. Tatsumo, H. Ogo, S. Masumoto, T. Fujibayashi, R. Nagata, U.S. Patent, 6,194,461 B1, 2001.

52 G. K. S. Prakash, Z. Zhang, F. Wang, M. Rahm, C. Ni, M. Iuliucci, R. Haiges and G. A. Olah, *Chem. - Eur. J.*, 2014, **20**, 831–838.
53 D. R. Duling, *J. Magn. Reson.*, 1994, 105–110.
54 V. Roubaud, H. Dozol, C. Rizzi, R. Lauricella, J.-C. Bouteiller and B. Tuccio, *J. Chem. Soc. Perkin Trans. 2*, 2002, 958–964.
55 R. Lauricella, A. Allouch, V. Roubaud, J.-C. Bouteiller and B. Tuccio, *Org. Biomol. Chem.*, 2004, **2**, 1304–1309.
56 C. Amatore, M. Azzabi, P. Calas, A. Jutand, C. Lefrou and Y. Rollin, *J. Electroanal. Chem. Interfacial Electrochem.*, 1990, **288**, 45–63.
57 C. A. Singer, X. A. Figueroa-Masot, R. H. Batchelor and D. M. Dorsa, *J. Neurosci.*, 1999, **19**, 2455–2463.
58 N. Callizot, M. Combes, R. Steinschneider and P. Poindron, *J. Neurosci. Res.*, 2013, **91**, 706–716.

Supporting Information For

Substituted α-Phenyl- and α-Naphthlyl-*N-tert*-butyl Nitrones: Synthesis and Spin-Trapping and Neuroprotection Evaluation

Table of contents

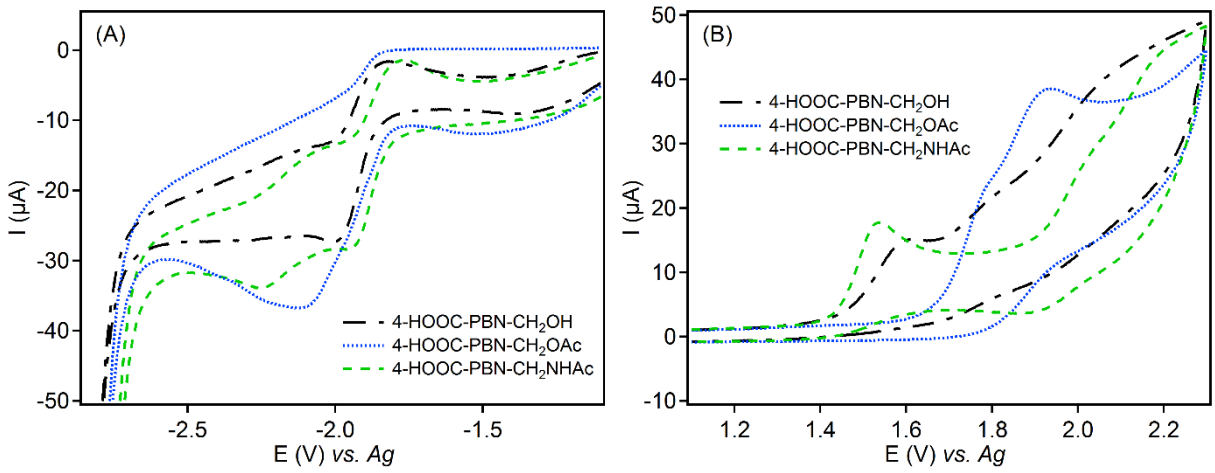

Figure S1. Cyclic voltammograms of 4-HOOC-PBN-CH_2Y derivatives in acetonitrile containing 0.1 M of TBAP at a GC electrode, potential scan rate υ = 0.1 V/s: (A) reduction and (B) oxidation.

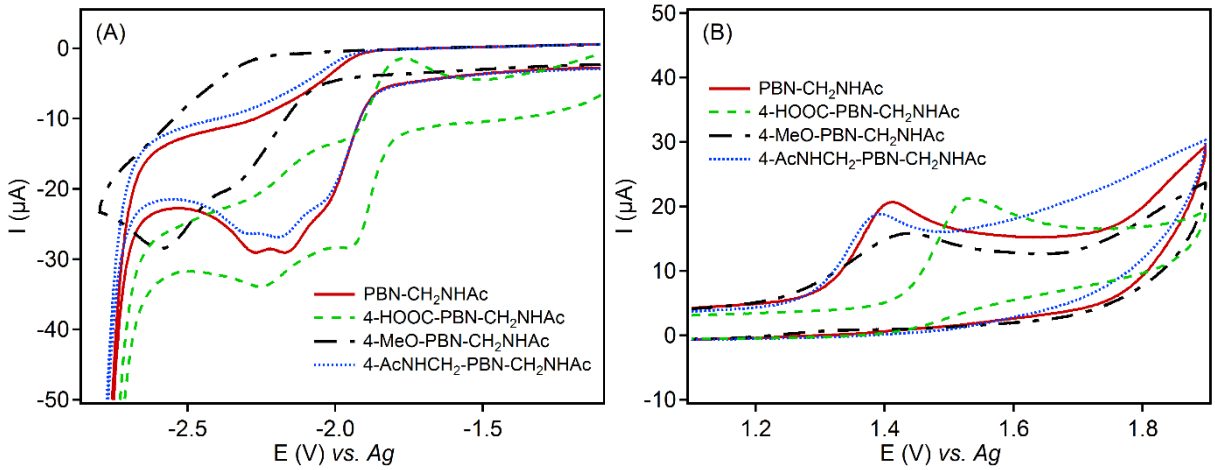

Figure S2. Cyclic voltammograms of X-PBN-CH_2NHAc derivatives in acetonitrile containing 0.1 M of TBAP at a GC electrode, potential scan rate υ = 0.1 V/s: (A) reduction and (B) oxidation.

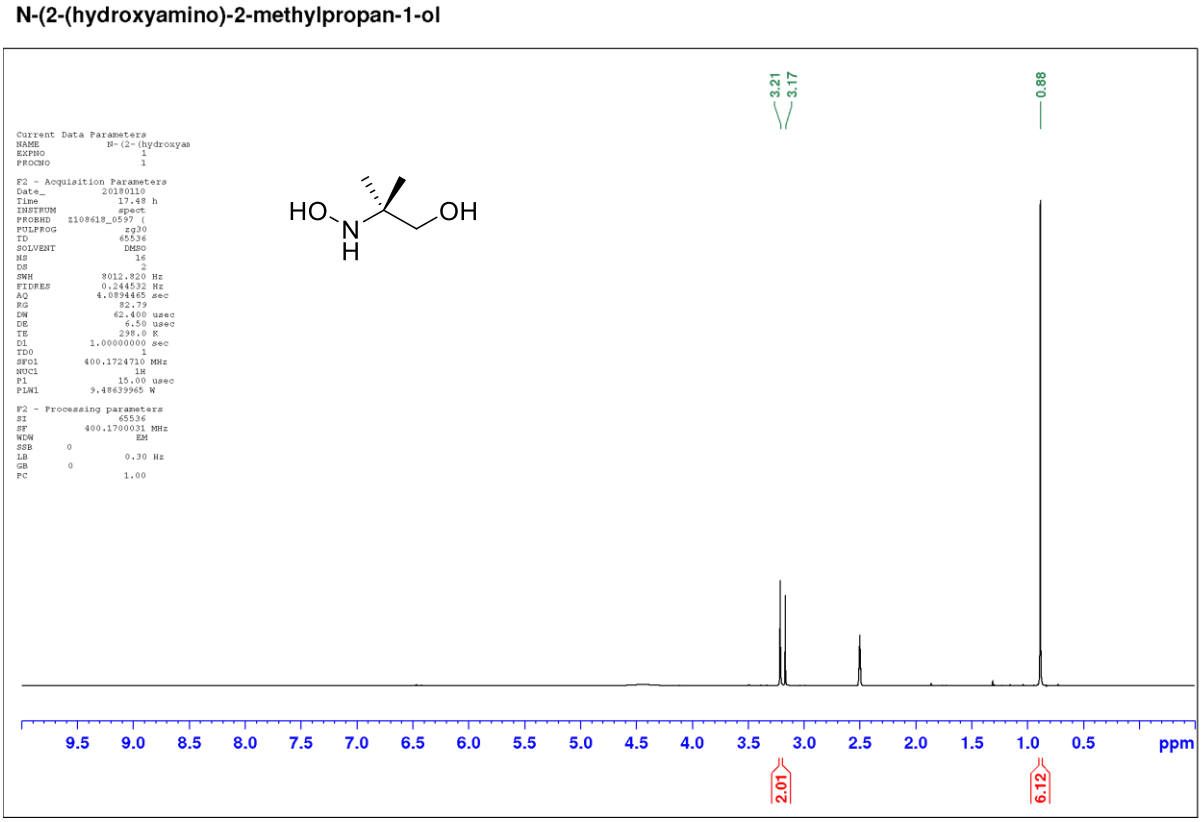

Figure S3. ^{1}H NMR spectrum of intermediate **14** in DMSO-d6.

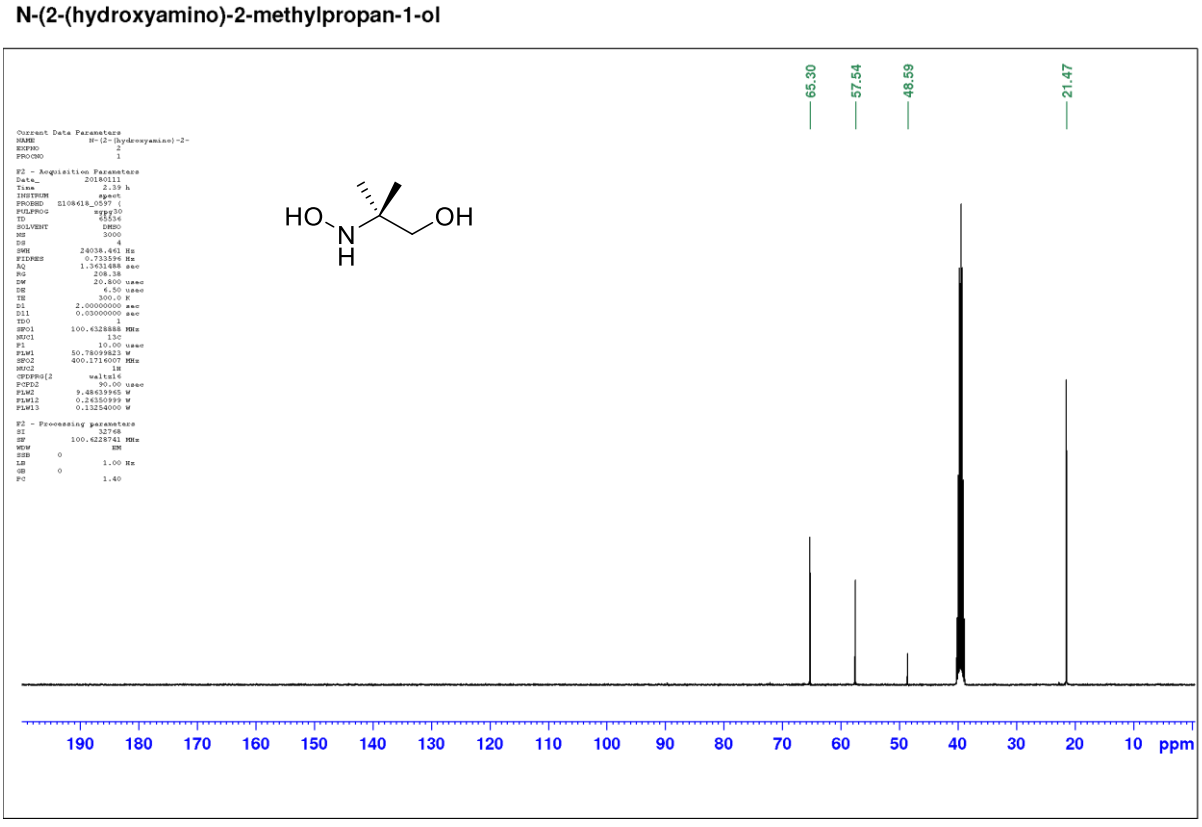

Figure S4. ^{13}C NMR spectrum of intermediate **14** in DMSO-d6.

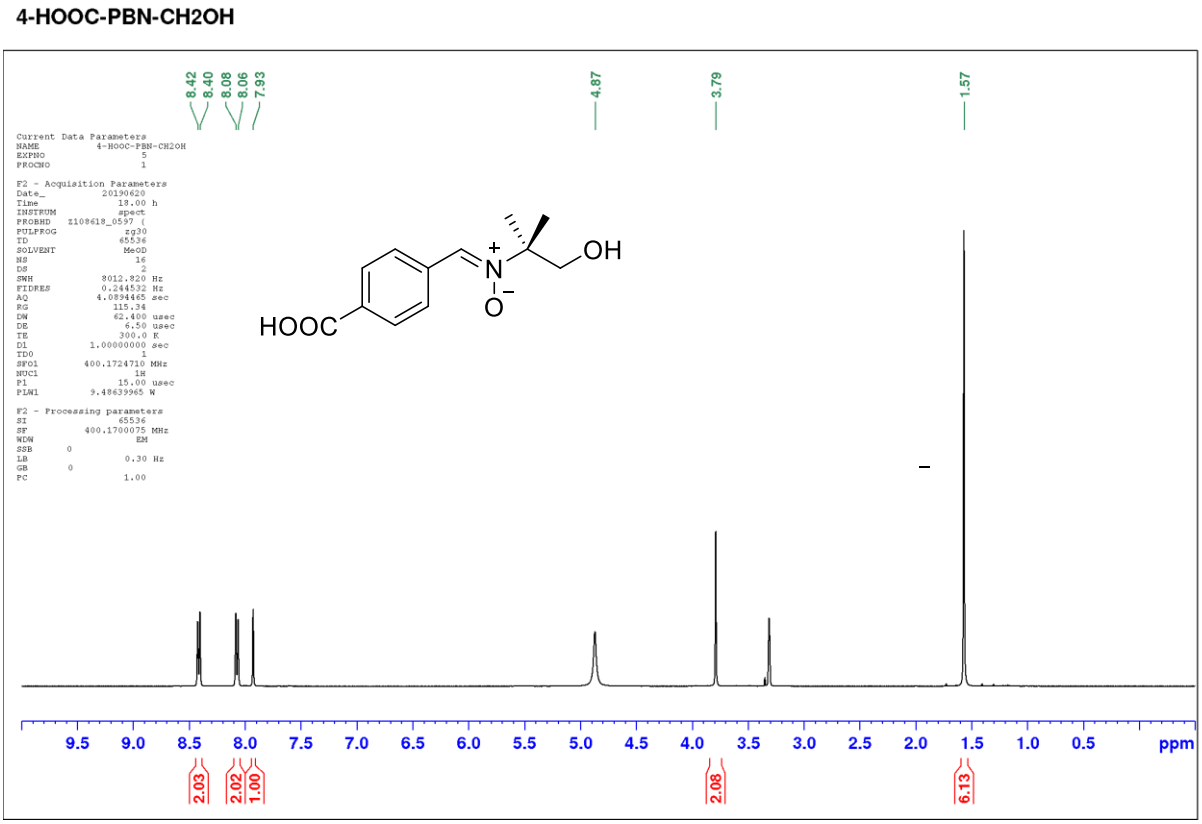

Figure S5. ^{1}H NMR spectrum of 4-HOOC-PBN-CH_2OH in MeOD.

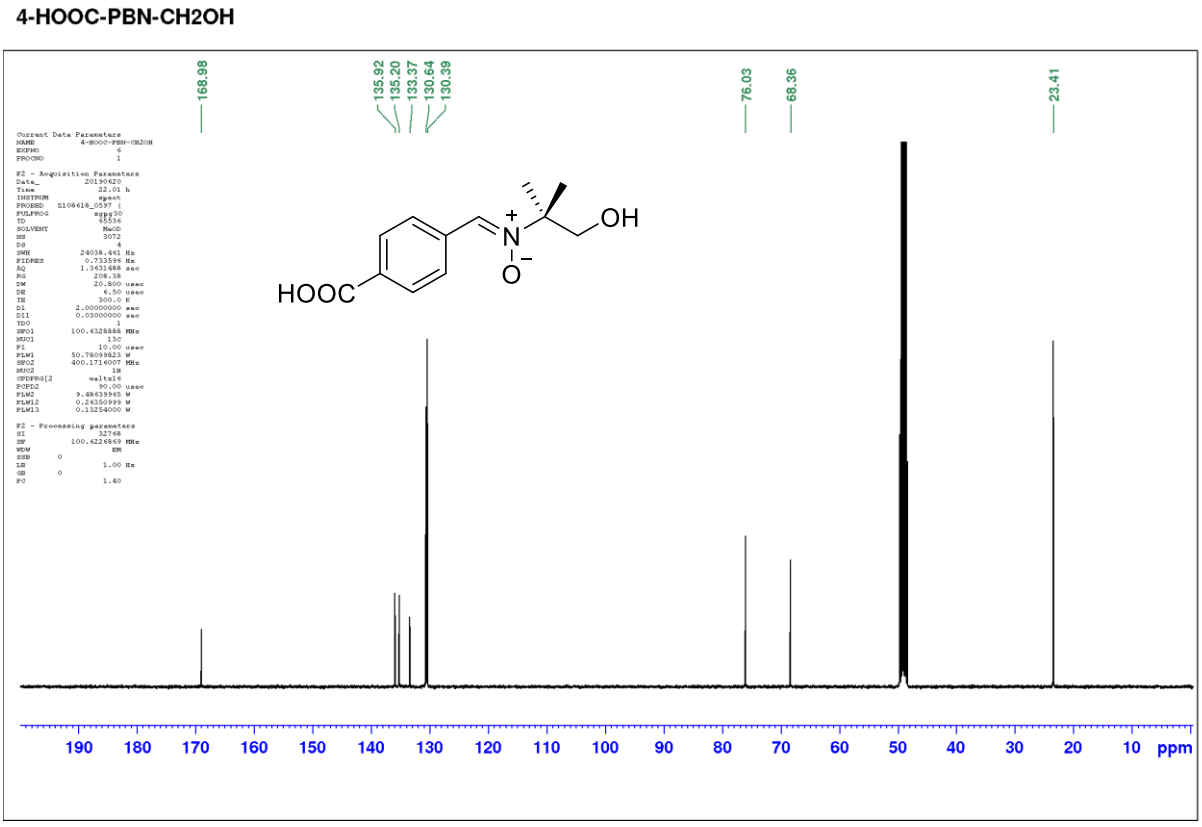

Figure S6. ^{13}C NMR spectrum of 4-HOOC-PBN-CH_2OH in MeOD.

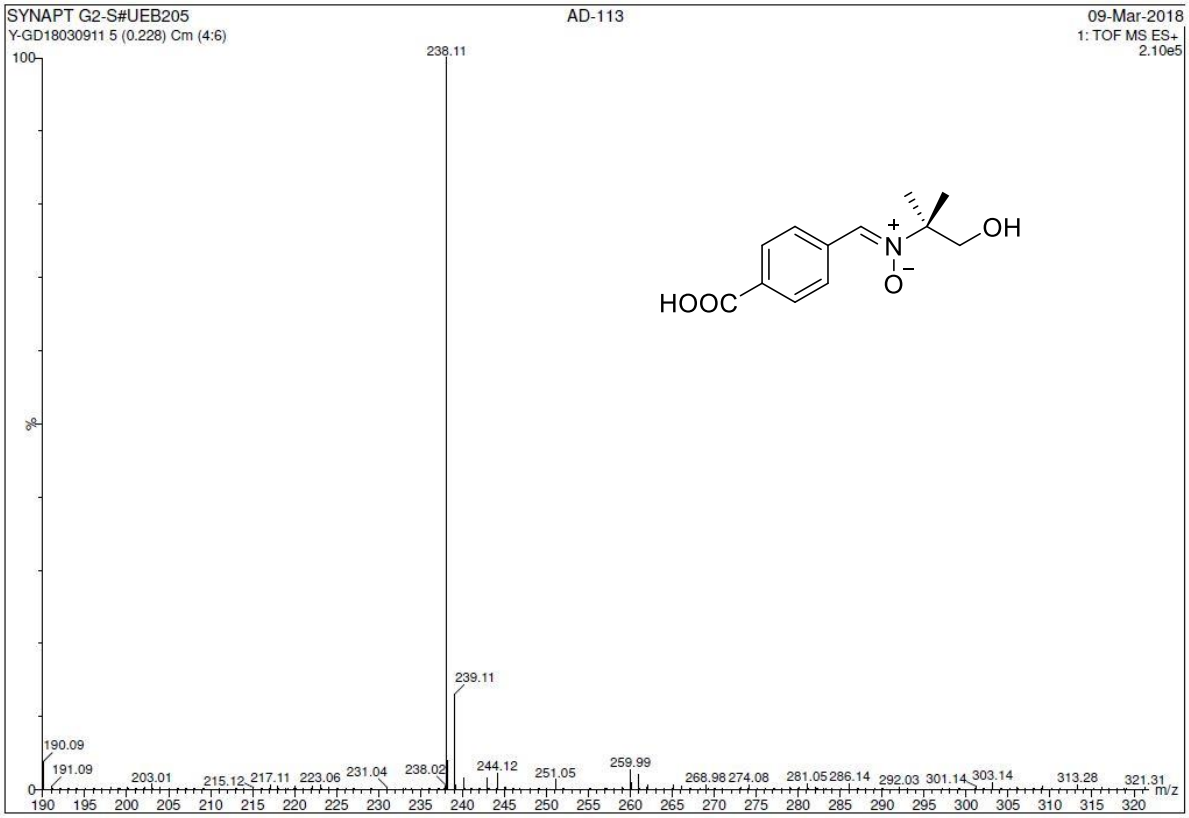

Figure S7. High-resolution mass spectrum of 4-HOOC-PBN-CH_2OH.

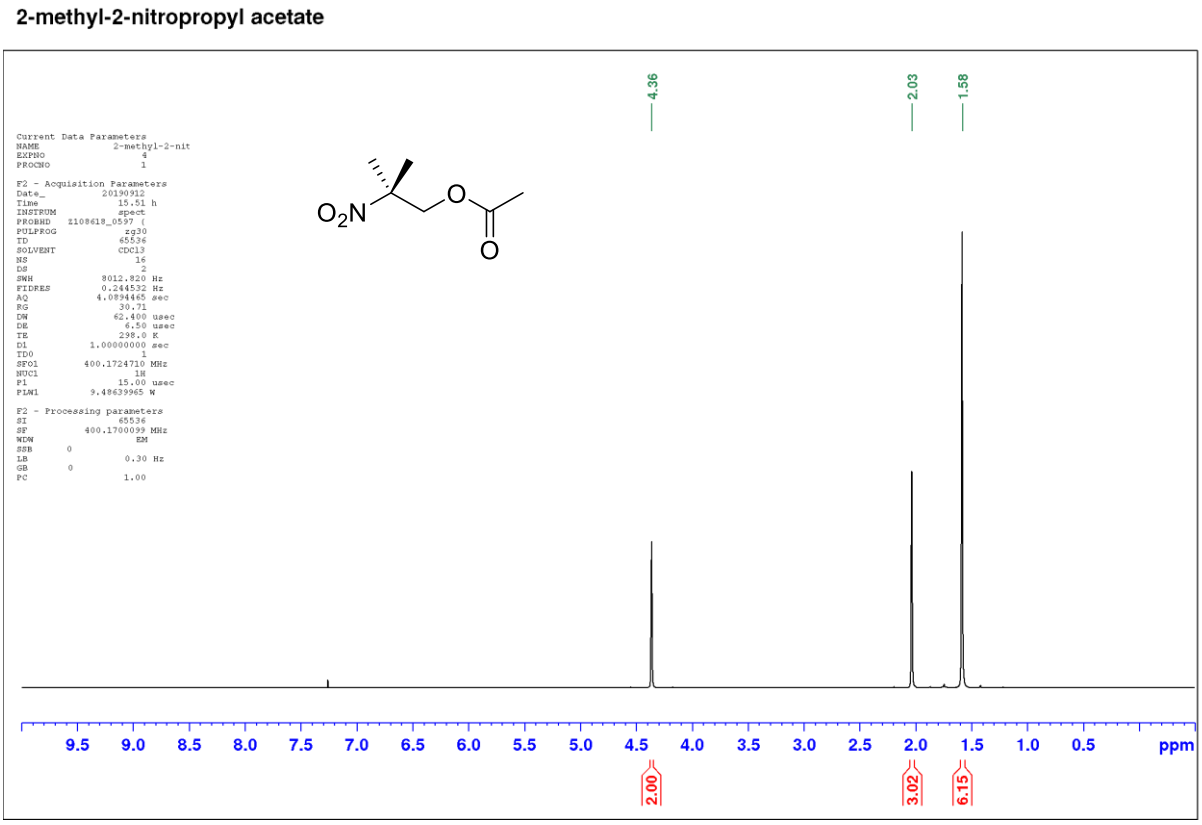

Figure S8. ^1H NMR spectrum of intermediate **15** in $CDCl_3$.

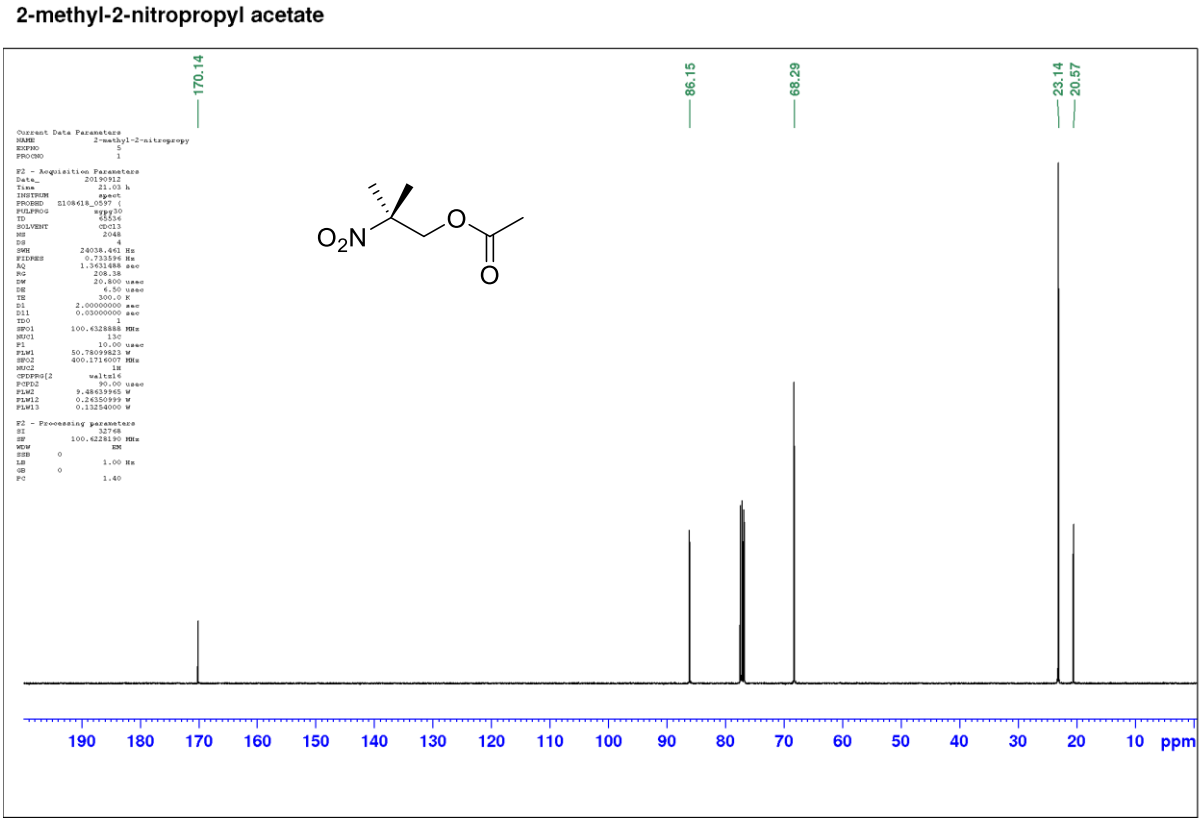

Figure S9. ^{13}C NMR spectrum of intermediate **15** in $CDCl_3$.

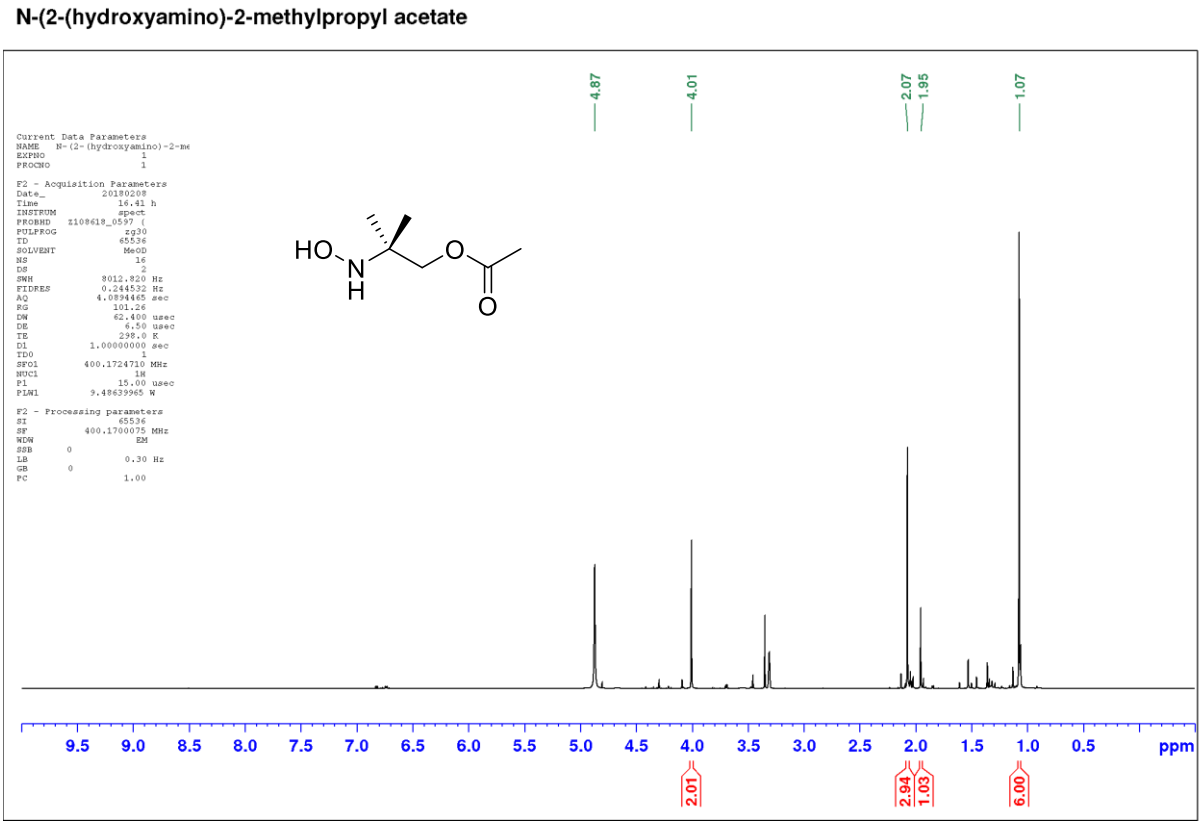

Figure S10. ^{1}H NMR spectrum of intermediate **16** in MeOD.

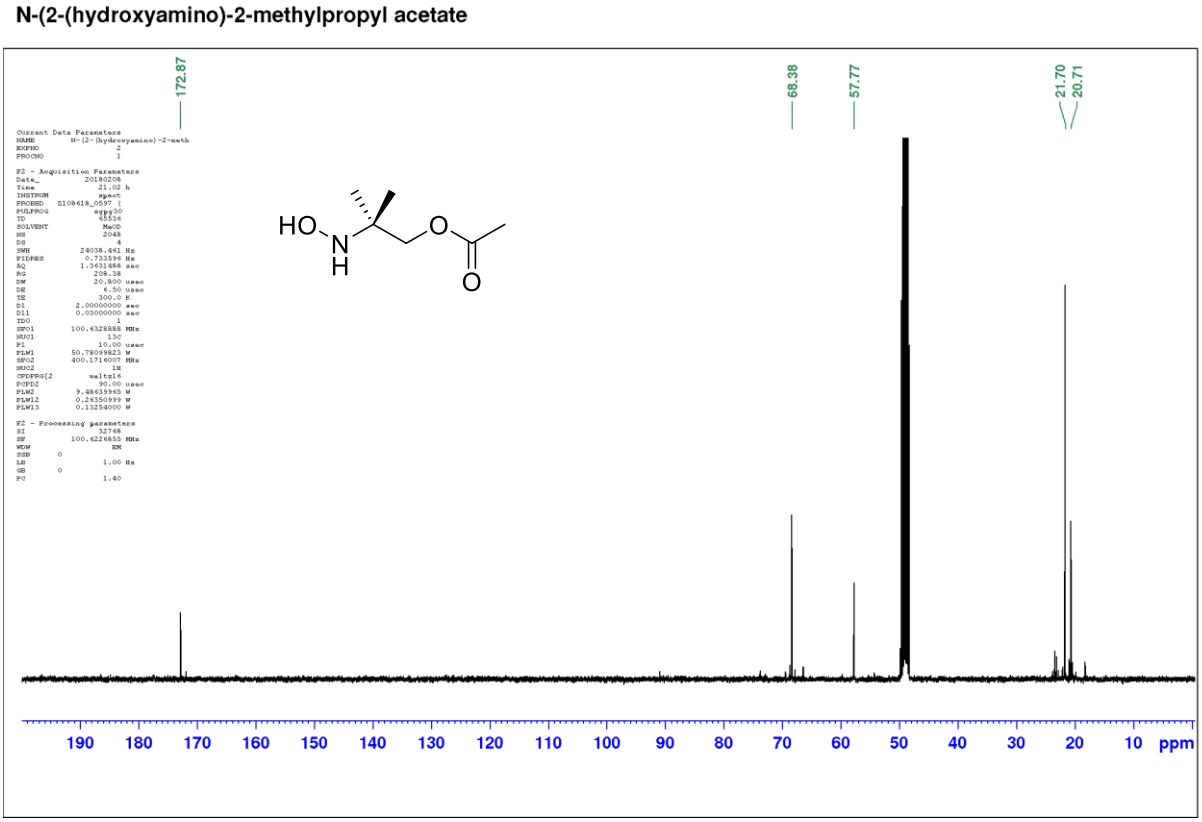

Figure S11. ^{13}C NMR spectrum of intermediate **16** in MeOD.

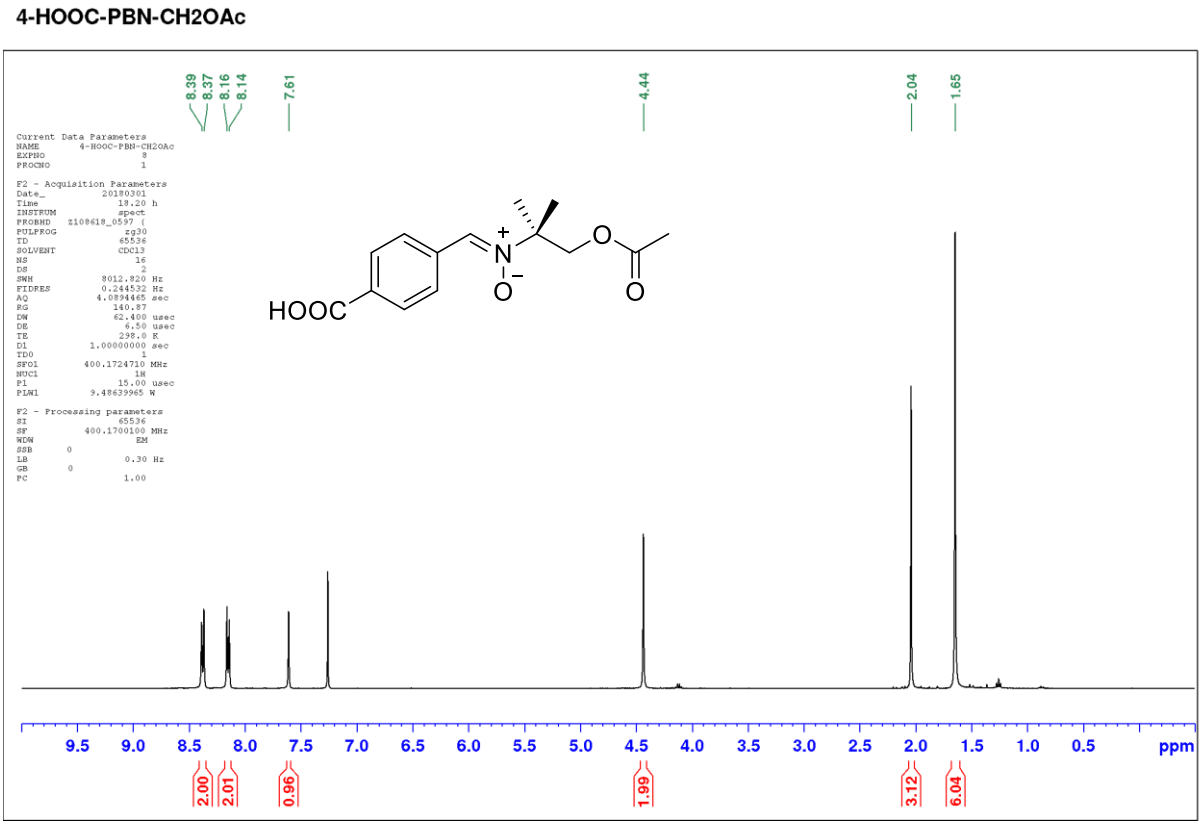

Figure S12. ^{1}H NMR spectrum of 4-HOOC-PBN-CH_2OAc in $CDCl_3$.

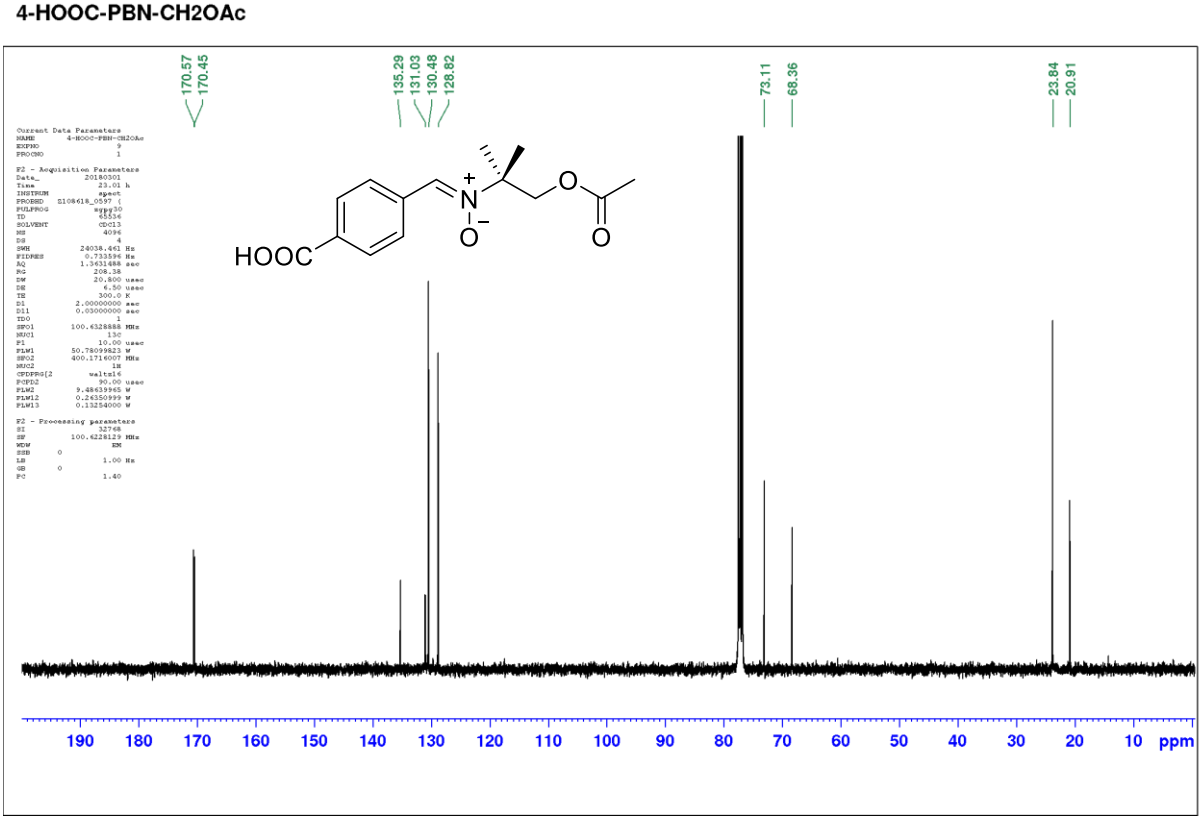

Figure S13. ^{13}C NMR spectrum of 4-HOOC-PBN-CH_2OAc in $CDCl_3$.

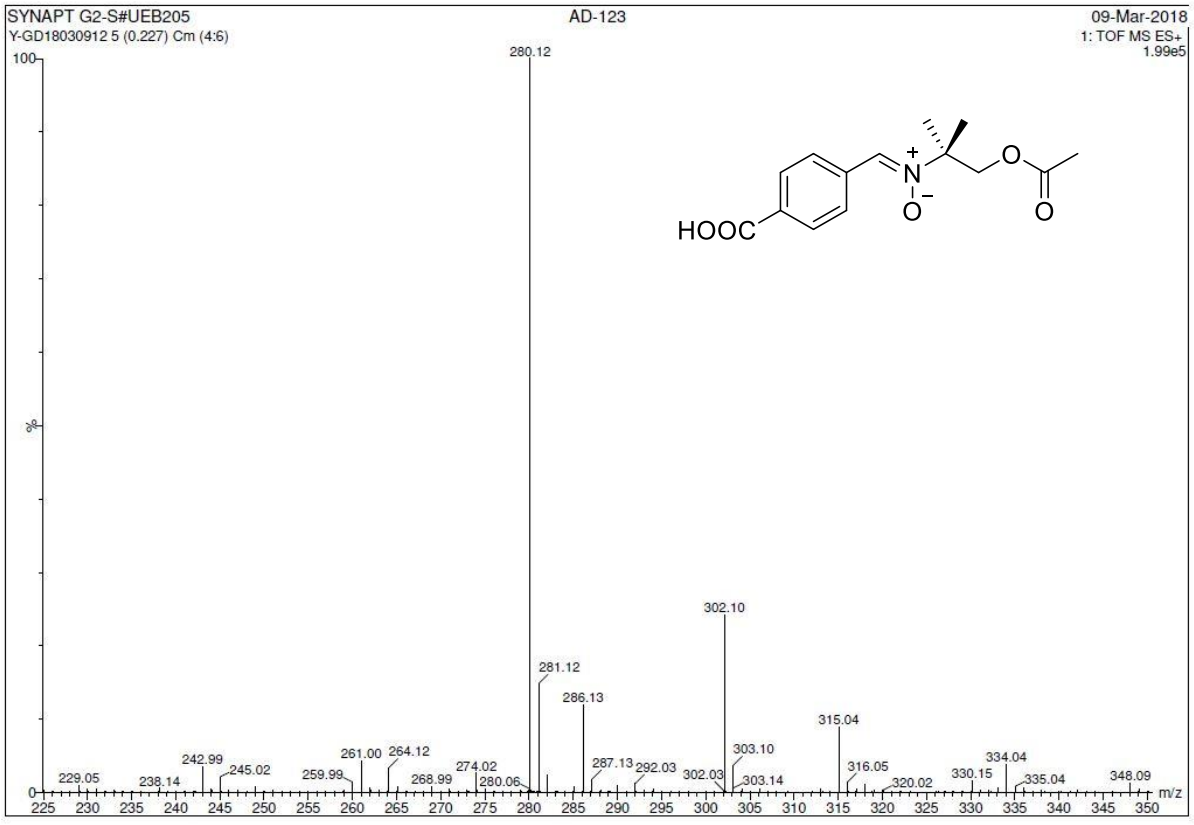

Figure S14. High-resolution mass spectrum of 4-HOOC-PBN-CH_2OAc.

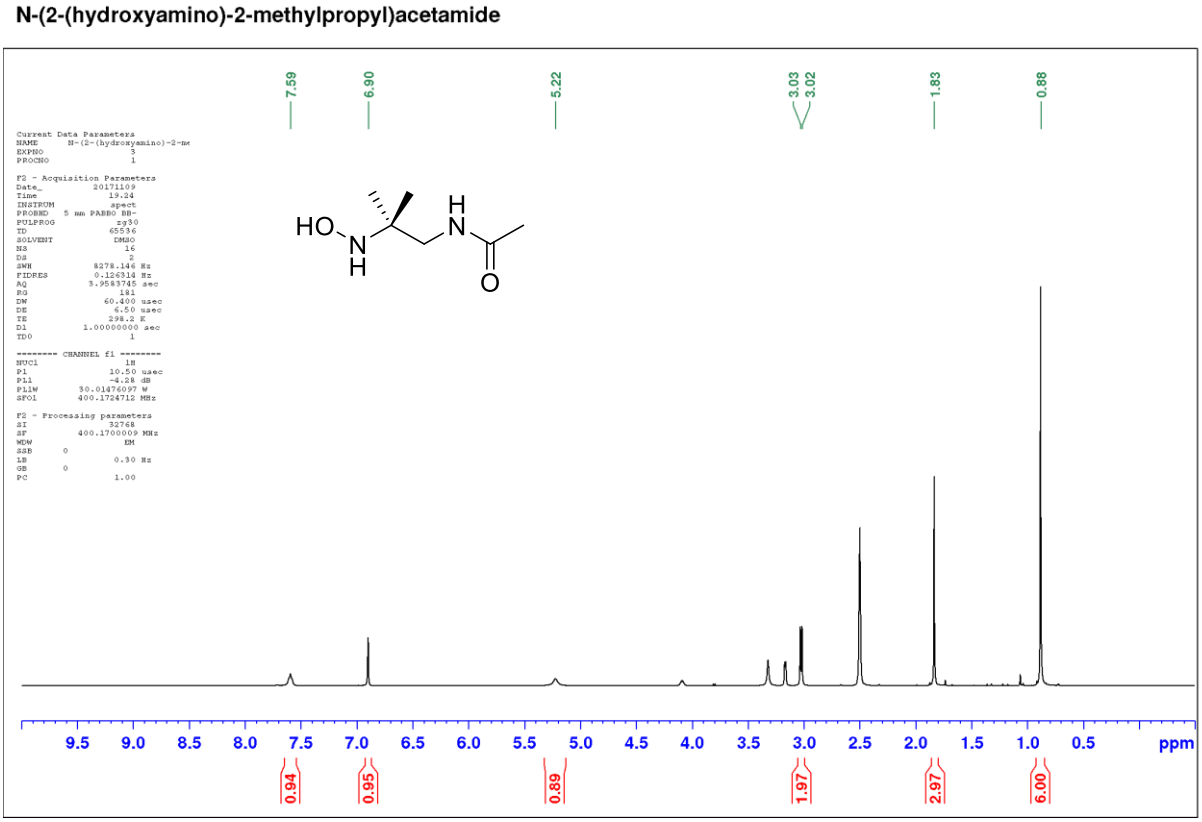

Figure S15. ^{1}H NMR spectrum of intermediate **18** in DMSO-d6.

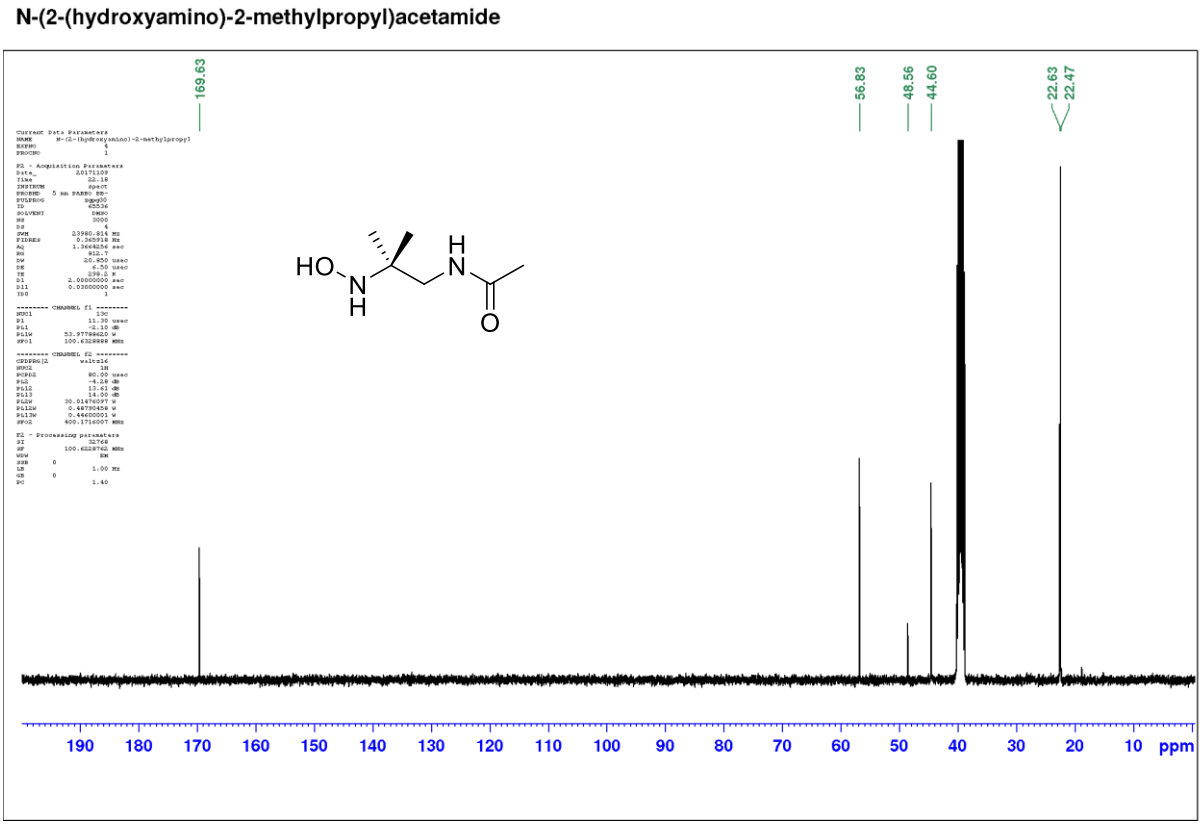

Figure S16. ^{13}C NMR spectrum of intermediate **18** in DMSO-d6.

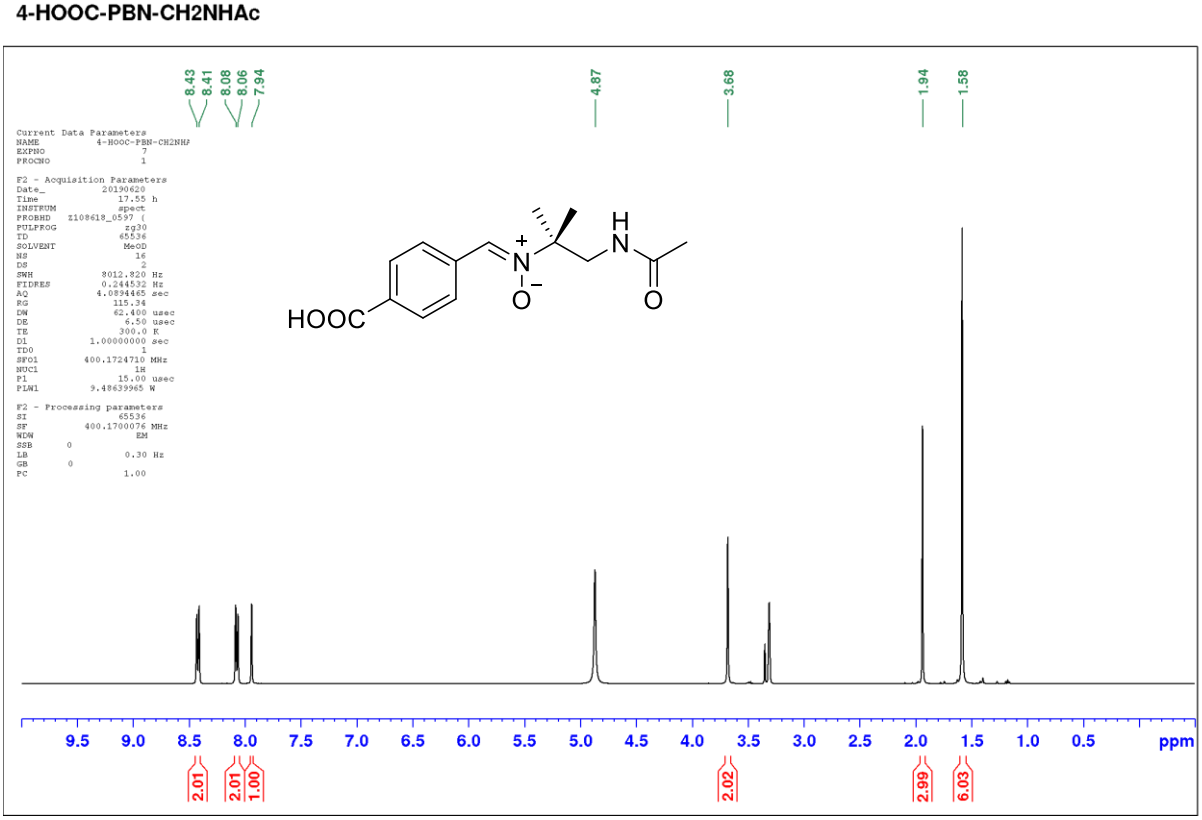

Figure S17. ^{1}H NMR spectrum of 4-HOOC-PBN-CH_2NHAc in MeOD.

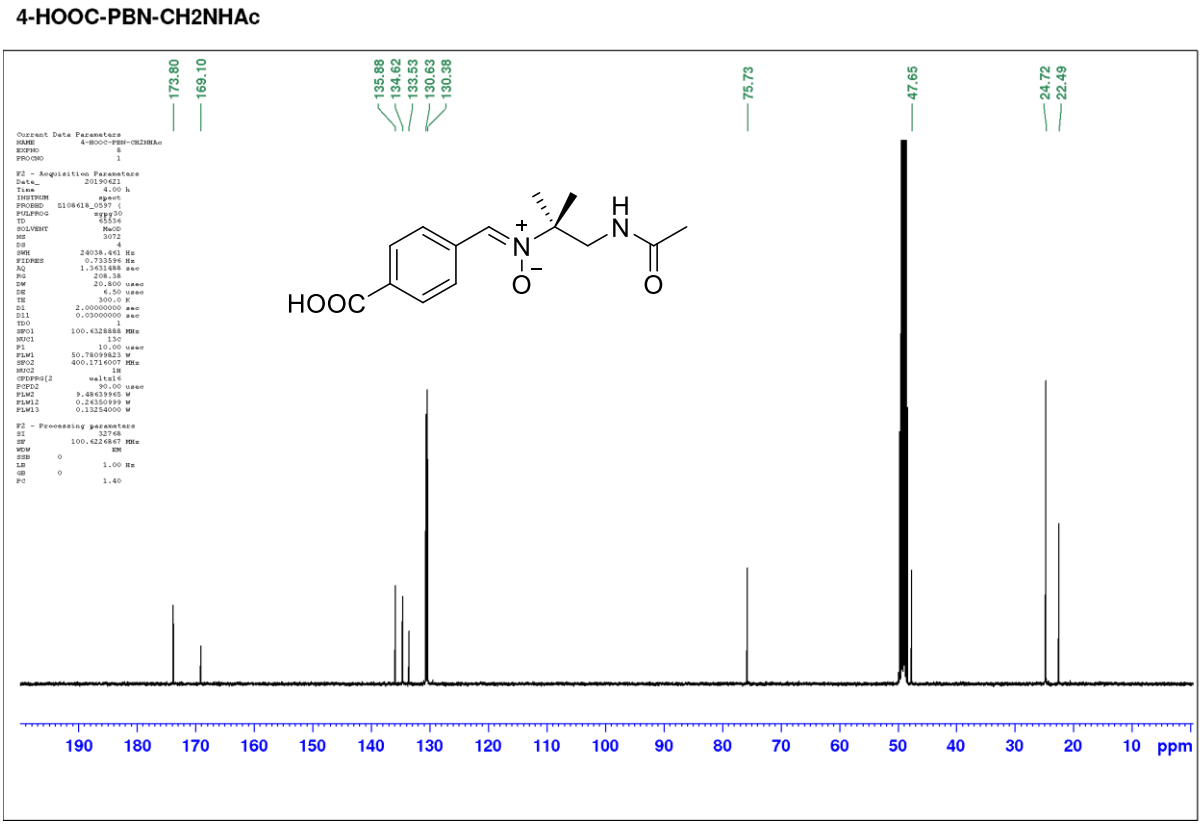

Figure S18. ^{13}C NMR spectrum of 4-HOOC-PBN-CH_2NHAc in MeOD.

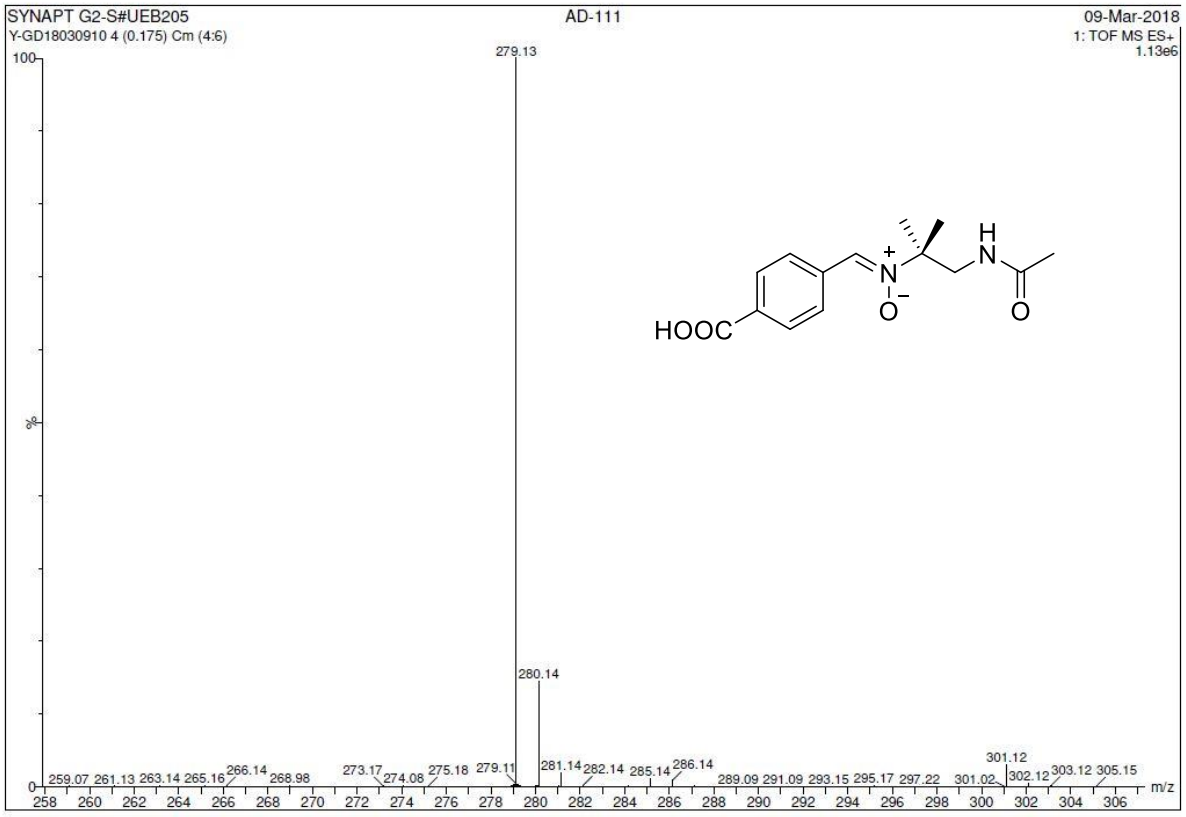

Figure S19. High-resolution mass spectrum of 4-HOOC-PBN-CH_2NHAc.

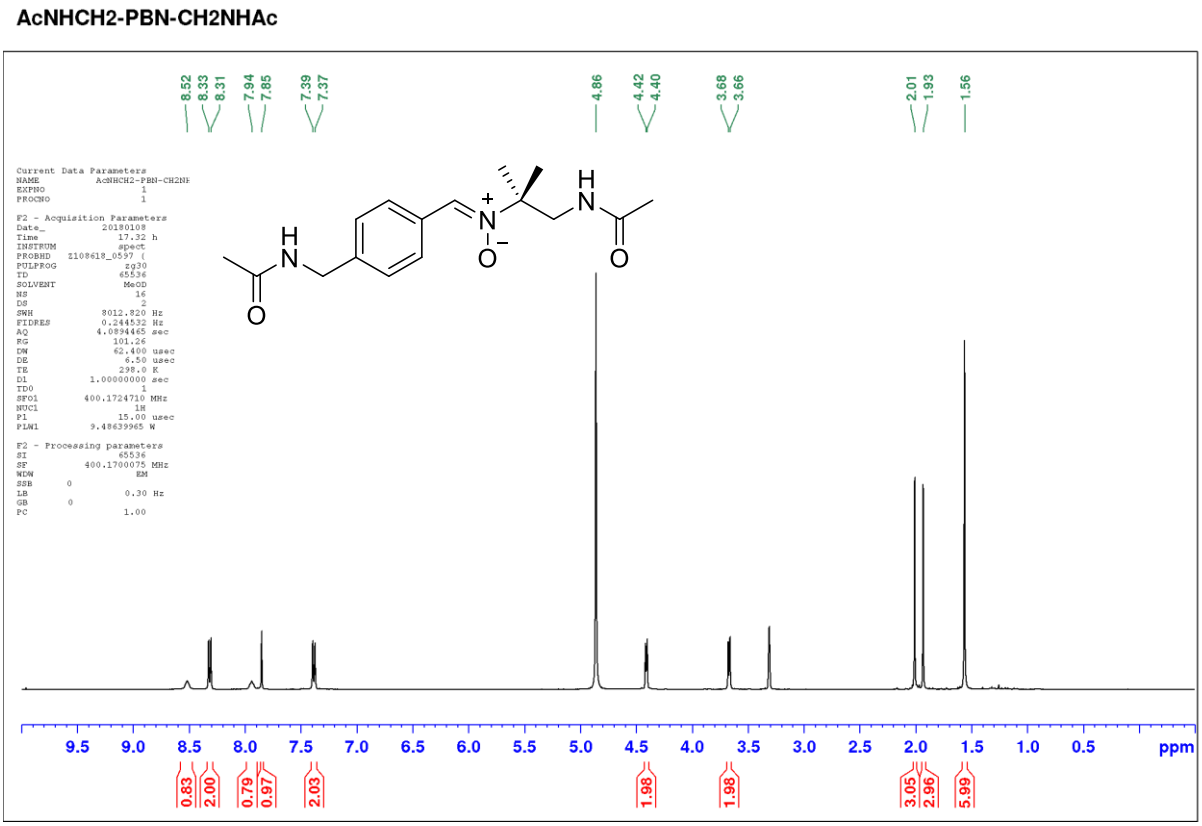

Figure S20. ^{1}H NMR spectrum of 4-AcNHCH_2-PBN-CH_2NHAc in MeOD.

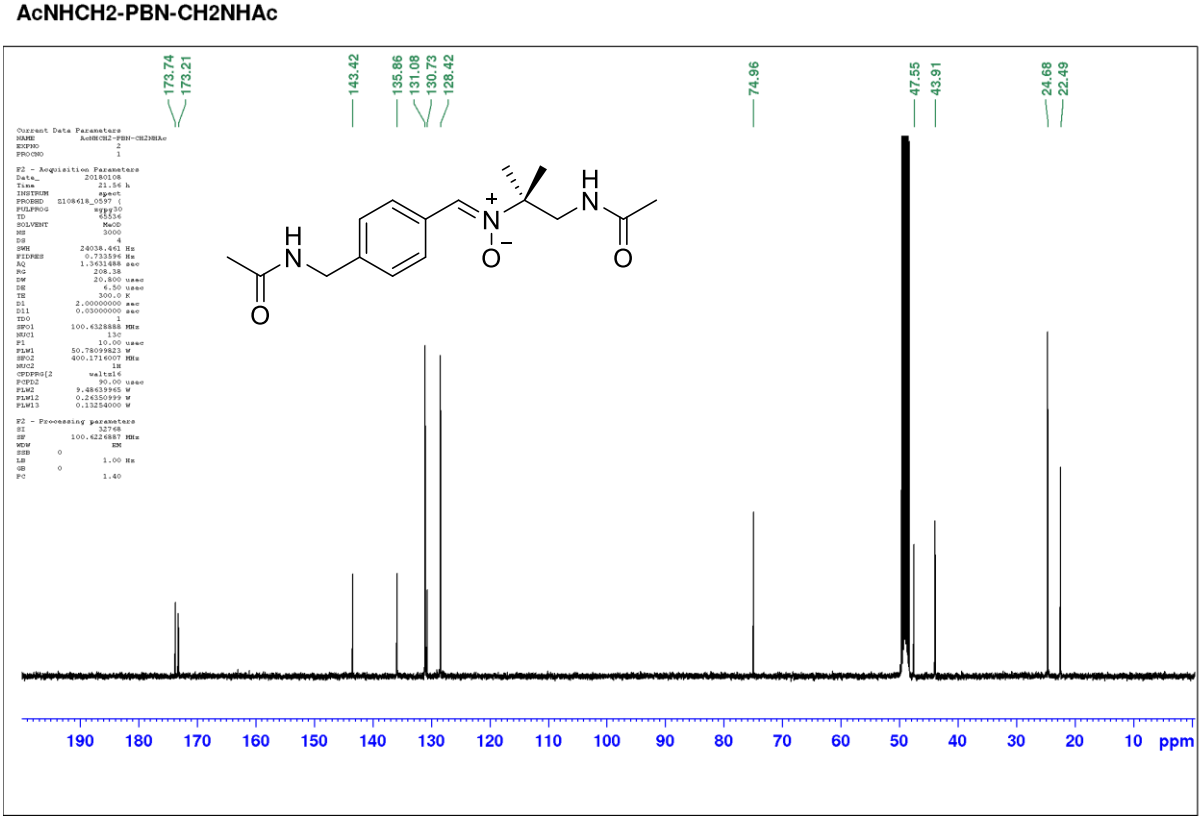

Figure S21. ^{13}C NMR spectrum of 4-AcNHCH$_2$-PBN-CH$_2$NHAc in MeOD.

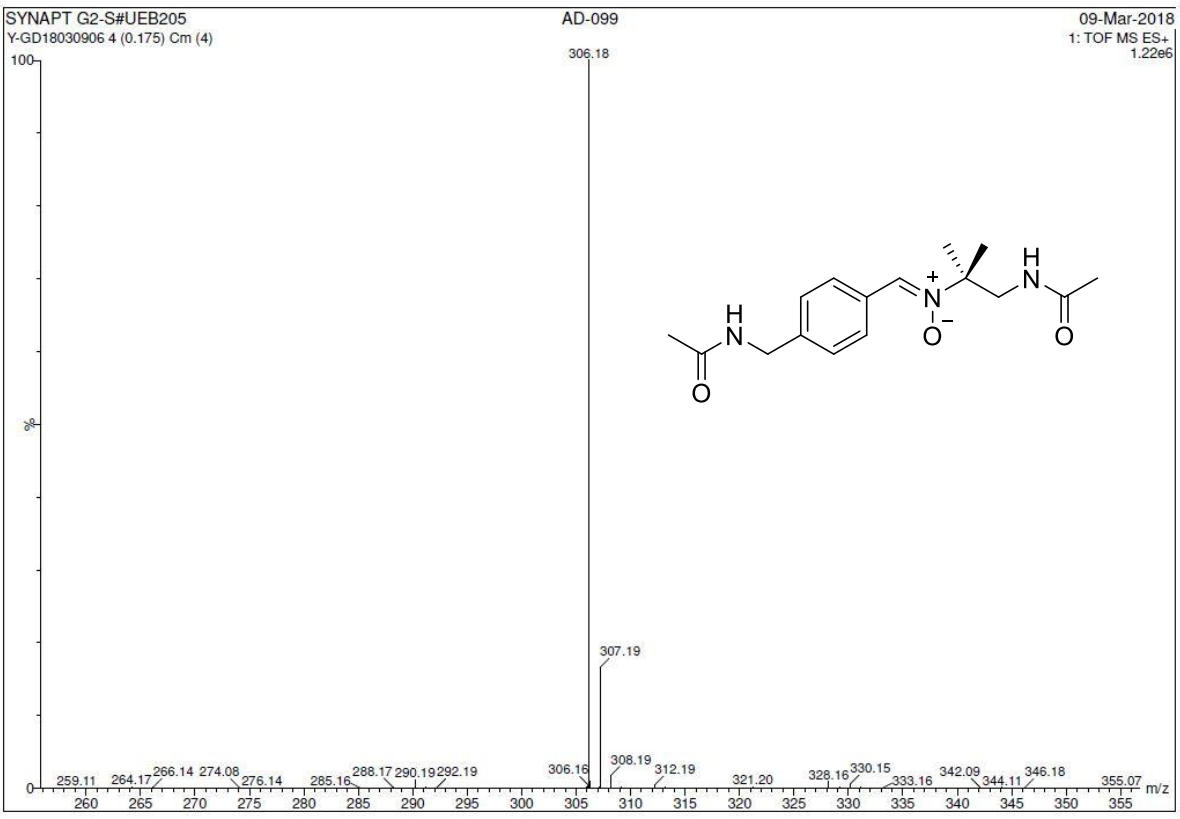

Figure S22. High-resolution mass spectrum of 4-AcNHCH$_2$-PBN-CH$_2$NHAc.

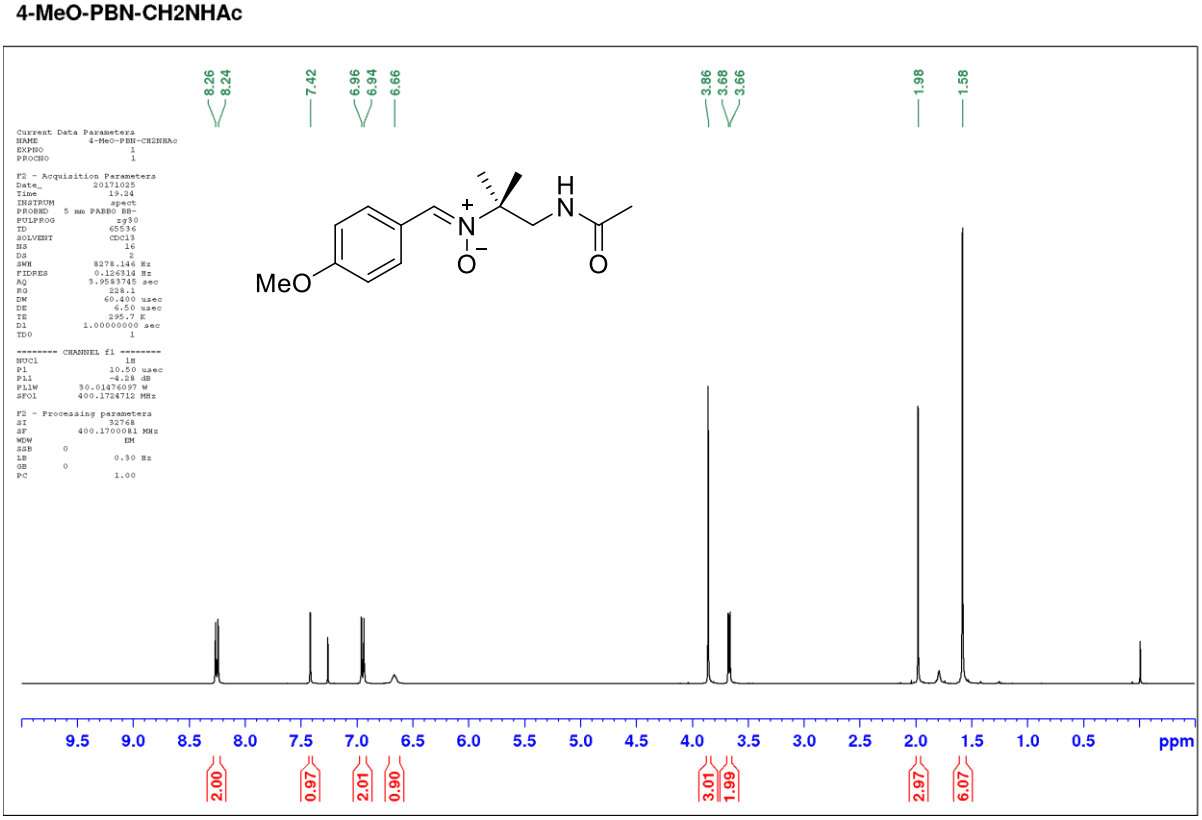

Figure S23. ^{1}H NMR spectrum of 4-MeO-PBN-CH_2NHAc in $CDCl_3$.

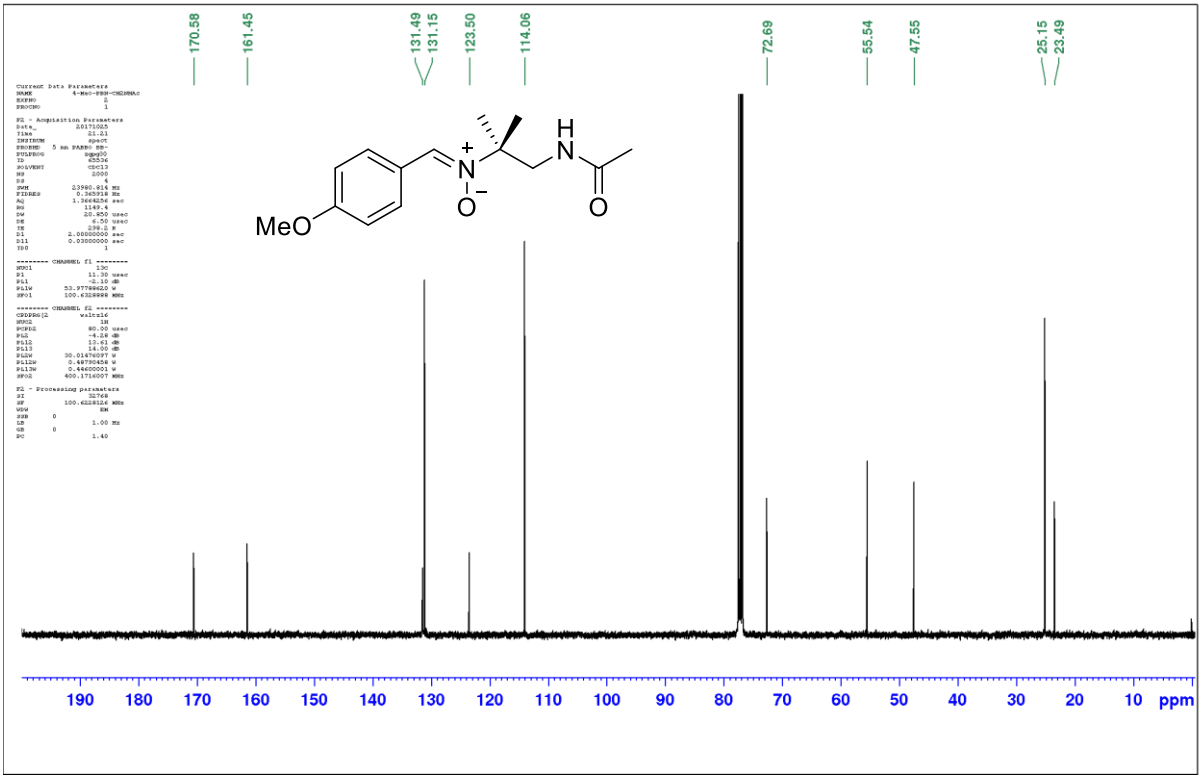

Figure S24. ^{13}C NMR spectrum of 4-MeO-PBN-CH_2NHAc in $CDCl_3$.

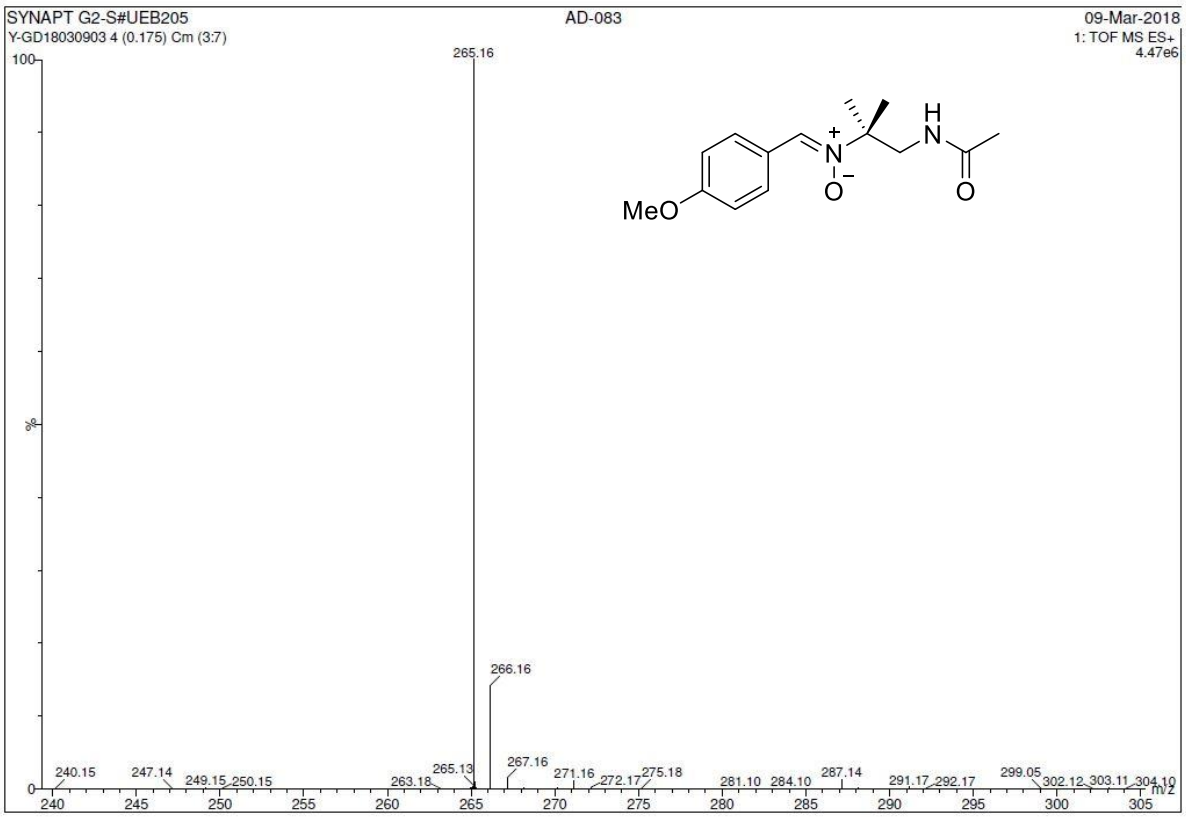

Figure S25. High-resolution mass spectrum of 4-MeO-PBN-CH_2NHAc.

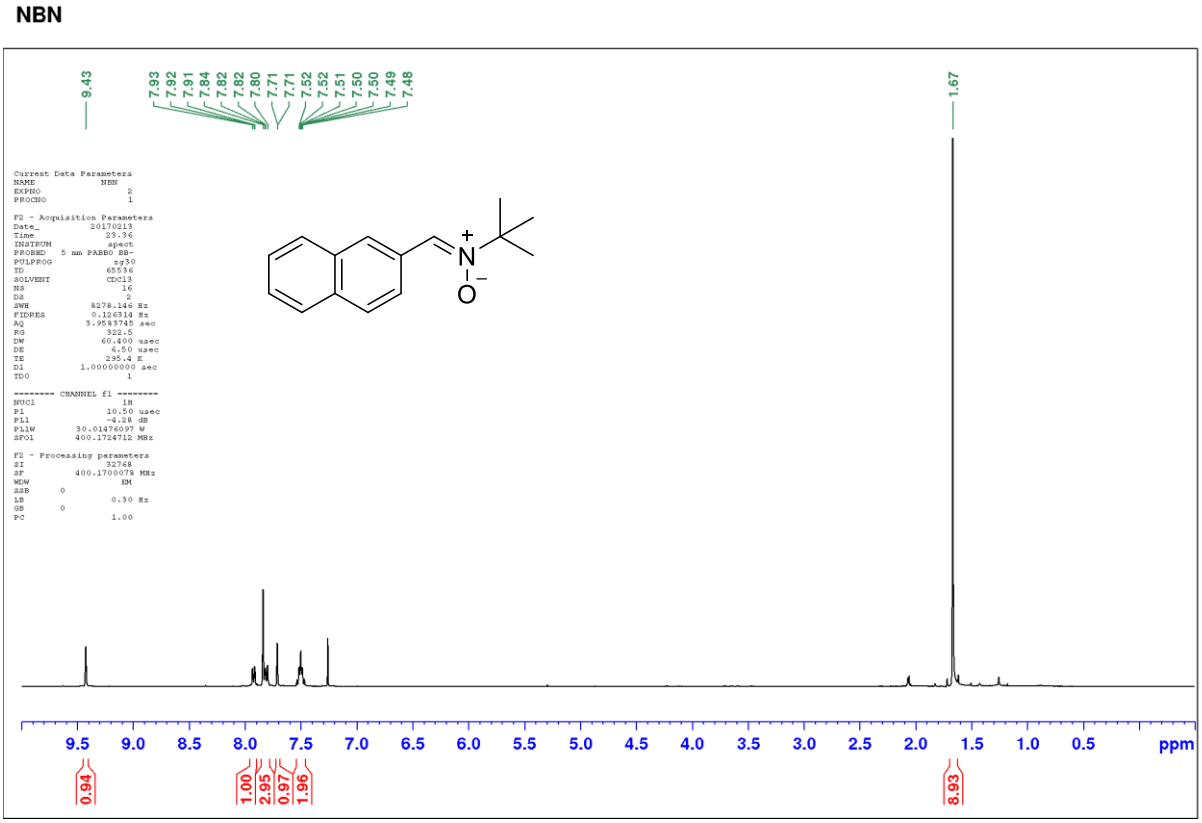

Figure S26. ^{1}H NMR spectrum of NBN in $CDCl_3$.

NBN

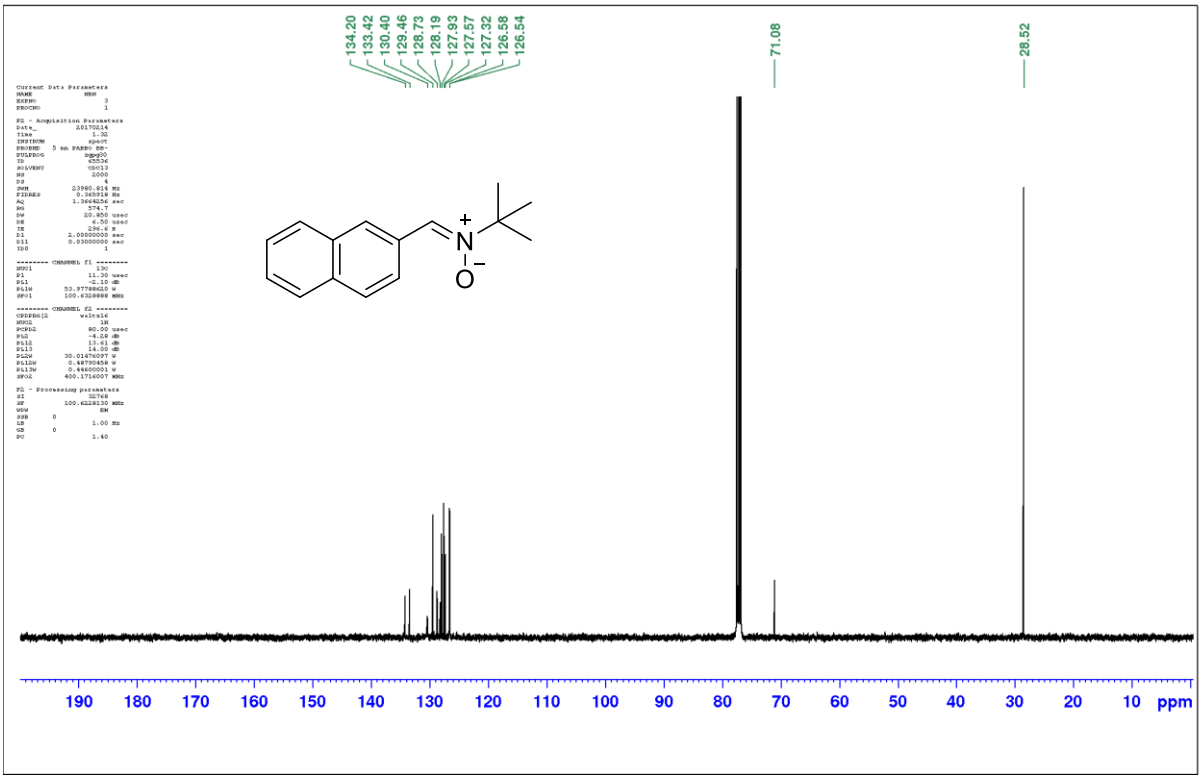

Figure S27. ^{13}C NMR spectrum of NBN in $CDCl_3$.

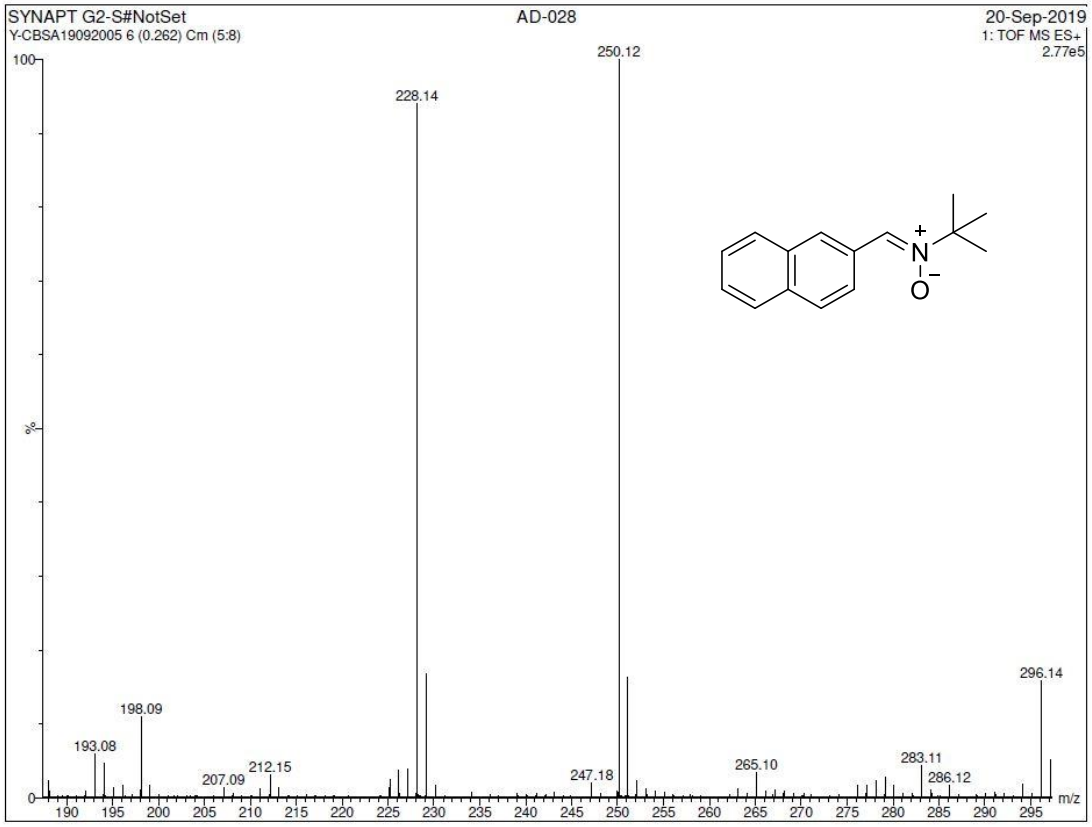

Figure S28. High-resolution mass spectrum of NBN.

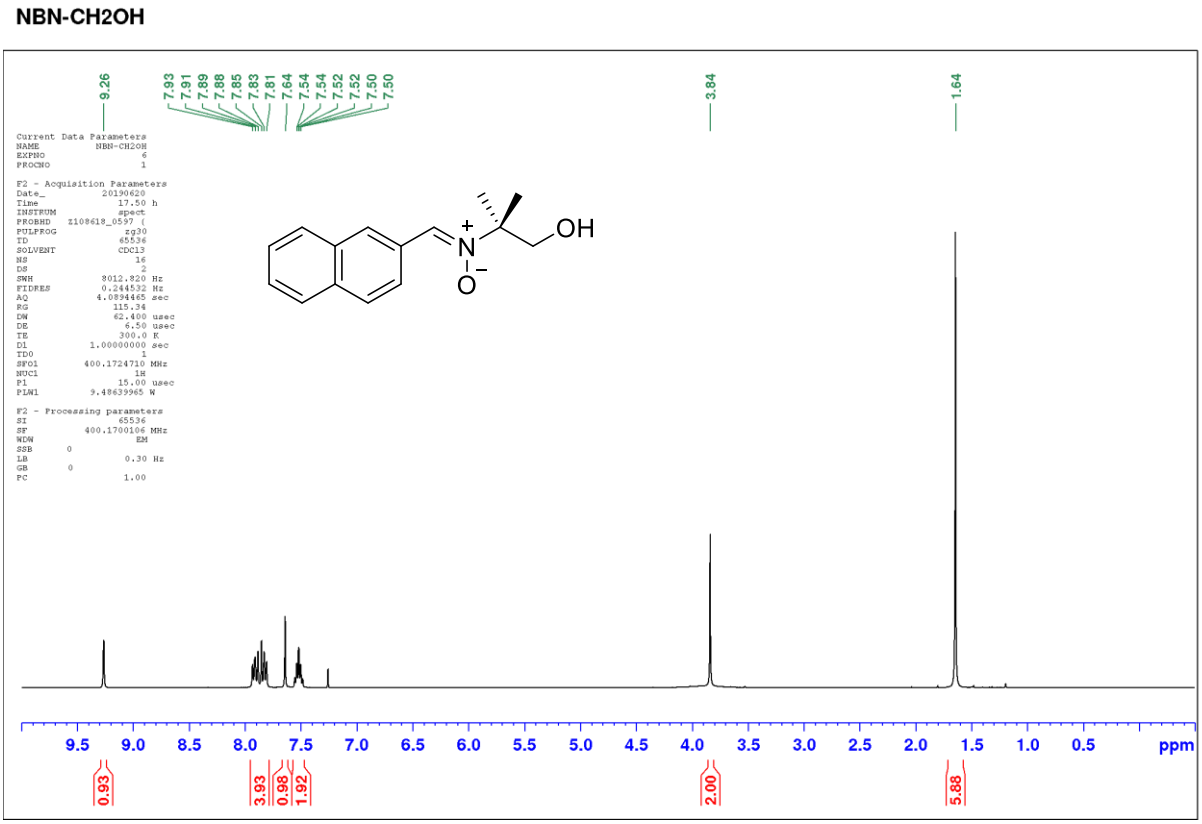

Figure S29. ^{1}H NMR spectrum of NBN-CH_2OH in $CDCl_3$.

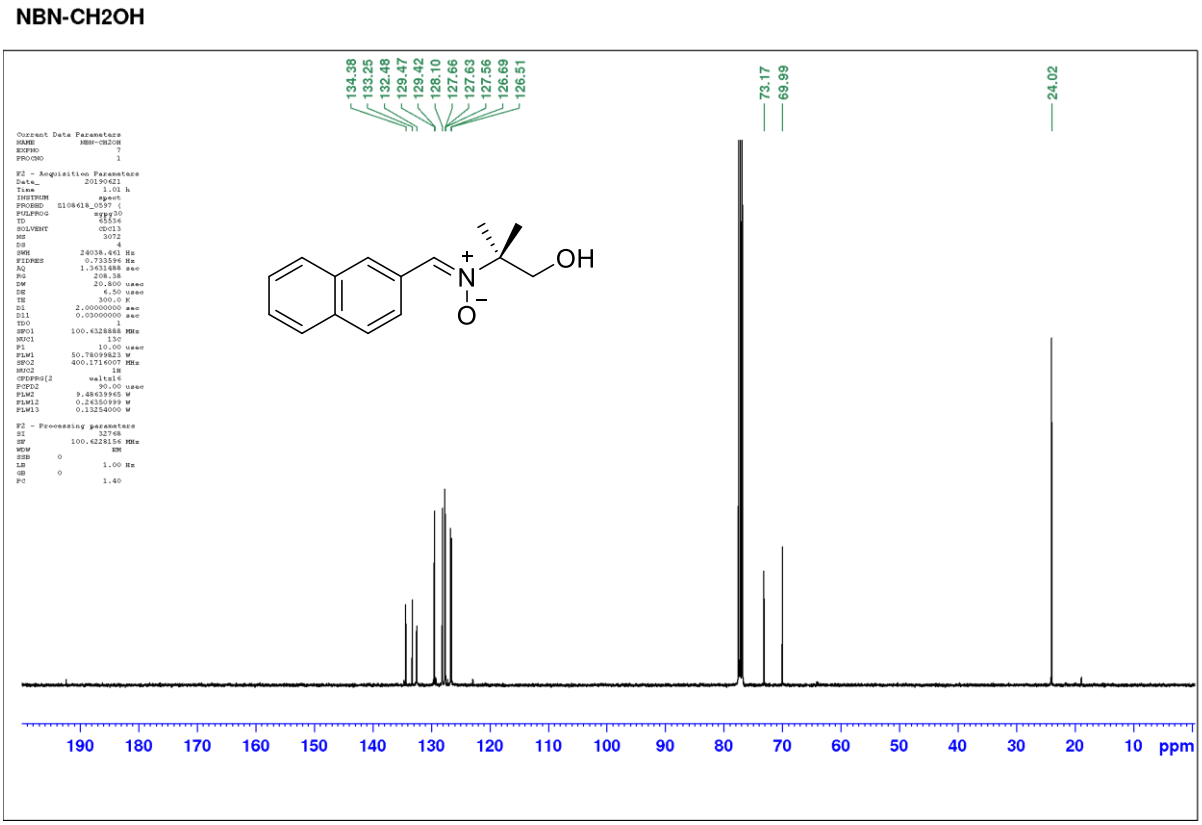

Figure S30. ^{13}C NMR spectrum of NBN-CH_2OH in $CDCl_3$.

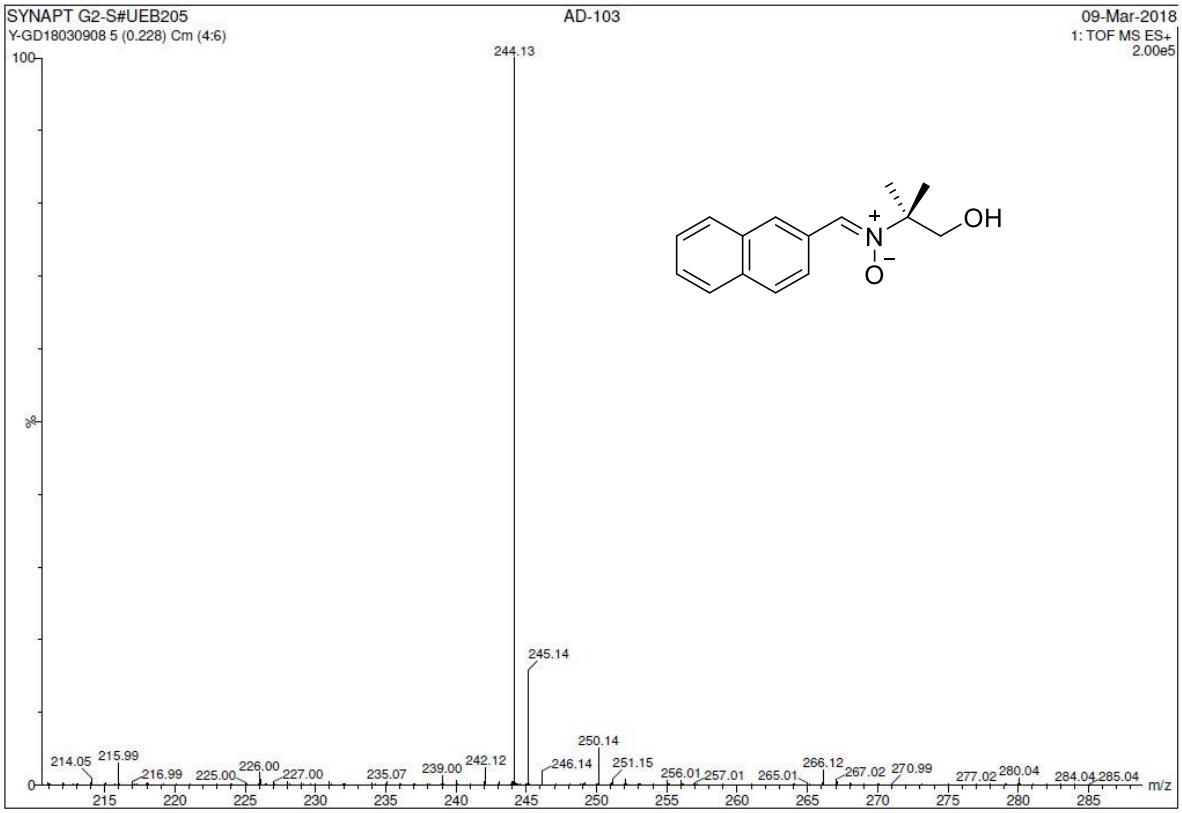

Figure S31. High-resolution mass spectrum of NBN-CH_2OH.

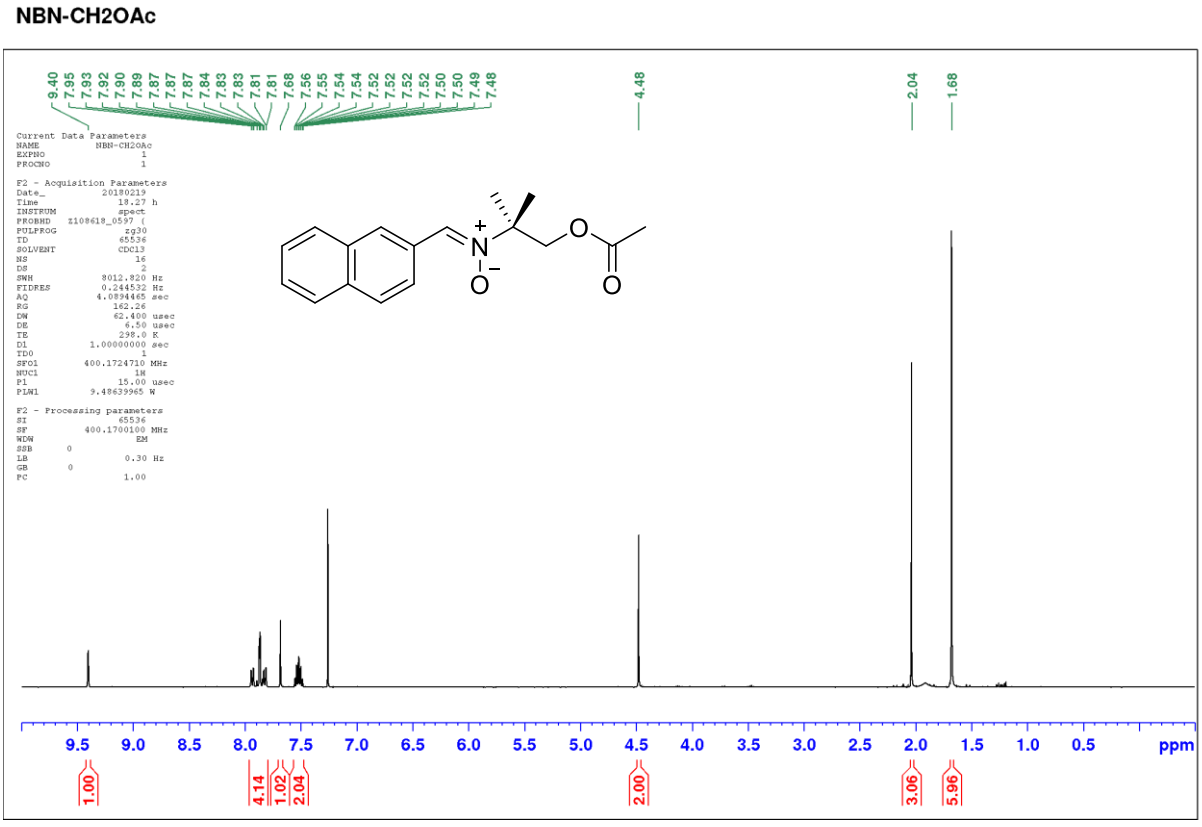

Figure S32. ^1H NMR spectrum of NBN-CH_2OAc in $CDCl_3$.

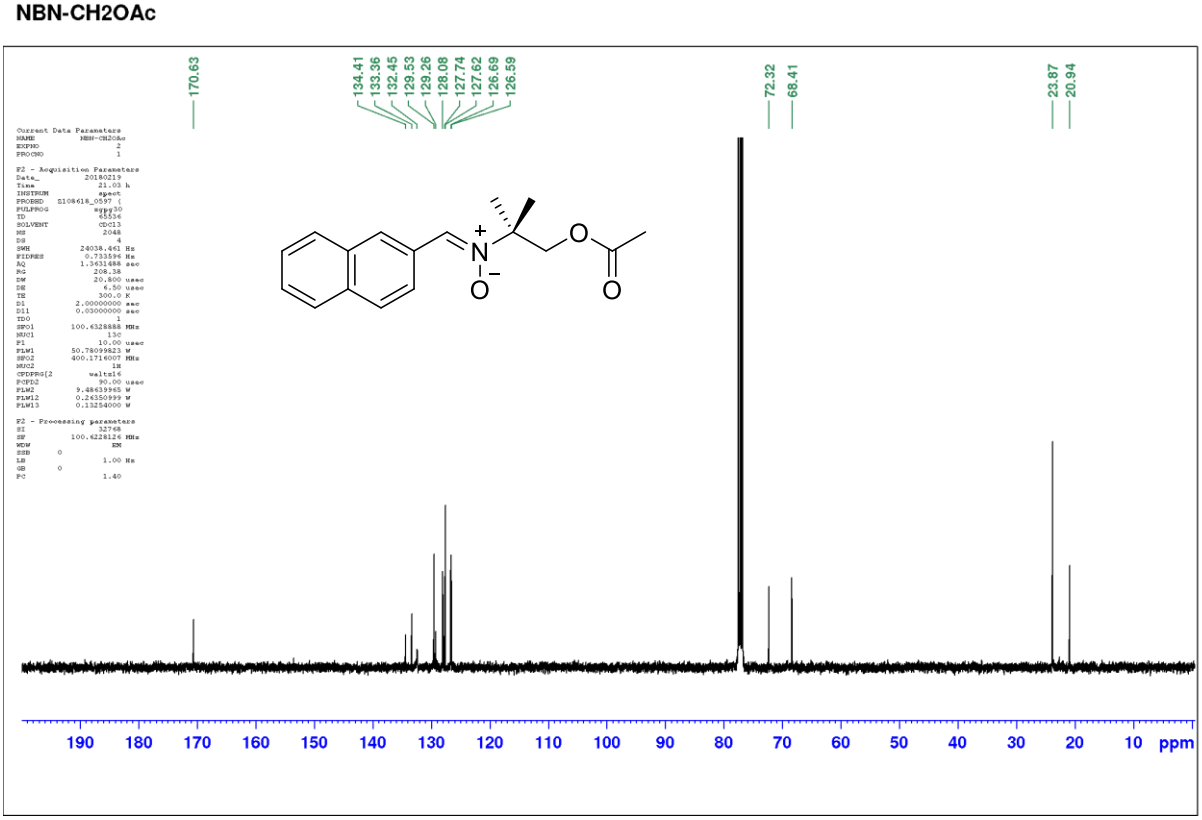

Figure S33. ^{13}C NMR spectrum of NBN-CH_2OAc in $CDCl_3$.

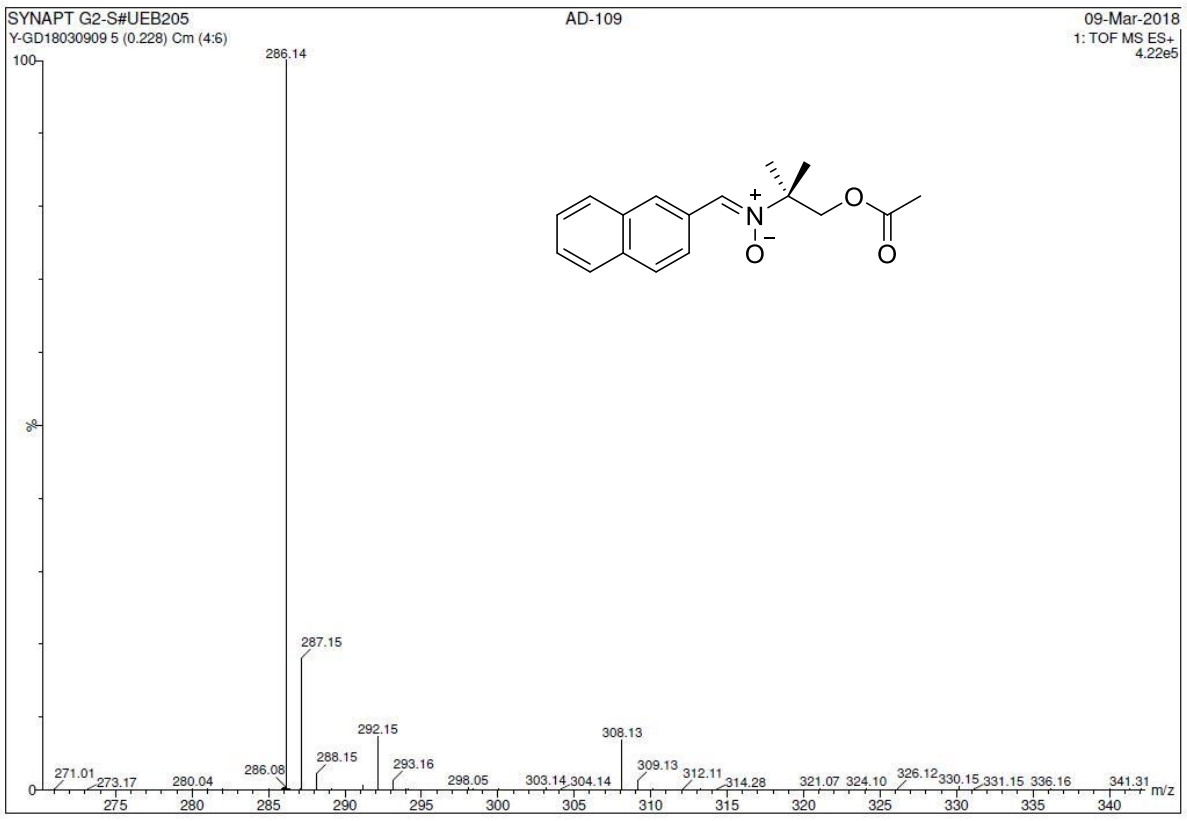

Figure S34. High-resolution mass spectrum of NBN-CH_2OAc.

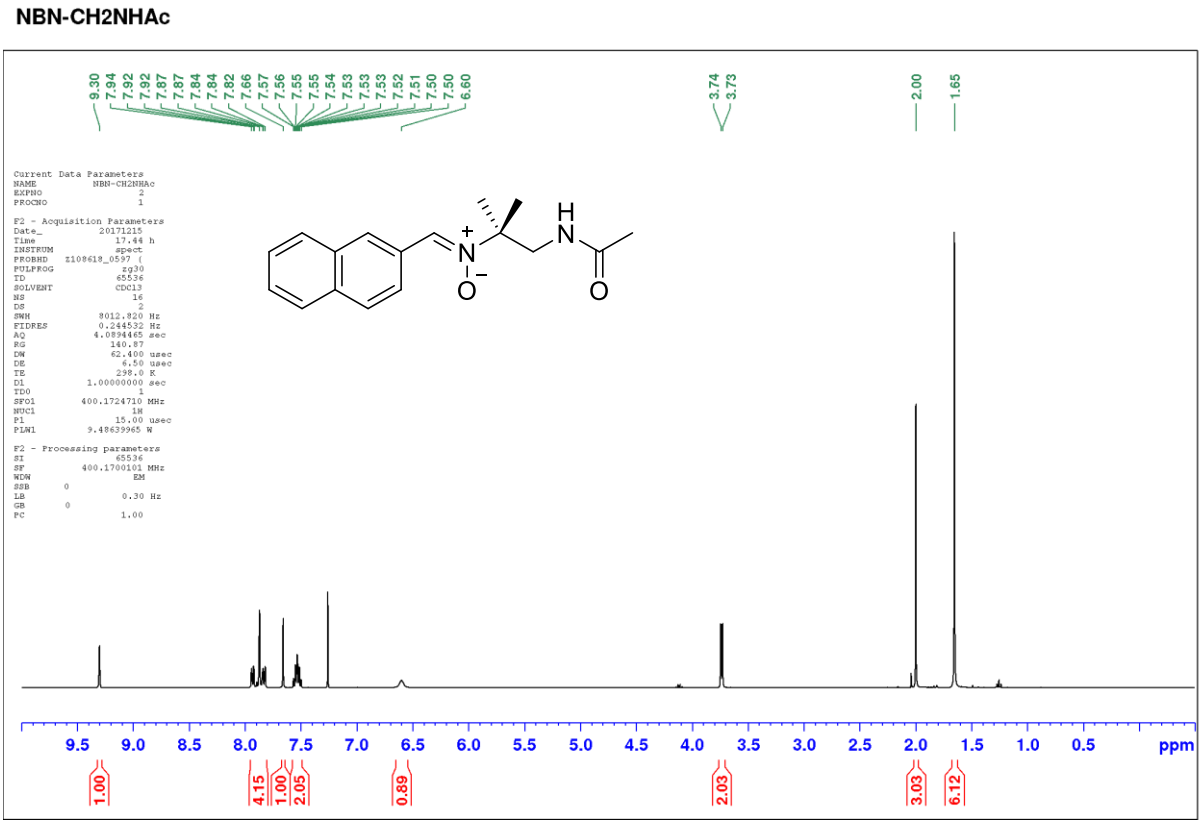

Figure S35. ^{1}H NMR spectrum of NBN-CH_2NHAc in $CDCl_3$.

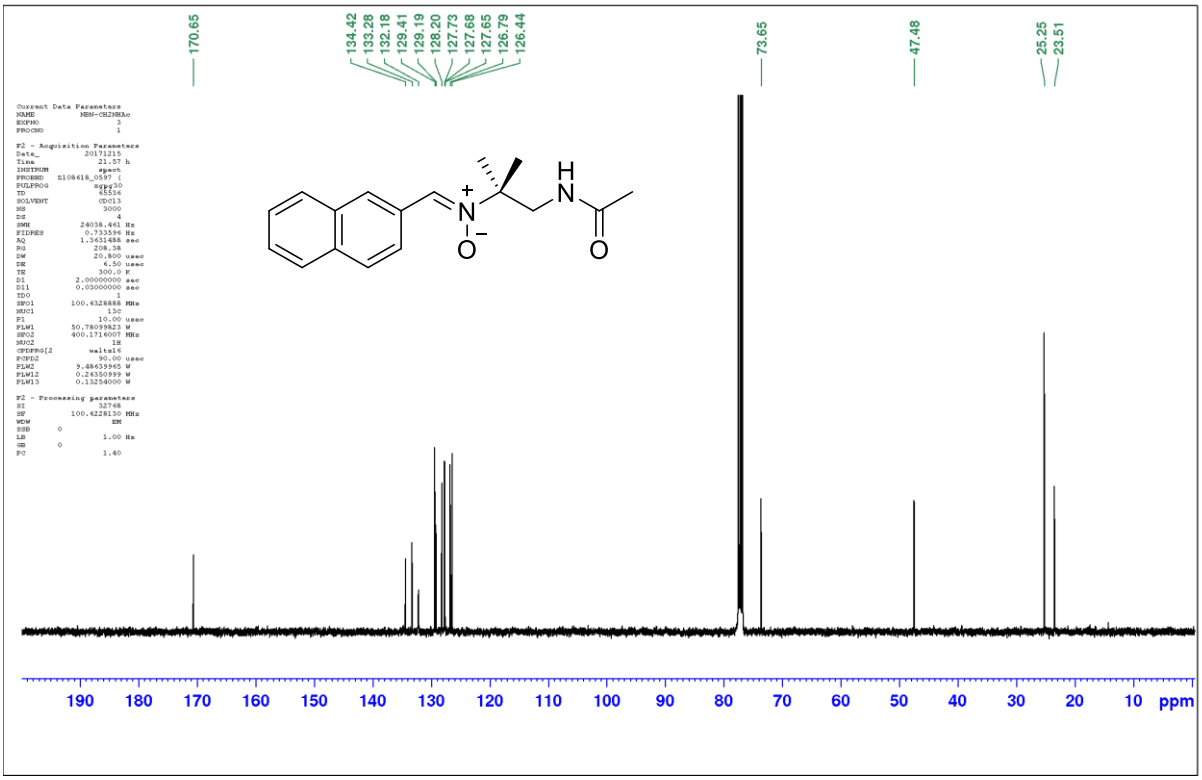

Figure S36. ^{13}C NMR spectrum of NBN-CH_2NHAc in $CDCl_3$.

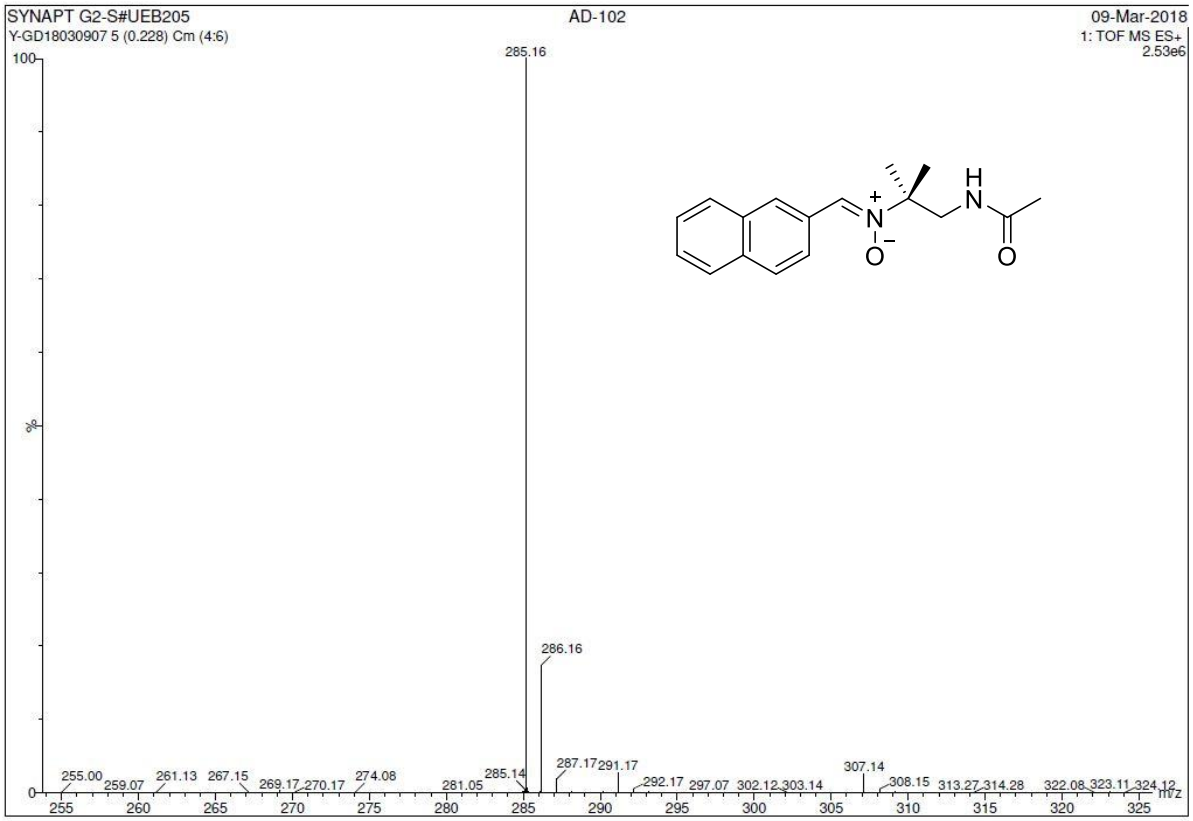

Figure S37. High-resolution mass spectrum of NBN-CH_2NHAc.

Discussion générale et Perspectives

Discussion générale et Perspectives

Table des matières

1. Objectifs du projet de thèse

Dans le cadre de cette thèse, nous nous sommes intéressés à l'α-phenyl-*N*-*tert*-butyl nitrone (PBN), une nitrone linéaire qui possède une bonne distribution cellulaire et tissulaire et qui a montré de nombreux effets protecteurs vis-à-vis du stress oxydant dans différents modèles d'étude *in vitro* et *in vivo*. La PBN permet une fonctionnalisation relativement aisée de part et d'autre de la fonction nitronyle, à la fois sur le cycle phényle et sur la partie *N*-*tert*-butyle, donnant accès à une grande variété de dérivés. Au cours de cette thèse nous nous sommes donc intéressés à la synthèse et à l'étude d'analogues de la PBN afin :

- De répondre à plusieurs questions, à savoir :

  (i) Quel est l'impact de la nature, de la position et du nombre de substituants sur les propriétés électrochimiques et la capacité de piégeage des nitrones ?

  (ii) Existe-t-il un lien entre l'ensemble de ces propriétés physico-chimiques et biologiques ?

  (iii) La modélisation moléculaire nous permettrait-elle de mieux comprendre et prédire la capacité des nitrones à piéger les radicaux libres et/ou leurs propriétés électrochimiques et antioxydantes ?

- D'identifier des nitrones prometteuses afin de pouvoir les utiliser comme sondes analytiques dans le piégeage de radicaux libres et/ou comme agents neuroprotecteurs.

Afin d'atteindre les objectifs que nous nous étions fixés, nous avons étudié les propriétés et l'activité de 33 molécules de type PBN incluant 9 dérivés précédemment synthétisés par notre laboratoire,[1–3] ainsi que la PPN et l'EPPN développées à l'université d'Aix Marseille.[4,5] Parmi toutes ces molécules, 11 n'ont jamais été mentionnées dans la littérature. Les nitrones que nous avons étudiées possèdent des modifications structurales diverses par rapport à la PBN :

- soit uniquement sur le cycle phényle (chapitres 2 et 3),
- soit uniquement sur la partie *N*-*tert*-butyle en position α ou β (chapitres 2 et 4),
- soit à la fois sur le cycle phényle en position *para* et sur la fonction *N*-*tert*-butyle en position α ou β (chapitres 2 et 4),

- soit en remplaçant le groupement phényle par un bicycle naphtalène et en modifiant la partie *N-tert*-butyle en position β (chapitre 4).

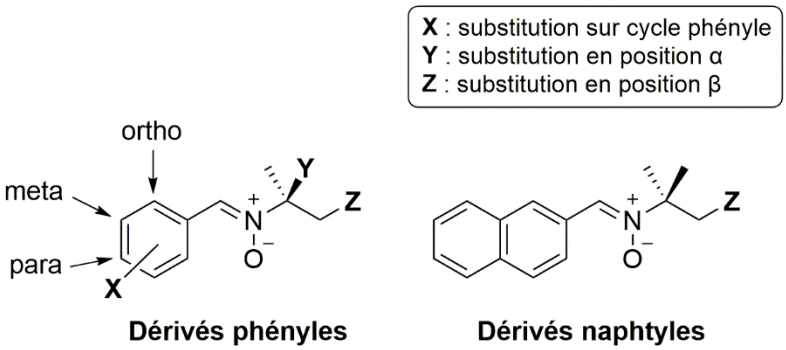

Figure 1. Structure chimique des différents dérivés envisagés.

2. Etude de la capacité à piéger le radical $^{\bullet}CH_2OH$

Dans un premier temps, nous avons étudié les propriétés de piégeage du radical hydroxymethyl ($^{\bullet}CH_2OH$) des différents dérivés synthétisés. Nous avons pour cela mesuré les constantes de vitesse relatives des nitrones par rapport à la PBN (k_N/k_{PBN}) en utilisant une méthode cinétique basée sur la compétition entre la nitrone N étudiée et la trinitrone TN. Il ressort de cette étude que la nature électronique des substituants introduits de part et d'autre de la fonction nitronyle a un fort impact sur la capacité de la nitrone à piéger des radicaux.

Effet de la nature des substituants sur le cycle phényle et la partie *N-tert*-butyle. L'introduction d'un groupement électroattracteur en *para* du cycle phényle ou en position α ou β de la partie *N-tert*-butyle a tendance à améliorer le piégeage du radical nucléophile $^{\bullet}CH_2OH$ sur la fonction nitronyle. Au contraire, la présence d'un groupement électrodonneur en position *para* du cycle aromatique diminue la capacité à piéger le radical $^{\bullet}CH_2OH$. Lorsque l'on modifie à la fois en *para* du cycle aromatique et sur la fonction *N-tert*-butyle, on remarque que les effets des substituants vont dans le même sens sans pour autant s'additionner complètement. Une rationalisation de la combinaison des effets sur la vitesse de piégeage du radical $^{\bullet}CH_2OH$ parait complexe mais néanmoins, la fonctionnalisation de la fonction *N-tert*-butyle semble avoir un plus fort impact sur la réactivité de la nitrone que celle de la position *para* du cycle aromatique. Lorsque le cycle phényle est remplacé par le bicycle naphtalène, qui apporte un fort effet mésomère donneur, la capacité de la fonction nitronyle à

piéger un radical est fortement réduite. Elle est cependant améliorée lorsqu'un groupement électroattracteur est également introduit en position β de la fonction *N*-*tert*-butyle, dépassant l'activité de la PBN et donc confirmant le fort impact des substituants en position β.

Effet de la position et du nombre de substituants sur le cycle phényle. Nous avons également étudié l'influence de la position et du nombre de substituants sur le cycle aromatique vis-à-vis de la capacité à piéger le radical $^{\bullet}CH_2OH$. Les résultats obtenus montrent que lorsqu'un seul substituant est présent, la position a peu d'impact sur la réactivité. Au contraire, lorsque deux groupements sont présents sur les positions *ortho* du cycle, la nitrone ne piège plus de radicaux. Cela pourrait être expliqué par l'encombrement stérique induit par les substituants sur ces positions qui pourrait gêner l'attaque du radical sur la fonction nitronyle. Toutefois, cette étude n'a été effectuée que sur le groupement methoxy (MeO), électrodonneur, et mériterait d'être reconduite avec un groupement électroattracteur, afin de confirmer cette hypothèse.

Mise en évidence de corrélations avec la constante de Hammett (σ_p). Dans le cas de modifications structurales en *para* du cycle aromatique, une prédiction de la capacité à piéger le radical $^{\bullet}CH_2OH$ par la nitrone peut être réalisée à partir de la constante de Hammett (σ_p) du substituant introduit.[6] En effet, une bonne corrélation entre cette constante qui traduit l'effet électronique du substituant et les constantes de vitesse relatives des dérivés a été obtenue (R^2 = 0,86). Cependant, il n'est plus possible de prédire l'activité de la nitrone par la constante de Hammett lorsque les modifications interviennent sur la partie *N*-*tert*-butyle. C'est pourquoi nous nous sommes tournés vers la modélisation moléculaire afin de vérifier si des paramètres théoriques nous permettraient de prédire la réactivité de la fonction nitronyle vis-à-vis du radical $^{\bullet}CH_2OH$.

Mise en évidence de corrélations avec les charges partielles des atomes de la fonction nitronyle. Les charges partielles des atomes de la fonction nitronyle (H, C, N et O) ont été calculées par la théorie de la fonctionnelle de la densité (DFT). Si on s'intéresse aux modifications en *para* du cycle aromatique, on obtient de très bonnes corrélations entre la constante de Hammett et les charges partielles des atomes de la fonction nitronyle (Figure 2), montrant bien l'impact électronique des substituants sur la répartition des charges de la fonction nitronyle.

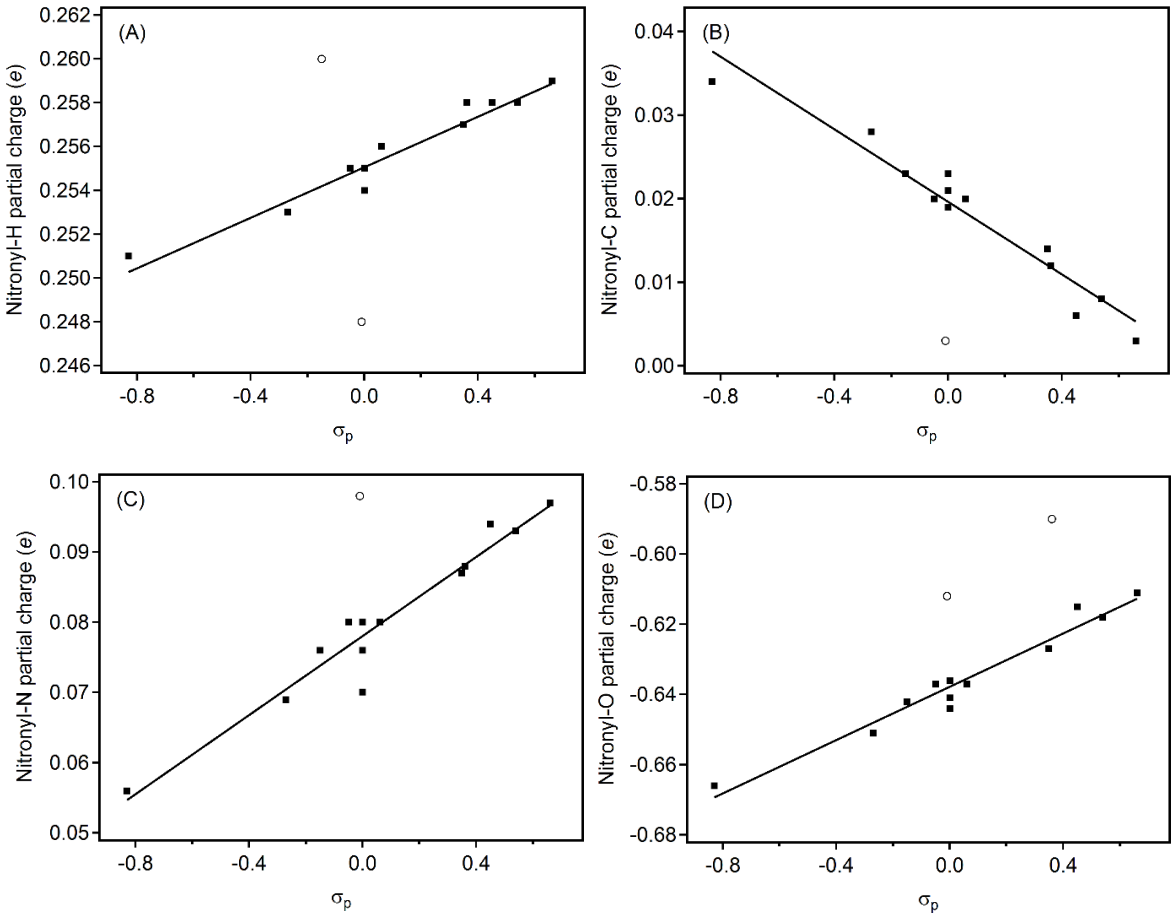

Figure 2. Corrélations entre la constante de Hammett (σ_p) du substituant et les charges partielles des atomes de la fonction nitronyle, (A) : proton (R^2 = 0,93), (B) : carbone (R^2 = 0,94), (C) : azote (R^2 = 0,93) et (D) : oxygène (R^2 = 0,95) des dérivés *para*, en excluant les valeurs aberrantes de 4-Ph-PBN, 4-iPr-PBN pour (A) et 4-MeNHCO-PBN pour (D) marqués avec un ○).

On obtient également une corrélation entre la vitesse de piégeage du radical $^{\bullet}CH_2OH$ et la charge partielle de l'atome de carbone de la fonction nitronyle, sur lequel le radical s'additionne (Figure 3A (■), R^2 = 0,87). Nous avons choisi de ne représenter que les nouveaux dérivés étudiés car les cinétiques de piégeage des nitrones précédemment étudiées n'ont pas été réalisées dans les mêmes conditions.[2] Les résultats montrent que la vitesse de piégeage est plus élevée lorsque la charge partielle du carbone est proche de zéro. Cependant, étant donné la nature nucléophile du radical $^{\bullet}CH_2OH$,[7] nous nous attendions à obtenir une tendance inverse, à savoir une augmentation de la vitesse de piégeage lorsque la charge partielle du carbone devient de plus en plus positive (site appauvri en électrons), qui traduirait une addition nucléophile du radical. Cette tendance est d'ailleurs observée lorsque la nitrone est modifiée sur la partie *N*-*tert*-butyle (Figure 3A (●), R^2 = 0,82), avec une corrélation positive entre la vitesse de piégeage et la charge partielle du carbone de la fonction nitronyle. Il

semblerait que la présence d'effets mésomères en position *para* du cycle phényle complexifie l'interprétation des résultats. Lorsque l'on modifie des deux côtés de la fonction nitronyle (dérivés bi-fonctionnalisés), une bonne corrélation négative est observée en excluant le dérivé 4-MeO-PPN (Figure 3A (▲), R^2 = 0,91). La fonctionnalisation de la position *para* du cycle aromatique semble donc avoir un plus fort impact sur la répartition de la charge partielle de l'atome de carbone que celle de la partie *N*-*tert*-butyle. Les tendances observées dépendant du lieu de fonctionnalisation de la nitrone, il semble difficile de généraliser l'influence de la répartition des charges de la fonction nitronyle sur la vitesse de piégeage du radical $^{\bullet}CH_2OH$. Pour finir, si l'on s'intéresse aux dérivés naphtalène, on remarque que la charge partielle du carbone ne varie pas lorsque l'on introduit un groupement électroattracteur en position β de la fonction *N*-*tert*-butyle.

Mise en évidence de corrélations avec la charge totale atomique de la fonction nitronyle. Nous nous sommes également intéressés à la charge totale atomique de la fonction nitronyle afin de voir si les vitesses de piégeage du radical $^{\bullet}CH_2OH$ ne corrélaient pas avec la charge globale du groupement nitronyle, où a lieu la réaction d'addition radicalaire. Dans le cas de modifications en *para* du cycle aromatique, une bonne corrélation positive est observée entre les deux paramètres (Figure 3B (■), R^2 = 0,83). La vitesse de piégeage est de plus en plus grande lorsque la charge totale atomique de la fonction nitronyle est de moins en moins négative et donc est appauvrie en électrons. Cette corrélation n'est malheureusement plus observée lorsque les modifications ont lieu sur la partie *N*-*tert*-butyle (Figure 3B (●)). Lorsque les modifications en *para* du cycle et en *N*-*tert*-butyle sont combinées (dérivés bi-fonctionnalisés), une légère tendance est observée (Figure 3B (▲), R^2 = 0,65) et est similaire à celle mise en évidence pour les dérivés *para*. Il semble donc difficile de généraliser la relation entre la vitesse de piégeage du radical $^{\bullet}CH_2OH$ des nitrones et la charge totale atomique de leur fonction nitronyle. La charge partielle du carbone et la charge totale atomique de la fonction nitronyle ne permettent pas de traduire à elles seules la réactivité de la nitrone vis-à-vis du radical $^{\bullet}CH_2OH$. Des études supplémentaires sont donc nécessaires pour mieux comprendre le mécanisme impliqué dans la réaction de piégeage du radical $^{\bullet}CH_2OH$. On peut par exemple envisager d'étudier la répartition des charges (densités de spin) et la thermodynamique de formation des adduits de spin formés.

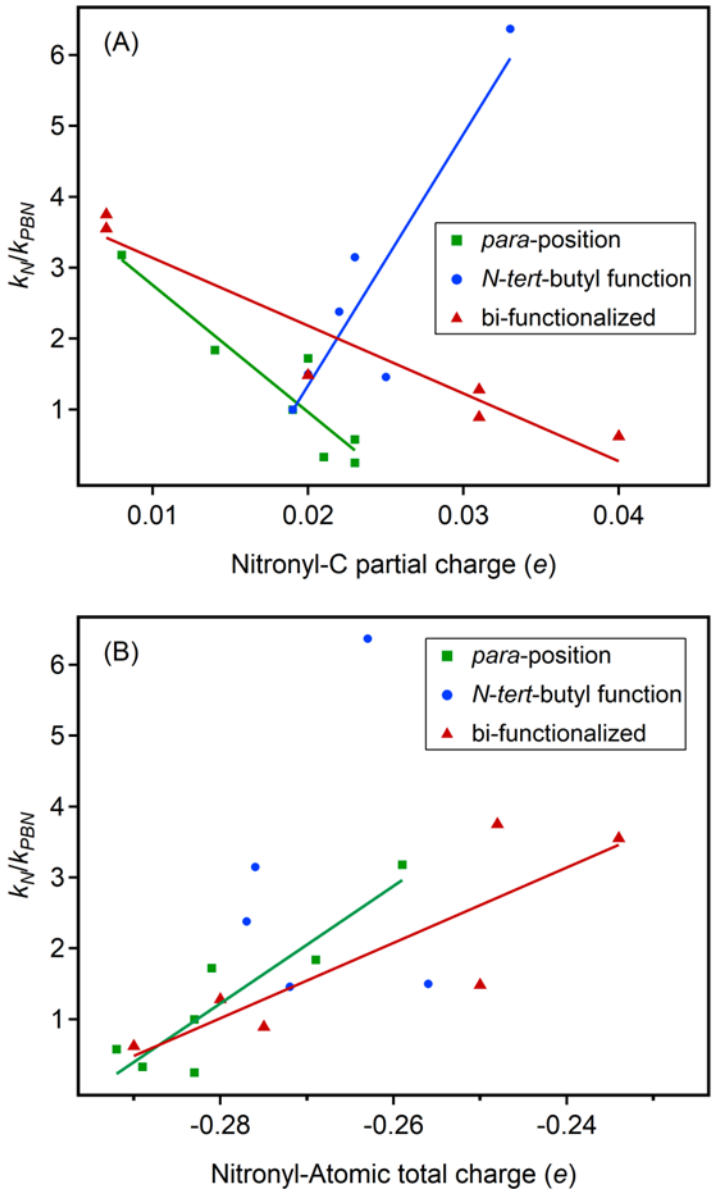

Figure 3. Tracé des constantes de vitesse relatives de piégeage du radical $^{\bullet}CH_2OH$ en fonction de (A) : la charge partielle du carbone et (B) : la charge totale atomique de la fonction nitronyle pour les dérivés modifiés en para (■) ((A) : R^2 = 0,87 et (B) : R^2 = 0,83, en excluant les valeurs aberrantes de 4-Ph-PBN et 4-MeO-PBN), ceux modifiés sur la partie N-tert-butyle (●) ((A) : R^2 = 0,82), et les dérivés bi-fonctionnalisés (▲) ((A) : R^2 = 0,91 et (B) : R^2 = 0,65 en excluant la valeur aberrante de 4-MeO-PPN).

3. Etude des propriétés électrochimiques

Nous avons ensuite étudié le comportement électrochimique des dérivés synthétisés et mesuré les potentiels de réduction et d'oxydation (E_p(c) et E_p(a)) de la fonction nitronyle par voltampérométrie cyclique afin d'avoir une idée du caractère antioxydant des différentes

nitrones synthétisées. La fonction nitronyle est capable à la fois de se réduire pour donner un radical anion et de s'oxyder pour donner un radical cation. Une fois de plus, les résultats obtenus sur les différents dérivés synthétisés montrent un effet important de la nature électronique des substituants.

Effet de la nature des substituants sur le cycle phényle et la partie *N*-*tert*-butyle. La présence d'un groupement électroattracteur sur le cycle aromatique a tendance à faciliter la réduction de la fonction nitronyle mais à rendre plus difficile son oxydation. L'inverse est observé lorsqu'un groupement électrodonneur est présent en position *para* du cycle. Concernant l'influence de la nature électronique des substituants en position α ou β de la fonction *N*-*tert*-butyle, un groupement électroattracteur a tendance à rendre la réduction plus facile alors que pour l'oxydation l'impact des substituants ne semble pas dépendre uniquement de leur nature électronique. En effet, on observe qu'une fonction acétamide a tendance à rendre l'oxydation plus facile tandis qu'un groupement acétate augmente le potentiel d'oxydation. La même tendance est observée pour les dérivés bi-fonctionnalisés. Toutefois, une addition des effets des substituants de part et d'autre de la fonction nitronyle n'est pas toujours observée pour les dérivés bi-fonctionnalisés, montrant qu'une généralisation des effets électroniques n'est pas possible. Pour finir, lorsque l'on introduit un bicycle naphtalène ayant un fort effet mésomère donneur, la réduction et l'oxydation de la fonction nitronyle sont facilitées.

Effet de la position et du nombre de substituants sur le cycle phényle. Une légère influence de la position du substituant sur le cycle phényle a également été observée ; la valeur du potentiel de réduction évoluant dans le sens *meta* ~ *ortho* < *para* et celle du potentiel d'oxydation évoluant en sens inverse : *para* < *ortho* < *meta*. Lorsque le nombre de groupements methoxy (MeO) est augmenté sur le cycle aromatique, une addition de l'effet électrodonneur est observé. Ainsi, le potentiel de réduction est plus grand et le potentiel d'oxydation plus faible lorsque trois groupements sont présents. Il convient cependant de noter que cette étude n'a été réalisée qu'avec le substituant MeO.

Mise en évidence de corrélations avec la constante de Hammett (σ_p). La connaissance de la constante de Hammett du substituant introduit en position *para* du cycle aromatique permet de prédire la valeur du potentiel de réduction ou d'oxydation de la fonction nitronyle du dérivé en question. En effet, de bonnes corrélations entre la constante de Hammett et les

potentiels de réduction et d'oxydation ont été observées pour les dérivés modifiés en *para* (R^2 = 0,78 et R^2 = 0,68). Cependant, cette prédiction ne peut plus être utilisée lorsque la fonctionnalisation de la nitrone a lieu en position α ou β.

Mise en évidence de corrélations avec le potentiel d'ionisation (IP). Nous nous sommes donc intéressés au calcul d'un paramètre théorique, le potentiel d'ionisation (IP), afin de vérifier si la modélisation moléculaire nous permettrait d'avoir une idée des potentiels d'oxydo-réduction des dérivés. En rassemblant les données de toutes les nitrones étudiées durant cette thèse, nous avons réussi à mettre en évidence une tendance entre le potentiel d'ionisation calculé et le potentiel d'oxydation de la fonction nitronyle mesuré (Figure 4, R^2 = 0,62). On remarque que les deux paramètres évoluent dans le même sens : plus le potentiel d'ionisation est grand et plus le potentiel d'oxydation est élevé et donc la fonction nitronyle difficilement oxydée. Par conséquent, ce paramètre théorique nous permettrait d'avoir une idée de la capacité des dérivés de la PBN à s'oxyder, sans nécessairement avoir à les synthétiser au préalable.

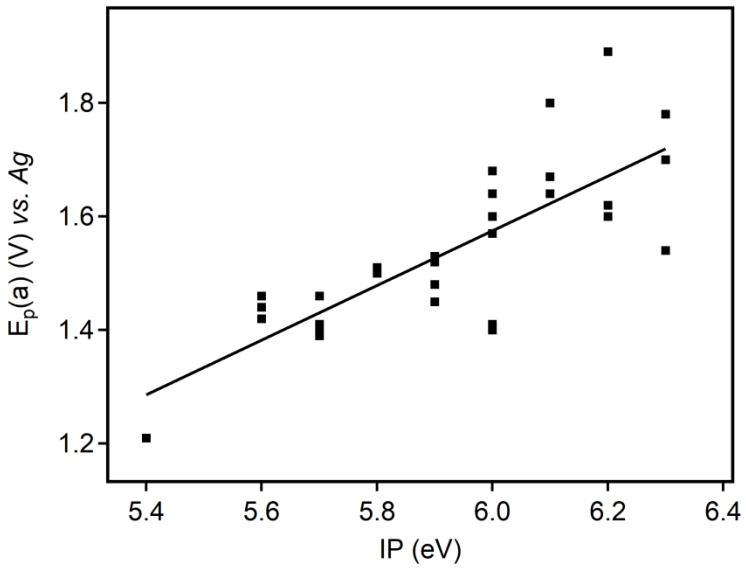

Figure 4. Tendance observée entre le potentiel d'ionisation (IP) et le potentiel d'oxydation ($E_p(a)$) de la fonction nitronyle de tous les dérivés, excluant les analogues 4-MeS-PBN et 4-Me_2N-PBN dont les processus d'oxydation sont plus compliqués (R^2 = 0,62).

Mise en évidence de corrélations avec la vitesse de piégeage du radical $^{\bullet}CH_2OH$. Etant donné la mise en évidence d'une influence des substituants sur les potentiels d'oxydo-réduction de la fonction nitronyle ainsi que sur la vitesse de piégeage du radical $^{\bullet}CH_2OH$, nous avons essayé de vérifier s'il n'existait pas de relation entre ces paramètres. Il ne semble

pas y avoir de lien entre le potentiel de réduction de la fonction nitronyle et la vitesse de piégeage (Figure 5A). Au contraire, de bonnes corrélations entre le potentiel d'oxydation de la fonction nitronyle et la vitesse de piégeage ont été identifiées pour chaque série de dérivés (Figure 5B), lorsque les analogues les plus réactifs sont exclus.

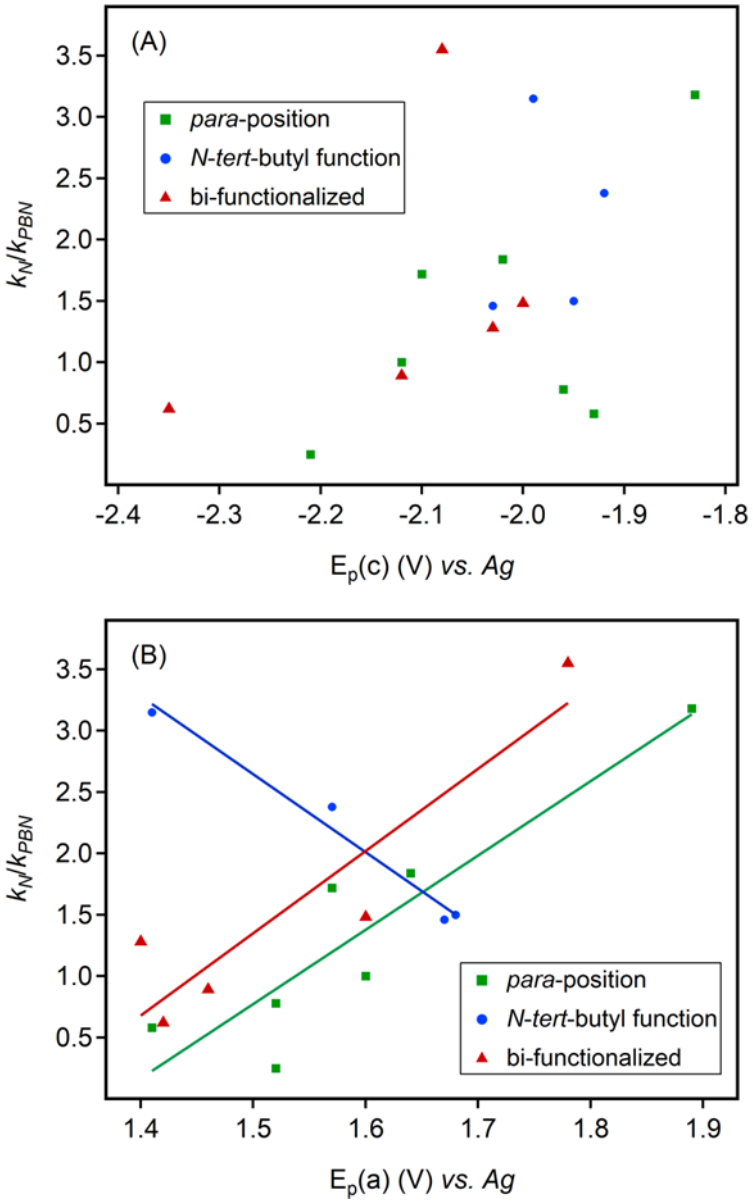

Figure 5. Tracé des constantes de vitesse relatives de piégeage du radical $^{\bullet}CH_2OH$ en fonction de (A) : le potentiel de réduction et (B) : le potentiel d'oxydation de la fonction nitronyle pour les dérivés modifiés en para (■) ((B) : R^2 = 0,72 en excluant la valeur aberrante de 4-MeS-PBN), ceux modifiés sur la partie N-tert-butyle (●) ((B) : R^2 = 0,96 en excluant la valeur aberrante de PPN), et les dérivés bi-fonctionnalisés (▲) ((B) : R^2 = 0,85 en excluant les valeurs aberrantes de 4-MeO-PPN et 4-HOOC-PBN-CH_2NHAc).

Comme reporté pour les charges atomiques de la fonction nitronyle, on obtient des tendances opposées selon le lieu de fonctionnalisation de la nitrone. En effet, pour une fonctionnalisation de la position *para* du cycle aromatique, la vitesse de piégeage augmente lorsque le potentiel d'oxydation augmente également, c'est-à-dire lorsque la fonction nitronyle accepte facilement un électron. La tendance inverse est observée pour une fonctionnalisation de la partie *N*-*tert*-butyle. Lorsque les fonctionnalisations ont lieu à la fois en *para* du cycle et en *N*-*tert*-butyle (dérivés bi-fonctionnalisés), la tendance observée est similaire à celle mise en évidence pour les dérivés *para*, montrant une plus forte influence de la fonctionnalisation de la position *para*. Il semble donc une fois de plus difficile de généraliser les relations observées et il semble également que la capacité des nitrones à piéger le radical $^{\bullet}CH_2OH$ ne dépende pas uniquement de leur facilité à transférer des électrons.

4. Etude de l'activité neuroprotectrice

Pour finir, les propriétés neuroprotectrices de l'ensemble des nitrones ont été étudiées sur deux modèles d'étude *in vitro* : (1) des cellules gliales intoxiquées à l'hydroperoxyde de *tert*-butyle (professeur M. Vignes) et (2) des neurones corticaux primaires intoxiqués par du glutamate (société Neuro-Sys).

Réflexions sur le mécanisme impliqué dans la neuroprotection. Nous nous sommes intéressés à la mise en évidence de liens entre l'activité neuroprotectrice des nitrones et leurs propriétés intrinsèques, notamment le potentiel d'oxydation de la fonction nitronyle. En effet, une étude de Rosselin *et al*. sur des dérivés substitués sur la fonction *N*-*tert*-butyle avait fait ressortir une bonne corrélation entre la cytoprotection à 50 µM de cellules endothéliales aortiques intoxiquées à l'H_2O_2 et le potentiel d'oxydation des dérivés. Cette corrélation montre que plus la fonction nitronyle donne facilement ses électrons (potentiel d'oxydation faible), meilleure est la cytoprotection de la nitrone ; supportant un mécanisme antioxydant.[3] Nous avons donc voulu vérifier cette relation avec les données déterminées dans le cadre de cette thèse et l'ensemble des nitrones étudiées mais aucune tendance significative n'a été observée (Figure 6A), supposant que le mécanisme impliqué dans la neuroprotection des cellules n'est pas seulement un mécanisme antioxydant. Il ne semble pas non plus exister de lien entre la capacité de la fonction nitronyle à capter des électrons (potentiel de réduction) et la neuroprotection de la nitrone (Figure 6B).

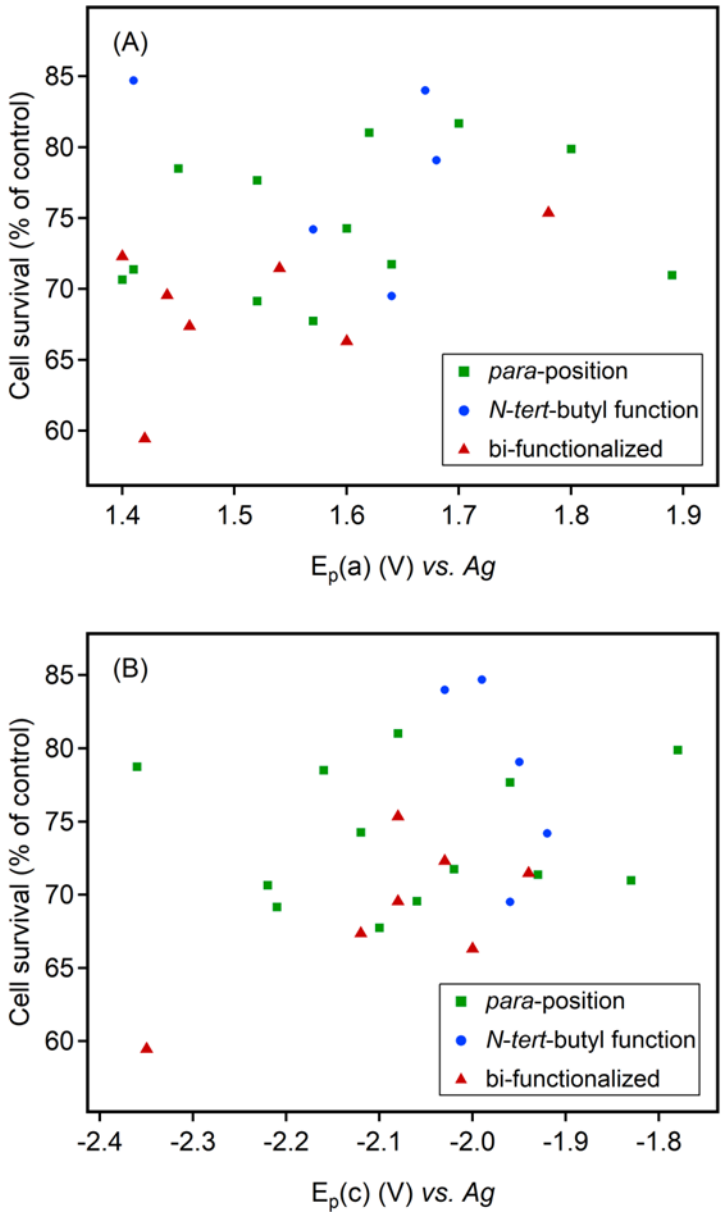

Figure 6. Tracé de la survie cellulaire de neurones corticaux primaires intoxiqués par du glutamate après 1 h d'incubation avec les dérivés à 10 µM en fonction de (A) : le potentiel d'oxydation $E_p(a)$ (en excluant les dérivés 4-MeS-PBN et 4-Me_2N-PBN pour lesquels les processus d'oxydation sont plus complexes) et (B) : le potentiel de réduction $E_p(c)$ de la fonction nitronyle.

Le mécanisme intervenant dans la neuroprotection des cellules ne semble pas non plus être un mécanisme de piégeage de radicaux puisqu'aucun lien entre la capacité de la nitrone à piéger le radical $^{\bullet}CH_2OH$ et ses propriétés neuroprotectrices n'a été démontré au cours de cette thèse (Figure 7A). En effet, les dérivés ayant la meilleure activité neuroprotectrice ne sont pas ceux qui piègent le mieux le radical $^{\bullet}CH_2OH$. De plus, l'activité biologique d'un composé chimique est affectée par de nombreux paramètres tels que sa solubilité dans l'eau, sa

lipophilie (Figure 7B) et sa toxicité, rendant la généralisation de relations structure – activité ou propriété – activité difficile, surtout sur une large série.

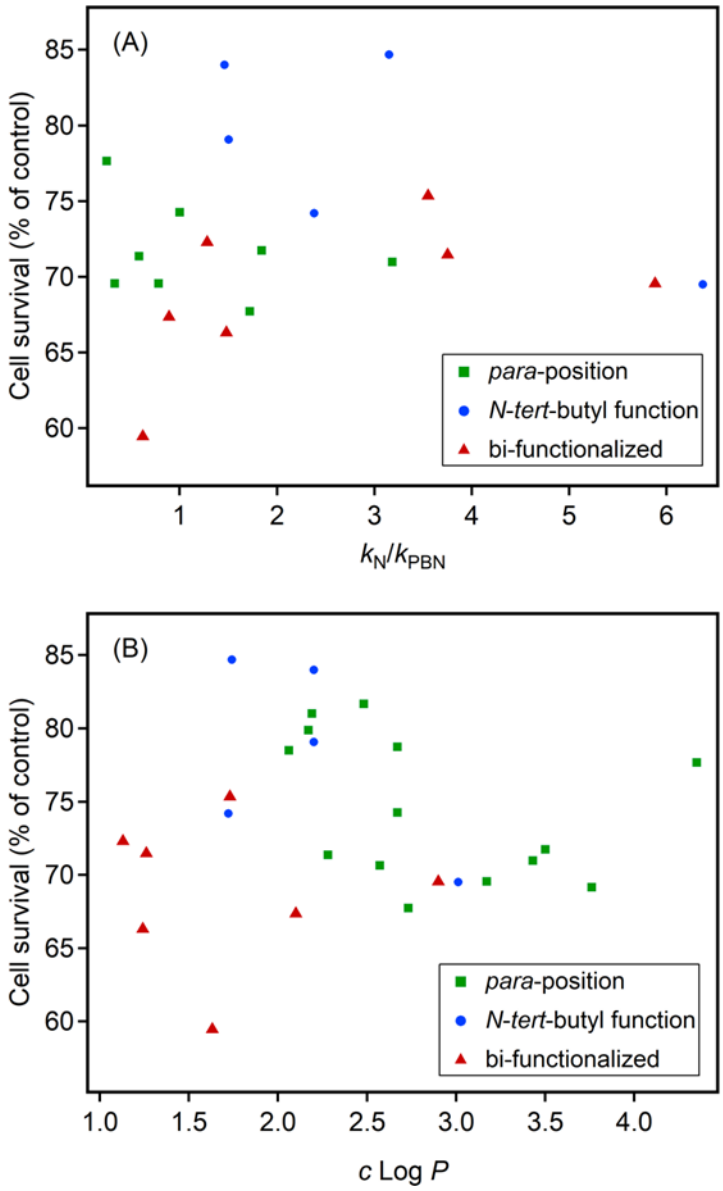

Figure 7. Tracé de la survie cellulaire de neurones corticaux primaires intoxiqués par du glutamate après 1 h d'incubation avec les dérivés à 10 µM en fonction de (A) : la constante de vitesse relative de piégeage du radical $^{\bullet}CH_2OH$ (k_N/k_{PBN}) et (B) : le coefficient de partage octanol-eau (c Log P) des dérivés.

5. Conclusion générale et perspectives

Pour conclure, cette thèse nous a permis de mieux comprendre l'influence de la nature électronique, de la position et du nombre de substituants sur les propriétés électrochimiques et

l'activité de piégeage du radical $^{\bullet}CH_2OH$ des nitrones et d'étudier les liens existants entre les différents paramètres étudiés. Nous avons aussi pu mettre en évidence des relations entre des paramètres théoriques calculés (charges atomiques et potentiels d'ionisation) et des propriétés propres aux dérivés (potentiels d'oxydo-réduction, capacité à piéger le radical $^{\bullet}CH_2OH$), confirmant le fait que la modélisation moléculaire pourrait nous aider à sélectionner des nitrones d'intérêt en balayant rapidement un large panel de molécules avant de les synthétiser. En revanche, l'influence de la nature électronique des substituants sur l'activité neuroprotectrice des nitrones n'a pu être identifiée.

Dans le cadre de cette thèse, nous avons également identifié des dérivés prometteurs soit en tant que piégeur de radicaux, soit en tant qu'agents neuroprotecteurs car nous avons observé qu'il est en effet rare qu'un même composé présente les deux activités. Les dérivés présentant les meilleures capacités de piégeage du radical $^{\bullet}CH_2OH$ sont la PPN et la 4-MeO-PPN, surpassant de 6 fois celles de la PBN et faisant d'elles les nitrones les plus prometteuses pour le piégeage de radicaux centrés sur le carbone. Ces deux dérivés possèdent un groupement phosphonate en position α de la fonction *N-tert*-butyle. Les dérivés 4-HOOC-PBN-CH_2NHAc, 4-HOOC-PBN-CH_2OAc, PBN-CH_2NHAc et 4-CF_3-PBN présentent également de très bonnes capacités de piégeage du radical $^{\bullet}CH_2OH$, de 3,8 à 3,2 fois supérieures à celles de la PBN. Aux vus des résultats obtenus, il serait donc opportun de synthétiser une série de nitrones possédant un groupement phosphonate ou amide en position α de la partie *N-tert*-butyle ainsi qu'un groupement électroattracteur en *para* du cycle aromatique tel qu'un trifluorométhyl (CF_3) ou un acide carboxylique (HOOC), par exemple. On pourrait également envisager d'étudier le piégeage d'un autre radical afin de déterminer si la nature du radical piégé a une influence sur la réactivité de la nitrone.

Concernant l'activité neuroprotectrice, les nitrones les plus prometteuses sont 4-HOOC-PBN-CH_2OH, 4-HOOC-PBN-CH_2NHAc, 4-Me_2N-PBN, 4-F-PBN, 4-MeS-PBN et 4-MeCONH-PBN dans le test du professeur M. Vignes et 4-HOOC-PBN, NBN, 4-Me_2N-PBN, 4-MeNHCO-PBN, 4-NC-PBN, PBN-CH_2OAc, PBN-CH_2NHAc et NBN-CH_2OH dans le test de la société Neuro-Sys. Seuls les dérivés PBN-CH_2NHAc et 4-HOOC-PBN-CH_2NHAc possèdent une bonne vitesse de piégeage du radical $^{\bullet}CH_2OH$ ainsi qu'une activité neuroprotectrice. Une étude plus approfondie de l'activité neuroprotectrice des nitrones les plus efficaces reste nécessaire. Il serait également intéressant de déterminer leur capacité à franchir la barrière hémato-encéphalique, une propriété indispensable pour un agent neuroprotecteur.

Pour finir, une autre perspective qui pourrait être envisagée par la suite serait de greffer les nitrones prometteuses sur un transporteur afin d'améliorer leur biodisponibilité. Dans cette éventualité, nous avons poursuivi les recherches menées au laboratoire sur l'élaboration d'un transporteur amphiphile divalent sur lequel deux antioxydants pourraient être greffés. Le transporteur étudié possède une structure amphiphile composée d'une tête sucre polaire et d'une queue perfluorée hydrophobe permettant d'assurer à la fois une bonne solubilité en milieu aqueux et une hydrophobie suffisante pour garantir un passage membranaire. Il est également constitué de deux acides aminés lysines portant des groupements fonctionnels sur lesquels les antioxydants peuvent être ensuite greffés (Figure 8). Nous nous sommes particulièrement intéressés au dérivé FATxPBN qui comporte un antioxydant de type nitrone : la PBN et un analogue synthétique de la vitamine E : le Trolox. En effet, ce dérivé développé par Rosselin *et al.* a montré un effet de synergie antioxydante, lui conférant d'excellentes propriétés protectrices dans un modèle *ex vivo* de tissus aortiques de rats soumis à un stress oxydant induit par une hyperglycémie, ainsi qu'une bonne activité antioxydante dans un modèle de peroxydation lipidique. En effet, FATxPBN a montré des capacités de localisation membranaire.[8,9]

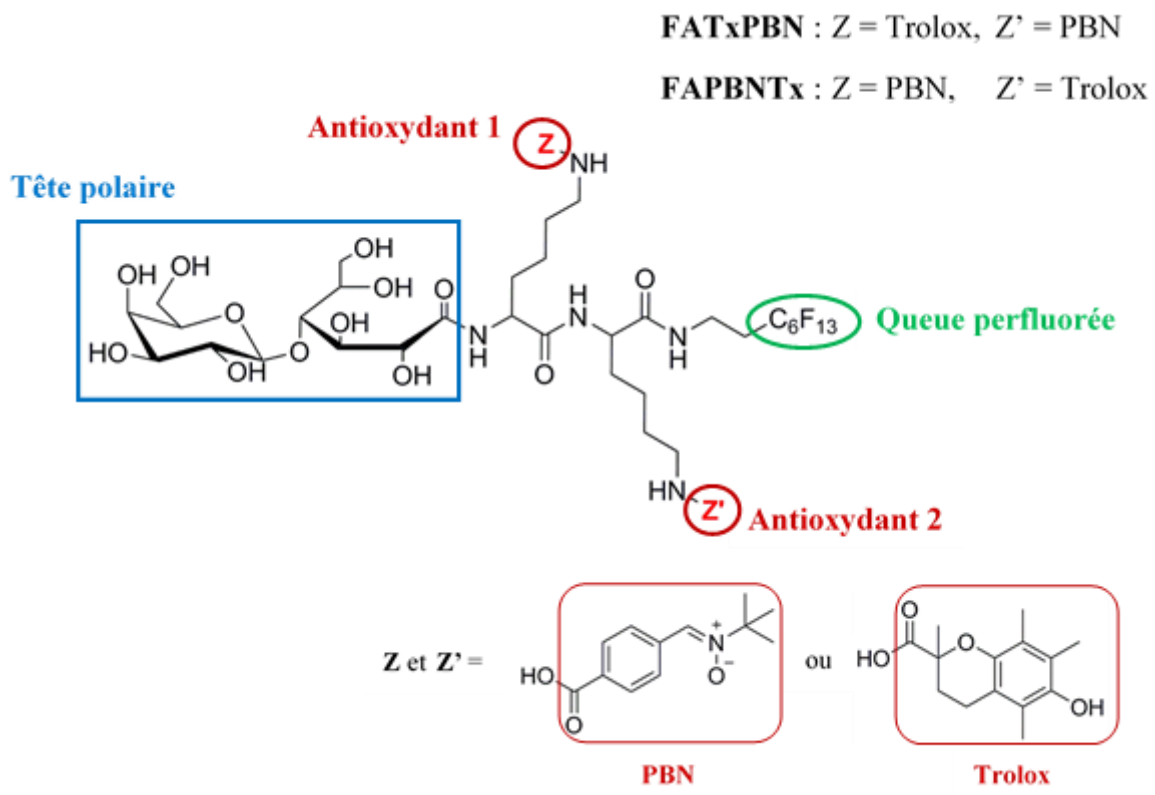

Figure 8. Représentation de la structure chimique des dérivés amphiphiles divalents FATxPBN et FAPBNTx.

Au cours de cette thèse, le FATxPBN a été obtenu en améliorant la voie de synthèse précédemment développée dans notre laboratoire. Nous avons également synthétisé le dérivé FAPBNTx dont la position des antioxydants PBN et Trolox a été inversée afin d'analyser l'influence de la position de l'antioxydant au sein du transporteur sur la réactivité de la molécule. L'activité neuroprotectrice des deux dérivés amphiphiles a été évaluée *in vitro* sur des neurones corticaux matures intoxiqués par du glutamate par la société Neuro-Sys (Figure 9). Les résultats montrent une très bonne neuroprotection des deux dérivés, même à faible concentration (1 nM). Le dérivé FAPBNTx présente une activité supérieure à celle du FATxPBN montrant que la position des antioxydants sur le transporteur amphiphile a une influence sur la neuroprotection de la molécule. L'activité neuroprotectrice du dérivé amphiphile divalent FAPBNTx est très supérieure à celle évaluée pour tous les dérivés de la PBN inclus dans cette thèse, montrant l'intérêt d'approfondir l'étude des propriétés de ce dérivé. Le greffage d'autres antioxydants sur le transporteur amphiphile pourrait être également envisagé, tels que les dérivés de la PBN que nous avons identifiés comme présentant les meilleures activités, tant en piégeage de radicaux qu'en neuroprotection. En effet, nous pourrions espérer que leur greffage sur un transporteur amphiphile améliorerait leur biodisponibilité, leur conférant une meilleure activité.

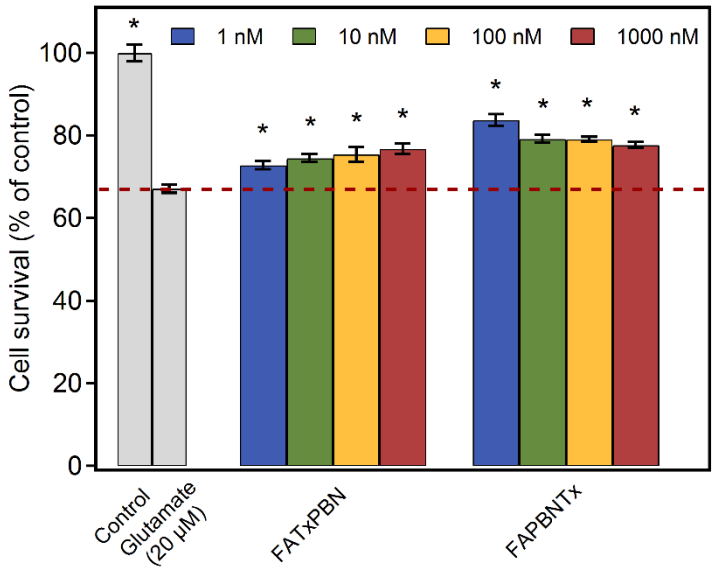

Figure 9. Effet neuroprotecteur des dérivés FATxPBN et FAPBNTx à 1 nM, 10 nM, 100 nM et 1000 nM sur des neurones corticaux primaires intoxiqués par du glutamate (20 µM, 20 min, évaluation réalisée 48 h après le lavage du glutamate) après 1 h d'incubation avec les dérivés. Evaluation de la survie cellulaire par un test MTT. La significativité statistique des résultats (*) a été déterminée avec $p < 0,05$ vs glutamate seul, par un test ANOVA à un facteur suivi d'un test Fischer PLSD.

REFERENCES

1 G. Durand, F. Choteau, B. Pucci and F. A. Villamena, *J. Phys. Chem. A*, 2008, **112**, 12498–12509.

2 M. Rosselin, B. Tuccio, P. Pério, Frederick. A. Villamena, P.-L. Fabre and G. Durand, *Electrochimica Acta*, 2016, **193**, 231–239.

3 M. Rosselin, F. Choteau, K. Zéamari, K. M. Nash, A. Das, R. Lauricella, E. Lojou, B. Tuccio, F. A. Villamena and G. Durand, *J. Org. Chem.*, 2014, **79**, 6615–6626.

4 A. Zeghdaoui, B. Tuccio, J.-P. Finet, V. Cerri and P. Tordo, *J. Chem. Soc. Perkin Trans. 2*, 1995, 2087–2089.

5 V. Roubaud, R. Lauricella, J.-C. Bouteiller and B. Tuccio, *Arch. Biochem. Biophys.*, 2002, **397**, 51–56.

6 C. Hansch, A. Leo and R. W. Taft, *Chem. Rev.*, 1991, **91**, 165–195.

7 F. De Vleeschouwer, V. Van Speybroeck, M. Waroquier, P. Geerlings and F. De Proft, *Org. Lett.*, 2007, **9**, 2721–2724.

8 M. Rosselin, G. Meyer, P. Guillet, T. Cheviet, G. Walther, A. Meister, D. Hadjipavlou-Litina and G. Durand, *Bioconjug. Chem.*, 2016, **27**, 772–781.

9 L. Socrier, M. Rosselin, A. M. Gomez Giraldo, B. Chantemargue, F. Di Meo, P. Trouillas, G. Durand and S. Morandat, *Biochim. Biophys. Acta BBA - Biomembr.*, 2019, **1861**, 1489–1501.